Pelagic Ecosystem and Carbon System Response to the K/Pg Boundary Mass Extinction

Heather S. Birch

Thesis submitted for the degree of Doctor of Philosophy.

July 2011

ProQuest LLC
789 East Eisenhower Parkway
P.O. Box 1346
Ann Arbor, MI 48106-1346

Abstract

The pelagic ecosystem plays an important role in cycling carbon between ocean and atmospheric reservoirs. This study explores the hypothesis that widespread extinctions experienced by the pelagic ecosystem at the Cretaceous/Paleogene (K/Pg) resulted in a reduction in surface-to-deep ocean organic carbon (C-org) flux, followed by a long period of recovery (3-4 myr). This hypothesis, coined the 'living ocean' model by previous authors, has potential problems. Firstly, benthic foraminifera, which are believed to be dependent on surface-exported food, do not show widespread extinction. Secondly, existing surface-to-deep ocean foraminiferal $\delta^{13}C$ records that are used to reconstruct C-org flux fail to account for the changing ecologies and potential isotopic disequilibrium effects on test calcite $\delta^{13}C$ of the newly evolved Paleocene planktonic foraminiferal indicator species. The goal of this study was to constrain such 'vital' effects in early Paleocene planktonic foraminifera and produce a refined reconstruction of the K/Pg marine carbon system response.

Multispecies $\delta^{18}O$ and $\delta^{13}C$ studies from a South Atlantic core (ODP Site 1262) constrain isotopic disequilibrium effects. The results provide the first species-specific $\delta^{13}C$ isotopic 'adjustment factors' that account for the influence of (i) unusually small test sizes (metabolic fractionation) and (ii) planktonic foraminiferal symbiosis. The adjustment factors were applied to a new stable isotope time series from Site 1262. In the refined reconstruction the apparent '$\delta^{13}C$ gradient-reversal' recognised in previous studies is eliminated, with benthic-planktic $\delta^{13}C$ differences now converging at zero. This period of minimum $\delta^{13}C$ gradient lasted ~200 kyr, thereafter the vertical $\delta^{13}C$ gradient gradually expanded until a pre-extinction gradient of 1 ‰ was reached, signalling full carbon pump recovery, at ~64.1 Ma. This is 1.58 myr after the K/Pg event and represents close to half the recovery time estimated previously. Under this model, recovery of the $\delta^{13}C$ gradient precedes the inferred evolutionary origin of photosymbiosis by 0.6 Ma. Sedimentological ($CaCO_3$), paleontological and bulk $\delta^{13}C$ changes indicate that full oligotrophic conditions did not take hold until ~61.4 Ma. This suggests that although C-org flux recovered after 1.58 myr, the extended pelagic ecosystem may have taken far longer (>4 myr) to fully recover from the catastrophe.

Acknowledgment

I would first like to say thank you to my supervisors Helen Coxall, Paul Pearson and Daniela Schmidt, for their help and guidance throughout my PhD. My particular thanks go to my main supervisor Helen who despite juggling family life and work always had time for me. Helen guided me through my PhD and was invaluable in increasing my understanding of my work and inspiring new ideas. I feel privileged to have been her first PhD student. I thank Paul for his expert instruction on foraminiferal taxonomy, especially for the 'foram school' when he took me to participate in the GLOW cruise. For his help and advice throughout my PhD, after he took me under his wing when Helen spent time in Stockholm. I am also grateful to Daniela who launched me into my PhD, as I met her on my first day when I flew to Bremen. She introduced me to many people at a variety of conferences and helped to secure the samples I used for analysis.

I also owe a large debt of gratitude to Dick Kroon for providing me with the Site 1262 samples. I would also like to thank the people who have provided technical support for my PhD. Julia Becker for running the stable isotope samples, Pete Fisher for his scanning electron microscope instruction, Alun Rodgers who assisted with graphics and printing, Lindsey Axe who helped with the light microscope facility and Lawrence Badham for producing my Tanzanian thin sections.

I would also like to thank the 2008 and 2009 TDP participants and the Tanzanian Petroleum Drilling Corporation (based in Dar es Salaam); Brian Huber, Helen Coxall, Jackie Lees, Álvaro Jiménez Berrocoso, Maria Rose Petrizzo, Amina Mweneinda, Joyce singano, Ken MacLeod, Ephrem Mchana, Michael Mkreme, Mr. K, Ines Wendler, Francesca Falzoni and Laura Cotton, for their help and guidance whilst on fieldwork and later back in Cardiff. A special thank you goes to Jackie Lees and Paul Bown who have given me advice and guidance for my PhD, but also about life in academia, as well as providing me with accommodation when I attended a conference in London.

The past 3 and a half years have been made even more enjoyable by the presence of my fellow PhD colleagues and the Paleoclimate group members, through many discussions, some of which were about science. Thanks to my 1.16 office mates, Martin Wolstencroft, Tracy Aze and Louis Emery (who loved 'fieldwork'). I would especially like to thank Heather Price, Elaine Mawbey and Helen Medley for their support through the good and bad times and for the many cups of tea. Last but not least a big thank you goes to my family and fiancée for all there help and support through the years leading up to my time here in Cardiff and during my PhD.

I would also like to show my gratitude to NERC who funded this project. Grant number 2007-2009 NE/F009038/1 and 2009- 2011 NE/H526394/1.

Citations

Conference abstracts:

Birch. H, Coxall. H, Lear. C and Schmidt. D (2008). Planktonic foraminifera ecology and pelagic ecosystem recovery after the K/Pg. The Palaeontological Association 52nd Annual Meeting.

Birch. H, Coxall. H, Lear. C and Schmidt. D (2009). Planktonic foraminifera ecology and pelagic ecosystem recovery after the K/Pg boundary mass extinction. UK IODP Symposium, 2009.

Birch, H., Coxall. H., Pearson, P., Schmidt. D (2009). Return to the light: Evolution of photosymbiosis after the end Cretaceous mass extinction. The Palaeontological Association 53nd Annual Meeting.

Birch, H., Coxall. H., Pearson, P., Schmidt. D (2010). Return to the light: Evolution of photosymbiosis after the end Cretaceous mass extinction. Geochemistry Group Annual Research in Progress Meeting 2010, London.

Birch, H., Coxall. H., Pearson, P., Schmidt. D (2010). Evolution of photosymbiosis and recovery of the carbon system after the End Cretaceous mass extinction. International Palaeontological Congress (IPC3), London.

Birch, H., Coxall. H., Pearson, P., Schmidt. D (2010). Planktonic foraminifera ecology and carbon system recovery after the end Cretaceous mass extinction. International symposium on foraminifera, FORAMS 2010, Bonn, Germany.

Birch, H., Coxall. H., Pearson, P., Schmidt. D (2011). Carbon system recovery and planktonic foraminifera ecology after the end Cretaceous mass extinction. Climate and Biota of the Paleogene (CBEP), Salzburg.

Papers:

Birch, H., Coxall, H., and Pearson, P. (2011). Evolutionary ecology of Early Paleocene planktonic foraminifera: Size, depth habitat and symbiosis. Submitted to Paleobiology (#11027).

Contents

List of Figures

List of Tables

1. Introduction

This introduction is organized into the following sections; an account of current understanding of the K/Pg extinction event and its possible causes and consequences, an outline of the biology and ecology of the microfossil group used in this study, i.e. planktonic foraminifera, and a review of the geochemical proxy methods used.

1.1. General background to the project

The Cretaceous – Tertiary (K/T), or Cretaceous – Paleogene (K/Pg) boundary, which is the International Commission on Stratigraphy (ICS) preferred name, occurred ~65 million years ago (Ma) and marks the end of the Mesozoic Era and the start of the Cenozoic (Figure 1.1). This boundary has long been associated with major changes in Earth's fauna and flora, including, most famously, the rapid demise of the dinosaurs. The question of whether the changes at this boundary were catastrophic, involving mass extinction, or more gradual, involving progressive faunal turnover resulting from gradual environmental change (D'Hondt, 2005), is controversial. However, the weight of evidence tips heavily in favour of the mass extinction theory (Schulte *et al.*, 2010), which implies vast and abrupt changes to Earth's ecosystems 65 million years ago as the result of some catastrophic event.

Now generally accepted as the second largest extinction event in Earth's history, the K/Pg boundary event has become a fascinating interval for study, offering many opportunities to explore the possible cause and consequences of a major disturbance to the Earth's biotic system. As on land, the marine realm suffered widespread extinctions at the K/Pg that appear to be associated with major perturbations of the marine carbon system. The purpose of this thesis is to explore the evidence for a carbon system crash and the pattern of post-K/Pg recovery in the pelagic realm using foraminifera evolutionary and geochemical analysis. The work builds on previous research by D'Hondt *et al.* (1998) and Coxall *et al.* (2006) who suggested that disruption of pelagic

food webs, because of extinction, interrupted the transport of organic matter to the seafloor. Making use of newly available stratigraphically continuous deep sea sediment records with an orbitally controlled age-framework will provide new constraints on the ocean vertical carbon gradient that will help resolve the tempo and mechanisms of ecosystem perturbation and recovery.

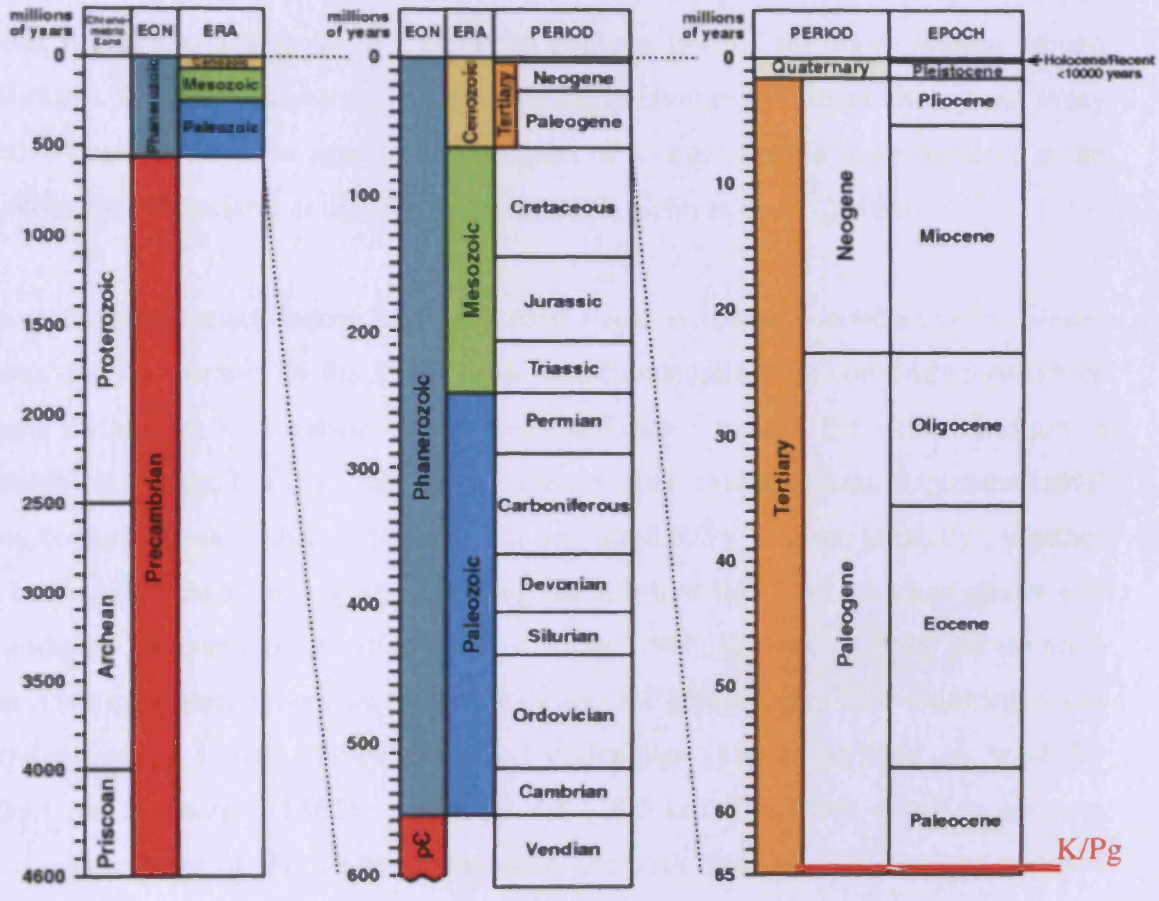

Figure 1.1 – Geological timescale with the K/Pg boundary indicated by a red line. Image taken from http://www.geo.ucalgary.ca/~macrae/timescale.html.

1.2. The cause of the K/Pg extinction event

The nature and mechanism of K/Pg extinction is a matter of heated and ongoing debate. Many possible causes have been proposed ranging from natural ongoing climate change and sea level rise (Haq *et al.*, 1987, Keller *et al.*, 1993 and Oms *et al.*, 2007), flood basalt volcanic eruptions associated with emplacement of the Deccan Traps in western India (Officer and Drake, 1985; Duncan and Pyle, 1988; Courtillot *et al.*, 1988) and asteroid impacts (Alvarez *et al.*, 1980) to name a few of the more widely argued possibilities. In general however, evidence strongly favours the impact theory and many scientists (but not all) now agree that an impact of a large asteroid body occurred at the K/Pg boundary (Macleod *et al.*, 2007; Kring, 2007; Schulte *et al.*, 2010).

Support for the impact theory can be traced back to research conducted by Walter Alvarez and co-workers in the 1980s who found unusually high concentrations of the element iridium in Cretaceous – Paleogene sediments around the world. Iridium is extremely rare in the Earth's crust but occurs at higher concentrations in extraterrestrial bodies, including asteroids and comets. The so-called K/Pg 'Iridium anomaly', together with other evidence of an object impacting the Earth at this time (shocked quartz and melt-induced glass spherules called tektites; Kring, 1993; D'Hondt, 1994a) led the team to the Alvarez impact theory as the cause of the K/Pg extinction. Still requiring a site for the proposed impact, Hildebrand and colleagues (1991), building on work by Penfield and Camargo (1981), suggested the ~300 km Chicxulub crater in Mexico. Buried on the coast of the Yucatan peninsula, the scale and age of this crater matched the other geochemical, sedimentary and palaeontological evidence for a devastating K/Pg asteroid impact. Since Alvarez' pioneering work, over 250 K/Pg boundary sites have now been located around the globe (Schulte *et al.*, 2010). These sites show varying thicknesses of ejecta debris depending on proximity to the Chicxulub impact site (Figure 1.2). These correlative horizons further strengthen the theory that a single impact at the K/Pg boundary had global consequences (Schulte *et al.*, 2010).

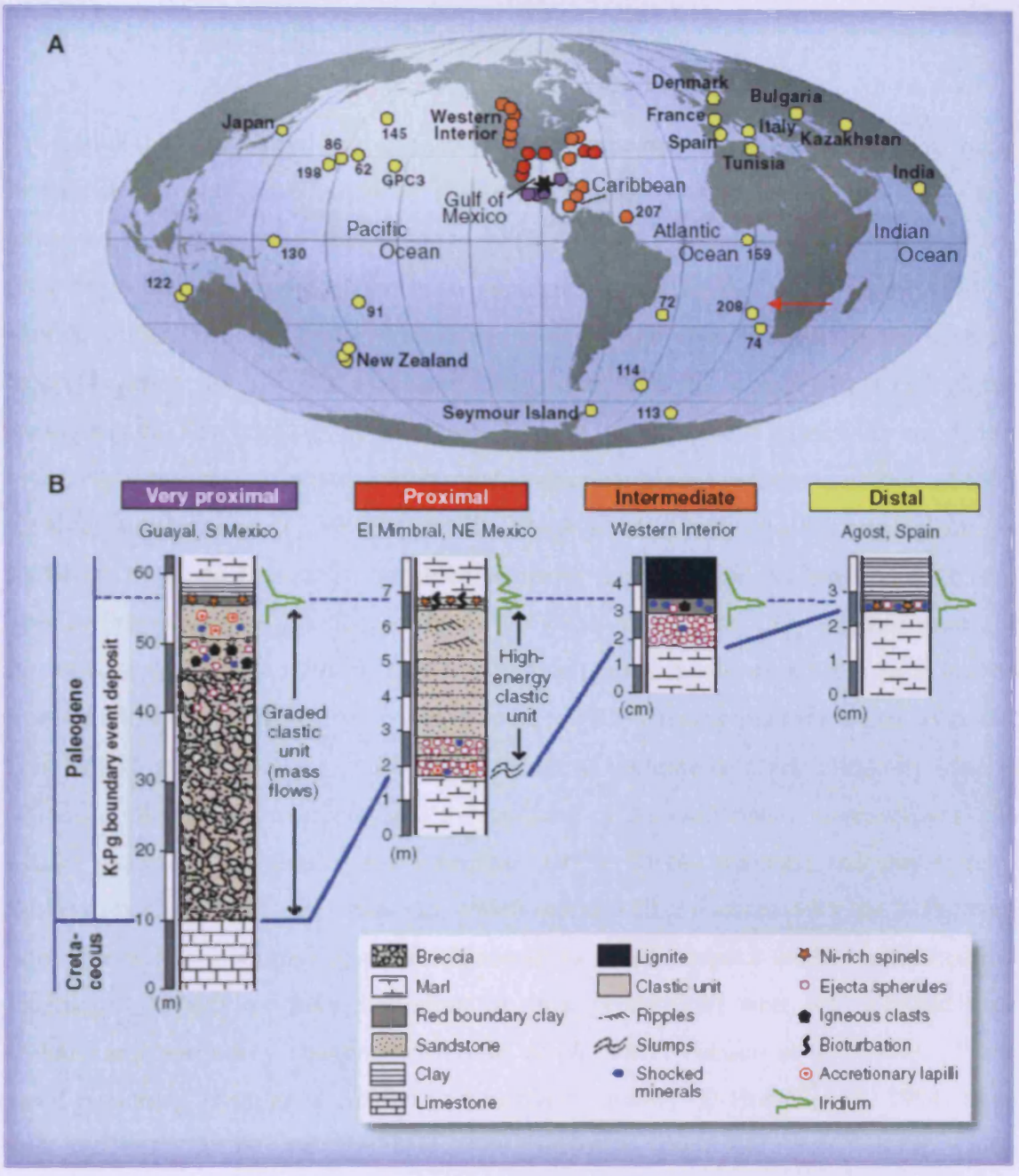

Figure 1.2 – A = Global distribution of key K/Pg boundary sites. Numbered sites equal deep sea drilling Legs. The asterisk indicates the location of the Impact site at Chicxulub and red arrow the Leg of interest in this study, 208. Yellow indicates distal sites (>5000 km away), orange indicates intermediate sites (1000 to 5000 km), Red indicates proximal sites (up to 1000 km), and purple indicates very proximal sites (up to 500 km). B = General lithologies at the 4 categories of distance. Taken from Schulte *et al.* 2010.

1.2.1. Immediate effects of the Chicxulub bolides impact

The initial shock blast and heat produced by the impact of a large extraterrestrial body on the Earth would have killed all plants and animals in the immediate vicinity and generated numerous wild fires (Kring, 1993). As the Chicxulub crater was near the coast large tsunamis would have been generated, affecting the whole of the Gulf of Mexico region (Kring, 1993). The iridium signal and other impact ejecta, such as spherules, have been found worldwide suggesting that the impact event had global consequences. The lithology of the upper 3 km at the Chicxulub impact site are rich in water, carbonate and sulphate, which upon impact could realise large quantities of SO_2, H_2O vapour (Pope *et al.*, 1998) and CO_2 (Pope *et al.*, 1997) into the atmosphere, as predicted by impact models. Sulphate aerosols are predicted to have lead to near freezing temperatures globally, despite the large amount of CO_2 released into the atmosphere (Pope *et al.*, 1997). The dust and sulphur aerosols would also have lead to global darkness for up to a year (Toon *et al.*, 1982) causing photosynthesis to cease. This lack of photosynthesis could have lead to an increase in ocean alkalinity (due to extinction of $CaCO_3$ producers) and a deepening of the carbonate compensation depth (CCD) (Hsu, 1980; Caldeira and Rampino, 1993). Global darkness and cessation of photosynthesis (Griffis and Chapman, 1988) seems a likely scenario for the K/Pg mass extinction and is supported by the fossil record as aquatic deposit feeders and terrestrial detritivores (which are less dependant on new production) were less affected than primary and secondary consumers (Arthur *et al.*, 1987; Hansen *et al.*, 1987). Trace metal poisoning (Jing *et al.*, 2010) and increased acidity (D'Hondt *et al.*, 1994) have been suggested as another mechanism for extinction within the marine realm, which could amplify the stress affects of global darkness (Schulte *et al.*, 2010).

1.2.2. Terrestrial biotic change at the K/Pg boundary

The K/Pg is most famous for the extinction of the dinosaurs (Sheehan *et al.*, 1991; MacLeod *et al.*, 1997). Dinosaurs, along with pterosaurs were the only major terrestrial vertebrate groups to become extinct at the K/Pg boundary (Milner, 1998). Lizards,

snakes, freshwater fish, turtles, crocodilians and amphibians all seem to have passed through the K/Pg boundary with little effect (Buffetaut, 1990; MacLeod *et al.*, 1997). Information on bird survival at the K/Pg boundary is patchy and no real conclusions can be made (Buffetaut, 1990; MacLeod *et al.*, 1997). Among mammalian taxa, the marsupials seem to have been most severely affected with nearly all species becoming extinct. In contrast the multituberculates and placental mammals seem to have actually expanded in diversity (Buffetaut, 1990; Erwin, 1998). The extinctions on land seems to have been selective with larger organisms dependent on plants, generally being more susceptible than smaller animals (carnivorous, insectivorous or omnivorous), in most cases (Buffetaut, 1990).

Among terrestrial plants the K/Pg boundary is also marked by a large extinction incurring a loss of 30 to 35 % of palynoflora (Nichols, 2007). Johnson *et al.* (1989) also found a 30 % palynofloral extinction at the K/Pg boundary and states that megaflora underwent a 79 % turnover at the boundary. Above the boundary a spike in fern-spores was found to be present by Nichols (2007) at a sampling site from western North America. This is inferred to represent pioneer plant communities re-occupying terrestrial terrains after the devastation of the extinction.

1.2.3. Marine biotic change at the K/Pg boundary

The marine ecosystem was also seriously affected with fossil records indicating that over 50 % of marine genera (particularly organisms that produced calcareous skeletons) were wiped out at the boundary across shelf and pelagic environments (Sepkoski, 1996; D'Hondt 2005). Some groups survived better than others, such as those with benthic lifestyles (e.g. benthic foraminifera) and those with the ability to form resting cysts (e.g. dinoflagellates, except calcareous forms) (Kitchell *et al.*, 1986). These lifestyles likely facilitated protection from the environmental upheaval.

Vertebrates

The fossil records of marine vertebrates are limited. Bony fish are generally thought to have passed through the K/Pg extinction with few losses (MacLeod *et al.*, 1997), but a review by Kriwet and Benton (2004) showed that the neoselachian sharks suffered major losses with 84 % (+/-5 %) of species going extinct. Batoids (rays) were also seriously affected with almost all identifiable species lost. Benthopelagic and deep-sea species of sharks and batoids were the only forms which showed little effect from the K/Pg event, when compared to open marine, open continental and shallow sea forms. Marine reptiles (e.g. mosasaurs and sauropterygians) also became extinct (MacLeod *et al.*, 1997).

Marine plankton

Calcareous nannoplankton, microscopic marine alga, suffered major losses at the K/Pg boundary (Pospichal, 1994; Henriksson, 1996; MacLeod *et al.*, 1997; Bown, 2005; Bernaola and Monechi, 2007). Of the 131 late Maastrichtian species only 10 survived into the Danian, resulting in a 90% loss of species diversity. The species that did survive tended to be r-selected (opportunistic) taxa that were either uncommon or only common in high latitude environments before the K/Pg boundary (Bown, 2005). The abundance of calcareous nannoplankton in sea floor sediments, as recorded by fine fraction carbonate sediment accumulation (D'Hondt, 2005), remained low for at least 150 kyrs after the boundary (Bernaola and Monechi, 2007). This would suggest that they were still living in a unfavourable environment or had changed their life cycle strategies (Bernaola and Monechi, 2007). There was a complete loss of all the Cretaceous calcareous dinoflagellates ('Calcispheres') assemblages at the K/Pg boundary with no Maastrichtian taxa continuing into the Paleocene. This was followed by a mass occurrence in the Danian, when completely new Cenozoic assemblages evolved (Futterer, 1990).

Although most marine plankton suffered some loss at the K/Pg boundary there was an unexpected high survival of marine diatoms (Kitchell *et al.*, 1986; MacLeod *et al.*,

1997) and the majority of siliceous plankton thrived. Radiolarians showed no mass extinction and diatoms actually increased in abundance relative to radiolarians. A possible explanation for this is that reduced numbers of calcareous plankton led to vacated niche space that allowed the opportunistic diatoms to bloom (MacLeod *et al.*, 1997). Enhanced upwelling or more efficient nutrient cycling may also explain this plankton bloom in the first 1 million years of the Paleocene (Hollis *et al.*, 1995).

Invertebrates

On the continental shelves, molluscan assemblages display major changes in taxonomic and ecological make-up across the K/Pg boundary. Maastrichtian faunas were dominated by diverse suites of suspension feeders but these were replaced by low diversity, deposit feeding or carnivorous species in the Paleocene (Hansen *et al.*, 1987; Hansena *et al.*, 2004). Veneroid bivalves suffered an 81 % loss of subgenera at the K/Pg boundary (Lockwood, 2004). Ammonoidea (Cephalopods) and rudist bivales along with nerineid and acteonellid gastropods (largely suspension feeders) all became extinct (MacLeod *et al.*, 1997). The late Cretaceous and K/Pg boundary was a period of major evolutionary turnover for ostrocods and echinoderms rather than obvious extinction, although the timing of these events has not been fully constrained (MacLeod *et al.*, 1997).

Between 30 and 32 % of scleractinian corals became extinct at the boundary (Kiessling and Baron-Szabo, 2004 and Baron-Szabo, 2006, respectively), with photosymbiotic (zooxanthellate) corals being more affected than azooxanthellate corals (Kiessling and Baron-Szabo, 2004). Approximately 13 % of bryozoan families went extinct at the K/Pg boundary however, this had little effect on the long term pattern of bryozoan evolution (MacLeod *et al.*, 1997). Research into the decopod crustaceans and more specifically the brachyura (true crabs) has shown that they did not suffer major extinction at the K/Pg boundary (Brösing, 2008).

One of the most severely affected marine groups were planktonic foraminifera (MacLeod *et al.*, 1997) with 90 % of species disappearing at the boundary (Smit, 1982;

D'Hondt *et al.*, 1996). One aspect of the K/Pg extinction is that open ocean faunal assemblages are marked by a sharper turnover than near-shore assemblages (Keller, 1988; D'Hondt and Keller, 1991). This is probably due to near-shore assemblages being dominated by small, opportunitstic multiserial taxa before the boundary extinction; whereas the larger open ocean specialists that dominated in the Cretaceous all went extinct (D'Hondt *et al.*, 1996).

It is widely believed that as few as five species of planktonic foraminifera survived the K/Pg extinction, of which three are believed to have seeded the radiation of the Paleocene (Olsson *et al.*, 1999). Other authors however, recognise additional Cretaceous survivors and values range up to 26 species (MacLeod and Keller, 1991). Keller *et al.* (1993), Keller (1988) and Canudo *et al.*, (1991) propose a gradual extinction caused by sea level regression rather than the rapid impact scenario, due to their findings of Cretaceous foraminifera into Paleogene sediments and last occurrences of foraminifera before the boundary. Other scientists however have argued that these findings are purely an artefact of re-working (Norris *et al.*, 1999) and the species whose last occurrence were below the boundary were found to be rare and do occur up to the boundary in other core sections (D'Hondt *et al.*, 1996). Keller *et al.* (1993) argues that if the foraminifera were simply an artefact or reworking then they would still display Cretaceous $\delta^{13}C$ values, but they display tertiary values instead. A study by Huber (1996) found no such $\delta^{13}C$ evidence that foraminifera had survived beyond the boundary. Another independent study by Macleod and Huber (1996) looked at the problem of Cretaceous 'survivors' versus reworking by looking at the $^{87}Sr/^{86}Sr$ ratios of foraminifera and inoceramids compared with $^{87}Sr/^{86}Sr$ seawater ratios and concluded that the Cretaceous foraminifera in Paleogene sediments were a result of re-working. A K/Pg sequence recovered from ODP Leg 207 on Demerara Rise in the Atlantic Ocean, contains a complete sedimentary sequence unaffected by tsunamis and impact induced shock waves (Macleod *et al.*, 2007). Below the spherule bed (which occurs exactly between the Maastrichtian and Danian sediment contacts) a complete Maastrichtian assemblage is recognised with no changes in diversity. Above this spherule bed rare, poorly preserved Cretaceous planktonic foraminifera are found only within the

planktonic foraminifera biochron P0, indicating a catastrophic single impact induced mass extinction (Macleod *et al.*, 2007).

1.3. Consequences of the K/Pg boundary extinctions

1.3.1. Biogeochemical collapse and recovery

There are two main lines of evidence for major disturbance to the marine carbon cycle at the K/Pg boundary; 1) a crash in carbonate sediment accumulation and 2) collapse in the surface to deep carbon isotope ($\delta^{13}C$) gradient, both of which appear, in existing records, to take ~3 myr to recover (D'Hondt, 2005, Figure 1.3). The dramatic reduction (approximately 50 to 85%, Zachos *et al.*, 1985; Zachos and Arthur, 1986; Arthur *et al.*, 1987; D'Hondt and Keller, 1991) in the rates of deep sea carbonate sedimentation in all ocean basins seems to be due to the major extinction of carbonate producers, i.e. nannoplankton, and to a lesser extent planktonic foraminifera (D'Hondt, 2005). Several lines of evidence suggest it was a reduction of sediment flux to the deep ocean rather than an increase in dissolution that lead to this reduction of carbonate sediments. These include increased preservation and reduced fragmentation in planktonic foraminifera (D'Hondt, 2005) at the K/Pg boundary. The carbonate crash coincided with a collapse of the vertical ocean $\delta^{13}C$ gradient between planktonic and benthic foraminifera (D'Hondt *et al.*, 1998). This has been interpreted as signalling a major reduction in the flux of organic carbon to the seafloor (D'Hondt *et al.*, 1998). The accumulation of barium (Ba), a proxy for organic matter flux also shows a large reduction at the K/Pg boundary (Zachos *et al.*, 1989).

A reduction in primary productivity was first proposed by Hsü *et al.* (1982) to be the cause of this reduced flux in a so called 'strangelove' ocean (Broecker and Peng, 1982). Loss of primary production may have been an immediate consequence of impact dust clouds that would have lead to global darkness and prevented photosynthesis. However, models of large impact events have dust clouds leaving the atmosphere after approximately only a year (Kring, 2000), which does not explain the apparent 3 myr delay in organic carbon flux recovery. D'Hondt *et al.* (1998) proposed that primary

production recovered quickly after the mass extinction event but that organic export from the surface waters remained low over the 3 myr period following the boundary because of a modified pelagic ecosystem caused by extinctions. This has been termed the 'Living Ocean Model' (D'Hondt *et al.*, 1998 and Adams *et al.*, 2004). This hypothesis proposes that in the absence of larger grazers and a reduction of mean phytoplankton size, the resultant smaller aggregates cannot survive dissolution before reaching the sea floor. One challenge to this hypothesis is that benthic foraminifera, which would have been major benefactors of surface derived food, appear to cross the boundary event with relatively few or no extinctions (Thomas, 1990; Alegret *et al.*, 2001; Alegret *et al.*, 2003; Culver, 2003; Coccini and Marsili, 2007).

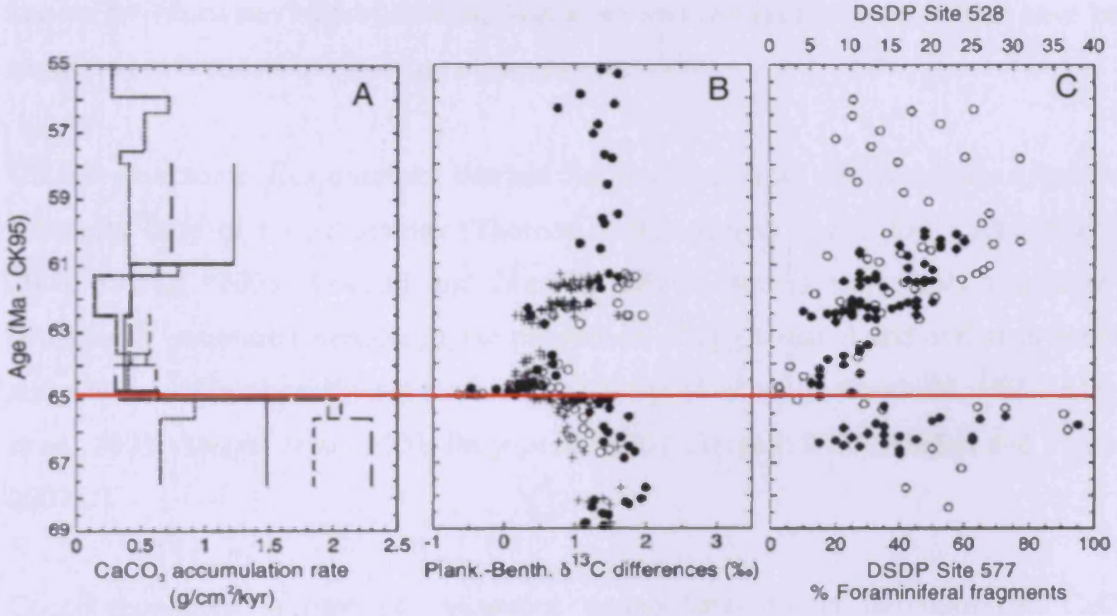

Figure 1.3 - Sediment and geochemical patterns at the K/Pg boundary. Panel C = Mean $CaCO_3$ accumulation rates at Central Pacific DSDP Site 577 (dotted line), South Atlantic DSDP Site 528 (line with short dashes), Site 527 (line with long dashes) and Caribbean ODP Site 1001A (solid line). Panel B = Carbon isotopic $\delta^{13}C$ differences between planktic foraminifera and benthic foraminifera at South Atlantic DSDP Site 528. The black circles represent $\delta^{13}C$ differences between fine carbonate (principally calcareous nannofossils) and benthic foraminifera, the white circles represent differences between mixed layer planktic foraminifera and benthic foraminifera, and the crosses represent differences between thermocline planktic foraminifera and benthic foraminifera. Isotopic data are from D'Hondt *et al.* (1998) and S. D'Hondt and J.C. Zachos (unpublished data). Panel C = Percent foraminiferal fragments at Site 577 (white circles) and Site 528 (black circles). Timescale is based on Cande and Kent (1995) and red line denotes the K/Pg boundary. Adapted from D'Hondt (2005). DSDP Site 527 and 528 are part of Leg 74 located on the map in Figure 1.1, Site 1001A is located as the middle point of the Caribbean sites on the map in Figure 1.1.

1.3.2. Recovery of the pelagic ecosystem

Only two to three species of planktonic foraminifera occur consistently more than a few centimetres above the many globally sampled boundary horizons (D'Hondt, 2005) and can be classified as Cretaceous K/Pg survivors. These few survivors are thought to have seeded the subsequent Paleogene evolutionary radiation of planktonic foraminifera (Olsson et al., 1999). Two waves of evolutionary expansion have been proposed by Coxall *et al.* (2006). The first stage of recovery was marked by the addition of 18 new species and 8 new genera establishing basic test shape and generic diversity, whilst the final recovery was marked by the addition of 16 new species and 3 new genera from a South Atlantic (DSDP site 528) record. At this second stage of evolution of the group known as 'muricates' (*Morozovella*, *Acarinina* and *Igorina*) evolved, which have been suggested to be hosts to symbiont algae (Norris, 1996).

Unlike planktonic foraminifera, benthic foraminifera cross the boundary event with relatively little or no extinctions (Thomas, 1990; Alegret *et al.*, 2001; Alegret *et al.*, 2003; Culver, 2003; Coccini and Marsili, 2007). Studies show only a change in community structure (increase in the proportion of agglutinated and epifaunal forams) and a decrease in diversity that lasted for ~200 kyr (Kuhnt and Kaminski, 1993; Alegret *et al.*, 2001; Alegret et al., 2003; Peryt *et al.*, 2002; Alegret, 2007; Alegret and Thomas, 2007).

Coccolithophores, a type of calcareous nannoplankton and the dominant $CaCO_3$ producers in the Cretaceous (Stanley *et al.*, 2005), suffered major extinctions at the K/Pg boundary and, like planktonic foraminifera, their recovery was delayed. However, their diversification after the boundary appeared to be slower than planktonic foraminifera. A reason for this delay may be that the niche of principle primary producer that they occupied in the Maastrichtian had been taken over by calcareous dinoflagellates (e.g. *Thoracosphaera* spp.) in the early Danian (Fornaciari *et al.*, 2007). *Thoracosphaera* spp. are a significant component of the assemblage up to the base of the calcareous nannofossil bizone *Prinsius dimorphosus* (Fornaciari *et al.*, 2007), which

correlates approximately with the upper part of the planktonic foraminifera biochron P1b.

Molluscs located in shelf habitats also showed a delay in recovery of approximately 2 myr (Hansen *et al.*, 2004). In the Cretaceous, molluscan populations were dominated by suspension feeders. At the K/Pg boundary, most of these were wiped out and the remaining species were predominately deposit feeders. Low diversity deposit feeders dominated communities while $\delta^{13}C$ surface to deep sea gradient values were reduced. Higher diversity, suspension feeding communities began to dominate as conditions and $\delta^{13}C$ returned to pre-extinction levels (Hansen *et al.*, 2004). Veneroid bivalves were found to have an even longer recovery as sub-genetic diversity did not return for approximately 12 myr (Lockwood, 2004). This recovery occurred in a step by step method from the survivors.

Aguirre *et al.*, (2007) also found delayed recovery in calcareous red algae or corallines after the K/Pg boundary. In the early Danian a total of 9 species were found, with Melobesioids and sporolithaceans (deep cooler water species) being the dominant groups. The largest species radiation occurred approximately 6 million years later as 29 species are recognised (19 of which were new) as the shallow warmer water species re-occupied their habitat after the extinction (Aguirre *et al.*, 2007). Reef facies and reef biota showed a two-stage recovery during the Paleocene after the K/Pg boundary (Vecsei and Moussavian, 1997).

For many groups (e.g. planktonic foraminifera [D'Hondt, 2005], molluscs [Gallagher, 2001] and echinoids [Markov and Soloviev, 1997]) the early stages of evolutionary recovery involved very low diversity assemblages, dominated by small, opportunistic taxa that could thrive in harsh environments (Erwin, 1998). Oceanic instability has been inferred by Zachos *et al.* (1989) after the K/Pg, as foraminiferal assemblage turnover rates were fast throughout the Danian, leading to the theory that a highly structured ecosystem may have been incapable of developing initially.

The wide variety of fossil evidence both on land and in the oceans suggests there was significant extinction and evolutionary turnover at the K/Pg boundary. The scarcity of high quality terrestrial fossil records spanning the event has led many scientists to concentrate on marine calcareous plankton, whose fossil records of evolutionary change, in contrast, are extensive and almost continuous in places. Foraminifera provide the added potential of recording environmental information, such as ocean temperatures and the state of carbon cycling, in their calcareous test chemistry. For this reason the remainder of this review will focus on planktonic foraminifera at the time of the K/Pg boundary and the subsequent multi-million year phase of recovery in the Paleocene.

1.4. Planktonic Foraminifera

Foraminifera, are protists and members of the rhizopod order Foraminiferida (Eichwald, 1830). They are mostly marine and build an external test, usually of calcium carbonate in the form of calcite. The majority of foraminiferal species live on the sea floor (benthic), but a relatively small number of species live in the water column (planktonic). Planktonic foraminifera, most of which are in the superfamily Globigerinacea (Carpenter, Parker and Jones, 1862), have relatively low species diversity but are far more abundant than their benthic counterparts (Haynes, 1981). The group is believed to have originated from benthic foraminifera in the mid Jurassic (Leckie, 1989; Schmidt *et al.*, 2006), although multiple derivations of planktonic ecologies from 'tacky pelagic' benthic ancestors is highly likely (Darling *et al*, 2009). There are approximately forty five modern planktonic species (Aze *et al.*, 2011), living mostly in the photic zones where food is most plentiful. However, some species can inhabit deeper levels of the water column. This species-specific depth specialization is useful for providing tracers of different water masses in space and over time, including thermal and nutrient stratification. Planktonic foraminifera make up a relatively small part of the marine zooplankton but the constant deposition of their tests at the seafloor makes a substantial contribution to sea floor sediments (Hemleben *et al.*, 1989; Schiebel 2002; Schiebel and Hemleben, 2005). Today 47 % of the global ocean seafloor that lies above the calcite compensation depth is covered by almost pure carbonate ooze (Leeder, 1999).

The living planktonic foraminifera consist of a mass of cytoplasm (endoplasm) with a nucleus and other organelles that inhabit the test, and a thinner layer of cytoplasm (ectoplasm) then surrounds the test. The most striking structures of the ectoplasm are the pseudopods, granular threads that stream out reaching lengths of up to three times the diameter of the test. These pseudopods can be retracted on one side and 'thrown' out on the other to allow the foraminifera to move, albeit slowly (Haynes, 1981). Foraminifera have a range of diets including unicellular algae, especially diatoms, dissolved and colloidal organic molecules, other protists and small crustaceans such as copepods (Anderson *et al.*, 1979; Haynes, 1981). They collect their food by means of the pseudopods. According to Walker and Bambach (1974) part of the success of foraminifera is due to the versatility of the pseudopodial network to utilise all the 6 main food classes. Unlike benthic foraminifers, whose laboratory study has revealed alternating cycles of sexual and asexual reproduction (Haynes, 1981), difficulties in capturing and retaining planktonic species means that very little is known about planktonic foraminifera reproduction. What has been learned indicates that they reproduce sexually, shedding gametes into the open ocean on what was thought to be an approximate lunar cycle (for review see Hemleben *et al.*, 1989). More recent literature has shown that shallower dwelling species reproduce once or twice a month (Bijma *et al.*, 1990; Schiebel *et al.*, 1997; Schiebel and Hemleben, 2005), but deeper dwelling species are thought to reproduce much less often (Hemleben *et al.*, 1989; Schiebel and Hemleben, 2005).

The majority of our knowledge and taxonomy of both recent and past planktonic foraminifera has come from the morphology of the adult test, the test wall ultrastructure (including distribution of spines and pores), chamber shape and wall ornamentation, which provide the diagnostic characters that define species (Hemleben *et al.*, 1989). Small juveniles grow by addition of chambers, usually in a spiral, until the onset of reproduction, when gametes are released and the empty test falls to the sea floor. Some planktonic foraminifera can be spinose, characterized by the presence of small, acicular spines (consisting of a single calcite crystal) radiating out from the surface. Spines are thought to be fundamental to the biology, probably serving to support food-gathering rhizopods (which secure prey items during digestion) and harbour algal symbionts.

Although rarely preserved in ancient specimens, the presence of spines is signalled by tiny scar-like 'spine-holes' in some well preserved fossils (Olsson *et al.*, 1999). The evolution of spinose morphologies for the first time in the early Paleocene is believed to represent a milestone in planktonic foraminifera biology that allowed ecological specialization and contributed to the success of these organisms in the pelagic realm for the remainder of the Cenozoic (Olsson *et al.*, 1999).

Many spinose species of modern planktonic foraminifera have algae living in their cytoplasm suggesting a symbiotic relationship (Bé *et al.*, 1982; Spero and DeNiro, 1987; Hemleben, *et al.*, 1989; Spero, 1992; Spero and Lea, 1993; Norris, 1996). During the day these symbionts are transferred to the pseudopodia where they can carry out photosynthesis but are transferred back to the cytoplasm at night (Haynes, 1981). The symbionts provide photosynthetically fixed carbon for the foraminifera in exchange for protection and nutrients from captured zooplankton (Hemleben *et al.*, 1989). Symbionts in foraminifera are predominately dinoflagellates but can also be chysophytes (Hemleben *et al.*, 1989; Schiebel and Hemleben, 2005).

The ecology of modern planktonic foraminifera has been the subject of many scientific investigations. Assemblages of planktonic foraminifera can be divided into five major faunal provinces; 1) Polar, 2) Subpolar, 3) Transition (temperate), 4) Subtropical, 5) Tropical (Bradshaw, 1959; Bé and Tolderlund, 1971), which are predominately dependent on food, which in turn is dependent on hydrographic conditions (such as temperature, salinity and upwelling). Recently Aze *et al.* (2011) have recognised 6 ecological groups among the Cenozoic macroperforate planktonic foraminifera (1. Open ocean mixed layer tropical/subtropical, with symbionts, 2. Open ocean mixed layer tropical/subtropical, without symbionts, 3. Open ocean thermocline, 4. Open ocean sub-thermocline, 5. High latitude and 6. Upwelling/High productivity). In general planktonic foraminifera are open water species with abundance and diversity reduced in shelf and coastal waters (Hemleben *et al.*, 1989). Superimposed on this general trend are seasonal variations (Bé, 1960; Schiebel and Hemleben, 2000), vertical distributions and patchiness (Bradshaw, 1959; Bé, 1960) linked to the physical-chemical environment, food resource, test morphology, population dynamics and reproductive

stages (Fairbanks *et al.*, 1982; Hemleben *et al.*, 1989; Schiebel and Hemleben, 2000; Schiebel and Hemleben, 2005). Changes in assemblages over time, therefore, provide indications of environmental change, which is used extensively in palaeoclimate studies.

1.5. Environmental proxies - Stable isotopes

Oxygen and carbon exist in nature in various stable isotope species. There are three stable isotopes of oxygen: ^{16}O, ^{17}O and ^{18}O, with relative natural abundances of 99.76 %, 0.04 % and 0.20 % respectively. Because of the greater mass difference and higher abundance of ^{16}O and ^{18}O, the ratio of $^{18}O/^{16}O$ is used in isotopic studies. Carbon occurs as two stable isotopes: ^{12}C and ^{13}C, with relative abundances of 98.89 % and 1.11 % respectively. The difference in these isotope ratios, relative to a standard, is reported as a delta (δ) value i.e. $\delta^{18}O$ and $\delta^{13}C$. Each of these isotopes shares the same number of electrons and protons but have a different number of neutrons. The different numbers of neutrons controls the mass of the element and as many physico-chemical reactions are mass dependent, each isotope of an element behaves differently. The partitioning of isotopes between substances with different isotopic composition is known as fractionation. Fractionation mainly results from: (1) isotopic exchange reactions, which are the partitioning of isotopes between phases that are in equilibrium. These processes are essentially temperature dependent. (2) Kinetic effects, which cause deviations from the simple equilibrium processes as a result of different rates of reaction for the various isotopic species (Libes, 1992; Cooke and Rohling, 2001).

The isotopic composition of foraminiferal tests has been a powerful tool in reconstructing past ocean climates. This work was pioneered by Emiliani (1954) and Shackleton and Opdyke (1973), building on studies of heavy isotopes by Urey (1947). The technique is based on the principle that foraminiferal calcite in the past records the ambient $\delta^{18}O$ and $\delta^{13}C$ of the water in which the organism was living and calcifying, although in practice foraminiferal stable isotope values usually deviate from equilibrium to some degree. These isotopic ratios, which are controlled by various physical and

chemical parameters, have bearing on environmental and climatic conditions and allow the construction of paleoceanographic time sequences. A more detailed explanation of the principles involved can be found in Cooke and Rohling (2001) and Hemleben *et al.*, (1989) but a summary is presented in the following paragraphs.

1.5.1. Oxygen

The oxygen isotope ratio of sea water is directly linked to the hydrological cycle as the lighter isotope of oxygen within the water molecule is preferentially evaporated, leaving the surrounding water enriched in $\delta^{18}O$. This means that the amount of water stored on land as ice also becomes an important factor, because the snow that forms the ice, derived by evaporation of ocean water at low latitudes, has a very low isotopic composition (-30 to -50 ‰) due to the 'Raleigh Distillation Effect' (Libes, 1992).

There are several processes which determine the oxygen isotope composition of newly formed foraminiferal carbonate; temperature and $\delta^{18}O$ of the surrounding water being the main two. It is this temperature effect that has been used by many paleoclimatologists to reconstruct past temperatures from analysing foraminiferal tests. The overall effect of equilibrium fractionation is roughly 0.2 ‰ depletion in carbonate $\delta^{18}O$ for every 1 °C temperature increase (Kim and O'Neil, 1997). Studies show that there was minimal ice during the K/Pg boundary time (e.g. Zachos *et al.*, 2001) so $\delta^{18}O$ variations are likely the result of local temperature and salinity values, biological changes or post mortem diagenesis.

Five main sources of deviation from sea water isotopic equilibrium, while the planktonic foraminifera are alive, are: (1) the ontogenic effect, through changes in incorporation of metabolic products; (2) symbiont photosynthesis; (3) respiration (the reverse of photosynthesis) within the water column and the use of these respiratory products for calcification; (4) gametogenic calcite; (5) and the effect of changes in $[CO_3^{2-}]$. The various effects may operate in opposing directions, masking one another. All of these influences are important for the interpretation of planktonic foraminifera

stable isotopic climate proxies (Crowley and Zachos, 2000; Cooke and Rohling, 2001). Diagenetic alterations of the planktonic foraminifera test after death can also alter $\delta^{18}O$ values (e.g. Sexton *et al.*, 2006). Many of these effects can largely be accounted for by using species specific records, narrow test size fractions, avoiding specimens with gametogenic calcite and being aware of the preservation state of the specimens.

1.5.2. Carbon

In the present day ocean there is an isotopic gradient, with respect to $\delta^{13}C$, between surface and deep water due to the preferential uptake of ^{12}C by primary producers in the photic zone. This leaves waters of the surface ocean enriched in ^{13}C relative to ^{12}C. If surface dwelling foraminifera secrete a calcium carbonate test in equilibrium (or close to equilibrium) with the surrounding waters they too would show this isotopic ratio enriched in ^{13}C. The ^{12}C enriched organic matter then sinks through the water column to the seafloor as it moves through the food chain into aggregates large enough to avoid oxidation. As the ^{12}C enriched organic matter sinks through the water column, it is available to microbes and is subject to remineralisation. This process of remineralisation leads to the release of ^{12}C to the surrounding waters. Once out of the photic zone remineralisation exceeds photosymbiosis, leading to a net release of ^{12}C to the surrounding waters. The benthic dwelling foraminifera then secrete their calcium carbonate tests in equilibrium with these waters and consequently have an isotopic ratio enriched in ^{12}C. In the modern ocean this ^{13}C depletion is strengthened in benthic foraminifera and the deep ocean waters, as you move from the Atlantic through to the Pacific Ocean, due to ocean circulation, that results in older, more ^{13}C-depleted water in the Pacific basin. The vertical gradient in ^{13}C can be used to establish a depth habitat for foraminiferal species and more importantly how efficiently the 'marine carbon pump' is working.

Differences in foraminiferal $\delta^{13}C$ values relative to dissolved carbon in ambient sea water may be caused by: (1) utilisation of metabolic CO_2 during shell formation; (2) photosynthetic activity of symbionts; (3) growth rate; and (4) variation in carbonate ion concentrations in ambient waters. The various effects are not strictly separate, and there

may be strong overlaps between their regulating processes (Cooke and Rohling, 2001 for a review; details are given in Chapter 4).

1.6. Aims and objectives

The pelagic ecosystem is thought to play an important role in regulating global climates by cycling carbon as biomineral skeletons and organic matter between ocean, sediments and atmospheric reservoirs. It is important therefore, to have a greater knowledge of the pelagic realm, with all its complexity as an integrated ecosystem, as its ability to recover after major perturbations has far reaching implications. Models have shown that complete cessation of oceanic productivity could lead to global warming of up to 3 °C due to increased pCO_2 levels by a factor of 2 or 3 on the time scale of a few 1,000 years (Caldeira *et al.*, 1988). Not only is the understanding of the pelagic realm necessary for climate studies but also for environmental and ecological implications. A study by Kirchner and Weil (2000) showed that smaller background extinctions, not just major extinction events, display a time lag in recovery.

The widespread extinctions experienced by the pelagic ecosystem at the K/Pg boundary, especially of calcareous producers, provides an excellent opportunity to better understand the link between pelagic ecosystem function, carbon cycling and climate. Much progress has been made in identifying the short and longer term consequences of marine extinctions to the carbon system, but additional constraints are required to gain confidence of geochemical reconstructions and improve understanding of ecosystem function. The main question raised is whether the K/Pg recovery was as long as proposed by carbon isotope gradients or is the $\delta^{13}C$ of planktonic foraminifera that are used to reconstruct vertical carbon gradients, influenced by strong disequilibrium vital effects because of a unique onset of environmental and ecological conditions in the early Paleocene. Another important question postulated by D'Hondt (2005) was the link between geochemical recovery and biological evolutionary recovery. The question at the K/Pg boundary is what the driving force was; did recovery of the marine carbon pump lead to increased pelagic speciation due to the availability of new ecospace or did the eventual re-appearance of larger species after the extinction facilitate the transfer of

organic matter to the deep sea and therefore play a role in 'fixing' the marine carbon pump.

Despite much work on this important event many previous studies have had to use patchy data from cores with rudimentary age models, which limit palaeoenvironmental reconstructions. An example of this is a former Deep Sea Drilling Program (DSDP) cruise, leg 74, from Walvis Ridge in the Eastern South Atlantic, one of the few places where it is possible to recover a complete K/Pg boundary section including Paleogene sediments. Leg 74 sampled at this location but due to the available technology at the time the cores were rotary drilled and consequently suffered poor recovery (25% - 75%) and severe drilling disturbance (ShipBoard Scientific Party, 2004). With a new, astronomically constrained age model (Westerhold *et al.*, 2008), complete core from Leg 208, drilled at the same location as Leg 74, important new insights into the palaeoenvironment and recovery after the K/Pg boundary can be gained. The newly recovered records will allow for better constraints on the timing and resolution of the recovery stages.

This project will explore the hypothesis that the vertical organic carbon flux that collapsed at the K/Pg boundary remained suppressed for up to 3 myrs into the Paleocene. The approach taken is to focus on constraining ecologies, depth habitats and possible disequilibrium effects of the indicator species (planktonic foraminifera) used to produce geochemical reconstructions. Focusing on the records from Ocean Drilling Program (ODP) Site 1262 the specifics of the project include:-

(1) Conducting multispecies size analysis on planktonic foraminifera to assess the effect of changing pelagic ecology, including the influence of test size on $\delta^{13}C$ throughout the K/Pg extinction and recovery interval (Chapter 4 and 5).

(2) Creating improved down-hole planktonic and benthic foraminifera $\delta^{13}C$ records across the K/Pg interval and extending 4 myr into the Paleocene, that ensure continuous coverage by appropriate indicator species and accounting for vital effects (Chapter 6).

(3) Exploring the pattern of planktonic foraminifera assemblage turnover and test size distribution in the early Paleocene, which has implications for carbonate production and provides additional insight into pelagic ecosystem function (Chapter 7).

(4) Auxiliary to the Site 1262 studies, well preserved Paleocene planktonic foraminifera from Tanzania will be studied. This will provide the first account of the K/Pg transition in southern coastal Tanzania as well as a snapshot of early Paleocene low latitude paleotemperatures as derived from rare 'glassy' planktonic foraminifera (Chapter 8).

1.7. Account of project

This PhD project was devised by my supervisor Dr. Helen Coxall after she recognised a gap in the understanding of the K/Pg marine geochemical records, especially in relation to the interpretation of the oceanic carbon system response. I began the project in October 2007 having been awarded a NERC studentship. At the beginning of this project I went to the IODP core repository in Bremen to participate in the ODP leg 208 sampling meeting. Whilst there I met one of my other supervisors for this project Dr Daniella Schmidt (University of Bristol) and benthic foram expert Prof Ellen Thomas (Yale University). The three of us were there to sample ODP Leg 208 Site 1267, and obtain Cretaceous/Paleogene (K/Pg) boundary core samples. We each took every third sample to wash and analyse in our various laboratories. This was a great opportunity for me to observe the core that I have worked on first hand, as well as interacting with members of the leg 208 scientific shipboard team, including co-chief scientist Prof. Jim Zachos.

During the spring of 2008 I visited the other co-chief scientist Prof. Dick Kroon in Edinburgh to collect washed ODP Leg 208 Site 1262 samples that have been the source for the majority of my analysis. Under the guidance of Helen Coxall I was trained in Paleocene planktonic foraminifera taxonomy and biostratigraphy and produced a range chart and biozonation scheme for this site. With this knowledge I was able to conduct the initial paleoecological analysis on multispecies at differing size fractions that helped constrained paleoecologies and select key species to focus on for the rest of the

analysis. These initial findings were presented at a number of conferences that I attended in 2008 (Geochemistry Group Annual Research in Progress Meeting (GSPSE) in London, The Micropalaeontological Society AGM in London and The Paleontological Association annual meeting in Glasgow).

In the summer of 2008 I joined an expedition of the Tanzanian Drilling Project (TDP) led by Dr. Brian Huber (Smithsonian Institution) to Tanzania. The main aims of the expedition were to recover excellently preserved calcareous microfossil sediment cores for scientific research spanning the Paleocene/Eocene, K/Pg and Cretaceous. Whilst in Tanzania I gained valuable experience of field drilling, including sediment core lithologic characterisation, logging, and biostratigraphy. The excellent preservation of Tanzanian planktonic foraminifera reported elsewhere in the clay rich sediments would have provided an excellent opportunity to study the K/Pg and its recovery, using high quality 'glassy' foraminifera based proxy tools. However, hopes of recovering the K/Pg boundary were short lived when drilling was terminated prematurely in 2008 because of bands of sandy porous sediments that prevented drilling. Despite the lack of finding the K/Pg boundary we were able to recover lower Paleocene sediment, which had always remained elusive on previous drilling seasons. This will help fill in the gaps of previous paleotemperature estimates for the region (Pearson *et al.*, 2001; 2007).

Back in Cardiff I picked multispecies samples of planktonic foraminifera at a range of test sizes to explore the role of test size and ontogeny on Paleocene planktonic foraminifera stable isotope signals. During this time the mass spectrometer at Cardiff University stopped working temporarily so I diverted my attention away from stable isotope records and concentrated on changing planktonic foraminifera assemblages and differing sample size weights through the recovery interval.

During February and March of 2009 I participated in a research cruise with my second supervisor Prof. Paul Pearson (Cardiff University) off the coast of Tanzania. The purpose of this cruise was to collect site survey data for future offshore scientific drilling, as well as the shallow coring of Holocene sediments. Whilst on board the ship I learnt many additional skills such as digital seismic surveying and sediment core

retrieval and Plio-Pleistocene planktonic foraminifera biostratigraphy. I was also very fortunate to see live planktonic foraminifera collected from plankton nets. During the cruise Plio-Pleistocene sediment was collected and I used this opportunity to obtain modern planktonic foraminifera to form an analogue to the multispecies test size work I was conducting in the Paleocene. I was awarded an ECORD scholarship in the summer of 2009, to attend the USSP summer school 'Past Global Change Reconstruction & Modelling Techniques' in Urbino. This course allowed me to broaden my view of past global climates and find out about other proxies and modelling approaches used throughout the paleoclimate community. Later on that year I returned to Tanzania with the TDP, where again we tried to locate the K/Pg boundary after the promising results of the previous season attempt. The hope was that by casing the hole the problems of loose sediment could be overcome. This approached worked and 172 m was recovered. However, we were still unsuccessful in drilling the K/Pg boundary because a hiatus was discovered at the K/Pg boundary. After spending much of the beginning and middle of the year away from Cardiff the end of the year was concentrated on finishing isotope multispecies/size fraction time slices and assemblage counts. The isotopic time slice data provided constraints on the phylogeny and timing of the evolution of symbiosis within the planktonic foraminifera. I presented the results of this work at the 2009 PalAss conference in Birmingham.

At the beginning of 2010 I focused my attention on picking planktonic and benthic foraminifera to produce a down-hole Site 1262 stable isotope record spanning 4 myrs from the late Maastrichtian through to the end of the proposed carbon system recovery period. Initial results of this work, along with the new understanding of planktonic foraminiferal ecology in the Paleocene were presented at the 'Forams 2010' conference in Bonn, Germany. With all my data collected I embarked on the task of writing my thesis, separating each discrete study into its own chapter before bringing all the results together in the final synthesis chapter.

2. Materials and Methods

This chapter focuses on the material studied within this thesis, giving an account of the geological and oceanographic setting of each location. Details of sample selection, preparation and analysis are also included.

2.1. Material

This thesis focuses on deep-sea sediment material recovered at Ocean Drilling Program (ODP) Site 1262 because it represents the most continuous and well-dated marine Cretaceous/Paleogene (K/Pg) boundary sequence available. I have also generated multispecies foraminiferal isotope data on exceptionally well-preserved 'glassy' foraminifera from i) a Holocene box core recovered from offshore Tanzania (Chapter 4) and ii) an early Paleocene sample from a new borehole drilled onshore coastal Tanzania (Chapter 8).

2.1.1. Walvis Ridge, ODP Site 1262

Walvis Ridge in the south eastern Atlantic is one of the few locations where recovery of continuous Paleocene sediments is possible. Leg 208 drilled close to previously drilled sites from Deep Sea Drilling Project (DSDP) Leg 74 and although a great deal of useful information was gleaned from that Leg the available technology at the time meant that the cores were rotary drilled, which resulted in some intervals of poor recovery and drilling disturbance. This lead to the subsequent ODP cruise Leg 208 where advances in ODP coring technology, as well as using the new methods of drilling multiple holes at each site, allowed for 100% recovery of the stratigraphy at these sites using Advanced hydraulic Piston Coring (APC) (Shipboard Scientific Party, 2004).

Geologic setting and oceanography

Walvis ridge is a northeast-southwest trending aseismic ridge that divides the South Atlantic Ocean into two basins, the Angola Basin to the north and the Cape Basin to the south. Water depth in the area varies between 2500 on top of the ridge to 4770 m at the sea floor (Shipboard Scientific Party, 2004). Pelagic sediments vary in thickness from ~300 to ~600 m, but generally increase in thickness towards the continental margin (Moore *et al.*, 1984). These Sediments are mainly calcareous oozes and chalks (≥ 90 % calcium carbonate) due to the predominance of calcite saturated NADW in the Angola Basin. The non carbonate fraction is predominately clay with very little biogenic opal (Moore *et al.*, 1984 and Shipboard Scientific Party, 2004).

In the modern day ocean the south eastern Atlantic is dominated by two subsurface water masses, North Atlantic Deep Water (NADW) and Antarctic Bottom Water (AABW). NADW dominates in the Angola basin (North of Walvis Ridge) and AABW dominates in the Cape Basin (south of Walvis Ridge) and the two meet at Walvis Ridge. The surface flow of water (Benguela current) is generally in a northern direction over Walvis Ridge, which is situated in the eastern part of the subtropical gyre. General circulation models (GCMs) demonstrate the influences that a narrower Paleocene Atlantic Ocean might have had on circulation, with far saltier waters (Brass *et al.*, 1982; Bice and Marotzke, 2001) and lack of a large sub tropical gyre (Barron and Peterson, 1991) in the South Atlantic Ocean. According to these models surface flow within this area would have been dominated by eastern and equatorward patterns (Barron and Peterson, 1991). The formation of deep water is proposed to have been from southern high latitudes in the early Paleocene ocean (Miller *et al.*, 1987; Corfield and Cartlidge, 1992) after a reorganisation and proposed shift in the source of deep water from the sub tropical North Atlantic that was thought to have dominated during the Cretaceous (Corfield and Norris, 1996; Cramer *et al.*, 2009).

Site 1262 coring

ODP Site 1262 was one of six sites (Sites 1262-1267) drilled on Walvis Ridge during ODP Leg 208 (Figure 2.1). Sites 1262 and 1267 both recovered Maastrichtian through

to Danian sediments, with reconstructed paleodepths of upper abyssal (~3000m) over this interval (Shipboard Scientific Party, 2004). Of these two sites, Site 1262 has better microfossil preservation and lower bioturbation (Shipboard Scientific Party, 2004), which is the reason why this site was chosen for this study.

Site 1262 was located at the north-western edge of the drilling area (Latitude 27°11.15'S and Longitude 1°34.62'E) and represents the deepest site, at 4.75 km. This site is above the present day lysocline and calcium compensation depth (CCD) and appears to have maintained its position above the CCD throughout the Cenozoic (Shipboard Scientific Party, 2004). Three holes were drilled, each offset by ~20 m using the advanced piston corer (APC) system. The recovered sequences were spliced together to form a single stratigraphic section with a total length of 236 meters composite depth (mcd) using similarities in magnetic susceptibility (MS) and colour reflectance (L*) data (Shipboard Scientific Party, 2004). The K/Pg boundary was located at 216.75 mcd. The K/Pg is identified in core by a dramatic change in lithology from carbonate-rich, clay-bearing nannofossil ooze with foraminifers to medium brown clayey nannofossil ooze and ash-bearing clay as the MS and L* data demonstrate. These physical changes coincide with the abrupt change in plankton assemblages and sudden disappearance of Cretaceous taxa (Shipboard Scientific Party, 2004).

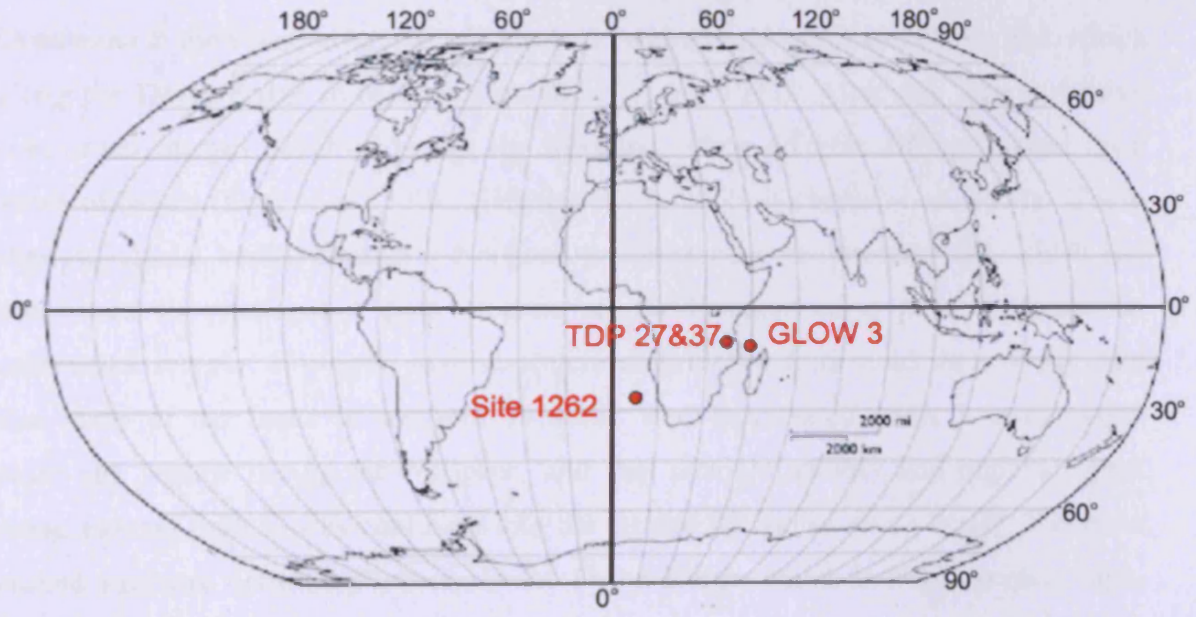

Figure 2.1 – World map showing locations of the samples used in this study.

Chronology

The age model for Site 1262 is based on the orbitally tuned chronology of Westerhold *et al.*, (2008). This age model was based on tuning of cyclical variations in X-ray fluorescence (XRF) measurements of iron and other elements to the long and short eccentricity cycles (405 kyr, 100 kyr, respectively), which have been found to be stable over geological time (Varadi *et al.*, 2003; Laskar *et al.*, 2004). This was calibrated relative to the detailed Leg 208 calcareous nannofossil biostratigraphy and magnetic reversal stratigraphy (Westerhold *et al.*, 2008), which gives three possible solutions for the K/Pg (Westerhold *et al.*, 2007). Westerhold *et al.*'s (2008) 'Option 2' age for the K/Pg of 65.68 Ma is this authors preferred solution, being most consistent with radiometric and argon dating, and the one that I have followed in this study. This calibration is 0.68 Ma older than the Cande and Kent (1995) K/Pg age estimate of 65.0 Ma and 0.18 Ma older than the Gradstein *et al.*, (2004) estimate of 65.5 Ma.

2.1.2. Offshore Tanzania, Paleogene GLObal Warming events (GLOW) Site 3

Geologic setting and oceanography

The area offshore Tanzania has a very tectonically active past. During the break-up of Gondwana in the Permian to Early Cretaceous Madagascar rifted away from East Africa along the Davie Ridge transform zone (Kent *et al.*, 1971). After this time a passive continental margin developed until the Miocene, when offshore rifting opened up a series of basins (Kent *et al.*, 1971; Nicholas *et al.*, 2006; Nicholas *et al.*, 2007). These shallow coastal basins contain a Neogene to Pleistocene sedimentary fill, which has been used to represent a post-Miocene re-establishment of a passive Tanzanian continental margin. However, diverse structural evidence from field surveys suggests that many of the faults in southern Tanzania were reactivated under a compressive strike-slip regime during the Neogene, and that tectonic activity and regional uplift along moving fault blocks continues into the Recent (Nicholas *et al.*, 2007). The main seabed structure offshore Tanzania is the Davie Ridge, which is a topographic high, dominated by a NW-SE trending normal fault which interrupts the continental slope

east of Tanzania. The Tanzania channel is a submarine channel at the northern end of the Davie ridge that can be traced to 800 km offshore (Bourget *et al.*, 2008).

Today, the northern part of the Indian Ocean is heavily influenced by the monsoon, which gives rise to changes in wind and current direction during different seasons. The southern Indian Ocean, from Africa to Australia, lies within a large anticyclonic 'supergyre' (Figure 2.2) and is characterized by the westward flowing South Equatorial Current (SEC). It splits at the east coast of Madagascar near 17°S into northward and southward branches, the Northeast and Southeast Madagascar Currents (NEMC and SEMC). The NEMC transports a supply of water for the Mozambique Channel flow (MCF) and the East African Coastal Current (EACC) (Schott *et al.*, 2009; Ali and Huber 2010).

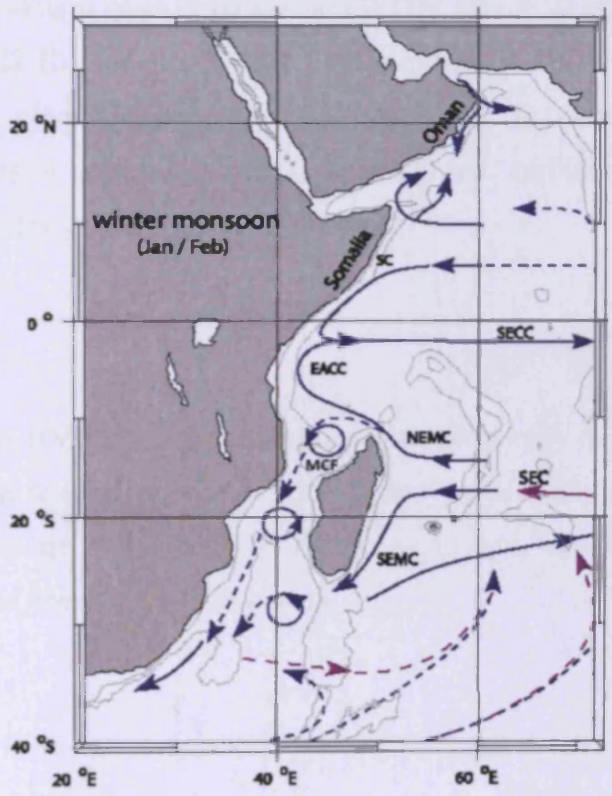

Figure 2.2 - Schematic representation of identified current branches during the winter (southwest) monsoon. Current branches indicated are the South Equatorial Current (SEC), South Equatorial Counter Current (SECC), Northeast and Southeast Madagascar Current (NEMC and SEMC), East African Coastal Current (EACC), Mozambique Channel flow (MCF) and Somali Current (SC). Depth contours shown are for 1000 m and 3000 m (grey). Adapted from Schott et al., (2009).

GLOW Site 3

GLOW 3 (Latitude 8°51.5538'S Longitude 41°26.4102'E; North of the Tanzania Channel) was recovered by the RV *Pelagica* whilst on the Paleogene Global warming events (GLOW) Cruise in the South West Indian Ocean off the coast of Tanzania between the 10th February and the 9th March 2009 (Figure 2.1) (Kroon *et al.*, unpublished). The purpose of this cruise was to collect site survey data for future offshore scientific drilling, as well as the shallow coring of Holocene sediments.

The GLOW Site 3 Box Core was taken using a Royal Netherlands Institute for Sea Research (NIOZ) designed box corer with a barrel diameter of 30 cm and height of 55 cm. Water depth at the site was 3006 m. 100 cc of sediment from the top 0-1 cm of the box core was sampled. A full profiling CTD (Conductivity, Temperature, and Depth measurer) Seabird system, was deployed at GLOW Site 2, (Latitude 10°65.243'S and Longitude 41°77.227'E), which is within 74 km of Site 3. The CTD cast provided data on water column physical and chemical properties. In addition to the standard measurements, oxygen concentrations, florescence and turbidity measurements were also taken. Water depth at that site was 2219 m.

Chronology

Whilst on board the RV *Pelagica* preliminary biostratigraphy of core top material was carried out using the scheme of Pearson (1995) and Wade *et al.* (2011), which dated the top of GLOW 3 to be Pleistocene to Holocene in age, due to the presence of *T. truncatulinoides* and absence of *T. tosaensis*.

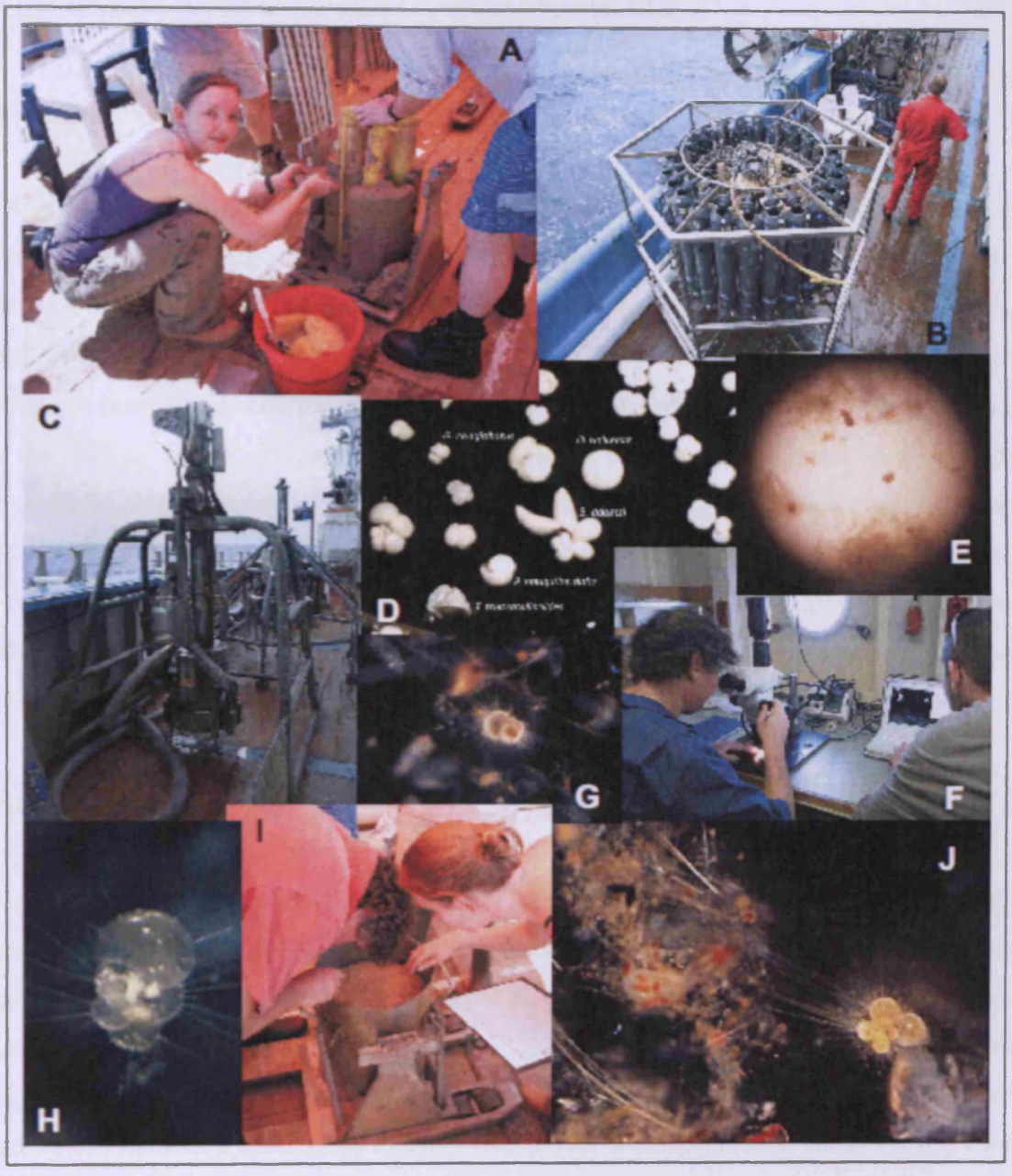

Figure 2.3 – Photographs taken during the GLOW cruise. A – Sampling the top 1 cm of sediment from box core, B – Profiling CTD (Conductivity, Temperature, and Depth measurer), C – Box corer before deployment, D – Example of foraminifera found after washing box core sediment, E – View down a light microscope at live foraminifera from plankton net, F – Looking at live planktonic foraminifera, G – *Globigerinoides trilobus* from plankton net, H & J – *Globigerinella siphonifera* from plankton net, I – Describing box core.

2.1.3. Onshore Tanzania Drilling Project (TDP) Site 27 & 37

Geologic setting

The geologic setting for these sites is similar to that of the offshore sites (Section 2.1.2). The east African margin was affected by a marine transgression, which accompanied seafloor spreading in the lower Cretaceous (Salman and Abdula, 1995; Jiménez Berrocoso *et al.*, 2010). During the Paleocene to Miocene period of tectonic stability, when the passive continental margin developed, a sequence of marine sediments know as the 'Kilwa group' (Figure 2.4) was laid down on the mid or outer shelf to upper continental slope (Nicholas *et al.*, 2006). A number of topographic highs (eg. Kimamba hill) can be found on the otherwise low-lying coastal plain that have been interpreted as a fault bounded tectonic unit and the surface expression of a deeper seated 'flower structure' that has locally 'popped-up' during the Miocene or younger (Nicholas *et al.*, 2007).

Site 27 and 37

Tanzanian Drilling Project (TDP) was first established in 2002 after initial reconnaissance work from surface exposures revealed exceptionally well preserved species (Pearson *et al.*, 2001; Nicholas *et al.*, 2006). TDP Site 27 was cited on top of Kimamba Hill (UTM 37L 574233, 8892237; 8° 55.448'S, 39 20.086' E, Figure 2.1 and Figure 2.4), 60 km from Kilwa Masoko. The Site was accessed via a track to a laterite quarry off the main Hotelitatu –Lindi road a few hundred metres north of the Ukuli River Bridge. TDP Site 27 spudded-in approximately 100 m south east of the quarry immediately off the track to the west. The objective was to drill and recover a sedimentary sequence through the K/Pg boundary. This was the third attempt at drilling this interval by TDP. Previous attempts (TDP Site 10 and TDP Site 19, Nicholas *et al.*, 2006) did not penetrate beyond the late Paleocene (planktonic Biozone P4). Kimamba Hill was selected as a candidate K/Pg site because reconnaissance work had identified upper Maastrichtian clays in the Ukuli River bank on the south-western flank of the hill and the hill itself has been described as Paleocene from the outcropping limestones

(Kent *et al.*, 1971; Nicholas *et al.*, 2006). Drilling at this site, however, faced various technical difficulties. Recovery was poor from the outset and no continuous clay sections were recovered. Drilling was terminated after 18.40 m of coring due to loose sands, which caused the core barrel to lock-up. There was not enough time in the drilling schedule to attempt another hole and TDP Site 27 was abandoned.

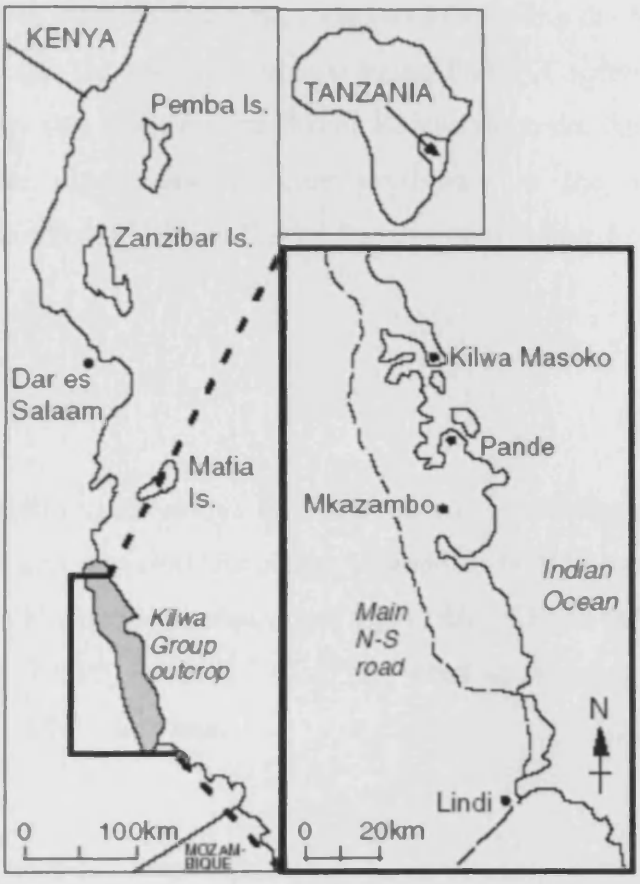

Figure 2.4 – Location of the Kilwa group in Tanzania adapted form Nicolas *et al.* (2006)

Encouraged by the indications of mid-Paleocene sediments in preliminary biostratigraphy of TDP Site 27, the TDP returned to Kimamba Hill in 2009 and drilled TDP Site 37 in another attempt at recovering a K/Pg sequence. TDP Site 37 was cited at the southern end of the laterite quarry and approximately 200 m north of TDP Site 27(UTM 37L 574233, 8892237; S 8° 55.248', 39° 19.938'E, Figure 2.1 and Figure 2.4). Coring proceeded relatively smoothly penetrating to a depth of 172.10 m before drilling was terminated.

A mobile rig (Longyear 38) capable of wireline coring to about 150 m, supplied and run by the Tanzanian State Mining Corporation (STAMICO), was used. The drill rig used NQ (48 mm) core barrels in 2008 drilling. Each NQ barrel had a liner which was split in half to allow the sediment core to be retrieved without disturbance. To improve on the drilling problems of 2008, drilling in 2009 had the addition of HQ (64 mm) core barrels, which were used for casing to stabilise the hole. Water was used to keep the diamond carbite bit cool. Cores were photographed and describe (using the Munsell colour chart system) with lithologic log produced on-site using PSICAT software, before samples for dating and laboratory studies were taken. Before shipment back to the UK, cores were stored in the air-conditioned core repository at the Tanzania Petroleum Development Corporation (TPDC), Dar-es-Salaam after being transported back from site.

Chronology

Planktonic foraminifera (this study) and nannofossil biostratigraphy (Lees, personal communication) on site revealed the oldest biozone to be P3a based on the Berggren and Pearson, (2005) biozonation scheme and age of 60 – 61 Ma based on the time scale of Cande and Kent, (1995) or 61.2 - 62.2 Ma when approximately converted to the Westerhold *et al.*, (2008) time scale.

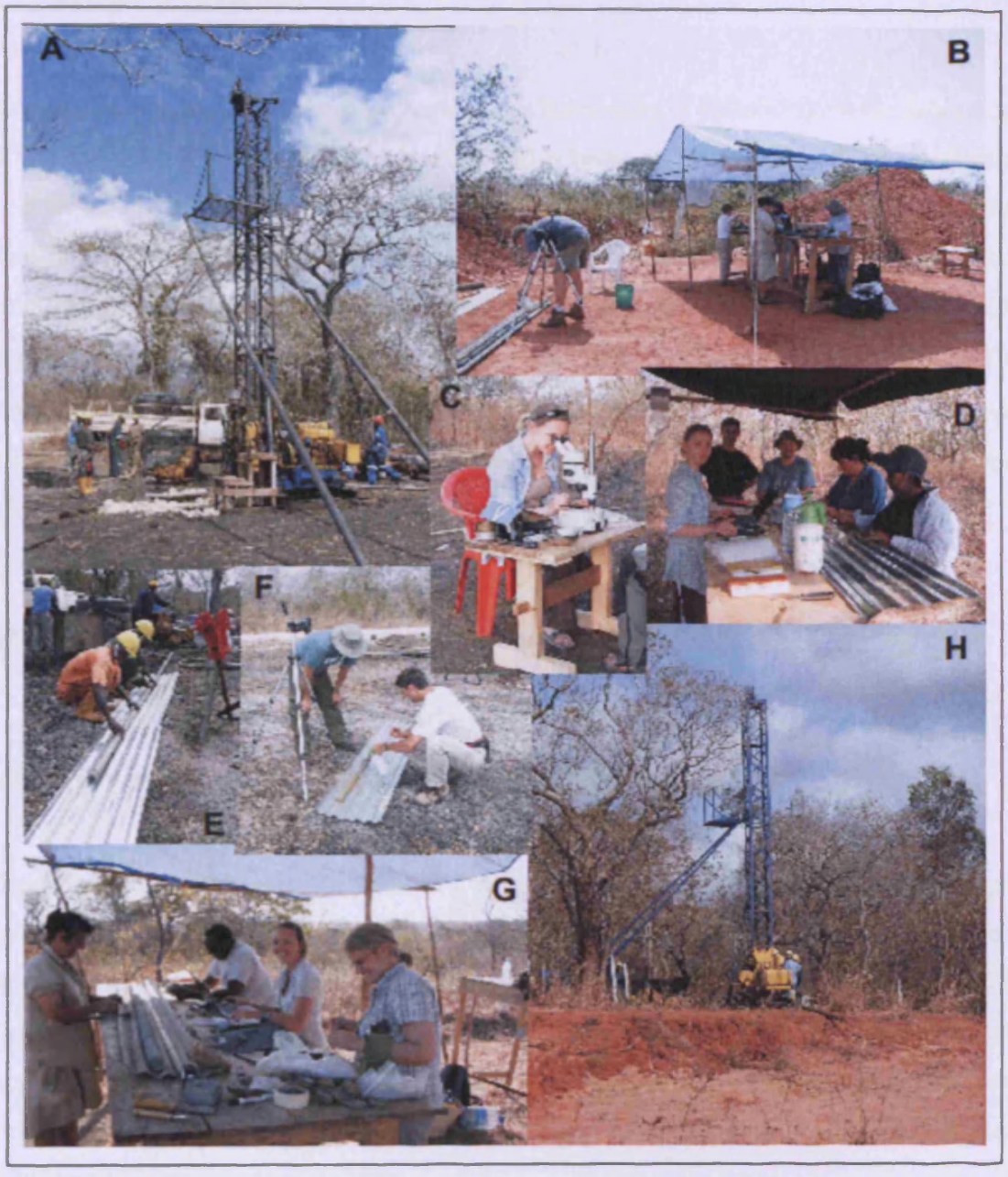

Figure 2.5 – Photographs taken during TDP drilling September 2008 and 2009. A – Drilling rig on location TDP Site 27, B – Logging and sampling, C – On site biostratigraphy, D – Logging and sampling, E – Core as it came out of core barrel, F – Washing and photographing core, G – Logging and sampling, H – Drilling rig on location TDP Site 37.

2.2. Sample preparation

Samples from Site 1262 were processed at the University of Edinburgh in the laboratory of Professor Dick Kroon. Sample spacing varies between 36 and 144 cm (equivalent to ~ 45.68 and 182.74 kyrs, respectively). The TDP and GLOW samples were prepared at Cardiff University. Samples were first dried for ~48 hours in a 40 °C oven before weighing to determine whole sample dry mass. They were then washed through a 38 μm sieve with de-ionised water, to separate the foraminifera-rich coarse fraction. The remaining fine (<38 μm) fraction was collected in a plastic bag. This fine sediment was left to settle before the water was siphoned off. Both coarse and fine fractions were dried in an oven at 40 °C and then weighed.

2.3. Analysis

2.3.1. Taxonomy, biostratigraphy and assemblage counts

The Site 1262 planktonic foraminifera assemblages were examined in detail using a light microscope to record species stratigraphic ranges. This was used to produce a biozonation, following the zonation scheme of Berggren and Pearson (2005). Taxonomy followed Olsson *et al.* (1999) for the Paleocene and Bolli *et al.* (1985), with guidance from Brian Huber for the upper Cretaceous. Identification for recent/modern foraminifera recovered during the GLOW cruise followed Kennett and Srinavasan, (1983) and Hemleben *et al.* (1989).

Planktonic foraminifera species abundance counts were made on 49 samples with a resolution of 72 cm (~91.37 kyrs). The >106 μm fraction and 38 – 106 μm fraction were analysed separately. In the >106 μm fraction, specimens were identified to species level, whilst in the 38 – 106 μm fraction, specimens were identified to genus. The samples were examined under a binocular light microscope on a picking tray. The foraminifera were identified and their number recorded out of a specimen total of 300. It

has become standard in micropalaeontology to count 300 specimens since this should allow 95 % of species that are present at >1 % abundance to be identified (Dennison and Hay, 1967; Buzas, 1990; Al-Sabouni *et al.*, 2007).

2.3.2. Scanning Electron Microscope (SEM) analysis

Species used for isotopic analysis (see below) were examined and imaged using a Veeco FEI (Philips) XL30 FEG (Field Emission Gun) Environmental Scanning Electron Microscope (SEM), fitted with a secondary electron detector (SE) to fully document morphology. Specimens were gold coated and imaged under high vacuum mode using SE, this has a resolution of 2 nm at 30 KV and magnification of x10 to x 500,000. Scales are indicated on images.

2.3.3. Sample selection for stable isotope analysis

Site 1262 – Paleoecological analysis

Six samples spanning the early Paleocene (1262C-10H-3, 187.26 [61.16 Ma], 1262B-20H-3, 193.27 [61. 90 Ma], 1262C-11H-3, 198.09 [62.47 Ma], 1262C-11H-4, 199.29 [62.65 Ma], 1262C-12H-4, 207.42 [63.99 Ma] and 1262B-22H-3, 214.03 [65.1 Ma]) were initially chosen for multispecies isotopic analysis. The goal was to document isotopic paleoecology in dominant species using isotope variability in different test size fractions. These sample time slices cover the recovery period after the K/Pg to assess changes in paleoecology through time and at differing size fractions (Table 2.1) as shown by the preliminary range chart analysis (Chapter 3). The total number of species analysed was 13. This included species from the genus *Morozovella*, which is interpreted to have been photosymbiotic (D'Hondt and Zachos, 1993; Pearson et al., 1993; D'Hondt et al., 1994; Norris, 1996; Coxall et al., 2006; Wade et al., 2008). *Praemurica*, the supposed ancestor of *Morozovella* were also included, as were several species believed to be asymbiotic belonging to the genera *Subbotina* and *Parasubbotina* (Douglas and Savin, 1978; Boersma and Shackleton, 1979; Shackleton et al., 1985;

Pearson et al., 1993; D'Hondt *et al.*, 1994). *Eoglobigerina eobulloides* and *Woodringina hornerstowensis* were also included as they have been suggested to have been symbiotic (D'Hondt and Zachos, 1993). Building on these original six time slices additional multispecies stable isotope analysis was also carried out on a 3 further time slices (63.57 Ma, 63. 54 Ma and 63.50 Ma) between 63.99 Ma and 62.65 Ma, as this appeared to represent a time of significant ecological change.

Size Fraction (μm)	Mean Size of size fraction (μm)	Minimum number of specimens used
>300	300	2
>250	250	3
250 – 300	275	3
212 - 250	231	4
180 – 212	196	9
150 – 180	165	17
125 – 150	137.5	27
106 – 125	114.5	38
80 – 106	93	80
63 – 80	71.5	100

Table 2.1 – Size fractions utilised for monospecific samples and the minimum number of specimens required by the mass spectrometer to achieve the necessary sample mass, derived from test runs by Cardiff Universities' stable isotope facility.

From each of the above samples every species that occurred in large enough quantities to be analysed were chosen and picked. The number of specimens required for analysis depended on the size fraction, but minimum numbers required to achieve the necessary sample mass are given next to each size fraction (Table 2.1). At least 2 individuals were always analysed to reduce individual variation. Care was taken to choose the best preserved and most representative of the differing species selected. Specimens were not cleaned prior to analysis due to their delicate nature and visible lack of organics and sediment infill.

Site 1262 – Down hole analysis

Results of the multispecies isotope analysis were used to infer relative isotopic depth ecologies. This information was subsequently used to select appropriate water column tracer species for the down hole paleoceanographic analysis. Cross plots of $\delta^{18}O$ against $\delta^{13}C$ were constructed, and using the method described by Spero and Williams, (1989) and Pearson *et al.*, (1993) a relative depth habitat could be assigned. This facilitated the selection of a thermocline dweller – ***Subbotina triloculinoides***, an intermediate dweller – ***Praemurica inconstans*** and surface dwellers – ***Morozovella praeangulata*** through to ***M. angulata*** for down hole isotopic comparison. The benthic species ***Nuttallides truempyi*** was also picked to provide a deep sea comparison, as this species is found throughout the studied interval and is believed to be an epifaunal species living in isotopic equilibrium with seafloor waters (Shackleton *et al.*, 1984). Nearer to the K/Pg boundary some of these planktonic species are not present, having not evolved yet and ***Subbotina trivalis*** and ***Praemurica taurica*** were used instead. Where these evolutionary species changes occur overlapping records have been produced so any changing ecology related to species changes could be taken into account. ***Guembelitria cretacea*** and ***Hedbergella holmdelensis*** were picked as the only species to cross the K/Pg boundary. While in the Late Cretaceous ***Globotruncana falsostuarti*** and ***Racemiguembelina fructicosa*** were chosen as intermediate/mixed layer dwellers (D'Hondt and Zachos, 1998; Houston and Huber, 1998; Houston *et al.*, 1999).

Initially a resolution of 72 cm (~91.37 kyr) was analysed for planktonic foraminifera and 144 cm (~182.74 kyr) for benthic foraminifera. Specimens were picked from the 180-212 μm, 212-250 μm or 250-300 μm size fraction depending on species natural size ranges. Nearer to the boundary benthic species were picked at the same resolution as the planktonic foraminifera. The size fraction, from which the planktonic foraminifera were picked, had to be reduced, as the average size of the foraminifera decreased nearer to the boundary. Above and below the boundary the resolution was increased to 36 cm (~45.68 kyr). Following D'Hondt and Arthur (2002) a correction factor for *N. truempyi* was not applied as this species is thought to be close to equilibrium (Shackleton *et al.*, 1984).

GLOW 3

Monospecific samples were picked from 13 size fractions in the Glow Site 3 Box core sample (Table 2.2) to provide a modern analogue for the Paleocene data. Twelve species from the modern core top assemblage were analysed; *Globigerina bulloides*, *Globigerinoides ruber*, *Globigerinita glutinata*, *Globorotaloides hexagonus* and *Globoturborotalita rubescens* (pink) as these were all relatively small species so could be comparable to the Paleocene small species. *Globigerinoides sacculifer*, *Globigerinella siphonifera* and *Orbulina universa* were selected as known photosymbiotic species and *Globorotalia tumida*, *Globorotalia ungulata*, *Truncorotalia truncatulinoides* and *Globorotalia scitula* were chosen as known deeper dwelling species (Hemleben *et al.*, 1989). For the larger samples in the modern to reduce variability, 3 or more specimens were crushed and part of the mixture was analysed.

Size Fraction (μm)	Mean Size of size fraction (μm)	Minimum number of specimens used
>710	710	1
600 - 710	655	1
500 - 600	550	1
425 - 500	462.5	1
400 - 425	412.5	2
355 - 400	377.5	2
300 - 355	327.5	2
250 – 300	275	3
180 – 250	231	4
150 – 180	196	9
125 – 150	165	17
106 – 125	137.5	27
80 – 106	114.5	38

Table 2.2 – Size fractions utilised for monospecific samples and the minimum number of specimens required, derived from test runs by Cardiff Universities' stable isotope facility.

TDP 27

Despite drilling problems and poor core recovery some thin intervals of Paleocene hemipelagic clays containing 'glassy' foraminifera were collected. The most diverse and well preserved of these samples (sample TDP27/7/1, 10-20 cm) was used for isotopic analysis. Though the planktonic foraminifera were exceptionally well preserved, some infill was present, so the foraminifera were gently crushed and the 'glassy' test removed for analysis. Due to this process only species and size fractions with sufficient quantities of calcite could be used for analysis. These were *Morozovella angulata* and *Praemurica uncinata* (surface mixed layer dwellers) and *Subbotina triangularis* (thermocline dweller). Size fractions utilised were 212-250 μm and 300-355 μm, where test, infill and a mixture of the two were also analysed as a control.

2.3.4. Carbon and Oxygen isotope analysis using mass spectrometry

A mass spectrometer separates a charged molecular mixture according to mass, using the motions of the molecules in a magnetic or electric field. Absolute values for minor isotopes cannot be determined accurately, however when compared to a known standard a sample can be measured precisely. Thus isotope ratios of a sample are always measured against a known standard and this difference is reported as a delta (δ) value that is defined as :-

Equation 2.1 $$\delta \text{ in } ‰ = \left[\frac{R \text{ sample} - R \text{ standard}}{R \text{ standard}} \right] x\, 1000$$

Where R is the isotopic ratio with the most abundant isotope in the denominator (i.e. $^{13}C/^{12}C$ or $^{18}O/^{16}O$).

The carbon dioxide (CO_2) gas produced, when phosphoric acid is added, was analysed to determine the relative abundances of ^{18}O to ^{16}O and ^{13}C to ^{12}C. The mass spectrometer used to carry out isotopic analyses was a ThermoFinnigan MAT252 with automated KIEL III carbonate preparation unit at Cardiff University stable isotope

facility. Stable isotope results were calibrated to the PDB scale by international standard NBS19 and analytical precision was better than 0.05 ‰ for $\delta^{18}O$ and 0.03 ‰ for $\delta^{13}C$.

2.3.5. Sample size fraction weights

Separated sieved size fractions (Table 2.3) were weighed in 94 samples with a resolution of 36 cm (~45.68 kyr) to (i) establish the individual contribution of species size classes of planktonic foraminifera (which dominate the coarse fraction) and (ii) document how this changed over time, to the overall coarse weight of the sample, as full sample weights were unavailable. Samples were weighed using an A & D semi-microbalance (standard deviation of 0.1 mg). This was repeated three times and the mean value taken, in all cases the standard error on the mean weight of the measuring cup plus contents was <0.0005 %. The cup was weighed between each sample to check for drift in the balance and the balance was re-zeroed if necessary.

Size Fraction
>300 μm
250 – 300 μm
180 – 250 μm
150 – 180 μm
125 – 150 μm
106 – 125 μm
80 – 106 μm
63 – 80 μm
38 – 63 μm

Table 2.3 – Size fractions utilised for weights.

2.3.6. Thin sections TDP Site 27 and 37

Sections of limestone were chosen throughout the two cores drilled at TDP 27 and 37 to give an even coverage of the distance drilled. Thin sections were processed back in Cardiff Universities 'Rock Preparation Facility' using 600 grit silicon carbide for lapping on a Logitech LP50. The resultant rock chips were mounted onto pre-ground glass slides using araldite 20/20 epoxy resin before being re-lapped down to 40 μm. The thin sections were then examined using a Lecia DMRX microscope mounted with a Leica DFC490 camera and pictures were taken using the IM1000 software. Identification of planktonic foraminifera within thin sections followed the same protocol as sediment samples (see section 2.3.1). Identification of other fauna within the thin sections followed descriptions and images from Flügel (2004).

3. Taxonomy and Biostratigraphy

This chapter gives an introduction to the taxonomy used throughout this thesis with descriptions and figures of the planktonic foraminifera used for isotope analysis. This chapter also contains the full stratigraphic ranges of planktonic foraminifera found at Site 1262 and along with refined biostratigraphy using the new astronomically tuned age calibrations for this site from Westerhold et al. (2008) may represent improvements in the stratigraphic and chronological age estimates of early Paleocene biozones.

3.1. Introduction

The extinction of many planktonic foraminifera at the K/Pg was followed by a rapid burst of evolution in the early Paleocene, including fundamental changes in test wall structure and consequently biology. The resulting wall structure underpins the fundamental classification of planktonic foraminifera (Olsson *et al.*, 1999). The first tier of classification is based on pore size, which separates species into macroperforate (pore diameter 2-7μm) and microperforate (pore diameter <1μm) forms (Olsson *et al.*, 1999). Several of the K/Pg survivors were microperforate species (Figure 3.1) i.e. *Guembelitria cretacea*, *Zeauvigerina waiparaensis* and *Rectoguembelina cretacea*. Of these *Guembelitria cretacea* has been proposed as the ancestor to the Cenozoic microperforates (D'Hondt, 1991; Liu and Olsson, 1992), although recent molecular studies suggest microperforates may have had multiple independent origin from benthic species (Darling, 2009). The only macroperforate (Figure 3.2) species to survive were from the genus *Hedbergella*. Radical morphological developments occurred rapidly in this genus resulting in the appearance of genus level structural modifications that determine the next important classification tier; spinose (having spines) and non-spinose (absent of spines). The spinose genera *Eoglobigerina*, *Parasubbotina* and *Subbotina* are believed to have all descended from *H. monmouthensis*. The non-spinose species can be further subdivided into smooth walled and cancellate walled varieties. The smooth walled genus *Globanomalina* is thought to have descended from *H. holmdelensis*. Other smooth walled genera may possess small surface pustules. When there is heavy

development of these pustules it can lead to the development of pointed structures known as 'muricate' (Blow, 1979). Muricate wall textures are found in the *Acarinina*, *Igorina* and *Morozovella* genera. This study supports the view (like Bolli, 1957a; Blow, 1979; Olsson *et al.*, 1999) that *Acarinina*, *Igorina* and *Morozovella* descended from the *Praemurica* genus, which in turn descended from *H. monmouthensis*. The cancellate wall structure is thought to have developed from the growth of pustules into ridges. This type of wall structure was common in the early Paleocene with species of *Eoglobigerina*, *Parasubbotina*, *Subbotina*, *Acarinina*, *Igorina* and *Praemurica* all possessing cancellate walls (Olsson *et al.*, 1999). Beyond wall structure, taxonomy is then heavily based on gross test morphological characteristics such as aperture position, number of chambers in final whorl, coiling direction and chamber shape.

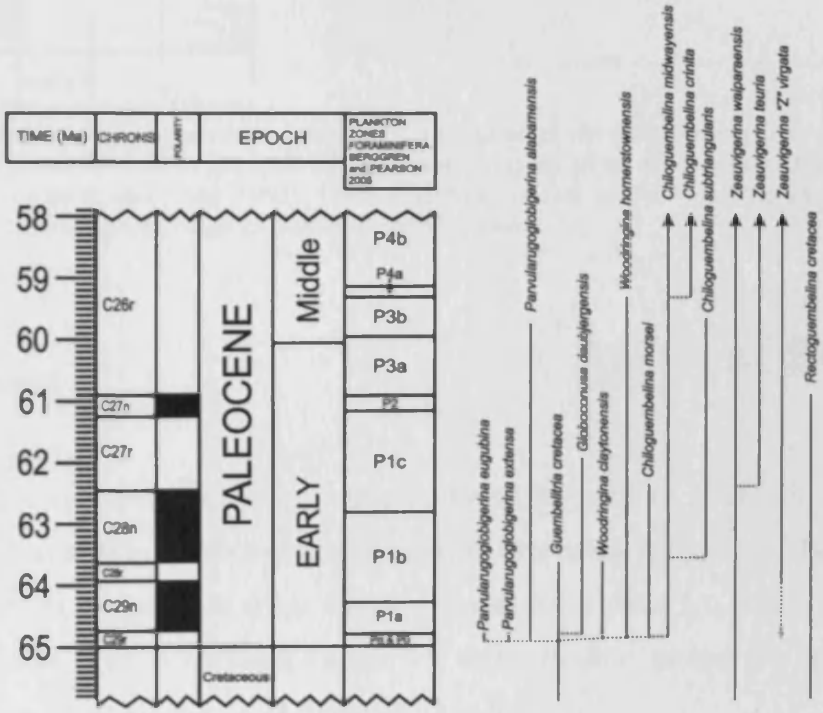

Figure 3.1 – Microperforate Paleocene planktonic foraminifera diversification and evolution, adapted from Olsson *et al.*, (1999). Age (Ma) based on the Geomagnetic Polarity Time Scale (GPTS) of Cande and Kent (1995), planktonic foraminifera biozons after Berggren and Pearson (2005).

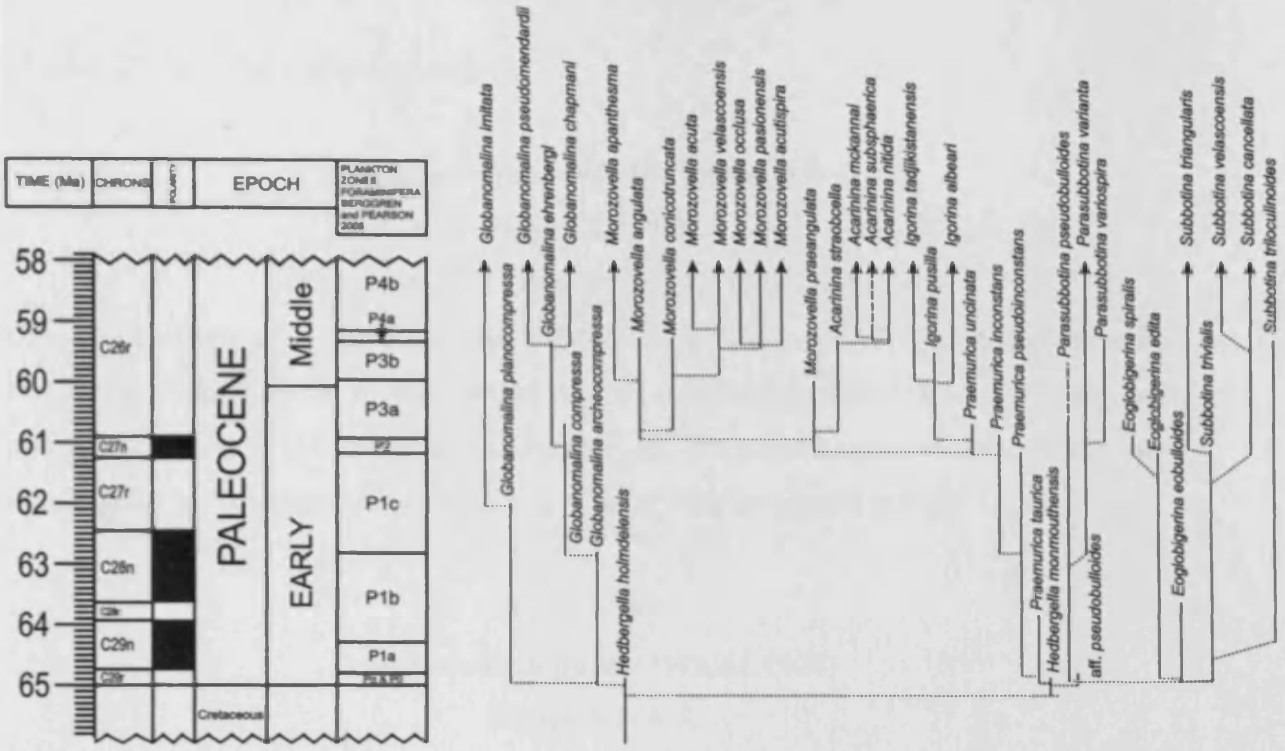

Figure 3.2 – Macroperforate Paleocene planktonic foraminifera diversification and evolution, adapted from Olsson *et al.*, (1999) and Aze *et al.* (2011). Age (Ma) based on the Geomagnetic Polarity Time Scale (GPTS) of Cande and Kent (1995), planktonic foraminifera biozons after Berggren and Pearson (2005). Dashed line represents range extension at high latitudes.

3.2. Taxonomy

The taxonomic schemes followed are discussed in section 2.3.1. However, when identifying foraminifera for isotope analysis strict taxonomy is required. For this reason detailed descriptions (adapted from Kennett J. and Srinavasan M., 1983; Hemleben *et al.*, 1989; Olsson *et al.*, 1999) and images for these specific species are included based on observations made on the study material included here.

3.2.1. Paleocene

Macroperforate (Non-spinose species)

***Morozovella praeangulata* (Blow, 1979)**

Figure 3.3; 7-9.

Olsson *et al.*, (1999), Plate 53: Figures 1-13

Diagnostic characters – Planoconvex, moderately lobulate test. Five to 6 chambers in last whorl. Chambers are more rounded than the angular chambers of *M. angulata*, and no keel is present. The umbilicus is narrow and deep with aperture interiomarginal, umbilical to extraumbilical slit stretching to nearly the peripheral margin.

***Morozovella angulata* (White, 1928)**

Figure 3.3; 4-6.

Tanzania Figure 3.8; 4-6, 11.

Olsson *et al.*, (1999), Plate 48: Figures 1-16

Diagnostic characters – Angulo-conical test, flat spiral side and convex umbilical side. Four to 6 angular chambers in the final whorl, increasing in size, with the final chamber often reasonably large (=/> than ½ the width). Keel present marked by an imperforate band along the peripheral margin. Umbilicus, deep due to elevated chamber sides. Aperture low, interiomarginal, umbilical to extraumbilical, with weakly developed lip. In edge view final chamber appears raised slightly from the keel line.

***Morozovella apanthesma* (Loeblich and Tappan, 1957)**

Figure 3.3; 1-3.

Olsson *et al.*, (1999), Plate 49: Figures 1-15

Diagnostic characters – Planoconvex, umbilicoconvex test, with 4 to 6 chambers in the final whorl. Chambers are more rounded than the angular chambers of *M. angulata*, as well as the keel being less distinct. Aperture interiomarginal, umbilical to extraumbilical, with continuous lip.

***Morozovella occlusa* (Loeblich and Tappan, 1957)**

Figure 3.3; 10-11.

Olsson *et al.*, (1999), Plate 51: Figures 1-15

Diagnostic characters – Planoconvex to biconvex circular test, much flatter than *M. praeangulata*, *M. angulata* and *M. apanthesma*. Four to 8 chambers in final whorl, keel very prominent, distinctly muricocarinate. Aperture interiomarginal, umbilical to extraumbilical arch.

***Praemurica taurica* (Morozova, 1961)**

Figure 3.4; 10-12.

Olsson *et al.*, (1999), Plate 61: Figures 1-15

Diagnostic characters – Very low trochospiral test with 5 – 7 sub-globular chambers in final whorl, increasing moderately in size. The last one or two chambers are often shifted towards umbilicus and may take on a more square shape. Umbilical to extraumbilical arched aperture, boarded by narrow lip. Umbilicus deep, broad and may contain relic aperture lips.

***Praemurica pseudoinconstans* (Blow, 1979)**

Figure 3.4; 7-9.

Olsson *et al.*, (1999), Plate 60: Figures 1-13

Diagnostic characters – Low trochospiral test with 5 – 6 sub-globular chambers in final whorl, increasing moderately in size to start and then increasing more rapidly. Aperture a high rounded arch boarded by a lip which broadens towards the umbilicus. Relic aperture lips may be present in umbilicus. More common than the superficially similar *P. psuedobulloides* (Figure 3.5; 1-3), which can be distinguished by the presence of a narrow lip bordering the aperture which does not broaden towards the umbilicus but stops before it reaches the umbilicus. The umbilicus of *P. pseudobullodies* is narrower and deeper than *Pr. pseudoinconstans*.

***Praemurica inconstans* (Subbotina, 1953)**

Figure 3.4; 4-6.

Olsson *et al.*, (1999), Plate 59: Figures 1-16

Diagnostic characters – Broadly oval to elongate test. Five to 7 sub-globular chambers, increasing moderately in size. Early chambers often tightly coiled but loosening in later chambers. Aperture interiomarginal, umbilical to extraumbilical slit with lipped rim often extending into umbilicus. Sutures radial and straight or only slightly curved.

***Praemurica uncinata* (Bolli, 1957)**

Figure 3.4; 1-3.

Tanzania Figure 3.8; 1-3, 10.

Olsson *et al.*, (1999), Plate 62: Figures 1-16

Diagnostic characters – Broadly oval to elongate test. Five to 8 sub-angular chambers in final whorl, increasing moderately in size but often very loosely coiled. Aperture interiomarginal, umbilical to extraumbilical arch extending to peripheral margin. Sutures radial and strongly re-curved. Muricae are often present on wall surface particularly around peripheral margin.

Macroperforate (Spinose species)

***Parasubbotina varianta* (Subbotina, 1953)**

Figure 3.5; 4-6.

Olsson *et al.*, (1999), Plate 22: Figures 6-16

Diagnostic characters – Four globular chambers in final whorl, increasing rapidly in size. Test a low trochospiral with a high arch umbilical to extraumbilical aperture boarded by a broad lip. Umbilicus is deep, rounded and small but open to surrounding chambers.

***Subbotina triloculinoides* (Plummer, 1926)**

Figure 3.5; 7-9.

Olsson *et al.*, (1999), Plate 27: Figures 1-13

Diagnostic characters – Three to $3^1/_2$ very globular chambers in the final whorl but only specimens with 3 chambers and not $3^1/_2$ chamber in final whorl were used. The final chamber encompasses the full width of the specimen. Umbilicus is narrow and deep and often covered by apertural lip. The aperture is umbilical with some asymmetry in the extraumbilical directions. The species is coarsely cancellate but is asymmetrical when compared to the smaller, often 4 chambered, *S. cancellata* species which is symmetrically cancellate.

***Subbotina trivalis* (Subbotina, 1953)**

Figure 3.5; 11-12.

Olsson *et al.*, (1999), Plate 28: Figures 1-13

Diagnostic characters – Three $^1/_2$ to four very globular chambers in final whorl, with compact chamber arrangement. The penultimate chamber in final whorl is equal in size or larger than the ultimate chamber. Umbilical aperture with lip.

***Subbotina triangularis* (White, 1928)**

Figure 3.8; 7-9, 12. (Tanzania only)

Olsson *et al.*, (1999), Plate 26: Figures 1-13

Diagnostic characters – Three $^1/_2$ globular chambers in final whorl, shape of test triangular in umbilical view. The penultimate chamber in final whorl is equal in size or larger than the ultimate chamber. Ultimate chamber can have squashed appearance to give an elongated oval. Aperture umbilical to extraumbilican borded by thin lip. Umbilical aperture with lip.

***Eoglobigerina eobulloides* (Morozova, 1959)**

Figure 3.5; 13-14.

Olsson *et al.*, (1999), Plate 19: Figures 1-15

Diagnostic characters – Elevated trochospire test with 4 to $4^1/_2$ very globular chambers in final whorl, increasing moderately in size. An umbilical to slightly extraumbilical rounded aperture, boarded by narrow lip. Umbilicus small but open to previous chambers. Overall size generally <250μm.

Microperforate

***Woodringina hornerstownensis* (Olsson, 1960)**

Figure 3.5; 10.

Olsson *et al.*, (1999), Plate 68: Figures 7-14

Diagnostic characters – Initial end of test consists of 3 chambers in the whorl, the rest of the test is biserial and twisted. The overall test shape tapers with straight sutures and often 6 or more pairs of globular chambers.

3.2.2. Modern

Macroperforate (Non-spinose species)

***Globorotalia tumida* (encrusted) (Brady, 1877)**

Figure 3.6; 5-6.

Kennett and Srinavasan, (1983), Plate 38; 1-3

Hemleben *et al.*, (1989), Figure 2.6; g-i

Diagnostic characters – Large trochospiral, biconvex test, equatorial periphery ovate with acute keel. Tear dropped shaped, fatter at base with final chamber slightly twisted in edge view. Five to 6 wedge shaped chambers in final whorl, increasing gradually in size. Aperture interiomarginal, extraumbilical to umbilical, low arch with a large plate like lip. The umbilicus is narrow and deep.

***Globorotalia ungulata* (Bermudez, 1960)**

Figure 3.6; 7-8.

Kennett and Srinavasan, (1983), Plate 38; 7-9

Hemleben *et al.*, (1989), Figure 2.6; k-m

Diagnostic characters – Trochospiral, biconvex test, equatorial periphery ovate with acute keel. Five chambers in final whorl, increasing slowly in size. Aperture interiomarginal, extraumbilical to umbilical, low arch with lip. Umbilicus narrow and deep. General shape similar to *Gr. tumida*, but is distinguished by thin delicate test.

***Globorotalia scitula* (Brady 1882)**

Figure 3.6; 1-2.

Kennett and Srinavasan, (1983), Plate 31; 1, 3-5

Hemleben *et al.*, (1989), Figure 2.5; a-c

Diagnostic characters – Medium to low trochospiral, biconvex test, axial periphery sub-angular to angular with a keel like rim. Four to 5 strongly compressed crescent shaped chambers in final whorl, increasing moderately in size. Surface mostly smooth except pustulose surface of early chambers on umbilical side. Aperture interiomarginal, umbilical to extraumbilical, low slit with pronounced lip.

***Truncorotalia truncatulinoides* (d'Orbigny, 1839)**

Figure 3.6; 3-4.

Kennett and Srinavasan, (1983), Plate 35; 4-6

Hemleben *et al.*, (1989), Figure 2.6; d-f

Diagnostic characters – Low trochospiral, planoconvex. Equatorial periphery almost circular with distinct keel. Five angular conical chambers in the final whorl, increasing slowly in size. Aperture interiomarginal, extraumbilical to umbilical, low arch with lip. Umbilicus wide and deep. Pustulate surface on umbilical side.

***Globorotaloides hexagonus* (Natland, 1938)**

Figure 3.6; 9-10.

Kennett and Srinavasan, (1983), Plate 54; 1, 3-5

Hemleben *et al.*, (1989), Figure 2.6; d-f

Diagnostic characters – Very low trochospiral, almost planispiral coarsely cancellate test. Five globular chambers in final whorl, increasing rapidly in size. Aperture interiomarginal, extraumbilical to umbilical, low arch boarded by plate or thick lip. Umbilicus wide but mostly covered by apertural plate.

Macroperforate (Spinose species)

***Globigerina bulloides* (d'Orbigny, 1826)**

Figure 3.7; 10-12.

Kennett and Srinavasan, (1983), Plate 6; 4-6

Hemleben *et al.*, (1989), Figure 2.1; a-c

Diagnostic characters – Low trochospiral test with 4 globular chambers in final whorl, increasing moderately in size. Aperture umbilical, a high symmetrical arch, no secondary apertures present.

***Globoturborotalita rubescens* (pink) (Hofker, 1956)**

Figure 3.7; 13-15.

Kennett and Srinavasan, (1983), Plate 9; 7-9

Hemleben *et al.*, (1989), Figure 2.1; g,h

Diagnostic characters – Small trochospiral test, pink in colour throughout test. Four globular chambers in final whorl, increasing rapidly in size. Aperture umbilical boarded by a rim, no secondary apertures present.

***Globigerinoides ruber* (d'Orbigny, 1839)**

Figure 3.7; 7-9.

Kennett and Srinavasan, (1983), Plate 17; 1-3

Hemleben *et al.*, (1989), Figure 2.2; k,l

Diagnostic characters – Low to high trochospiral test, white in colour. Three globular chambers in final whorl, increasing moderately in size. Primary aperture intermarginal, umbilical wide arch boarded by a rim, 2 secondary apertures present on spiral side sutures.

***Globigerinoides sacculifer* (Brady, 1877)**

Figure 3.7; 4-6.

Kennett and Srinavasan, (1983), Plate 14; 4-6

Hemleben *et al.*, (1989), Figure 2.2; m-r

Diagnostic characters – Low trochospiral test with 4 chambers in final whorl, increasing moderately in size. The first 3 chambers are globular and the last one elongate and lobulate in shape. Primary aperture intermarginal, umbilical arch boarded by a rim, secondary apertures present on spiral side.

***Globigerinella siphonifera* (type I and II) (d'Orbigny, 1839)**

Figure 3.7; 2-3.

Kennett and Srinavasan, (1983), Plate 60; 4-6

Hemleben *et al.*, (1989), Figure 2.3; i,k

Diagnostic characters – Low trochospiral test in early stage before becoming planispiral. Five to 6 globular chambers in final whorl, increasing rapidly in size. Aperture intermarginal, wide equatorial arch.

***Orbulina universa* (d'Orbigny, 1839)**

Figure 3.7; 1.

Kennett and Srinavasan, (1983), Plate 20; 4-6

Hemleben *et al.*, (1989), Figure 2.3; n,o

Diagnostic characters – Spherical test, composed of single chamber. Often densely perforate with openings of two sizes.

Microperforate

***Globigerinita glutinata* (with bulla) (Egger, 1893)**

Figure 3.6; 11-12.

Kennett and Srinavasan, (1983), Plate 56; 1, 3-5

Hemleben *et al.*, (1989), Figure 2.7; e-h

Diagnostic characters – Small low to medium trochospriral test with 3 – 4 globular chambers, increasing rapidly in size. Primary aperture intermarginal, umbilical low arch with lip obscured by an irregular bulla, which leads to secondary apertures along the bulla margins.

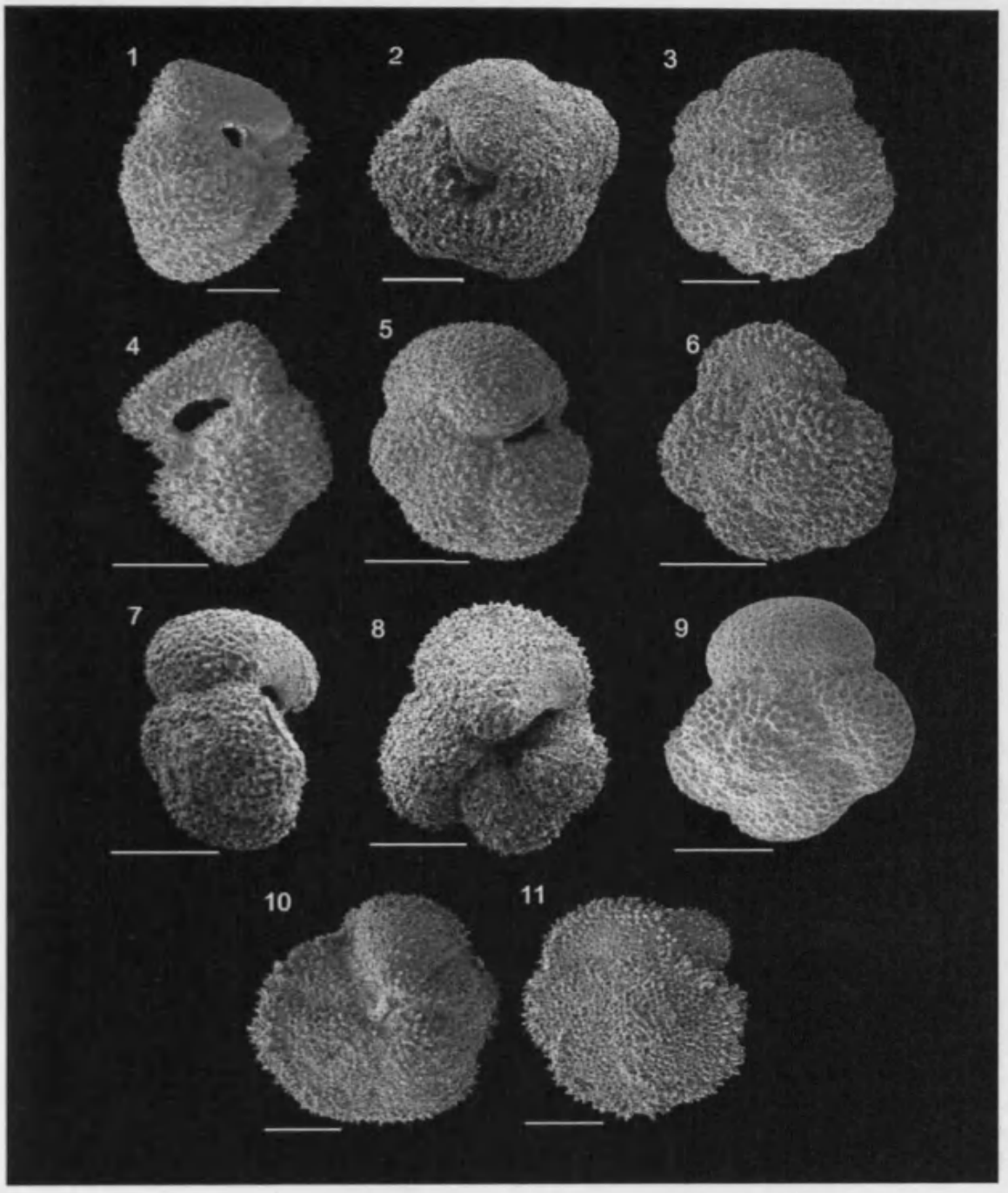

Figure 3.3 - Scanning electron microscope images of Paleocene planktonic foraminifera used in this study. **1-3**: *Morozovella apanthesma* (from 1262C-10H-4, 187.89cm), **4-6**: *Morozovella angulata* (from 1262C-10H-4, 187.89cm) **7-9**: *Morozovella praeangulata* (from 1262C-11H-2, 196.29cm), **10-11**: *Morozovella occlusa* (from 1262C-10H-4, 187.89cm). Scale bar = 100μm.

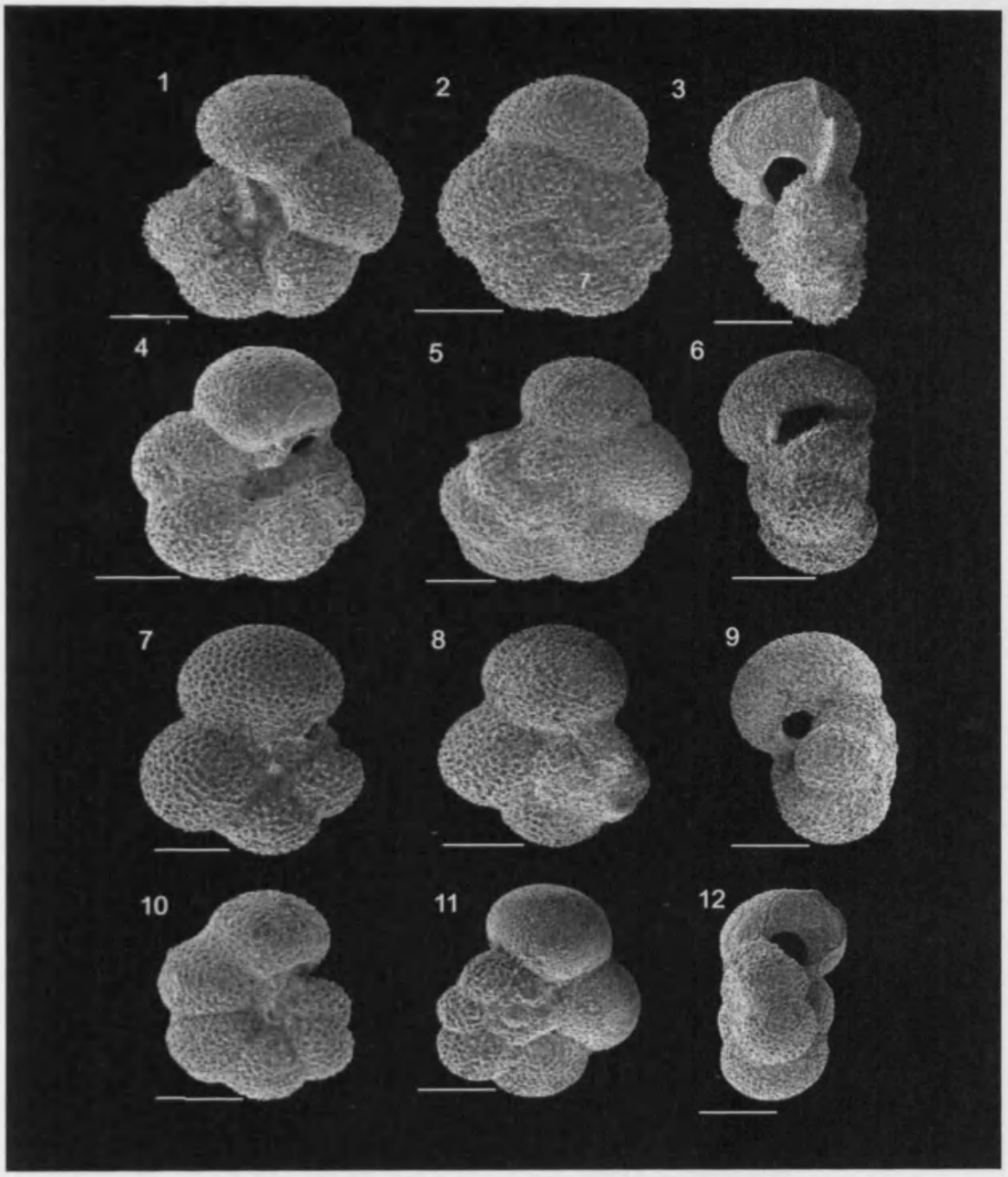

Figure 3.4 - Scanning electron microscope images of Paleocene planktonic foraminifera used in this study. **1-3**: *Praemurica uncinata*, **4-6**: *Praemurica inconstans*, **7-9**: *Praemurica pseudoinconstans* (all from 1262C-11H-2, 195.84cm), **10-12**: *Praemurica taurica*, (from 1262B-22H-3, 214.0cm). Scale bar = 100μm.

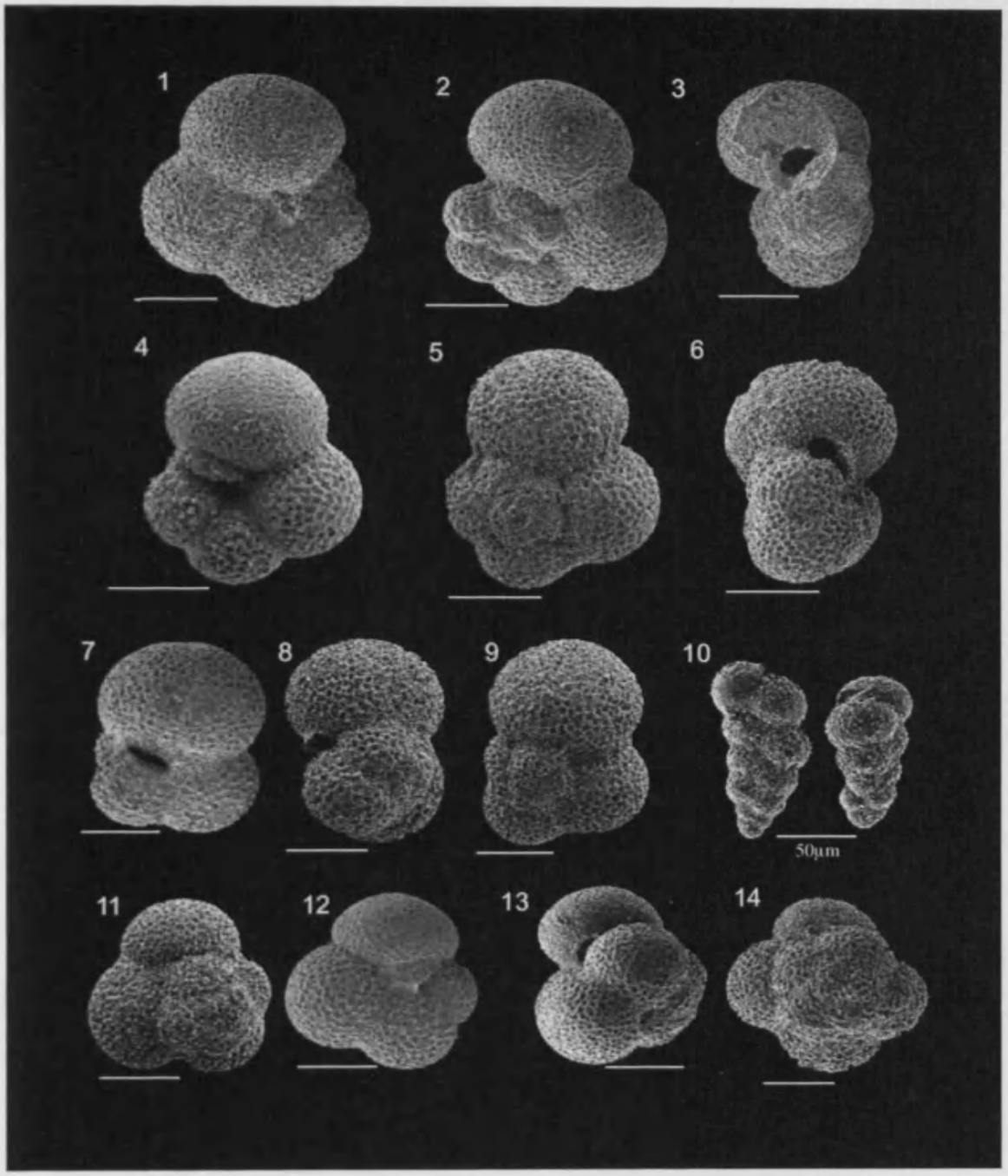

Figure 3.5 - Scanning electron microscope images of Paleocene planktonic foraminifera used in this study. **1-3**: *Parasubbotina pseudobulloides* (from 1262B-20H-4, 194.41cm), **4-6**: *Parasubbotina varianta* (from 1262C-11H-2, 196.29cm), **7-9**: *Subbotina triloculinoides* (from 1262B-20H-4, 194.41cm), **10:** *Woodringina hornerstownensis* (from 1262C-12H-3, 206.01cm.**11-12**: *Subbotina trivalis* (from 1262C-11H-2, 195.84cm),**13-14**: *Eoglobigerina eobulloides* (from 1262B-22H-3, 214.0cm). Scale bar = 100µm except *Woodringina hornerstownensis* where scale bar = 50µm.

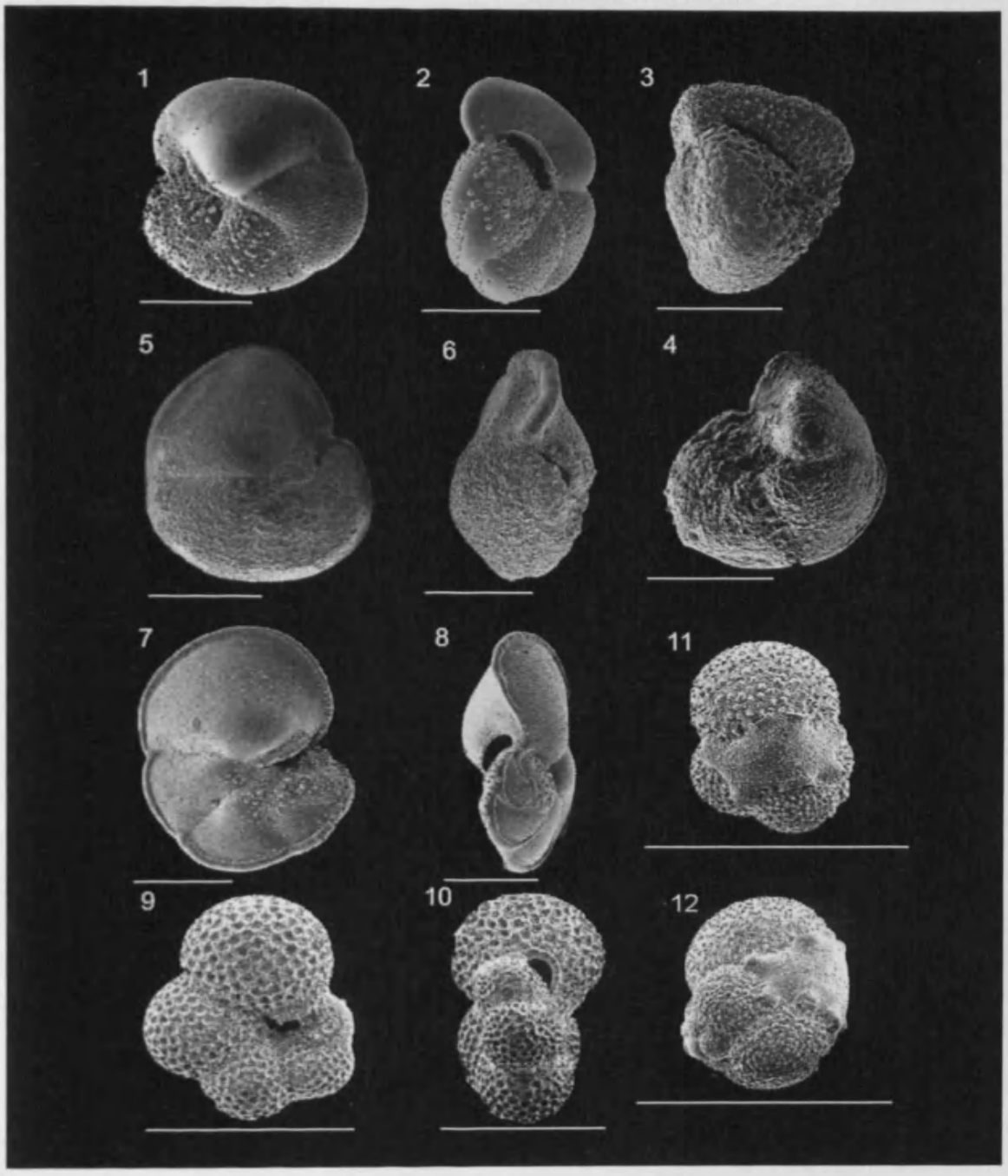

Figure 3.6 - Scanning electron microscope images of modern planktonic foraminifera used in this study. **1-2:** *Globorotalia scitula*, **3-4:** *Truncorotalia truncatulinoides*, **5-6:** *Globorotalia tumida* (encrusted), **7-8:** *Globorotalia ungulata*, **9-10:** *Globorotaloides hexagonus*, **11-12:** *Globigerinita glutinata* (with bulla). Scale bar = 200μm.

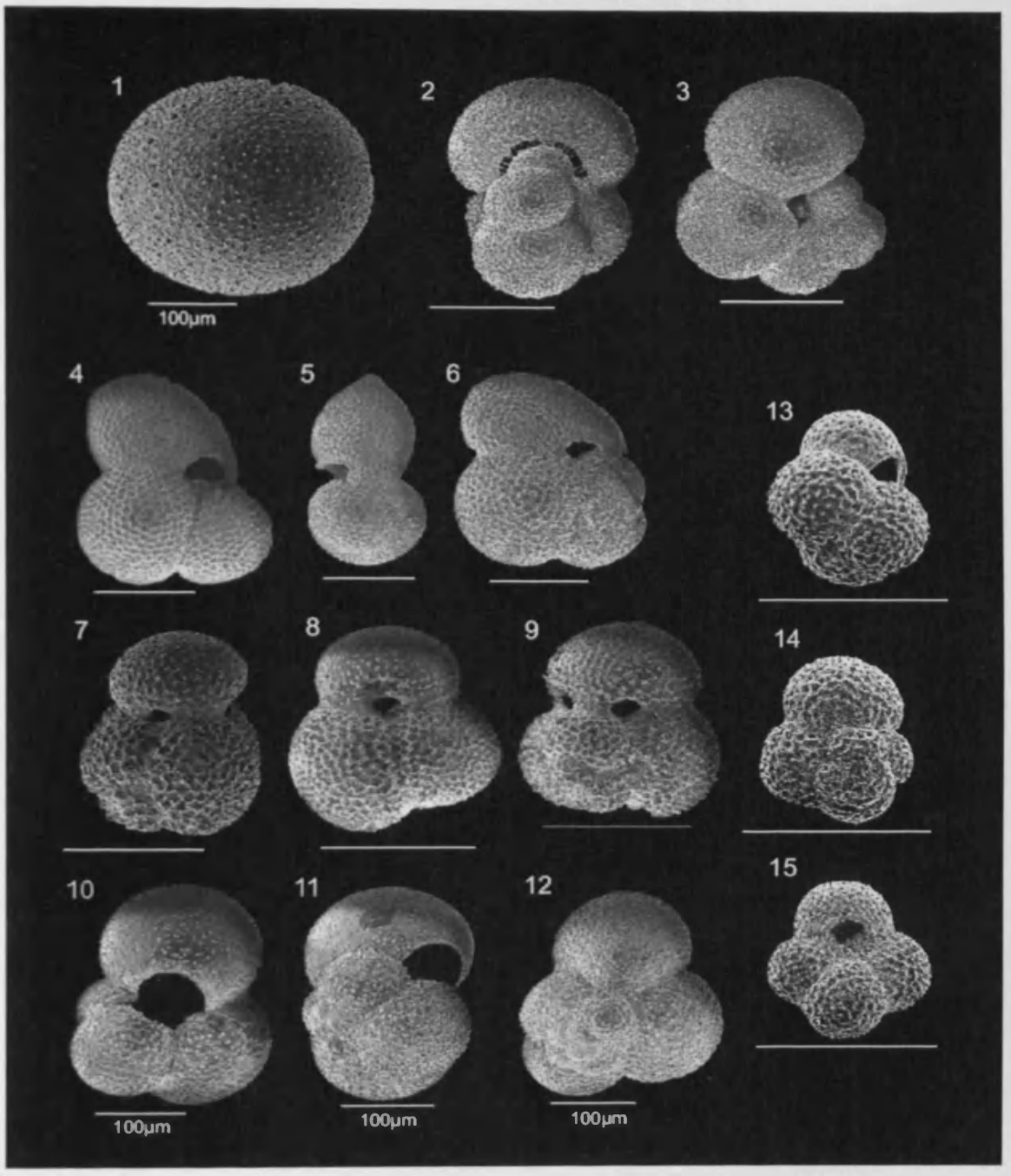

Figure 3.7 - Scanning electron microscope images of modern planktonic foraminifera used in this study. **1:** *Orbulina universa*, **2-3:** *Globigerinella siphonifera*, **4-6:** *Globigerinoides sacculifer*, **7-9:** *Globigerinoides ruber*, **10-12:** *Globigerina bulloides*, **13-15:** *Globoturborotalita rubescens* (pink). Scale bar = 200µm, except for *Orbulina universa* and *Globigerina bulloides* who's scale bar = 100µm.

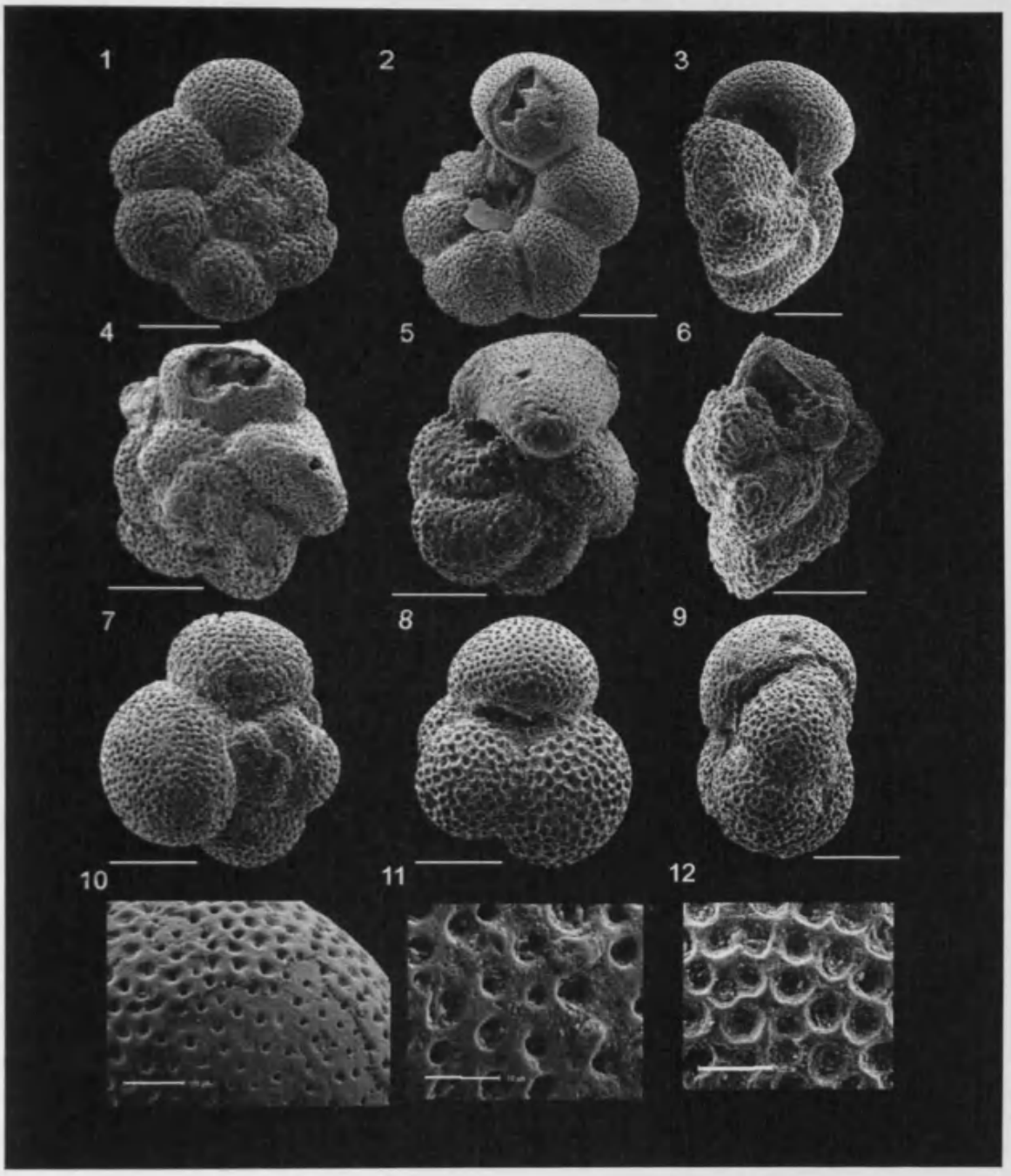

Figure 3.8 - Scanning electron microscope images of Tanzanian Paleocene planktonic foraminifera used in this study. **1-3**: *Praemurica uncinata*, **4-6**: *Morozovella angulata*, **7-9**: *Subbotina triangularis*. Scale bar = 100µm. **10;** *Praemurica uncinata* wall structure, scale 20 µm **11;** *Morozovella angulata* wall structure, scale 10 µm **12**: *Subbotina triangularis*, wall structure, scale 20 µm.

3.3. Site 1262 species stratigraphic ranges and preservation state

Site 1262 contains a typical suite of low-mid latitude planktonic foraminifera. Light microscope analysis reveals that Site 1262 planktonic foraminifera were free of particulate carbonate infilling and show good preservation of large scale test morphological features. The test surface appears milky and coarse in texture, which SEM analysis revealed to be micron scale recrystallisation (Figure 3.3 to Figure 3.5) as is typical of deep-sea carbonate oozes. Although indicative of diagenetic alteration a number of studies suggest that original ecological isotope differences between species are preserved (Corfield *et al.*, 1990; Spero, 1992; Pearson *et al.*, 2001; Sexton *et al.*, 2006). The ranges of all species found in Site 1262 are shown in Figure 3.9 and Figure 3.10 as well as Table 3.1. No species of *Acarinina* were present in the set of samples used for bistratigraphic analysis. However, rare specimens of *A. strabocella* were noted in two of the samples when picking for isotope analysis (1262C-10H-3, 186.66cm and 1262C-10H-3, 187.26cm). Conversion of the sample depth horizons on to the Site 1262 age model indicates that a number of species appear earlier and disappear earlier than indicated by previous global estimates (Figure 3.1 and Figure 3.2), even when differences in time scale are taken into account. *G. chapmani*, *E. edita*, *P. varianta*, *S. cancellata*, *Pr. inconstans* and *M. occlusa* all have first occurrences over 1 myr earlier than previous records.

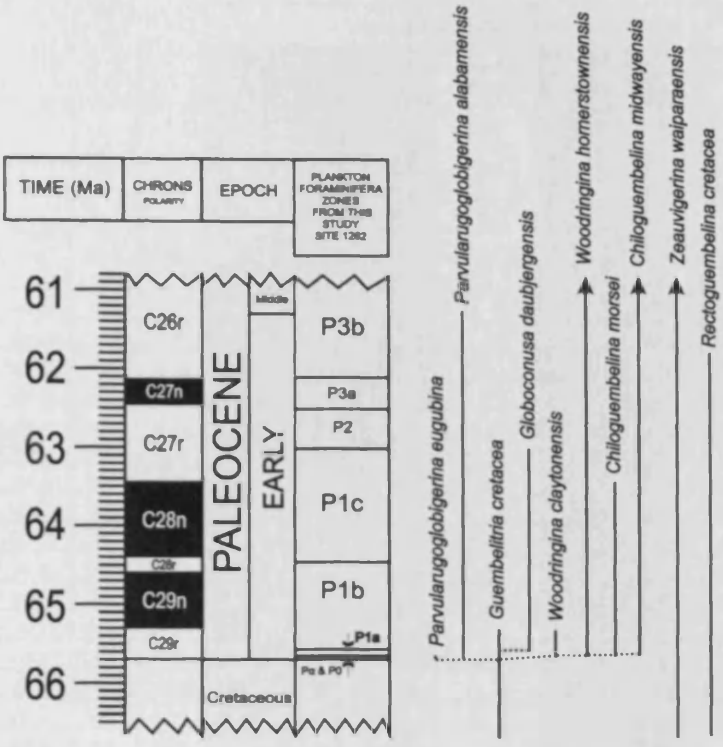

Figure 3.9 – Microperforate Paleocene planktonic foraminifera diversification, evolution and ranges found in this study Site 1262. Age (Ma) based on the time scale from Westerhold *et al.*, (2008) with orbital chronology from site 1262). Adapted from Olsson *et al.*, (1999).

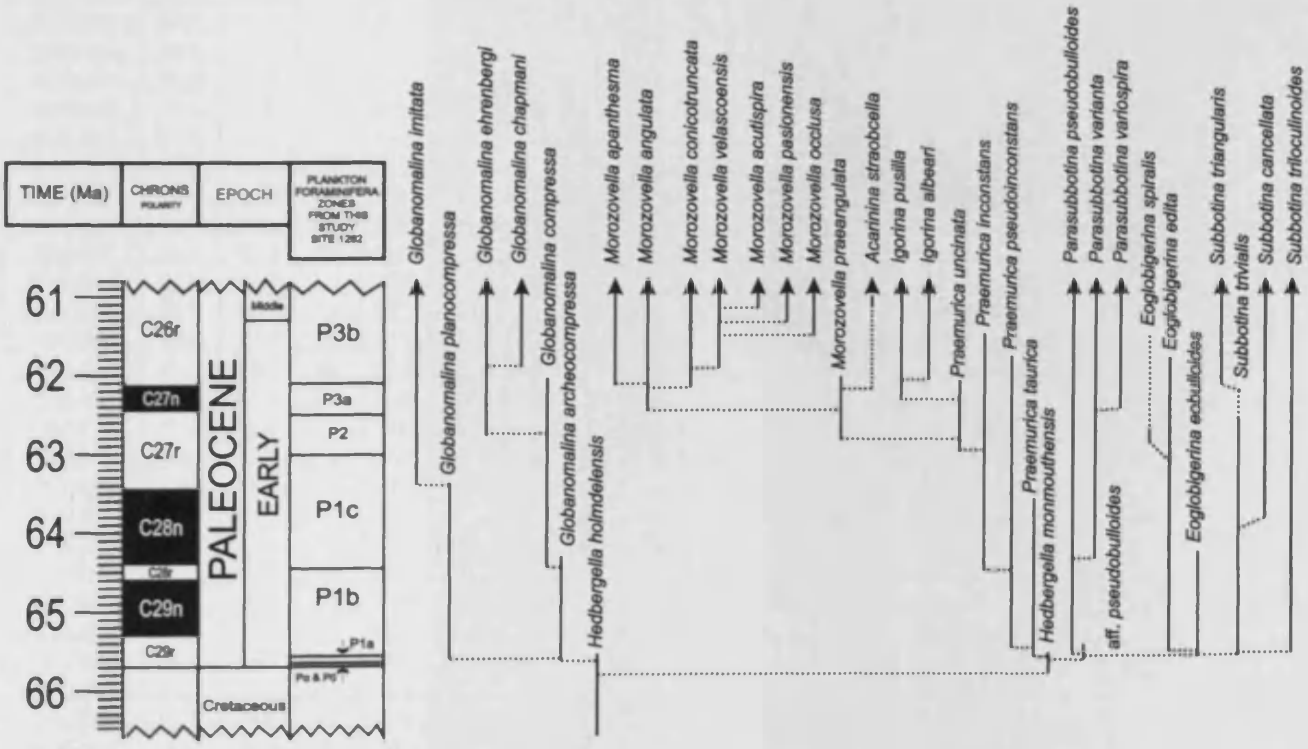

Figure 3.10 - Macroperforate Paleocene planktonic foraminifera diversification, evolution and ranges found in this study Site 1262. Age (Ma) based on the time scale from Westerhold *et al.*, (2008) with orbital chronology from site 1262). Adapted from Olsson *et al.*, (1999) and Aze *et al.* (2011). Dashed ranges indicate the full range observed by Olsson et al., (1999), which is not present in this study.

					Macroperforate Planktonic Foraminifera																
					Globanomalina						Eoglob-igerina			Para-subbotina				Subbotina			
Sample	Depth (mbsf)	Depth (mcd)	PF Zone	Age (Ma)	archaeocompressa	chapmani	compressa	chrisbergi	imitata	planocompressa	edita	eobulloides	spiralis	ad. pseudobulloides	pseudobulloides	variata	wanuspira	cancellata	triangularis	trilociformoides	trivialis
1262B-19H-5	198.96	185.05	P3b	60.86		X		X							X	X	X	X	X	X	
1262C-10H-2	170.87	185.79	P3b	60.95		X			X							X		X	X	X	
1262C-10H-3	171.59	185.51	P3b	61.05		X			X							X	X	X	X	X	
1262C-10H-3	172.31	187.23	P3b	61.16		X		X	X							X	X	X	X	X	
1262C-10H-4	173.03	187.95	P3b	61.26		X		X	X							X	X	X	X	X	
1262C-10H-4	173.75	188.67	P3b	61.35		X		X								X	X	X	X	X	
1262C-10H-5	174.47	189.39	P3b	61.44		X		X	X							X	X	X	X	X	
1262C-10H-5	175.19	190.11	P3b	61.52		X		X								X	X	X	X	X	
1262C-10H-6	175.91	190.83	P3b	61.61		X		X							X	X	X	X	X	X	
1262B-20H-2	174.23	191.56	P3b	61.70		X		X	X							X	X	X	X	X	
1262B-20H-3	174.95	192.28	P3b	61.79		X		X							X	X	X	X	X	X	
1262B-20H-3	175.67	193.00	P3b	61.87		X		X							X	X	X	X	X	X	
1262B-20H-3	176.39	193.72	P3b	61.95		X		X								X	X	X	X	X	
1262B-20H-4	177.14	194.47	P3b	62.03		X		X	X							X	X	X	X	X	
1262B-20H-4	177.86	195.19	P3b	62.12		X		X							X	X	X	X	X	X	
1262C-11H-2	179.38	195.90	P3a	62.21		X	X	X							X	X	X	X	X	X	
1262C-11H-3	181.18	197.70	P3a	62.42				X							X	X	X	X		X	
1262C-11H-3	181.9	198.42	P3a	62.51			X	X	X						X	X	X	X		X	
1262C-11H-4	182.62	199.14	P2	62.62			X	X							X	X		X		X	X
1262C-11H-4	183.34	199.86	P2	62.73			X	X							X	X		X		X	X
1262C-11H-5	184.06	200.58	P2	62.84			X	X							X	X		X		X	X
1262C-11H-5	184.51	201.35	P2	62.95			X	X					X		X	X		X		X	X
1262B-21H-1	182.2	202.14	P2	63.05			X				X				X	X		X		X	X
1262B-21H-2	182.92	202.86	P1c	63.13			X				X				X	X		X		X	X
1262C-12H-1	184.8	203.58	P1c	63.25			X				X				X	X		X		X	X
1262C-12H-2	185.52	204.30	P1c	63.41			X			X	X				X	X		X		X	X
1262C-12H-2	186.24	205.02	P1c	63.54			X			X	X				X	X		X		X	X
1262C-12H-2	186.99	205.77	P1c	63.68			X			X	X				X	X		X		X	X
1262C-12H-3	187.71	206.49	P1c	63.82			X			X	X				X	X		X		X	X
1262C-12H-3	188.43	207.21	P1c	63.95			X			X	X				X	X		X		X	X
1262C-12H-4	189.15	207.93	P1c	64.08			X			X	X				X	X				X	X
1262C-12H-4	189.93	208.71	P1c	64.21			X			X	X				X	X				X	X
1262C-12H-5	190.65	209.43	P1c	64.33			X			X	X				X	X				X	X
1262C-12H-6	191.58	210.36	P1c	64.48			X			X	X				X	X				X	X
1262C-12H-6	192.3	211.08	P1b	64.59	X					X	X				X					X	X
1262B-22H-1	191.04	212.03	P1b	64.74	X					X	X	X			X					X	X
1262B-22H-2	192.04	213.03	P1b	64.92	X					X	X	X			X					X	X
1262B-22H-3	193.01	214.00	P1b	65.1	X					X	X	X			X					X	X
1262C-13H-1	193.86	214.90	P1b	65.29	X					X	X	X			X					X	X
1262B-22H-3	194.09	215.08	P1b	65.32	X					X	X	X			X					X	X
1262B-22H-4	194.24	215.23	P1b	65.36	X					X	X	X			X					X	X
1262C-13H-1	194.6	215.64	P1b	65.46	X					X	X	X			X					X	X
1262C-13H-1	194.86	215.90	P1b	65.53	X					X	X	X			X					X	X
1262C-13H-2	195.06	216.10	P1b	65.57	X					X	X	X			X					X	X
1262C-13H-2	195.28	216.32	P1b	65.61	X					X	X	X			X					X	X
1262C-13H-2	195.53	216.57	P1a	65.66	X					X	X	X			X						X
1262C-13H-2	195.65	216.69	Pu	65.68	X					X	X	X		X							X

Table 3.1 - Planktonic foraminiferal presence/absence range charts at Site 1262. PF = Planktonic foraminiferal zones based on Olsson *et al.*, 1999 and Berger & Pearson, 2005.

					Macroperforate Planktonic Foraminifera															
					Praemurica				Igo-rina		Morozovella									
Sample	Depth (mbsf)	Depth (mcd)	PF Zone	Age (Ma)	inconstans	pseudoinconstans	taurica	unicinnata	albicans	pusilla	acutispira	angulata	apanthesma	conicorotunda	occlusa	panamensis	praeangulata	velascoensis	Hedbergella holmdelensis	Hedbergella monmouthensis
1262B-19H-5	198.96	185.05	P3b	60.86					X	X	X	X	X		X	X				
1262C-10H-2	170.87	185.79	P3b	60.95					X	X		X	X		X			X		
1262C-10H-3	171.59	186.51	P3b	61.05					X		X	X	X	X	X	X		X		
1262C-10H-5	172.31	187.23	P3b	61.16					X		X	X	X	X	X	X		X		
1262C-10H-4	173.03	187.95	P3b	61.26					X		X	X	X	X	X	X		X		
1262c-10h-4	173.75	188.67	P3b	61.35					X			X	X	X	X	X		X		
1262C-10H-5	174.47	189.39	P3b	61.44					X	X		X	X	X	X	X		X		
1262C-10H-5	175.19	190.11	P3b	61.52					X	X		X	X		X			X		
1262C-10H-6	175.91	190.83	P3b	61.61					X			X	X		X					
1262B-20H-2	174.23	191.56	P3b	61.70					X	X		X	X	X						
1262B-20H-3	174.95	192.28	P3b	61.79					X	X		X	X					X		
1262B-20H-3	175.67	193.00	P3b	61.87					X			X	X					X		
1262B-20H-3	176.39	193.72	P3b	61.95					X			X	X	X				X		
1262B-20H-4	177.14	194.47	P3b	62.03					X	X		X	X					X		
1262B-20H-4	177.86	195.19	P3b	62.12					X	X		X	X	X						
1262C-11H-2	179.38	195.90	P3a	62.21	X			X				X	X				X			
1262C-11H-3	181.18	197.70	P3a	62.42	X			X		X		X					X			
1262C-11H-3	181.9	198.42	P3a	62.51	X			X				X					X			
1262C-11H-4	182.62	199.14	P2	62.62	X	X		X									X			
1262C-11H-4	183.34	199.86	P2	62.73	X	X		X									X			
1262C-11H-5	184.06	200.58	P2	62.84	X	X		X									X			
1262C-11H-5	184.51	201.30	P2	62.95	X	X		X									X			
1262B-21H-1	182.2	202.14	P2	63.05	X	X		X									X			
1262B-21H-2	182.92	202.86	P1c	63.13	X	X														
1262C-12H-1	184.8	203.58	P1c	63.25	X	X														
1262C-12H-2	185.52	204.30	P1c	63.41	X	X														
1262C-12H-2	186.24	205.02	P1c	63.54	X	X														
1262C-12H-2	186.99	205.77	P1c	63.68	X	X														
1262C-12H-3	187.71	206.49	P1c	63.82	X	X	X													
1262C-12H-3	188.43	207.21	P1c	63.95	X	X	X													
1262C-12H-4	189.15	207.93	P1c	64.08	X	X	X													
1262C-12H-4	189.93	208.71	P1c	64.21	X	X	X													
1262C-12H-5	190.65	209.43	P1c	64.33	X	X	X													
1262C-12H-6	191.58	210.36	P1c	64.48	X	X	X													
1262C-12H-6	192.3	211.08	P1b	64.59		X	X													
1262B-22H-1	191.04	211.03	P1b	64.74		X	X													
1262b-22H-2	192.04	213.03	P1b	64.92		X	X													
1262B-22H-3	193.01	214.00	P1b	65.1		X	X													
1262C-13H-1	193.86	214.90	P1b	65.29		X	X													
1262B-22H-3	194.09	215.08	P1b	65.32		X	X													
1262B-22H-4	194.24	215.23	P1b	65.36		X	X													
1262C-13H-1	194.6	215.64	P1b	65.45		X	X													
1262C-13H-1	194.86	215.90	P1b	65.53		X	X													
1262C-13H-2	195.05	216.10	P1b	65.57		X	X													
1262C-13H-2	195.28	216.32	P1b	65.61		X	X													
1262C-13H-2	195.53	216.57	P1a	65.66		X	X													
1262C-13H-2	195.65	216.69	Pα	65.68			X												X	X

Table 3.1 – Continued.

					Microperforate Planktonic Foraminifera												
Sample	Depth (mbsf)	Depth (mcd)	PF Zone	Age (Ma)	Guembelitria cretacea	Rectoguembelina cretacea	Zeauvigerina SP	Zeauvigerina waiparaensis	Parvularugoglobigerina alabamensis	Parvularugoglobigerina eugubina	Globoconusa daubjergensis	Woodringina SP	Woodringina claytonensis	Woodringina hornerstownensis	Chiloguembelina SP	Chiloguembelina midwayensis	Chiloguembelina morsei
1262B-19H-5	198.96	185.05	P3b	60.86											X		
1262C-10H-2	170.67	185.79	P3b	60.95				X								X	
1262C-10H-3	171.59	186.51	P3b	61.05			X								X		
1262C-10H-3	172.31	187.23	P3b	61.16			X					X			X		
1262C-10H-4	173.03	187.95	P3b	61.26			X		X			X			X		
1262c-10h-4	173.75	188.67	P3b	61.35			X					X			X		
1262C-10H-5	174.47	189.39	P3b	61.44			X					X				X	
1262C-10H-5	175.19	190.11	P3b	61.52			X					X				X	
1262C-10H-6	175.91	190.83	P3b	61.61				X				X				X	
1262B-20H-2	174.23	191.56	P3b	61.79				X				X				X	
1262B-20H-3	174.95	192.28	P3b	61.79		X						X				X	
1262B-20H-3	175.67	193.00	P3b	61.87			X		X					X		X	
1262B-20H-3	176.39	193.72	P3b	61.95			X					X				X	
1262B-20H-4	177.14	194.47	P3b	62.03				X						X		X	
1262B-20H-4	177.86	195.19	P3b	62.12			X					X				X	
1262C-11H-2	179.38	195.90	P3a	62.21		X	X					X				X	
1262C-11H-3	181.18	197.70	P3a	62.42			X		X			X				X	
1262C-11H-3	181.9	198.42	P3a	62.51		X	X					X			X		
1262C-11H-4	182.62	199.14	P2	62.62			X		X			X				X	
1262C-11H-4	183.34	199.86	P2	62.73		X	X							X		X	
1262C-11H-5	184.06	200.58	P2	62.84		X						X				X	
1262C-11H-5	184.51	201.30	P2	62.95			X					X				X	
1262B-21H-1	182.2	202.14	P2	63.05			X				X	X				X	
1262B-21H-2	182.92	202.86	P1c	63.13			X				X			X		X	
1262C-12H-1	184.8	203.58	P1c	63.25			X				X	X				X	
1262C-12H-2	185.52	204.30	P1c	63.41			X				X	X				X	X
1262C-12H-2	186.24	205.02	P1c	63.54		X	X				X	X				X	
1262C-12H-2	186.99	205.77	P1c	63.68		X	X		X		X			X		X	X
1262C-12H-3	187.71	206.49	P1c	63.82							X	X		X		X	
1262C-12H-3	188.43	207.21	P1c	63.95		X			X		X	X				X	X
1262C-12H-4	189.15	207.93	P1c	64.08		X	X				X	X				X	
1262C-12H-4	189.93	208.71	P1c	64.21		X	X				X	X				X	X
1262C-12H-5	190.65	209.43	P1c	64.33		X					X			X		X	X
1262C-12H-6	191.58	210.36	P1c	64.48		X	X				X			X		X	
1262C-12H-6	192.3	211.08	P1b	64.59			X		X		X			X		X	
1262B-22H-1	191.04	211.03	P1b	64.74			X				X			X		X	X
1262B-22H-2	192.04	213.03	P1b	64.92			X				X			X		X	
1262B-22H-3	193.01	214.00	P1b	65.1			X				X			X		X	X
1262C-13H-1	193.86	214.59	P1b	65.29	X		X				X			X		X	X
1262B-22H-3	194.09	215.05	P1b	65.32	X		X				X		X	X		X	X
1262B-22H-4	194.24	215.23	P1b	65.36	X		X				X			X		X	X
1262C-13H-1	194.6	215.64	P1b	65.46	X		X				X			X		X	X
1262C-13H-1	194.86	215.90	P1b	65.53	X		X				X			X		X	X
1262C-13H-2	195.06	216.10	P1b	65.57	X						X			X		X	X
1262C-13H-2	195.28	216.32	P1b	65.61	X	X					X			X		X	X
1262C-13H-2	195.53	216.57	P1a	65.66	X						X		X	X		X	X
1262C-13H-2	195.65	216.69	Pa	65.68	X			X		X			X	X		X	X

Table 3.1 – Continued.

3.4. Biostratigraphy

This section presents the results of biostratigraphic analysis carried out on Site 1262. It represents the first treatment of this kind after the low resolution core catcher analysis onboard Leg 208 (Shipboard Scientific Party, 2004). Table 3.3 shows the base datum events defined by the biozones and the ages for these bioevents from Site 1262. Table 3.3 compares the results of this study to that of previously published zonation schemes (Berggren and Pearson, 2005; Olsson *et al.*, 1999). As mentioned above, the ranges of many species are different in Site 1262. Of particular significance are the datum marker species, differences in age calibrations of S. *triloculinoides* the marker species for the base of P1b is ~0.82 myr older, *G. compressa* (P1c) is ~0.91 myr older, *Pr. uncinata* (P2) is ~0.79 myr older and *I. albeari* (P3b) is ~ 0.83 myr older.

Biozone	Base Datum	Sample Bottom	Depth mbsf	Depth mcd	Sample Top	Depth mbsf	Depth mcd	Error	Estimated Age (Ma) of Base datum (this study)
P3b	FAD *Igorina albeari*	1262B-20H-4, 146-147	177.86	195.19	N/A	N/A	N/A	N/A	62.12
P3a	FAD *Morozovella angulata*	1262C-11H-3, 140-141	181.90	198.42	1262C-11H-2, 38-39	179.38	195.90	+/- 0.36	62.51
P2	FAD *Praemurica uncinata*	1262B-21H-1, 80-81	182.20	202.14	1262C-11H-4, 62-63	182.62	199.14	+/- 0.36	63.05
P1c	FAD *Globanomalina compressa* &/or *Praemurica inconstans*	1262C-12H-6, 8-9	191.58	210.36	1262B-21H-2, 2-3	182.92	202.86	+/- 0.36	64.48
P1b	FAD *Subbotina triloculinoides*	1262C-13H-2, 28-29	195.28	216.32	1262C-12H-6, 80-81	192.30	211.08	+/- 0.36	65.61
P1a	LAD *Parvularugo-globigerina eugubina*	1262C-13H-2, 53-54	195.53	216.57	1262C-13H-2, 53-54	195.53	216.57	+/- 0.36	65.66
Pα	FAD *Parvularugo-globigerina eugubina*	N/A	N/A	N/A	1262C-13H-2, 65-66	195.65	216.69	N/A	65.68
P0	LAD Cretaceous Taxa	Not present	Not present	Not present	Not present	Not present	Not present	Not present	Not present

Table 3.2 – Biozonation of the Paleocene from Site 1262 this study, with age estimates for the base of each zone based on Westerhold *et al.*, (2008) age model. LAD = Last appearance Datum, FAD = First appearance datum.

Paleocene Biozone	Base Datum	Age (Ma) Beggren & Pearson, 2005	Age (Ma) Olsson et al., 1999	Age (Ma) this study	This study converted to Cande and Kent (1995)
P5	LAD *Globanomalina pseudomenadii*	55.90	55.90		
P4c	FAD *Acarinina soldadoensis*	56.50	56.50		
P4b	LAD *Parasubbotina variospira* &/or *Acarinina subsphaerica*	59.20	57.10		
P4a	FAD *Globanomalina pseudomenardii*	59.40	59.20		
P3b	FAD *Igorina albeari*	60.00	60.00	62.12	60.88
P3a	FAD *Morozovella angulata*	61.00	61.00	62.51	61.33
P2	FAD *Praemurica uncinata*	61.37	61.20	63.05	61.99
P1c	FAD *Globanomalina compressa* &/or *Praemurica inconstans*	62.87	63.00	64.48	63.81
P1b	FAD *Subbotina triloculinoides*	64.30	64.50	65.61	65.12
P1a	LAD *Parvularugo-globigerina eugubina*	64.80	64.90	65.66	65.18
Pα	FAD *Parvularugo-globigerina eugubina*	64.97	64.97	65.68	65.00
P0	LAD Cretaceous Taxa	65.00	65.00	Not present	
K/ Pg		65.00	65.00	65.68	

Table 3.3 – Biozonation of the Paleocene, with age estimates for the base of each zone from Olsson *et al.*, (1999); Berggren and Pearson, (2005) based on Cande and Kent (1995) Geomagnetic Polarity Time Scale (GPTS) and this study based on Westerhold *et al.*, (2008) age model. LAD = Last appearance Datum, FAD = First appearance datum. The final column shows boundary ages when converted from Westerhold *et al.*, (2008) to the Cande and Kent (1995) time scale, by linear interpolation.

3.5. Discussion and summary

The cause of the trend towards earlier first occurrences in this study when related to previous studies could be related to the sites used to construct the biozonation scheme. Although Berggren and Pearson (2005) updated the biostratigraphy of the Paleogene, much of the early Paleocene work was based on existing studies and no new stratigraphic information was included (Berggren *et al.*, 1995). Berggren *et al.* (1995) placed planktonic foraminifera datum levels with observed magnetic polarity stratigraphy and age estimates based on Cande and Kent (1995). This framework was based on records from DSDP Site 577 and Site 384 and ODP Site 689, Site 690 and Site 738. The cores from these sites were collected using extended core barrel (XCB) or rotary drilling (RCB), in the case of DSDP, which resulted in often poor core recovery and disturbance. These factors can seriously compromise the quality of geomagnetic data and therefore the ability to construct reliable geomagnetic polarity reversal stratigraphy. This brings into question the age estimates of the bioevents at several of the calibration sites. Many of these sites are located at higher latitudes than Site 1262 (i.e. Site 689 and 690 were taken in the Southern Ocean and Site 577 the western north Pacific), which could affect the timing of first occurrences. Alternatively the differences could be explained by differences in taxonomic practises. Publication of the '*Atlas of Paleocene Planktonic Foraminifera*' (Olsson *et al.*, 1999) has standardised the taxonomy but these updates have not been built into the zonation scheme. A final possibility is that there are inconsistencies in the Westhold *et al.* (2008) age model and Leg 207 paleomagnetic interpretation, althought the optimised recovery and data quality suggest that this is unlikely. A combination of poor data quality in old DSDP and ODP cores along with taxonomic difficulty could explain the offsets mentioned above and the biostratigraphy at Site 1262 would appear to allow for improvements in the stratigraphic and chronological age estimates of early Paleocene biozones.

4. Stable Isotope Ecology of Modern Planktonic Foraminifera

This chapter focuses on the carbon and oxygen stable isotope trends throughout a range of size fractions for twelve species of modern planktonic foraminifera taken from a core top sample in the western Indian Ocean. As the ecology of these species is known through observations and laboratory analysis, the isotopic trends observed can be matched up to these ecologies and any disequilibrium effects assessed. These are then applied to the fossil Paleocene data presented in Chapter 5. Despite a wealth of literature available for modern planktonic foraminifera, most studies focus on the large species and larger size fractions, making correlation to the smaller Paleocene species difficult. Here small species and size fractions have been included to allow for better direct correlation to Paleocene species.

4.1. Introduction

Planktonic foraminifera are especially useful in modern and ancient ecosystem studies owing to their widespread occurrence, species specific ecological niches and ability to secrete calcite tests, which record the geochemical composition of the waters they live in. The ecology and stable isotopic composition of modern planktonic foraminifera tests are studied to enable comparison with fossil forms and allow reconstructions of past water column thermal and nutrient structure. The interpretation of stable isotopes from planktonic foraminifer tests relies on the assumption that the foraminiferal calcite is secreted in isotopic equilibrium with the surrounding waters at the time they were living. It is clear, however, that in many cases this assumption does not hold and the affects of biological processes related to ecology are known to result in test $\delta^{13}C$ and $\delta^{18}O$ values that are not in equilibrium with sea water (Berger *et al.*, 1978; Kahn, 1979; Turner, 1982; McConnaughey, 1989a,b; Spero and Williams, 1989; Spero *et al.*, 1991; Cooke and Rohling, 1999; Bijma *et al.*, 1999; Schmidt *et al.*, 2008).

4.1.1. Foraminiferal isotopic values and depth habitat

The primary control on the isotopic composition of planktonic foraminiferal calcite relates to the depth preference of the species in question, due to water column differences set up with respect to carbon and oxygen isotopes. The $\delta^{18}O$ of calcite generally increases with depth habitat due to a decrease in temperature from the surface to deep water, affecting fractionation of ^{16}O and ^{18}O (Cooke and Rohling, 1999). The $\delta^{13}C$ of seawater generally decreases with depth as remineralisation of organic matter and release of ^{12}C takes over from the stripping of ^{12}C by photosynthesising organisms in the photic zone. Different species occur throughout the upper water column. Therefore a typical shallow living species will have relatively low $\delta^{18}O$ and high $\delta^{13}C$ compared to a deeper species. The preferred depth habitats of individual species are linked to temperature, light, chlorophyll concentrations and food availability (Fairbanks and Wiebe, 1980; Hemleben *et al.*, 1989; Ortiz *et al.*, 1995; Schiebel and Hemleben, 2000; Schiebel and Hemleben, 2005) which are dependent on hydrography. This preferred depth can change through ontogeny, which greatly influences the $\delta^{13}C$ and $\delta^{18}O$ values of the tests (Emiliani, 1954 and 1971; Shackleton *et al.*, 1985; Berger, 1978; Douglas and Savin, 1978; Bé, 1982). Spero and Williams (1989) showed that a combination of seasonality and habitat depth can influence the carbon and oxygen isotope values of the calcite test within a foram assemblage.

4.1.2. Foraminiferal isotopic disequilibrium and vital effects

Empirical studies have shown that a variety of factors can lead to isotopic disequilibrium in planktonic foraminifera. According to McConnaughey (1989a,b) there are two types of isotopic disequilibrium in planktonic foraminifera calcite; metabolic and kinetic. Metabolic effects are $\delta^{13}C$ deviations from the kinetic pattern. Metabolic effects result from changes in the $\delta^{13}C$ of dissolved inorganic carbon (DIC) near the site of calcite precipitation because of symbiont photosynthesis or foraminifera cell respiration (the offset can be negative or positive). Kinetic effects influence both carbon and oxygen by discriminating the heavier isotopes ^{13}C and ^{18}O during hydration and

hydroxylation of CO_2. This can lead to skeletal depletion in ^{13}C and ^{18}O from equilibrium that tends to fall along a line away from equilibrium seawater values (McConnaughey 1989a,b). Rapid skeletal growth is often associated with strong kinetic disequilibria.

Another factor that can influence planktonic foraminiferal calcite $\delta^{13}C$ and $\delta^{18}O$ is the carbon pool from which the CO_2 is extracted, which can change through ontogeny. Changes in the importance of the carbon pool utilised for calcification can alter from internal respired CO_2 to external CO_2 of seawater, due to the changing rates of growth and metabolic activity through ontogeny. Small foraminifera (<150μm) tend to grow rapidly and have high metabolic activity (Bé 1982), leading to increased kinetic fractionation and an increase in respired CO_2 (which is preferentially enriched in ^{12}C) being incorporated into the test. Larger foraminifera grow more slowly and show decreased metabolic activity with less kinetic fractionation (Berger *et al.*, 1978; Kahn, 1979; Berger and Vincent 1986; Wefer and Berger, 1991; Ravelo and Fairbanks, 1995; Spero *et al.*, 1997; Schmidt *et al.*, 2008). When viewing a test size / $\delta^{13}C$ plot a positive correlation may be observed if metabolic fractionation is influencing the smaller sizes of the species in question, as illustrated schematically in Figure 4.1.

Foraminiferal diet (Bé *et al.*, 1977) is another potential influence on shell isotopic composition. However, laboratory studies have found very little isotopic variation resulting from respiration of food source with different isotopic compositions (Spero *et al.*, 1991). Carbonate ion concentration of the surrounding waters is an additional factor that has been found to alter the $\delta^{13}C$ and $\delta^{18}O$ of calcite through kinetic and metabolic fractionation factors and appears to be independent of photosymbiosis (Spero *et al.*, 1997; Bijma *et al.*, 1999). For $\delta^{13}C$ of foraminifera calcite however, photosymbiosis has been found to have the largest effect (Spero *et al.*, 1991; Spero and Lea, 1993). This is especially true for test >150μm.

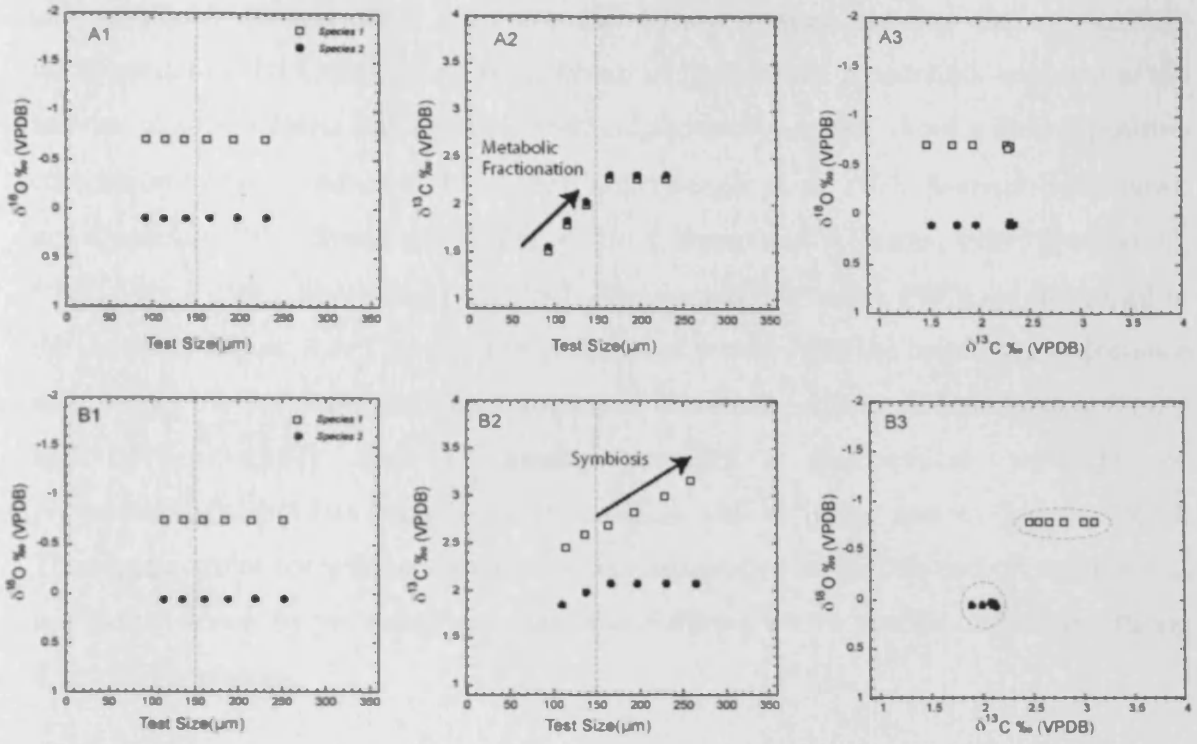

Figure 4.1 - Schematic model showing the influences that algal symbionts and incorporation of metabolic CO_2 has on stable carbon and oxygen isotope signals of planktonic foraminifera tests, adapted form Norris, (1996) based on modern core tope data from Ravelo and Fairbanks, (1995) and Berger *et al.*, (1978).

4.1.3. Foraminiferal photosymbiosis

Symbiotic relationships with photosynthetic algae have been found in many species of extant planktonic foraminifera (Bé *et al.*, 1982; Spero and DeNiro, 1987; Hemleben, *et al.*, 1989; Spero, 1992; Spero and Lea, 1993; Norris, 1996). This ecological strategy is thought to aide the host foraminifera in occupying new niche space (by providing photosynthetic compounds, Schiebel and Hemleben [2005]) in oligotrophic environments that would otherwise be unavailable. In extant foraminifera these symbionts are either chrysophytes or dinoflagellates, living in the host's cytoplasm or among the rhizopodial network and spines (Hemleben *et al.*, 1989; Schiebel and Hemleben, 2005).

Modern symbiosis causes planktonic foraminifera test calcite to be enriched in ^{13}C relative to ^{12}C by 0.5 to >1.0 ‰ (Norris, 1996). This occurs because algal

photosynthesis preferentially removes the lighter isotope leaving the surrounding microhabitat of the foraminifera, from which the test calcite is secreted, enriched in the heavier isotope (Spero and DeNiro, 1987). Laboratory studies show a strong positive correlation between calcite $\delta^{13}C$ and test size (Berger et al. 1978; Bouvier-Soumagnac and Duplessy, 1985; Spero and Williams, 1988; Spero and Williams, 1989; Spero *et al.*, 1991; Spero, 1992; Spero and Lea, 1993; Ravelo and Fairbanks, 1995), as illustrated in the model of Figure 4.1. This positive correlation results from the increasing importance and density of symbionts through ontogeny as the foraminifera reaches maturity (Spero and DeNiro, 1987). This relationship provides a geochemical 'signature' of photosymbiosis that has been found in fossil as well as living species (Norris, 1996). This is important for paleoceanographic reconstructions of marine carbon cycling that use extinct forms by providing a means of identifying which species might have strong $\delta^{13}C$ disequilibrium.

4.1.4. Limitations of existing constraints

The isotopic composition of modern planktonic foraminifera species reflects the ambient environments throughout the water column. This information forms the basis for the assumptions made when dealing with ancient environments and fossil species. For this reason a modern core top sample from the tropical Indian Ocean was analysed to provide ground truthing for the subsequent Paleocene data (Chapter 5). This ground truthing will help to understand the disequilibrium factors mentioned above so that fossil data can be correctly interpreted. Core tops and not plankton nets were used, despite core tops having generally higher $\delta^{18}O$ values (Bouvier-Soumagnac and Duplessy, 1985), as this is representative of the fossil material. Previous studies focus on the larger sizes of modern planktonic foraminifera, but to be of value as a comparison to the Paleocene, when smaller test sizes predominate (Schmidt *et al.*, 2004a), smaller modern species and small life stages of typically larger species were analysed here. To fully appreciate changing isotope values through ontogeny a full suite of size fractions is needed. This is currently lacking in existing data and will be a focus of the present study.

4.2. Results

4.2.1. Hydrographic data from GLOW Site 2

Figure 4.2 shows the results from the CTD cast taken at Site 2. The vertical temperature profile shows a relatively rapid decrease from surface temperatures of 29.14 °C to 13 °C at a depth of 250 m, indicating a surface mixed layer of ~30 m overlying a thick thermocline. Over the rest of the water column, to the depth of 2203 m, temperatures decrease gradually to a minimum of 2.4 °C. Salinity increases rapidly to a subsurface peak of 35.5 PSU at 135 m, where it then decreases to its minimum value of 34.7 PSU at 665 m. Below this point salinity values increase slightly before stabilising. Oxygen concentrations show an initial increase to 165.4 µmol/kg just below the surface at 53.6 m, before a rapid decrease to 97.2 µmol/kg at the shallow oxygen minimum (SOMZ) at 165 m. Values then increase almost as rapidly as they decrease until 321 m when there is slow decrease to a deep oxygen minimum zone (DOMZ) of 56.7 µmol/kg at 1013 m. Turbidity (the measure of particulate loading in the water column) and fluorescence (a measure of Chlorophyll) both share a similar profile with a subsurface maximum at 137 m and 95 m, respectively, before values stabilise and remain constant throughout the remainder of the lower water column.

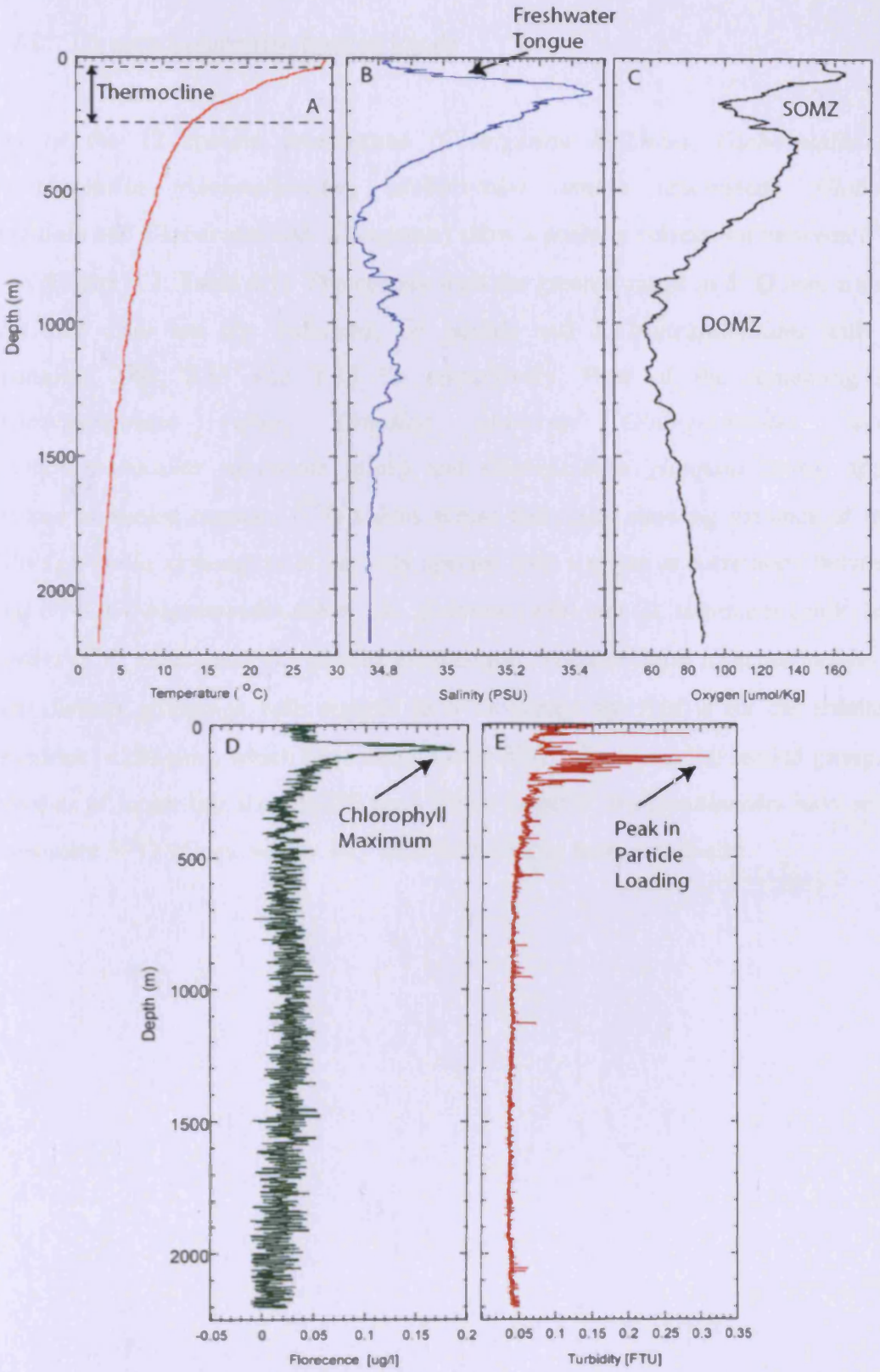

Figure 4.2 – CTD cast data from the upward section. Plot A – Temperature (°C), Plot B – Salinity (PSU), Plot C – Oxygen (µmol/Kg), Plot D – Fluorescence (µg/l) and Plot E – Turbidity (FTU). SOMZ = surface oxygen minimum zone and DOMZ = deep oxygen minimum zone.

4.2.2. Oxygen isotope size fraction trends

Six of the 12 species investigated (*Globigerina bulloides*, *Globorotalia scitula*, *Truncorotalia truncatulinoides*, *Globorotalia tumida* (encrusted), *Globorotalia ungulata* and *Globorotaloides hexagonus*) show a positive correlation between $\delta^{18}O$ and size (Figure 4.3; Table 4.1). The species with the greatest range in $\delta^{18}O$ over a specified test size class are *Gg. bulloides*, *Gr. scitula* and *T. truncatulinoides* with ranges spanning 2.46, 2.35 and 2.25 ‰ respectively. Five of the remaining species (*Globigerinoides ruber*, *Orbulina universa*, *Globigerinoides sacculifer*, *Globoturborotalita rubescens* (pink) and *Globigerinita glutinata* [w/b]) appear to remain at almost constant $\delta^{18}O$ values across test sizes, showing variance of <0.4 ‰. *Globigerinella siphonifera* is the only species with a negative correlation between size and $\delta^{18}O$. *Globigerinoides ruber*, *Ga. glutinata* (w/b) and *Gt. rubescens* (pink) have the lowest $\delta^{18}O$ values and *Gr. scitula* the heaviest. *Truncorotalia truncatulinoides* shows two distinct groupings with regards to $\delta^{18}O$ values; the first is for the smallest size fractions (<250 μm), which have much lower $\delta^{18}O$ values than the second group, which consists of larger test sizes (>250 μm). These larger *T. truncatulinoides* have relatively consistent $\delta^{18}O$ values, which vary little with further increases in size.

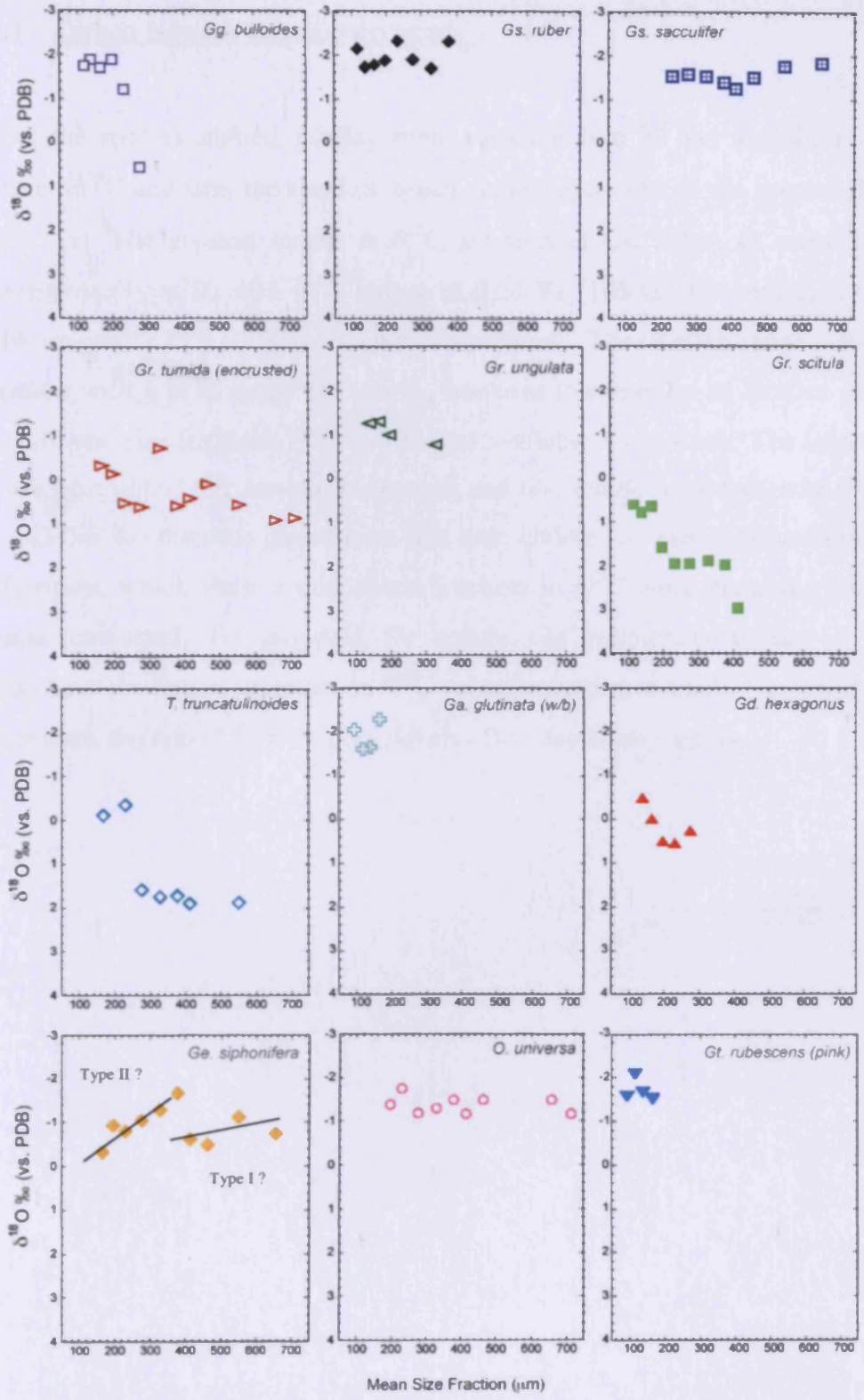

Figure 4.3 - Test size – oxygen isotope ($\delta^{18}O$) relationships for 12 species of modern extant planktonic foraminifera. Test size represents the average of the sieve size range. Genera abbreviations as follows Ge= *Globigerinella*, Gd = *Globorotaloides*, O = *Orbulina*, T = *Truncorotalia*, Gg = *Globigerina*, Ga = *Globigerinita*, Gt = *Globoturborotalita*, Gr = *Globorotalia* and Gs. *Globigerinoides*. w/s = with sac like final chamber, w/b = with bulla.

4.2.3. Carbon Isotopes size fraction trends

All of the species studied, display some variation in $\delta^{13}C$ and a positive correlation between $\delta^{13}C$ and size, the slope of which varies depending on the species (Figure 4.4; Table 4.1). The greatest ranges in $\delta^{13}C$ are seen in *Gs. ruber*, *O. universa* and *Ge. siphonifera* (Type II) with $\delta^{13}C$ ranges of 2.54 ‰ (106 to 400 μm), 2.18 ‰ (180 to >710 μm) and 2.73 ‰ (150 to 710 μm), respectively. The smallest range is found in *Gr. ungulata* with a $\delta^{13}C$ range of 0.56 ‰, however this may be an artefact of the small range of test size fractions (125 to 355 μm) available for analysis. The largest test size for *Gs. sacculifer*, *Gr. tumida* (encrusted) and *Gr. scitula* record slightly lower values (by 0.3-0.6 ‰) than the penultimate test size. Unlike *Gs. ruber*, *O. universa*, and *Ge. siphonifera*, which show a continuous increase in $\delta^{13}C$ with increasing test size, *Gr. tumida* (encrusted), *Gr. ungulata*, *Gr. scitula*, *Ga. glutinata* (w/b) and *Gt. rubescens* (pink) have the largest increases in $\delta^{13}C$ values occurring at smaller test sizes and in the larger tests, the rate of $\delta^{13}C$ increase levels off or decreases slightly.

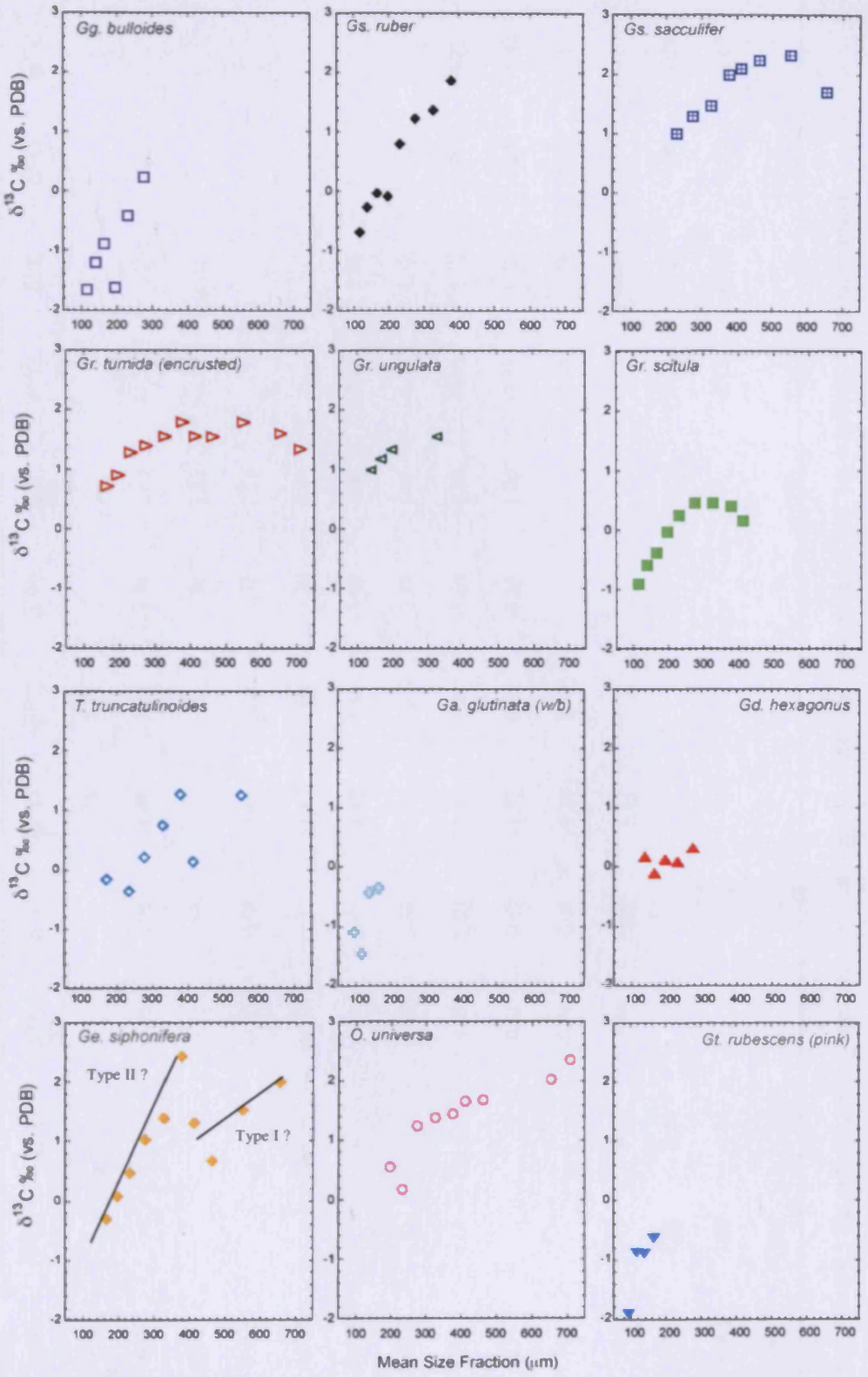

Figure 4.4 - Test size – carbon isotope ($\delta^{13}C$) relationships for 12 species of modern extant planktonic foraminifera. Test size represents the average of the sieve size range. Genera abbreviations as Figure 4.3. w/s = with sac like final chamber, w/b = with bulla.

Size Fraction (μm)	Mean Size (μm)	*Gt. rubescens* (pink)		*Ge. siphonifera*		*O. universa*		*Gs. sacculifer* (w/s)		*Gs. ruber* (white)		*Gg. bulloides*	
		$\delta^{18}O$	$\delta^{13}C$	$\delta^{18}O$	$\delta^{13}C$	$\delta^{18}O$	$\delta^{13}C$	$\delta^{18}O$	$\delta^{13}C$	$\delta^{18}O$	$\delta^{13}C$	$\delta^{18}O$	$\delta^{13}C$
>710	710					-1.18	2.36						
600-710	655			-0.75	1.99	-1.47	2.03	-1.84	1.69				
500-600	550			-1.13	1.53			-1.78	2.33				
425-500	462.5			-0.50	0.68	-1.48	1.68	-1.52	2.24				
400-425	412.5			-0.62	1.31	-1.18	1.66	-1.26	2.09				
355-400	377.5			-1.68	2.43	-1.48	1.45	-1.40	2.00	-2.32	1.86		
300-355	327.5			-1.29	1.39	-1.31	1.37	-1.55	1.47	-1.70	1.37		
250-300	275			-1.05	1.03	-1.17	1.24	-1.60	1.30	-1.90	1.22	0.56	0.22
212-250	231			-0.81	0.47	-1.75	0.19	-1.53	1.00	-2.33	0.80	-1.21	-0.42
180-212	196			-0.94	0.08	-1.36	0.55			-1.88	-0.08	-1.90	-1.61
150-180	165	-1.53	-0.62	-0.32	-0.30					-1.79	-0.03	-1.71	-0.89
125-150	137.5	-1.68	-0.88							-1.72	-0.27	-1.90	-1.20
106-125	114.5	-2.10	-0.86							-2.15	-0.68	-1.75	-1.67
80-106	93	-1.59	-1.89										

Table 4.1 - GLOW 3 Site sample stable isotope data this study (genera abbreviations as in Figure 4.3). w/s = with sac like final chamber.

Size Fraction (μm)	Mean Size (μm)	*Gd. hexagonus*		*Ga. glutinata* (w/b)		*T. truncatulinoides*		*Gr. scitula*		*Gr. ungulata*		*Gr. tumida (encrusted)*	
		$\delta^{18}O$	$\delta^{13}C$	$\delta^{18}O$	$\delta^{13}C$	$\delta^{18}O$	$\delta^{13}C$	$\delta^{18}O$	$\delta^{13}C$	$\delta^{18}O$	$\delta^{13}C$	$\delta^{18}O$	$\delta^{13}C$
>710	710											0.87	1.33
600-710	655											0.92	1.59
500-600	550					1.88	1.25					0.57	1.78
425-500	462.5											0.09	1.54
400-425	412.5					1.90	0.14*	2.96	0.16			0.42	1.55
355-400	377.5					1.73	1.26	1.98	0.41			0.59	1.79
300-355	327.5					1.74	0.75	1.87	0.47	-0.78	1.55	-0.72	1.55
250-300	275	0.26	0.32			1.59	0.21	1.96	0.46			0.63	1.39
212-250	231	0.55	0.09			-0.35	-0.36	1.96	0.24			0.53	1.28
180-212	196	0.50	0.13					1.57	-0.03	-1.00	1.33	-0.13	0.90
150-180	165	-0.01	-0.11	-2.30	-0.35	-0.11	-0.16	0.64	-0.38	-1.31	1.18	-0.32	0.72
125-150	137.5	-0.49	0.18	-1.66	-0.42			0.79	-0.59	-1.26	0.99		
106-125	114.5			-1.61	-1.45			0.61	-0.91				
80-106	93			-2.05	-1.10								

Table 4.1 – Continued. * indicates erroneous data which has been excluded from interpretation. w/b = with bulla.

4.2.4. Foraminiferal water column temperatures reconstructions

Foraminifera oxygen stable isotopes can be used to calculate seawater temperatures due to the temperature dependence of the fractionation process between the light (^{16}O) and heavy (^{18}O) oxygen isotopes (Emiliani, 1954; Cooke and Rohling, 1999) if the isotopic composition of the water is known. A variety of temperature calibrations exists, some of which are species specific. Since there are no species specific calculations for all the species investigated in this study then the general equation devised by Erez and Luz (1983) was used:

Equation 4.1 $$T\,(°C) = 16.998 - 4.52(\delta c - \delta w) + 0.028(\delta c - \delta w)^2$$

Where δc is the $\delta^{18}O$ of the foraminiferal calcite and δw is the $\delta^{18}O$ of seawater. The δw value assumed here is 0.41 ‰ based on seawater values in the area (Schmidt *et al.*, 1999) and modelling data (LeGrande and Schmidt, 2006). This δw value is the result of high salinities in the area (Srivastava *et al.*, 2010) and indicates net evaporation, which preferentially removes the ^{16}O leaving the surface waters enriched in ^{18}O (Cooke and Rohling, 1999).

Table 4.2 shows the calculated temperatures, the temperature range that results from the various test size fractions, as well as average for each planktonic foraminifera species. *Globigerinoides ruber* produces the highest overall temperature of 29.6 °C, as well as the highest average value of 27.9 °C. *Globorotalia scitula* generates the lowest temperature of 5.7 °C and lowest average temperature of 11.7 °C. *Globigerina bulloides*, *Gr. tumida* (encrusted), *Gr. scitula* and *T. truncatulinoides* all exibit large temperature ranges, ΔT = 11.3 °C, 7.4 °C, 10.4 °C and 10.1 °C, respectively. The majority of species register the lowest temperatures at the largest test sizes and their highest temperatures at the smaller test sizes, except *Gs. sacculifer* (w/s), *Ge. siphonifera* and *Ga. glutinata* (w/b).

Size Fraction (µm)	*Gg. bulloides*	*Gs. ruber* (white)	*Gs. sacculifer* (w/s)	*O. universa*	*Ge. siphonifera*	*Gt. rubescens* (pink)	*Gr. tumida* (encrusted)	*Gr. ungulata*	*Gr. scitula*	*T. truncatulinoides*	*Ga. glutinata* (w/b)	*Gd. hexagonus*
>710				24.3			14.9					
600-710			27.3	25.6	22.3		14.7					
500-600			27.0		24.0		16.3			10.4		
425-500			25.8	25.7	21.1		18.4					
400-425			24.6	24.2	21.7		16.9		5.7	10.3		
355-400		29.5	25.3	25.6	26.6		16.2		10.0	11.1		
300-355		26.7	25.9	24.9	24.8		22.1	22.4	10.5	11.0		
250-300	16.3	27.6	26.2	24.2	23.7		16.0		10.1	11.7		17.7
212-250	24.4	29.6	25.9	26.9	22.5		16.4		10.1	20.5		16.4
180-212	27.6	27.5		25.1	23.1		19.4	23.4	11.8			16.6
150-180	26.7	27.1			20.3	25.9	20.3	24.9	16.0	19.4	29.4	18.9
125-150	27.6	26.8				26.6		24.6	15.3		26.5	21.1
106-125	26.9	28.8				28.5			16.1		26.2	
80-106						26.1					28.3	
Temperature Range (°C)	11.3	2.9	2.6	2.7	6.2	2.6	7.4	2.4	10.4	10.1	3.2	4.7
Average temperature (°C)	24.9	27.9	26	25.2	23	26.8	17.4	23.8	11.7	16.1	27.6	18.1
Average $\delta^{18}O$	-1.32	-1.97	-1.56	-1.38	-0.91	-0.11	0.31	-1.09	1.59	1.41	-1.90	0.16

Table 4.2 – Calculated seawater temperatures (°C) from GLOW Site 3 core top, stable oxygen isotopes based on the equation from Erez and Luz (1983). Values in red indicate the highest temperatures and values in blue the lowest for each species. Genera abbreviations as Figure 4.3. w/s = with sac like final chamber, w/b = with bulla.

The calculated average temperatures for every species studied were then placed on to the temperature curve of the CTD cast so that definitive depth habitats could be inferred (Figure 4.5 - A). The depth habitat of the planktonic foraminifera divide into 3 main groups: Group 1 the surface dwellers (*Gs. ruber*, *Ga. glutinata*, *Gt. rubescens*, Gs. sacculifer, *O. universa*, *Gg. bulloides*, *Gr. ungulata* and *Ge. siphonifers*), occupy the upper 100 m of the water column. Group 2 consist of *Gd. hexagonus*, *Gr. tumida* and *T. truncatulinoides* and are located at the SOMZ at ~165m. Group 3 consists of *Gr. scitula* which is found much deeper at ~330 m. The surface dwellers in Group 1 can be further subdivided into 3 groups: Group A the shallowest group consists of *Gs. ruber*, *Ga.*

glutinata and ***Gt. rubescens***. Group B consists of Gs. sacculifer, ***O. universa*** and ***Gg. bulloides***. Group C the deepest group consists of ***Gr. ungulata*** and ***Ge. siphonifers***.

Another way to determine depth habitats is to use temperature and salinity data, from the CTD cast, to calculate δw and estimate δc. Following the protocol of Anand *et al.* (2003), based on the salinity $\delta^{18}O$ relationship described by Duplessy *et al.* (1991) and a re-arrangement of the temperature equation of Erez and Luz (1983), the following equations can be used to calculate δw and estimate δc.

Equation 4.2 $\delta w = -5.31 + 0.16 \times \text{salinity}$

When calculating δw the regional $\delta^{18}O$ salinity relationship of slope 0.16 and intercept -5.31 were taken from LeGrande and Schmidt (2006).

Equation 4.2 $\delta c = (\delta w - 0.27) + [4.64 - (4.64^2 - 4 \times 0.09(16.998 - T))^{0.5}] / 0.18$

Where T = Temperature (°C).

The average $\delta^{18}O$ for every species studied were then placed on the depth line estimate for δc, similar to estimated temperatures above, to help further refine the depth habitats of these planktonic foraminifera (Figure 4.5 - B). The depth habitats of the planktonic foraminifera are similar to the temperature estimates and divide into 3 main groups. The only major difference seen between the temperature estimated depth and δc estimated depth is for ***T. truncatulinoides***, which now plots in Group 3 with ***Gr. scitula***.

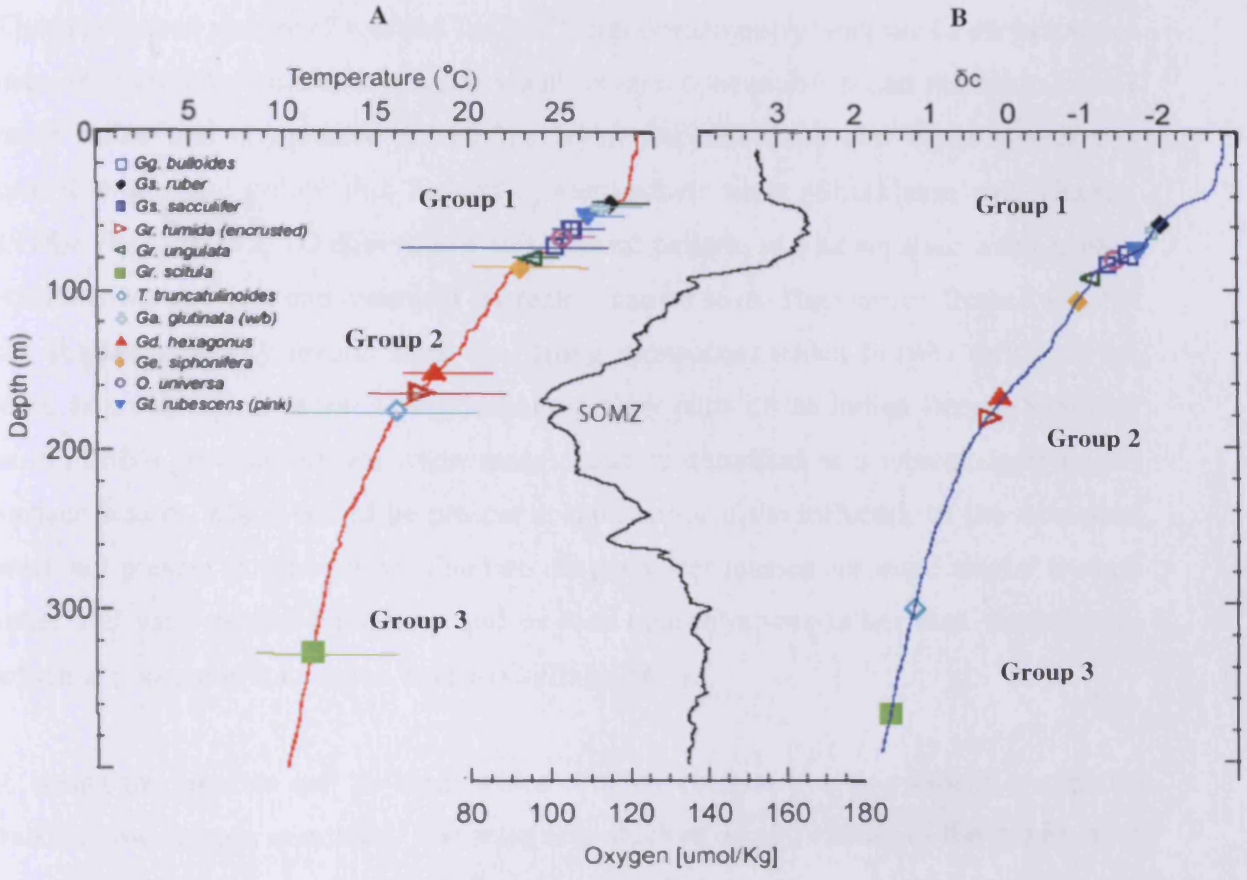

Figure 4.5 – Average planktonic foraminifera inferred depth habitat of the 12 species investigated at GLOW Site 3. A = average calculated $\delta^{18}O$ temperatures for foraminiferal calcite (Table 4.2) plotted with the temperature profiles from the CTD cast. Error bars on plot A denote full temperature ranges calculated from Table 4.2. B = average $\delta^{18}O$ of foraminifera calcite plotted on the calculated line of δc (using CTD temperature and salinity data and following the protocol of Anand *et al.* [2003], with regional $\delta^{18}O$ salinity relationship from LeGrande and Schmidt [2006]). The oxygen profile from the CTD cast is also shown. Genera abbreviations as Figure 4.3. SOMZ = surface oxygen minimum zone, w/b = with bulla. Group 1 = Surface mixed layer dwellers, Group 2 = Thermocline dwellers and Group 3 = Sub-thermocline dwellers.

4.3. Discussion

4.3.1. Hydrographic setting and water column conditions

The generalised picture of western Indian Ocean oceanography indicates a surface water mass of high temperature, low salinity and oxygen concentration that overlies a cooler more saline and oxygenated subsurface layer. Beneath these two water masses lies central water and below this Antarctic intermediate water (Shackleton and Vincent, 1978). The GLOW CTD data follow this general pattern, as four separate water masses with distinct physical and chemical characters can be seen. The warmer fresher water at the surface probably results from the strong monsoons, which heavily influence the area, as precipitation exceeds evaporation in many parts of the Indian Ocean (Sardessai *et al.*, 2010). The subsurface water mass could be classified as a typical upper mixed surface waters, which would be present at the surface if the influence of the monsoons were not present in this region. The two deeper water masses are more similar to each other and vary mostly in salinity and oxygen concentrations rather than temperature, which are common for deeper waters (Colling, 2001).

A strong thermocline can be seen, which roughly correlates with a salinity maximum and shallow oxygen minimum. The relatively shallow depth (~30 m) of the mixed layer compared to other parts of the world's oceans is relatively common in the Indian Ocean (Rao *et al.*, 1989; Pollehne *et al.*, 1993) and results from highly variable hydrographic conditions. Just above these physical property changes, the peak in fluorescence and turbidity, are seen indicating the probable depth of highest biological production. The chlorophyll maximum is relatively deep in the Indian Ocean and below the mixed layer, having a greater affinity with peaks in nutrient concentrations than with light levels, as the phytoplankton appears to be well adapted to the lower light conditions and thrive at these deeper depths (Neveux and Billy, 1986; Pollehne *et al.*, 1993). The CTD data collected in the area shows an oligotrophic water column with a relatively shallow thermocline and deep chlorophyll maximum (Figure 4.2). The double OMZ has been observed by others (Shackleton and Vincent, 1978; Naqui, 2006) in the Indian Ocean, with the SOMZ resulting from the remineralisation of organic matter. However, the

DOMZ is due to changing hydrographic conditions as the influential water mass change from central water to Antarctic intermediate water.

In the summer months (July and August) the north-western Indian Ocean is subject to intense upwelling (Schott *et al.*, 2009), which may affect stable isotope chemistry of any planktonic foraminifera that secretes the majority of its calcite test at this time. Sediment seafloor planktonic foraminifera assemblages, as represented by the core top samples, represent a time average mixture of such seasonal variations, a fact that must be considered in the following discussion.

4.3.2. Depth habitat

As indicated by the CTD data, physical properties of the water column such as temperature, oxygen concentrations and food availability vary greatly with depth. It is these factors that are said to influence the depth habitat and abundances of planktonic foraminifera (Fairbanks *et al.*, 1982; Hemleben *et al.*, 1989; Schiebel and Hemleben, 2000; Schiebel and Hemleben, 2005). Data from depth stratified plankton nets show that many species of foraminifera appear to increase in numbers at the chlorophyll maximum (Fairbanks and Wiebe, 1980), where a balance between light and nutrients favours maximum primary production. This occurs just above the thermocline, where there is still enough light for photosynthesis and enough nutrients being mixed up from deep water (where organic matter has been remineralised) to provide phytoplankton with ideal conditions for growth (Tait and Dipper, 1998). At GLOW Site 3 this occurs at ~95 m as indicated by the peak in fluorescence (Figure 4.2).

The foraminifera $\delta^{18}O$ temperatures and δc estimates (Figure 4.5; Table 4.2) indicate depth habitats inline with the known ecologies of the investigated species (Shackleton and Vincent, 1978; Hemleben et al., 1989). The data support relatively warm, surface mixed layer habitats for *Gg. bulloides*, *Gs. ruber* (white), *Gs. sacculifer* (w/s), *O. universa*, *Ge. siphonifera*, *Gt. rubescens* (pink), *Gr. ungulata* and *Ga. glutinata* (w/b), Group 1. The fresh water tongue (Figure 4.2), which is found year round (Sardessai *et al.*, 2010) appears to have little effect as a physical barrier to the planktonic

foraminifera, as many species (Group 1 from Figure 4.5) have $\delta^{18}O$ temperatures which indicate they have calcified within this zone. These lower salinities could affect $\delta^{18}O$ values and cause $\delta^{18}O$ temperature estimates to be lower. However, as some species record temperatures near the maximum of that recorded by the CTD and in line with sea surface temperature in the region (Sardessai *et al.*, 2010), this appears unlikely. The δc estimated depth, which do take into account salinity, agree well with the $\delta^{18}O$ temperature estimate depths (Figure 4.5). Of the surface, group 1, species *Gs. ruber* (white), *Gs. sacculifer* (w/s), *O. universa* and *Ge. siphonifera*, are photosymbiotic and would need light as much as nutrients (Faul *et al.*, 2000) for their symbiotic algae. This species thus inhabit the clear surface waters above the turbidity maximum at 137 m (Figure 4.2), where maximum light can penetrate. Among the mixed layer dwellers there is further inter species separation with *Gs. ruber* (white), *Ga. glutinata* (w/b), *Gt. rubescens* (pink) and *Gs. sacculifer* (w/s) inhabiting the shallowest depths. Observations were made by Fairbanks *et al.* (1982), who classed these species as 'true' oligotrophic species, best adapted for the low food conditions. Similar to the data presented here, Dekens *et al.* (2002), found *Gs. ruber* and not *Gs. sacculifer* (w/s), which is often used for paleotemperature surface reconstructions, has the lightest $\delta^{18}O$ and therefore registers the highest temperatures. This suggests that *Gs. ruber* would be the best choice for estimating sea surface temperatures (SST) as it appears to be the shallowest dwelling species in the western Indian Ocean. The slightly deeper dwelling mixed layer species (Group 1 – C) *Ge. siphonifera* and *Gr. ungulata*, are associated with the depth just above maximum fluorescence at 95 m (Figure 4.2) where the chlorophyll maximum is located and food would be readily available. *Globorotalia ungulata* is not a symbiotic species and would require food from additional sources. *Globigerinella siphonifera* is a symbiotic species but its dependence on its symbiotic algae for food maybe less than that of other symbiotic species (see section 4.3.3 for more details).

The $\delta^{18}O$ values of *Gr. tumida* (encrusted), *Gd. hexagona* and *T. truncatulinoides* indicate a deeper dwelling habitat in cool waters, well within the thermocline and at the shallow oxygen minimum ~ 165 m. *Globorotalia scitula* has the highest $\delta^{18}O$ values, indicating a very deep sub-thermocline habitat or growth in a colder season (Figure

4.2). The deep habitat is consistent with the suggestion from foraminiferal dietary studies that this species prefers fine, settling, particulate organic matter (Hemleben *et al.*, 1989; Itou *et al.*, 2001), which would sink down to these depths. Buzas and Sen Gupta, (1982) ordered *Gs. ruber* and *Gs. sacculifer* as shallow dwellers (0-65m), *O. universa* an intermediate dweller (65-85m) and *T. truncatulinoides* a deep dweller (105-200m). The findings presented here would generally agree with these, apart from *O. universa*, which is very close to the shallow dwellers in terms of $\delta^{18}O$ inferred depth. Unlike Ortiz *et al.* (1996) *Gr. scitula* and not *Gd. hexagona* was the deepest dwelling foraminifera, but this may be due to; plankton tows rather than sediment core top samples being utilised, or differences in water column structure and nutrient availability in the different ocean basins studied (Indian Ocean this study, Pacific Ocean sediments, Ortiz *et al.*, 1996), or a lack of larger *Gd. hexagona* specimens present in this study.

The $\delta^{18}O$ size trends provide insight into ontogenetic ecological trends assuming that different test sizes of a particular species correspond to different growth life stages (Brummer *et al.*, 1987). Correlation between $\delta^{18}O$ and test size indicates a change in depth habitat through ontogeny (as argued by Emiliani 1954; Bé 1982). *Globorotalia scitula*, *T. truncatulinoides*, *Gr. tumida* (encrusted), *Gg. bulloides* and to a lesser extent *Gd. hexagona* all display a positive correlation between $\delta^{18}O$ and size, suggesting a shift to deeper, cooler water in adult (larger) stages, which is consistent with previous findings (Hemleben *et al.*, 1989; Lohmann and Schweitzer, 1990; Schiebel and Hemleben, 2000; Itou *et al.*, 2001). These generally deeper dwelling species tend to have longer reproductive cycles and are known to vary their depth through their differing life stages (Hemleben *et al.*, 1989). The groupings within *T. truncatulinoides* $\delta^{18}O$ values suggest that the smaller (<250 μm) pre-adult forms lived near the bottom of the surface mixed layer, whereas the larger (>250 μm) adult forms migrated to a deeper habitat close to that of *Gr. scitula*. This depth related size trend has also been observed by Mulitza *et al.* (1997) in subtropical waters, but not in tropical waters. Lohmann and Schweitzer (1990) have suggested that *T. truncatulinoides* requires water column conditions where there is deep mixing and low-density stratification to introduce juveniles (pre-calcification stage, as the isotopes do not show any deeper water signal) from the deep into surface waters. The monsoon season in the summer months leads to

intense upwelling (Schott *et al.*, 2009) at the study site, which would provide the mechanism needed to move the juveniles to surface waters. Another possibility is that deep mixing allows the adults to move to surface water before undergoing gametogenesis; however they must not calcify at this stage as no surface water isotope signal is seen in these adult forms. The second suggestion appears more likely, as reproduction in planktonic foraminifera, in general, follows that of primary production (Berger *et al.*, 1988; Antoine *et al.*, 1996; Schiebel and Hemleben, 2005). During the upwelling season's primary productivity would increase, due to the increased supply of nutrients from the deep ocean.

4.3.3. Carbon isotopes and planktonic foraminifera symbiosis

Globigerinoides ruber, *Gs. sacculifer*, *Ge. siphonifera* and *O. universa* clearly show a strong positive correlation between $\delta^{13}C$ and test size throughout the full range of test sizes available, as well as a lack of a size trend in $\delta^{18}O$. Based on the model shown in Figure 4.1 this trend is interpreted as the geochemical signature of photosymbiosis. The absence of this pattern in *Gg. bulloides*, *Gr. tumida* (encrusted), *Gr. ungulata*, *Gr. scitula* and *T. truncatulinoides* indicates a non-symbiotic ecology. These data are in general agreement with what is known about the biology of these modern species (Emiliani, 1954; Berger *et al.*, 1978; Shackleton and Vincent, 1978; Erez and Honjo, 1981; Spero and DeNiro, 1987; Hemleben *et al.*, 1989; Spero and Lea, 1993; Ravelo and Fairbanks, 1995) but there are some interesting deviations from the existing isotope model for some species.

The $\delta^{13}C$ of *Gs. sacculifer* presented here shows a decrease at terminal life stages. This differs from laboratory studies that show no terminal excursion (Spero and Lea, 1993). The laboratory data, however used specimens that lack a 'sac like' final chamber and when specimens with a 'sac like' final chamber were analysed 'younger' (24hr old) specimens show more enriched $\delta^{13}C$ values compared to 'older' (3-5 days old) specimens and may account for the terminal excursion seen in the larger older specimens here. Lohmann, (1995) demonstrated that *Gs. sacculifer* grows in the surface waters until it sinks to deeper water and adds a secondary calcite layer. However, the

$\delta^{18}O$ values do not suggest migration to deeper waters. Instead another possibility for the reduced $\delta^{13}C$ values in the final life stages may reflect ingestion or loss of symbionts before gametogenesis, as previously suggested by Houston and Huber (1998).

Although *Ge. siphonifera* was not separated out into its two types (designated Type I and Type II based on morphological, genetic, physiological and test geo-chemical differences [Huber *et al.*, 1997; Bijma *et al.* 1998]) before analysis the two types can be distinguished in the data presented here (Figure 4.4 and Figure 4.3). Laboratory culture experiments found Type II is enriched in ^{13}C and ^{18}O compared to Type I, which is also seen in the results presented here. The less steep $\delta^{13}C$ / test size trend of the larger Type I is interpreted as being the result of overall lower symbiont density, hence lower photosynthetic rates and facultative rather than obligate symbiont nature, when compared to Type II (Bijma *et al.* 1998). This maybe the reason why average $\delta^{18}O$ *Ge. siphonifera* inferred temperatures place this foraminifera close to the chlorophyll maximum (Figure 4.2; Figure 4.5) where food availability is highest for a species not as dependent on its symbionts.

4.3.4. Metabolic fractionation influences on carbon isotopes

Positive correlations between test size and $\delta^{13}C$ values in mixed layer species can be explained by photosymbiosis. Size trends in deeper living, asymbiotic species need further explanation. Hemleben and Bijma, (1994) and Lohmann, (1995) show that foraminifera often migrate to deeper levels of the water column through ontogeny. Juveniles of *Gr. tumida* and *T. truncatulinoides* often start out in surface waters and have similar $\delta^{18}O$ as mixed layer species before migrating to deeper waters as they become adults. The $\delta^{13}C$ / size trend observed in known asymbiotic species *Gg. bulloides*, *Gr. scitula Gr. tumida* (encrusted) and *T. truncatulinoides* can't be explained by vertical migrations during ontogeny.

Although there are large $\delta^{18}O$ / size trends for these species and a tendency towards cooler $\delta^{18}O$ temperatures at larger test sizes, the trend in carbon isotopes goes in the

opposite direction to the predicted pattern if depth were the cause (Kroopnick, 1985). D'Hondt and Zachos (1998) and Spero and Lea (1996) also argue that the $\delta^{13}C$ trend is not caused by the formation of calcite at different depth and suggest kinetic or metabolic fractionation instead. The hypothesis of a strong size related negative vital effect in small planktonic foraminifera results from the decreasing influence of metabolic (isotopically light) CO_2 on test calcite $\delta^{13}C$ through ontogeny (Berger *et al.*, 1978). Support for this interpretation comes from laboratory experiments that show that small (young) foraminifera (<150μm) tend to grow rapidly and have high metabolic activity (Bé, 1982) leading to increased kinetic fractionation and an increase in respired CO_2 being incorporated into the test. Larger (older) foraminifera tend to grow more slowly and show decreased metabolic activity with less kinetic fractionation (Berger *et al.*, 1978; Kahn, 1979; Wefer and Berger, 1991; Ravelo and Fairbanks, 1995; Ortiz *et al.*, 1996; Spero *et al.*, 1997).

Lohmann (1995) however found that when analysis was restricted to primary test calcite there was no $\delta^{13}C$ / size trend, and therefore concluded that the trend was the result of the addition of secondary (crust) calcite only. This secondary calcite is added in some species of planktonic foraminifera, either before it undergoes gametogenesis or simply added at greater depths (Hemleben *et al.*, 1989; Schiebel and Hemleben, 2005). However, the species investigated here displayed no visible additional crust (except *Gr. tumida*, which was encrusted throughout the size ranges analysed). Elderfield *et al.* (2002) noted a continued trend in $\delta^{13}C$ with increasing size, far above 150 μm, for *T. truncatulinoides*. This trend was suggested to reflect a move to equilibrium with seawater $\delta^{13}C$ values, as larger individuals grow slower (Elderfield *et al.*, 2002). This trend showed a 0.5 ‰ change in $\delta^{13}C$ over a size increase of 288 μm (212 to 500 μm) for *T. truncatulinoides*, (Elderfield *et al.*, 2002). However, in the data presented here an increase of 1.6 ‰ was noted over a 200 μm size increase, which was most prominent in the smaller size fractions, suggesting that despite this continued $\delta^{13}C$ / size trend in larger individuals of some non-symbiotic species, this trend generally tails off as the individual grows larger. Despite these challenges, metabolic fractionation appears to be the most favourable explanation for these $\delta^{13}C$ disequilibrium effects in non-symbiotic species. The $\delta^{13}C$ / size trend for these species is generally stronger in the smaller

specimens (which would not be expected to have a gametogenic crust) and tends to level off with increasing test size, though not always at the 150 μm cut off point. This would suggest metabolic fractionation, as the model presented in Figure 4.1 demonstrates that metabolic fractionation effects decrease with increasing size. This metabolic fractionation affect does not mean that depth migration is not also occurring, as $\delta^{18}O$ do indicate some change, but that metabolic fractionation rather than changing depth habitat is an overriding influence on $\delta^{13}C$ values. These results indicate the importance of metabolic fractionation in a number of species that are not mentioned in the current literature, due to a lack of studies on smaller test sizes.

4.3.5. Determining the overriding disequilibrium effect

The positive correlation of $\delta^{13}C$ with test size is seen in both photosymbiosis and metabolic fractionation disequilibrium effects. However, there is an important need especially in the fossil record, where ecologies cannot be observed, to distinguish between them. This can be achieved in three main ways: first by assessing where the greatest $\delta^{13}C$ test size trend exists, i.e. if this is greatest in the smaller size fractions typically below 150 μm, after which $\delta^{13}C$ values start to level off then metabolic fractionation is most likely. However, if the $\delta^{13}C$ test size trend continues throughout all the different test sizes (except perhaps for terminal life stages) particularly above 150 μm, then photosymbiosis is the likely cause. Secondly, a photosymbiotic $\delta^{13}C$ test size trend will plot above any non symbiotic species present that inhabit a similar depth. Thirdly, on a $\delta^{13}C$ / $\delta^{18}O$ cross plot symbiotic species will be enriched compared to $\delta^{13}C$ equilibrium values and species subject to metabolic fractionation will be depleted.

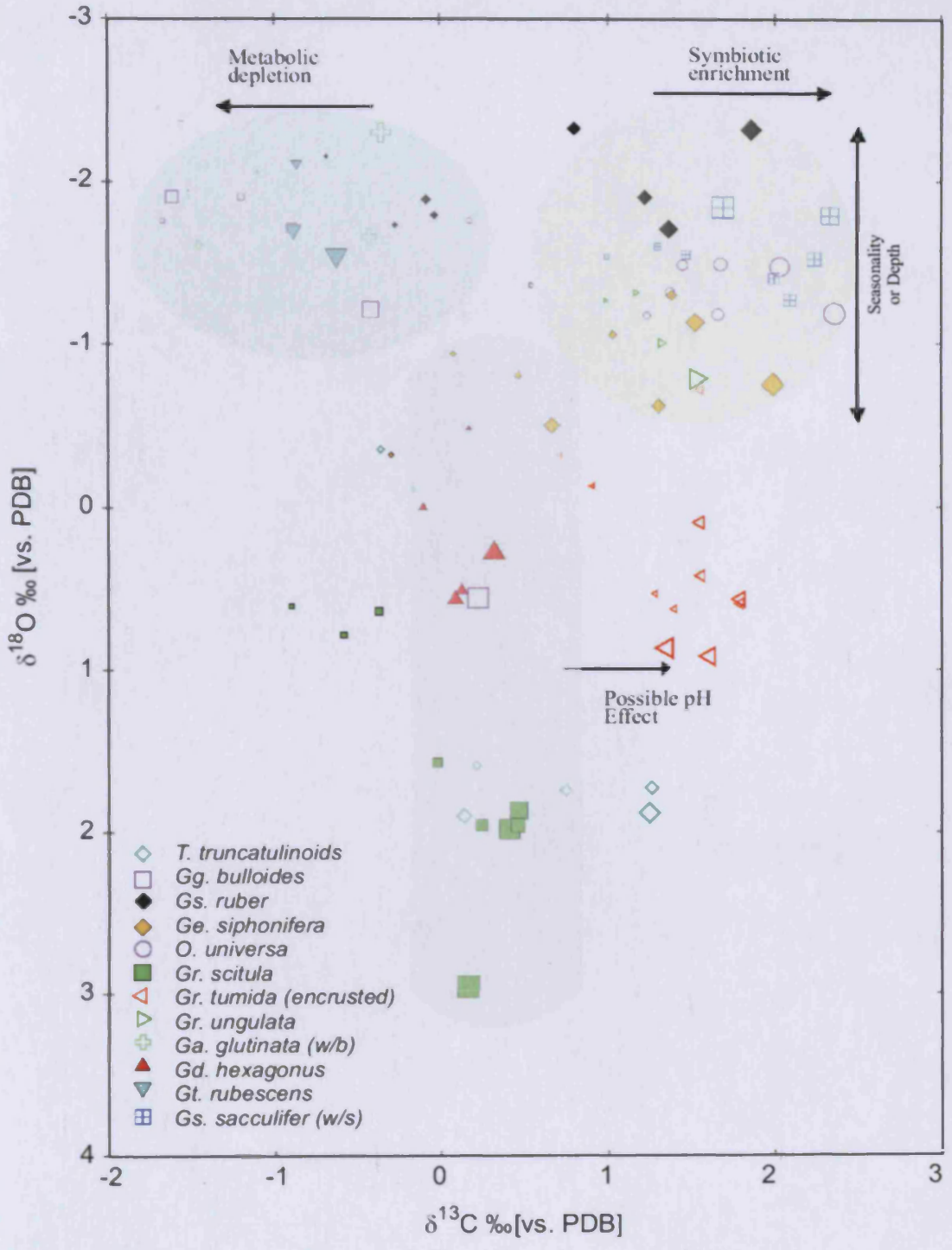

Figure 4.6 - Carbon isotope ($\delta^{13}C$) - oxygen isotope ($\delta^{18}O$) cross plots for 12 species of extant planktonic foraminifera based on interpretations of Pearson and Wade (2009). A possible pH effect is identified in this way for the first time. Genera abbreviations as Figure 4.3. w/s = with sac like final chamber, w/b = with bulla. Note that different symbol sizes are used to denote (approximately) separate test sizes of individual species (Table 4.1).

In Figure 4.6 the entire $\delta^{13}C$ and $\delta^{18}O$ data set for the 12 species studied, including measurements of the separate test size classes of each species are plotted on a single cross plot. Similar to the larger Oligocene multispecies data set, produced by Pearson and Wade (2009), ecological strategies and disequilibrium effects can be distinguished from a $\delta^{13}C$ / $\delta^{18}O$ cross plot. Some foraminifera (*Gg. bulloides*, *Gt. rubescens* (pink), *Ga. glutinata* and smaller *G. ruber*) congregate into the top left corner and can be said to be out of $\delta^{13}C$ equilibrium due to metabolic fractionation. Those in the top right hand corner are out of $\delta^{13}C$ equilibrium due to reliance on symbiotic algae. The vertical variation in $\delta^{18}O$ of these mixed layer species could be accounted for by calcification in different seasons or by changes in preferred depth habitat. An equilibrium line would be much harder to draw in the data presented here compared to that of Pearson and Wade (2009), as many species seem to be out of equilibrium with respect to $\delta^{13}C$ values, especially *Gr. tumida*, and to a lesser extent *T. truncatulinoides*, which is enriched by ~1.0 ‰ compared to *Gr. scitula* and *Gd. hexagonus*.

Globorotalia tumida is an interesting case as the only planktonic foraminifera to be analysed with a heavy calcite crust that may have contributed to the non equilibrium $\delta^{13}C$ values. The $\delta^{18}O$ inferred temperature depth places this species at the shallow oxygen minimum zone (OMZ) (Figure 4.5) which may also affect its isotope chemistry. The OMZ is associated with a significant decrease in pH (of >0.5; Park, 1966; Libes, 1992; Chen, 1994) due to the release and subsequent hydrolysis of CO_2 as organic matter is remineralised. Laboratory experiments have found that as pH and / or carbonate ion concentrations increase planktonic foraminiferal calcite $\delta^{13}C$ and to a lesser extent $\delta^{18}O$ values decrease (Spero *et al.*, 1997; Bijma *et al.*, 1999) and the reverse is also true that as pH decreases $\delta^{13}C$ and $\delta^{18}O$ values increase (Bowen *et al.*, 2004). The effect is species specific and appears to be the result of a combination of kinetic and metabolic fractionation processes (Bijma et al., 1999). The OMZ sees a decrease of at least 0.5 pH, which according to culture studies (Bijma et al., 1999; Uchikawa and Zeebe, 2010) would be sufficient to account for the 1.0 ‰ enrichment in $\delta^{13}C$ values of *Gr. tumida*. This $\delta^{13}C$ enrichment in a deep dweller may provide a means of identifying potential OMZ species in fossil data. The other species (*T.*

truncatulinoides and ***Gd. hexagonus***), which $\delta^{18}O$ temperature reconstructions suggest lived close to the OMZ do not appear to be as significantly affected by this pH affect. ***Globorotaloides hexagonus***, produces much smaller test sizes compared to *Gr. tumida* and it is possible that any pH effect is counteracted by metabolic influences, which may account for the lack of any pH influence in this OMZ dwelling species. ***Truncorotalia truncatulinoides***, according to $\delta^{18}O$ inferred depth and previous studies (Lohmann, 1995), spends less time at the OMZ and would be less affected by any pH influence. In addition to this the δc inferred depth profile shows *T. truncatulinoides* predominantly calcites deeper than the OMZ (Figure 4.5 – B). In contrast, *Gr. tumida*, $\delta^{18}O$ inferred depth places this species at the OMZ for the majority of its life.

4.4. Summary

- Hydrographic conditions demonstrate a typical sub-tropical oligotrophic site, with thermal stratification and permanent thermocline.
- Consistent with previous studies $\delta^{18}O$ inferred depths place *Gs. ruber* as the shallowest species and *Gr. scitula* as the deepest dwelling planktonic foraminifera.
- In *Gs. ruber*, *Gs. sacculifer*, *Ge. siphonifera* and *O. universa* there are strong positive correlations between $\delta^{13}C$ and test size trend which is interpreted as the geochemical signature of photosymbiotic influence in accordance with their known ecology.
- The $\delta^{13}C$ / size trends, particularly in smaller size fractions, found in *Gg. bulloides*, *Gr. scitula* *Gr. tumida* (encrusted) and *T. truncatulinoides*, which are known asymbiotic taxa, can be explained by metabolic fractionation. This causes the smaller sizes of each species to be depleted in ^{13}C. This depletion reduces with increasing size which gives the overall trend that resembles symbiotic enrichment. However, it can be distinguished from symbiotic trends as it occurs in the smaller size fractions typically below 150 μm, after which $\delta^{13}C$ values start to level off.
- *Globigerina bulloides*, *Gr. scitula*, *T. truncatulinoides*, *Gr. tumida* (encrusted), *Gr. ungulata* and *Gd. hexagonus* show a positive correlation between $\delta^{18}O$ and test size indicating migration to deeper waters through ontogeny for these species.
- The decreased pH values at the OMZ can lead to enrichment in $\delta^{13}C$, this is especially true for *Gr. tumida* (encrusted). This $\delta^{13}C$ enrichment in a deep dweller may provide a means of identifying potential OMZ species in fossil data.

5. Ecology of Paleocene Planktonic Foraminifera and the Evolutionary Radiation of Photosymbiosis

This chapter focuses on a number of time slices taken throughout the recovery period of the carbon system in the early Paleocene from Site 1262. Disagreement between planktonic and benthic foraminifera data has lead to questions about the value of planktonic foraminifera to accurately record seawater chemistry during this time interval. Carbon and oxygen stable isotope trends in a range of size fractions for thirteen species of Paleocene planktonic foraminifera, along with interpretations from Chapter 4, are used to understand the ecologies of these species and evaluate any disequilibrium effects that may be occurring.

5.1. Introduction

The K/Pg mass extinction seriously affected the marine ecosystem, causing widespread extinctions and a major disturbance to the carbon system. Among the carbon system responses, foraminiferal carbon stable isotopes ($\delta^{13}C$) show a collapse in the planktonic to benthic $\delta^{13}C$ gradient ($\Delta\delta^{13}C$), which has been interpreted as evidence for a significant reduction in ocean biological carbon pumping (D'Hondt *et al.*, 1996; Adams *et al.*, 2004; Coxall *et al.*, 2006; Alegret and Thomas, 2007; Ridgwell, unpublished data). The $\Delta\delta^{13}C$ proxy relies on the ability of different species of planktonic foraminifera to faithfully 'sample' ambient dissolved inorganic carbon (DIC) $\delta^{13}C$.

Potential problems with this interpretation are changes in planktonic foraminifera depth habitats during ontogeny and isotopic disequilibrium effects related to foraminiferal biology, that can affect the isotopic composition of the test calcite (Emiliani, 1954; Berger *et al.*, 1978; Kahn, 1979; Bé, 1982; Turner, 1982; McConnaughey, 1989a,b; Spero and Williams, 1989; Spero *et al.*, 1991; Ortiz *et al.*, 1996; Cooke and Rohling, 1999; Bijma *et al.*, 1999; see Chapter 4 for details). Post death diagenesis is an additional factor that can influence isotopic values (Corfield *et al.*, 1990; Spero, 1992;

Pearson *et al.*, 2001; Sexton *et al.*, 2006). The problem of biologically controlled disequilibrium effects is especially relevant in the early Paleocene when an entirely new set of species evolved after mass extinction of Cretaceous assemblages at the K/Pg boundary (Sepkoski, 1998; Molina *et al.*, 1998; Olsson *et al.*, 1999; Coxall *et al.*, 2006).

Early Danian planktonic foraminifera assemblages include scarce K/Pg survivor taxa and a suite of small 'microperforate' opportunistic species that diversified in the immediate aftermath of the extinction. The first wave of 'macroperforate' species, that includes ancestors of the main Cenozoic phylogenetic clades, followed rapidly (within ~15 kyrs) behind (Olsson *et al.*, 1999; Coxall *et al.*, 2006). This morphological and taxonomic diversification has been studied in detail (Sepkoski, 1998; Molina *et al.*, 1998; Olsson *et al.*, 1999; Coxall *et al.*, 2006). However, the ecological and biological evolution of early Paleocene species is less well understood, such that there are currently gaps in our understanding of the influence of habitat and isotopic disequilibrium effects on important palaeoclimate tracer species.

The early Paleocene saw systematic changes in ecology as no Cretaceous symbiotic foraminifera survived the K/Pg event. Cenozoic photosymbiosis had to re-evolve from a few survivors and despite past work on photosymbiosis in the early to mid Paleocene (D'Hondt & Zachos, 1993; D'Hondt *et al.*, 1994; Norris, 1996; Kelly *et al.*, 1996) the exact timing and ancestor of photosymbiosis in the Early Cenozoic is still unclear. Norris (1996) looked at a range of Paleocene species and showed positive correlations between size and $\delta^{13}C$ developing after 61.0 Ma (Cande and Kent, 1995, age model) during the evolution of *Pr. inconstans* to *Pr. uncinata* and suggested this reflected photosymbiotic ecology. D'Hondt and Zachos (1993) suggested that very early Paleocene species (*Eoglobigerina eobulloides*, *Woodringina* sp and *Parvularugoglobigerina eugubina*) were photosymbiotic after noting a positive correlation between size and $\delta^{13}C$ in these species.

To help further investigate these uncertainties new $\delta^{13}C$ and $\delta^{18}O$ test size fraction measurements for multiple species of early Paleocene planktonic foraminifera are presented. Based on suites of data from nine time slices (Figure 5.1), the results detail

the evolution of planktonic foraminiferal depth ecologies and $\delta^{13}C$ signatures in the first four million years after the K/Pg mass extinction. In particular, (i) potential disequilibrium $\delta^{13}C$ effects in small (small species and the smaller sizes of typically larger species) foraminifera tests are examined, as occur in the immediate aftermath of the K/Pg, and (ii) the evolution of foraminiferal photosymbiosis, an ecological adaptation associated with enriched $\delta^{13}C$ in modern symbiotic analogues is assessed. The results provide insight into isotopic disequilibrium effects on foraminiferal $\delta^{13}C$ in early Paleocene species that will help constrain reconstructions of oceanic carbon cycling after a critical episode in life history.

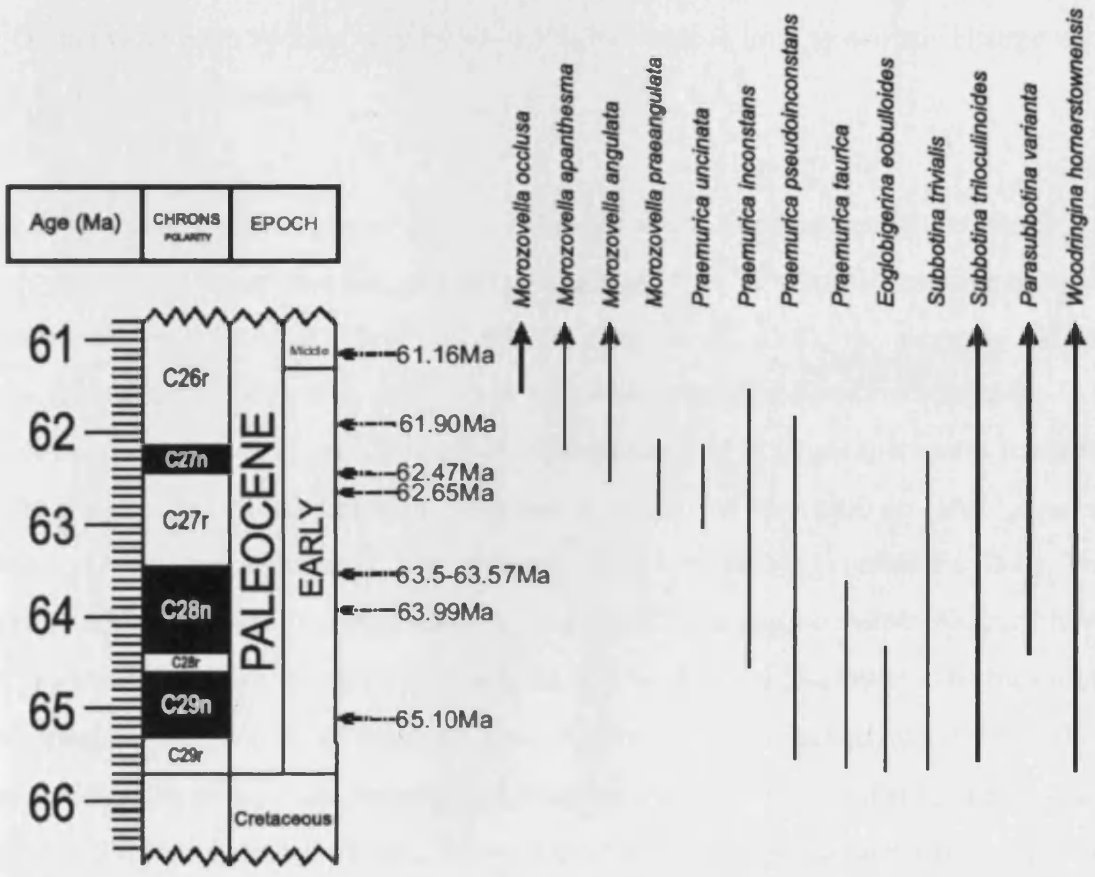

Figure 5.1 - Position of time slices in relation to age (Ma) based on the time scale from Westerhold *et al.*, (2008) with orbital chronology from Site 1262 and Paleocene planktonic foraminifera ranges for the species used in this study as observed from Site 1262.

5.2. Results

5.2.1. Oxygen isotope size fraction trends

Interspecies $\delta^{18}O$ offsets occur at all time intervals but the magnitude of the offsets change across test size-spectra over time. At 65.10 and 63.99Ma (Figure 5.2 A and B), planktonic $\delta^{18}O$ varies between 0.2 to -0.75‰ with *Subbotina* spp. *and E. eobulloides* having the highest values (0.2 to -0.2‰) and species with the smallest tests, i.e. *W. hornerstownensis* and *Pr. taurica*, registering lowest $\delta^{18}O$ values. In these early time slices $\delta^{18}O$ is almost identical for all species of *Praemurica* spp. across the range of test sizes. Values are negatively offset from *Subbotina/Parasubbotina* by ~0.1-0.3‰, except for *Pr. taurica* at 63.99 Ma, which is isotopically lighter again (Figure 5.2 B). Absolute $\delta^{18}O$ values for each species vary by +/- 0.3‰ but there is little systematic change with size in these oldest samples.

The $\delta^{18}O$-test size trajectories of *S. triloculinoides* and *P. varianta* remain relatively flat across the entire study interval, exhibiting the highest $\delta^{18}O$ values compared to other species (Figures 5.2 A-F). From 62.65 Ma (Figure 5.2 C-F), the negative offsets between of *Pr. inconstans/Pr. uncinata* and *Subbotina/Parasubbotina* increased to ~0.3-0.4‰ in specimens <150 μm. This offset further increased in larger specimens resulting in an inverse correlation between $\delta^{18}O$ and test size for tests 200 μm and larger in *Praemurica* sp. and *Morozovella* sp. between 62.47 - 61.90 Ma (Figures 5.2 D-F). The large specimens of *M. apanthesma, M. occlusa* and *M. angulata* (~250-300 μm) have the lowest $\delta^{18}O$ relative to other species in each time slice, ~0.5‰ lower even than mid-size specimens (150 μm) of the same species. *Pr. pseudoinconstans,* which is studied here for the first time, is the exception, exhibiting a $\delta^{18}O$ trajectory that is intermediate between *Pr. inconstans/uncinata, Morozovella* sp. and *Subbotina/Parasubotina.* At 61.90 Ma, *Pr. inconstans* $\delta^{18}O$ is higher than co-occurring *Morozovella* sp. over all test sizes, and exhibits a flat profile that is very similar to *Subbotina/Parasubbotina* (Figure 5.2 E).

$\delta^{18}O$ measurements for three additional time slices (Figure 5.3 A-C) that fall between 63.99-62.65 Ma on (Figure 5.2 B and C) show that the $\delta^{18}O$ trajectory of *Pr. inconstans* had become differentiated from *Pr. pseudoinconstans* by 63.57 Ma. At this time small individuals of *Pr. pseudoinconstans* have $\delta^{18}O$ that is similar to *S. trivialis,* but values decrease relative to this species in tests >200 μm.

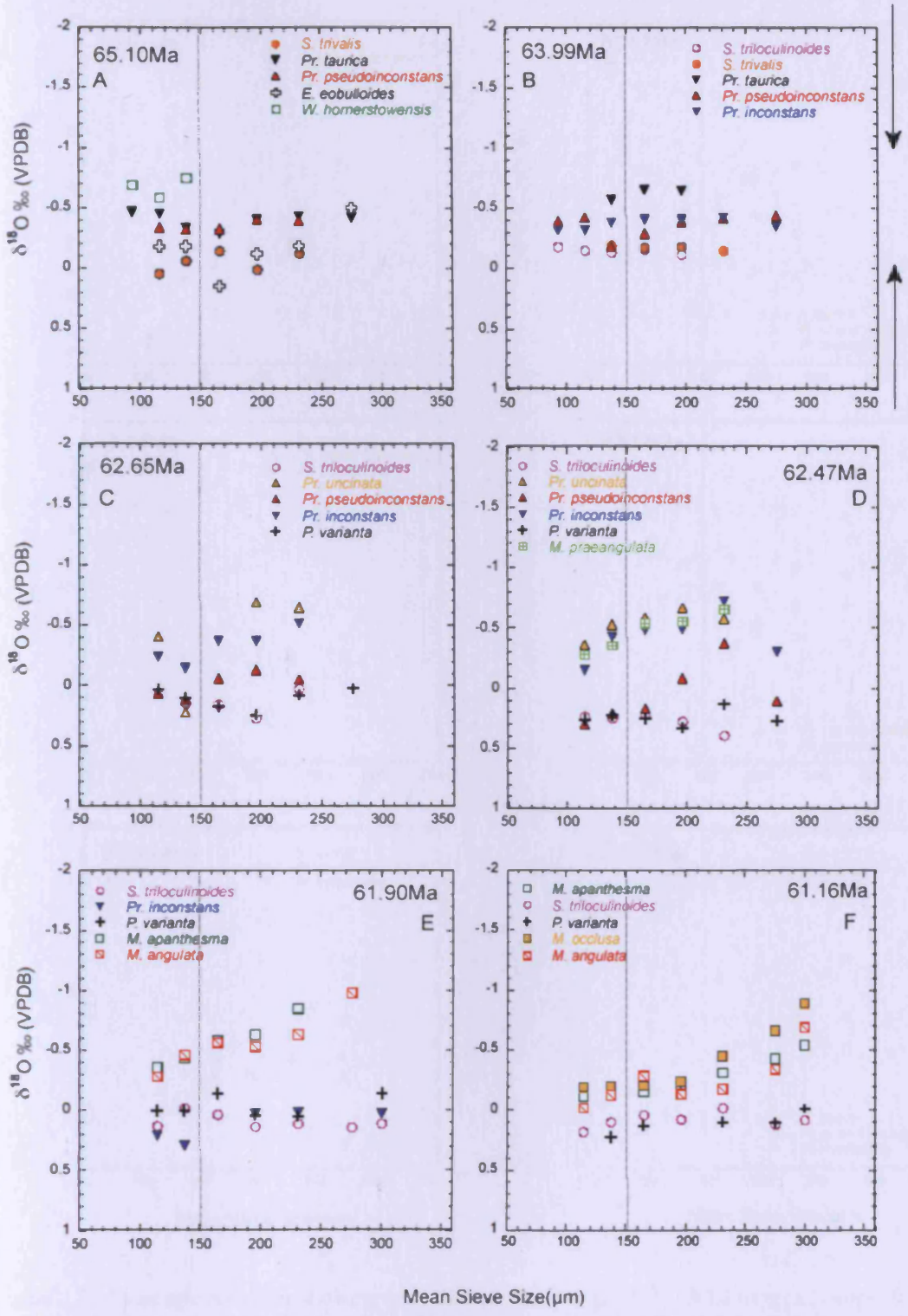

Figure 5.2 - Test size – oxygen isotope ($\delta^{18}O$) relationships for 6 time slices during the Paleocene from ODP site 1262. Ages are based on the time scale from Westerhold *et al.*, (2008) with orbital chronology from site 1262. Test size represents the average of the sieve size range. Genera abbreviations as follows M= *Morozovella*, Pr = *Praemurica*, S = *Subbotina*, P = *Parasubbotina*, E = *Eoglobigerina* and W = *Woodringina*. Arrows indicate position of Figure 5.3 close up time slices. Grey dashed line indicate approximate onset of adult ecology for planktonic foraminifera according to Brummer *et al.*, 1987.

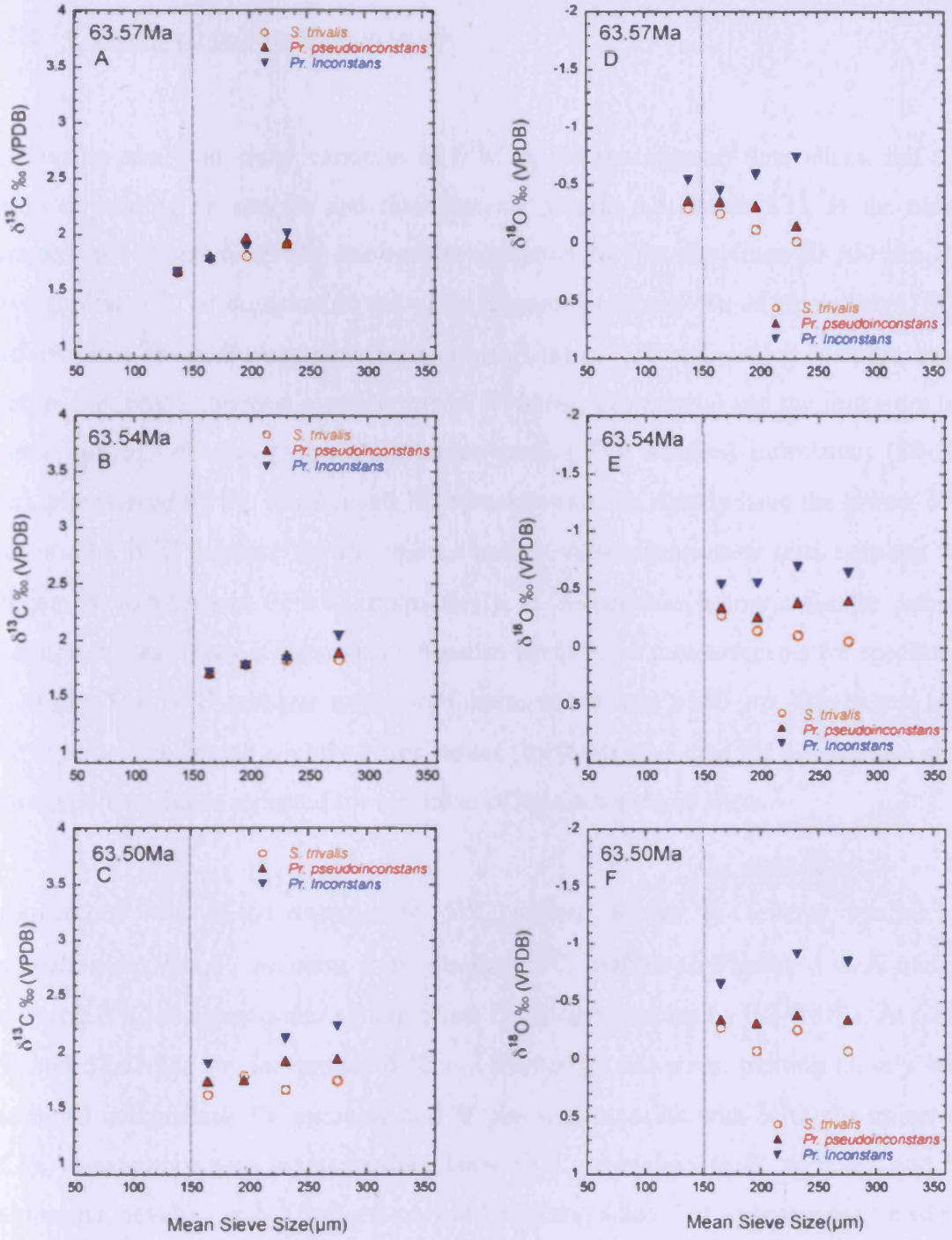

Figure 5.3 - Close up time slices showing test size – carbon isotope ($\delta^{13}C$) A-C/ oxygen isotope ($\delta^{18}O$) D-E relationships from between 63.99 and 62.65Ma (arrows in Figure 5.2 and 5.4). Ages are based on the time scale from Westerhold *et al.*, (2008) with orbital chronology from site 1262. Test size represents the average of the sieve size range. Genera abbreviations as Figure 5.2. Grey dashed line indicate approximate onset of adult ecology for planktonic foraminifera according to Brummer *et al.*, 1987.

5.2.2. Carbon isotope size fraction trends

All species analysed show variation in $\delta^{13}C$ in the investigated time slices, but this varies depending on species and time interval (Figure 5.4, Table 5.1). In the oldest samples (65.10 and 63.99Ma) the species analyzed vary in size from 80-300 μm and have similar $\delta^{13}C$ at comparable test sizes (Figure 5.4 A and B). At these times, $\delta^{13}C$ and test size are positively correlated in small tests <150 μm, which includes small species (i.e. post extinction recovery taxon *W. hornerstownensis*) and the immature life stages (juvenile-neanic) of typically larger species. The smallest individuals (80-106 μm), represented by *Pr. taurica* and *W. hornerstownensis*, clearly have the lowest $\delta^{13}C$ values. The $\delta^{13}C$ increase for *Pr. taurica* and *W. hornerstownensis* tests between 80-150 μm is ~0.5 ‰ and 0.33 ‰, respectively. *E. eobulloides* follow a similar pattern, although the trajectory is abbreviated because we have no measurements for specimens <100 μm. This $\delta^{13}C$–test size trajectory flattens out in tests >150 μm. The largest tests (>250 μm) often record slightly lower values (by 0.1-0.2‰) than the penultimate size-class, a pattern that is repeated for a number of taxa across time slices.

From 62.65 Ma clear interspecies $\delta^{13}C$ offsets appear in several species. *S. triloculinoides* and *P. varianta* show similar $\delta^{13}C$ profiles to Figures 5.4, A and B, however, $\delta^{13}C$ of *Praemurica* sp. are offset from these species by 0.3-0.8 ‰. At 62.65 Ma and 62.47 Ma *Pr. inconstans* $\delta^{13}C$ is offset at all test sizes, plotting closely with presumed descendants *Pr. uncinata* and *M. praeangulata*. As with $\delta^{18}O$, the trajectory of *Pr. pseudoinconstans* is intermediate between *S. triloculinoides/P. varianta*, and *Pr. inconstans*, developing $\delta^{13}C$ offsets only at larger test sizes. The appearance of positive $\delta^{13}C$ offsets is accompanied by the development of a further strong positive correlation between test size and $\delta^{13}C$ in tests >150 μm in *Praemurica* and *Morozovella* (Figure 5.4 C-F). *Pr. pseudoinconstans*, *Pr. inconstans* and *Pr. uncinata* show progressive $\delta^{13}C$ enrichment of ~0.2-0.3 ‰ in tests >150 μm. This trend increases in the 61.90 Ma and 61.16 Ma time slices to produce $\delta^{13}C$ offsets from 150 μm-sized specimens of ~1.5 ‰ between *S. triloculinoides* and *M. occlusa* in the largest tests (~300 μm) (Figures 5.4 E

and F). ***Pr. inconstans***, which was the last surviving species of the genus, reverted back to a ***Subbotina/Parasubbotina*** type trajectory by 61.90 Ma (Figure 5.4 E).

The $\delta^{13}C$ measurements for *S. trivialis*, *Pr. pseudoinconstans* and *Pr. inconstans* in the three additional time slices between Figure 5.4B and C (Figure 5.3; Table 5.2) show that the $\delta^{13}C$-test size relationship characteristic of *Praemurica* and *Morozovella* developed simultaneously in *Pr. pseudoinconstans* and *Pr. inconstans* between 63.54-63.50 Ma. The $\delta^{13}C$ offset from *S. trivialis* in *Pr. inconstans* was larger than in *Pr. psuedoinconstans* across the range of test sizes, such that the two morphotypes have clearly distinguishable isotopic signatures from 63.50 Ma (Figure 5.3).

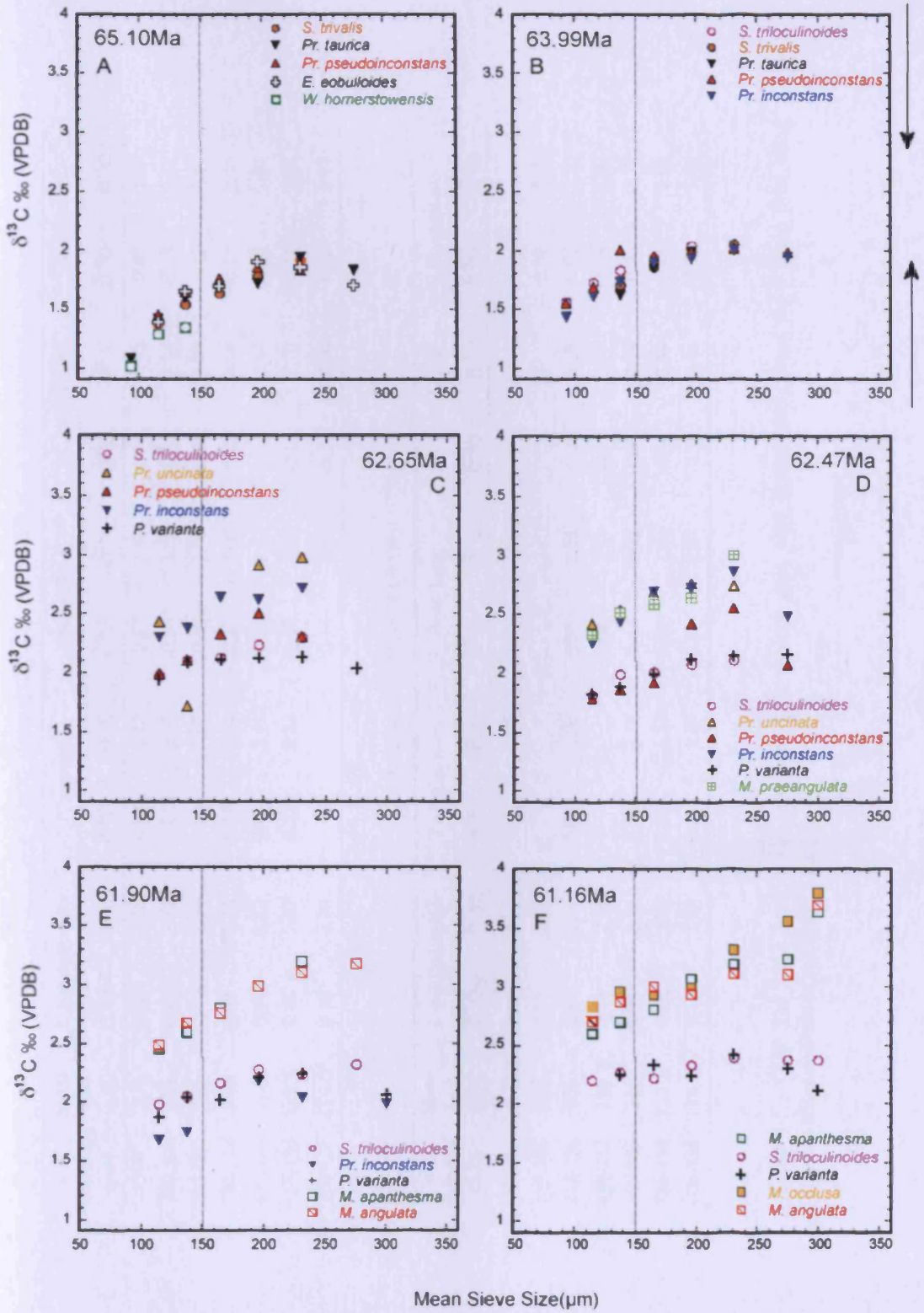

Figure 5.4 - Test size – carbon isotope ($\delta^{13}C$) relationships for 6 time slices during the Paleocene from ODP site 1262. Ages are based on the time scale from Westerhold *et al.*, (2008) with orbital chronology from site 1262. Test size represents the average of the sieve size range. Genera abbreviations as Figure 5.2. Arrows indicate position of Figure 5.3 close up time slices. Grey dashed line indicate approximate onset of adult ecology for planktonic foraminifera according to Brummer *et al.*, 1987.

1262C-10H-5, 187.26 cm, 61.16 (Ma)

Size Fraction (μm)	Mean Size (μm)	*S. triloculinoides*		*P. varianta*		*M. occlusa*		*M. apanthesma*		*M. angulata*	
		$\delta^{18}O$	$\delta^{13}C$	$\delta^{18}O$	$\delta^{13}C$	$\delta^{18}O$	$\delta^{13}C$	$\delta^{18}O$	$\delta^{13}C$	$\delta^{18}O$	$\delta^{13}C$
>300	300	0.08	2.38	-0.01	2.12	-0.89	3.80	-0.54	3.65	-0.69	3.69
250-300	275	0.12	2.37	0.11	2.30	-0.66	3.56	-0.43	3.24	-0.34	3.11
212-250	231	-0.02	2.39	0.10	2.42	-0.45	3.32	-0.31	3.20	-0.17	3.11
180-212	196	0.08	2.33	-0.19	2.24	-0.23	3.00	-0.22	3.04	-0.13	2.96
150-180	165	0.04	2.22	0.13	2.33	-0.20	2.92	-0.13	2.84	-0.28	2.97
125-150	137.5	0.10	2.27	0.22	2.24	-0.18	2.96	-0.13	2.70	-0.14	2.87
106-125	114.5	0.18	2.20			-0.18	2.83	-0.12	2.60	-0.02	2.70

1262B-20H-3, 193.27 cm, 61.9 (Ma)

Size Fraction (μm)	Mean Size (μm)	*S. triloculinoides*		*Pr. inconstans*		*P. varianta*		*M. apanthesma*		*M. angulata*	
		$\delta^{18}O$	$\delta^{13}C$	$\delta^{18}O$	$\delta^{13}C$	$\delta^{18}O$	$\delta^{13}C$	$\delta^{18}O$	$\delta^{13}C$	$\delta^{18}O$	$\delta^{13}C$
>300	300	0.11	2.04	0.03	1.98	-0.14	2.06				
250-300	275	0.14	2.32							-0.98	3.18
212-250	231	0.11	2.23	0.02	2.03	0.05	2.24	-0.85	3.18	-0.63	3.12
180-212	196	0.14	2.28			0.04	2.21	-0.63	2.99	-0.53	2.99
150-180	165	0.04	2.16	0.03	2.18	-0.14	2.02	-0.58	2.79	-0.57	2.77
125-150	137.5	-0.02	2.05	0.29	1.74	0.00	2.04	-0.44	2.59	-0.46	2.68
106-125	114.5	0.13	1.98	0.21	1.68	0.01	1.87	-0.34	2.46	-0.29	2.48

Table 5.1 - ODP Site 1262 Sample horizons and stable isotope data used in this study from the 6 main time slices (genera abbreviations as in Figure 5.2).

1262C-11H-3, 198.09 cm, 62.47 (Ma)

Size Fraction (μm)	Mean Size (μm)	*S. triloculinoides*		*Pr. uncinata*		*Pr. pseudoinconstans*		*Pr. inconstans*		*P. varianta*		*M. praeangulata*	
		$\delta^{18}O$	$\delta^{13}C$	$\delta^{18}O$	$\delta^{13}C$	$\delta^{18}O$	$\delta^{13}C$	$\delta^{18}O$	$\delta^{13}C$	$\delta^{18}O$	$\delta^{13}C$	$\delta^{18}O$	$\delta^{13}C$
250-300	275					0.11	2.07	-0.30	2.48	0.27	2.17		
212-250	231	0.39	2.11	-0.58	2.75	-0.37	2.55	-0.71	2.86	0.13	2.15	-0.66	3.00
180-212	196	0.28	2.07	-0.66	2.76	-0.08	2.42	-0.50	2.73	0.33	2.12	-0.54	2.64
150-180	165	0.22	2.01	-0.56	2.66	0.17	1.93	-0.50	2.69	0.26	1.99	-0.54	2.60
125-150	137.5	0.25	1.99	-0.53	2.53	0.21	1.87	-0.42	2.44	0.23	1.88	-0.36	2.51
106-125	114.5	0.24	1.81	-0.34	2.40	0.30	1.79	-0.15	2.25	0.26	1.83	-0.29	2.33

1262C-11H-4, 199.29 cm, 62.65 (Ma)

Size Fraction (μm)	Mean Size (μm)	*S. triloculinoides*		*Pr. uncinata*		*Pr. pseudoinconstans*		*Pr. inconstans*		*P. varianta*	
		$\delta^{18}O$	$\delta^{13}C$	$\delta^{8}O$	$\delta^{13}C$	$\delta^{18}O$	$\delta^{13}C$	$\delta^{18}O$	$\delta^{13}C$	$\delta^{18}O$	$\delta^{13}C$
250-300	275									0.03	2.04
212-250	231	0.03	2.30	-0.64	2.98	-0.05	2.31	-0.52	2.72	0.08	2.13
180-212	196	0.27	2.23	-0.69	2.91	-0.13	2.50	-0.37	2.62	0.24	2.13
150-180	165	0.16	2.12			-0.06	2.32	-0.37	2.64	0.18	2.11
125-150	137.5	0.15	2.10	0.22*	1.71*	0.12	2.10	-0.15	2.37	0.10	2.09
106-125	114.5	0.06	1.97	-0.40	2.43	0.07	1.99	-0.24	2.30	0.03	1.94

Table 5.1 – Continued. * indicates erroneous data which has been excluded from interpretation.

1262C-12H-4, 207.39 cm, 63.99 (Ma)

Size Fraction (μm)	Mean Size (μm)	*S. trivalis*		*S. triloculinoides*		*Pr. taurica*		*Pr. pseudoinconstans*		*Pr. inconstans*	
		$\delta^{18}O$	$\delta^{13}C$	$\delta^{8}O$	$\delta^{13}C$	$\delta^{18}O$	$\delta^{13}C$	$\delta^{18}O$	$\delta^{13}C$	$\delta^{18}O$	$\delta^{13}C$
250-300	275							-0.44	1.98	-0.35	1.94
212-250	231	-0.15	2.05					-0.42	2.01	-0.42	2.01
180-212	196	-0.18	1.98	-0.11	2.03	-0.65	1.98	-0.39	1.99	-0.41	1.93
150-180	165	-0.17	1.86	-0.16	1.93	-0.66	1.85	-0.29	1.95	-0.41	1.90
125-150	137.5	-0.19	1.70	-0.13	1.83	-0.57	1.63	-0.18	2.00	-0.38	1.73
106-125	114.5			-0.15	1.72			-0.42	1.69	-0.32	1.61
80-106	93			-0.18	1.56			-0.39	1.55	-0.32	1.44

1262B-22H-3-214-958 cm, 65.1 (Ma)

Size Fraction (μm)	Mean Size (μm)	*E. eobulloides*		*W. hornerstowensis*		*S. trivalis*		*P. pseudbulloides*		*Pr. taurica*		*Pr. pseudoinconstans*	
		$\delta^{18}O$	$\delta^{13}C$	$\delta^{18}O$	$\delta^{13}C$	$\delta^{8}O$	$\delta^{13}C$	$\delta^{18}O$	$\delta^{13}C$	$\delta^{18}O$	$\delta^{13}C$	$\delta^{18}O$	$\delta^{13}C$
250-300	275									-0.42	1.84		
212-250	231	-0.19	1.86			-0.12	1.91	-0.46	1.88	-0.43	1.94		
180-212	196	-0.12	1.90			0.01	1.78	-0.07	1.93	-0.40	1.72	-0.40	1.85
150-180	165	0.15	1.70			-0.14	1.63	-0.31	1.82	-0.29	1.68	-0.32	1.76
125-150	137.5	-0.18	1.65	-0.75	1.35	-0.06	1.54	-0.30	1.63	-0.34	1.60	-0.32	1.65
106-125	114.5	-0.18	1.39	-0.58	1.29	0.05	1.37			-0.45	1.42	-0.34	1.45
80-106	93			-0.69	1.02					-0.47	1.08		

Table 5.1 - Continued

1262C-12H-2, 204.81 cm, 63.50 (Ma)							
Size Fraction (μm)	Mean Size (μm)	*Pr. inconstans*		*Pr. pseudoinconstans*		*S.trivalis*	
		$\delta^{13}C$	$\delta^{18}O$	$\delta^{13}C$	$\delta^{18}O$	$\delta^{13}C$	$\delta^{18}O$
250 - 300	275	2.23	-0.85	1.93	-0.34	1.74	-0.07
212 - 250	231	2.12	-0.92	1.92	-0.38	1.66	-0.26
180 - 212	196	1.89	-0.65	1.74	-0.31	1.79	-0.07
150 - 180	165			1.74	-0.34	1.62	-0.28

1262C-12H-2, 204.99 cm, 63.54 (Ma)							
Size Fraction (μm)	Mean Size (μm)	*Pr. inconstans*		*Pr. pseudoinconstans*		*S.trivalis*	
		$\delta^{13}C$	$\delta^{18}O$	$\delta^{13}C$	$\delta^{18}O$	$\delta^{13}C$	$\delta^{18}O$
250 - 300	275	2.04	-0.64	1.89	-0.40	1.82	-0.05
212 - 250	231	1.83	-0.70	1.86	-0.39	1.82	-0.10
180 - 212	196	1.77	-0.55	1.79	-0.26	1.78	-0.14
150 - 180	165	1.72	-0.55	1.70	-0.34	1.70	-0.28

1262C-12H-2, 204.99 cm, 63.54 (Ma)							
Size Fraction (μm)	Mean Size (μm)	*Pr. inconstans*		*Pr. pseudoinconstans*		*S.trivalis*	
		$\delta^{13}C$	$\delta^{18}O$	$\delta^{13}C$	$\delta^{18}O$	$\delta^{13}C$	$\delta^{18}O$
212 - 250	231	2.02	-0.74	1.93	-0.15	1.92	-0.01
180 - 212	196	1.89	-0.59	1.98	-0.32	1.81	-0.12
150 - 180	165	1.78	-0.45	1.81	-0.36	1.79	-0.25
125 - 150	137.5	1.67	-0.54	1.68	-0.37	1.66	-0.30

Table 5.2 - ODP Site 1262 Sample horizons and stable isotope data used in this study from the additional 3 close up time slices (genera abbreviations as in Figure 5.2)

5.3. Discussion

The data on size-related variation in whole test $\delta^{13}C$ and $\delta^{18}O$ provides new insights into foraminiferal ecology and isotopic disequilibrium effects that are important for interpreting proxy records of environmental change in the first four million years of the Paleocene.

5.3.1. Oxygen isotope depth ecology

Consistent with previous studies, high $\delta^{18}O$ in *Subbotina* sp. and *Parasubbotina varianta* in our data indicate calcification in a cool subsurface, likely thermocline habitat, while *Morozovella* sp., having the lowest $\delta^{18}O$ values likely occupied warm shallower levels of the surface mixed layer (Boersma and Premoli Silva 1983; Corfield and Cartlidge, 1991; Pearson *et al.* 1993; D'Hondt *et al.*, 1994; Norris, 1996; Kelly *et al.* 1996; Quillévéré *et al.* 2001; Coxall *et al.*, 2000; 2007). *Woodringina hornerstownensis*, registering the lowest $\delta^{18}O$ of all species analysed in the oldest sample, is also consistent with previous work (D'Hondt and Zachos, 1993) that suggests this small thin-walled species lived in the surface mixed layer, and/or calcified during the warmest months. The lack of any strong correlation between test size and $\delta^{18}O$ in *Subbotina* and *Parasubbotina* is consistent with previous suggestions that these genera maintained a relatively constant depth habitat during their life cycle (Pearson *et al.*, 1993; 'D'Hondt *et al.*, 1994; Norris 1996; Quillévéré *et al.*, 2001).

The pronounced inverse relationship between test size and $\delta^{18}O$ in *Morozovella* sp. recorded in our data, and elsewhere (D'Hondt *et al.*, 1994; Norris 1996; Houston and Huber, 1998; Quillévéré *et al.*, 2001), might reflect vertical (upward) depth migration. The *Morozovella* sp. were probably phytosymbioitic and would need the light for their photosynthesising algae, thus moving into shallower waters is probable. Alternatively, as suggested by D'Hondt *et al.*, (1994), the progressive ontogenetic $\delta^{18}O$ decrease could have been caused by increased kinetic isotopic fractionation that has been shown to discriminate against the 'heavy' ^{18}O isotope at higher levels of symbiont activity in

adult life stages. The reduced $\delta^{13}C$ values that would also accompany increased kinetic isotopic fractionation are likely overprinted by the photosymbiotic enrichment effect on $\delta^{13}C$. This interpretation is supported by the results of culturing experiments that document light-enhanced calcification rates and clear negative correlations between photosymbiont activity and $\delta^{18}O$ in living phyotosymbiotic taxa *Orbulina universa* and *Globigerinioides sacculifer* (Bouvier-Soumagnac and Duplessy, 1985; Spero, 1992; Spero and Lea, 1993; Wit *et al.*, 2010). However, this $\delta^{18}O$ depleting effect is not seen in all modern symbiotic planktonic foraminifera and as values in other Paleocene species are at these lower $\delta^{18}O$ values then depth migration to shallower waters is a more likely scenario.

Mean maximum and minimum 'ice-free' calcification temperatures for the youngest time slice based on the highest and lowest $\delta^{18}O$ values of inferred surface dweller *M. occlusa* are ~13°C and 17°C. These are very likely to be underestimates because of the effect of post-burial recrystallization on foraminiferal test $\delta^{18}O$, as indicated by SEM studies (Chapter 3), that has been shown to depress tropical surface ocean palaeotemperature estimates based on pelagic carbonate ooze samples, by 6°C or more (Pearson *et al.*, 2001; Sexton *et al.*, 2006).

The isotopic depth ecology of *Praemurica* sp. is complex. In the oldest sample (Figure 5.2A), *Pr. taurica* and *Pr. pseudoinconstans,* appear to have lived at a depth intermediate between presumed surface dweller *W. hornerstownensis* and subsurface dwellers *Subbotina trivialis/E. eobulloides*, whereas *Pr. taurica* is interpreted as the shallowest living planktonic species in Figure 5.2 B (see also Norris, 1996). At 62.65 and 62.47 Ma *Pr. inconstans* and *Pr. uncinata* both posses surface-ocean signatures, apparently co-existing with *M. praeangulata*, a typical surface species. Over the same interval, *Pr. pseudoinconstans* appears to have occupied variable depths during its life cycle (Figures 5.2 C and D). Small and/or juveniles appear to have calcified at subsurface levels, whereas larger, mature forms apparently migrated across thermal and or salinity gradients to shallower levels. Close to the end of its evolutionary range, and once the morozovellids started to diversify (Figure 5.1, Olsson *et al.*, 1999), however, *Pr. inconstans* returned to a thermocline habitat (Figure 5.2 E).

5.3.2. Carbon isotopes: Metabolic and photosymbiotic disequilibrium effects

The overall similarity of $\delta^{13}C$ between species at different test sizes in the oldest time slices, despite corresponding interspecies $\delta^{18}O$ differences that indicate interspecies depth stratification, supports a relatively low background upper water column $\delta^{13}C$ gradient for at least two million years after the K/Pg event (D'Hondt *et al.*, 1998; Coxall *et al.*, 2006). The general pattern of increased $\delta^{13}C$ with increasing test size seen is consistent with previous studies that indicate increased reliance on ambient CO_2 for calcification at smaller test sizes (Berger *et al.*, 1978; Erez, 1978; D'Hondt and Zachos, 1993). Building on earlier interpretations (D'Hondt and Zachos, 1993), we emphasize the importance of subdividing this general pattern into two broad test size classes; 'small tests' <150 μm and 'large tests' >150 μm (shown as a grey dashed lines on Figures 5.2 -5.4).

Tests <150 μm show increasing $\delta^{13}C$ with increasing test size for all species. This is most apparent in the oldest time slices where small species are common and data could be collect for three sub-150 μm size fractions (Figures 5.4 A and B). The results are consistent with the hypothesis of a strong size related negative vital effect in small early Paleocene planktonic foraminifera that results from the decreasing influence of metabolic (isotopically light) CO_2 on test calcite $\delta^{13}C$ (D'Hondt and Zachos, 1993) through ontogeny. Support for this interpretation comes from laboratory experiments that show that small foraminifera (<150μm) tend to grow rapidly and have high metabolic activity (Bé, 1982) leading to increased kinetic fractionation and an increase in respired CO_2 being incorporated into the test. Larger foraminifera tend to grow more slowly and show decreased metabolic activity with less kinetic fractionation (Berger *et al.*, 1978; Kahn, 1979; Wefer and Berger, 1991; Ravelo and Fairbanks, 1995; Ortiz *et al.*, 1996; Spero *et al.*, 1997; Pearson and Wade, 2009). Another possibility is that like the larger forms (see below), the $\delta^{13}C$-size correlation is the result of foraminifera photosymbiosis (D'Hondt and Zachos, 1993). However, since all small species exhibit this trend, including forms interpreted as being asymbiotic at larger test sizes, it seems more likely that the $\delta^{13}C$ trend is related to metabolic effects related to small size and

follows the model presented in Chapter 4 with greatest increases in $\delta^{13}C$ occurring in the smaller size fractions.

Woodringina hornerstownensis, as with other Danian species such as *Guembelitria cretacea*, *Parvularugoglobigerina eugubina* and *Chiloguembelina midwayensis* (D'Hondt and Zachos, 1993) barely attain sizes >150 μm. Where they do (D'Hondt and Zachos, 1993), their test $\delta^{13}C$ continues to show high $\delta^{13}C$ compared to co-existing species of the same test size. These species also show the strongest $\delta^{13}C$-size range among the small species (D'Hondt and Zachos, 1993). These species are all classed as microperforates and therefore posses a very thin walled test. It is possible that metabolic $\delta^{13}C$ fraction has a greater influence on test $\delta^{13}C$ in these thin walled forms, most of which are thought to be opportunistic r-strategists, possibly 'tycho-pelagic', that flourished in the post-extinction Paleocene ocean, expanding into the pelagic realm from shelf environments and/or benthic environments (Kroon and Nedebragt, 1990; D'Hondt and Zachos, 1993; Darling *et al.*, 2009).

Tests >150 μm show different $\delta^{13}C$ trajectories depending on species. *Subbotina* sp., *P. varianta* and *Pr. taurica* show minimal $\delta^{13}C$ increases at larger test sizes whereas there is a pronounced positive correlation between $\delta^{13}C$ and test size in *Pr. pseudoinconstans*, *Pr. inconstans*, *Pr. uncinata* and species of *Morozovella* sp. This supports the view that this latter trend is the result of a vital effect caused by $\delta^{13}C$ disequilibrium related to algal photosymbiosis in these surface mixed layer species (D'Hondt and Zachos, 1993; Pearson *et al.*, 1993; D'Hondt *et al.*, 1994; Norris, 1996; Quillevere *et al.*, 2004; See also Chapter 4). Symbiotic relationships with photosynthetic algae have been found in many species of extant planktonic foraminifera (Bé *et al.* 1982; Hemleben *et al.* 1989; See also Chapter 4) and may aide the host foraminifera in occupying oligotrophic pelagic niche by providing food. Culture experiments show that photosymbiosis causes planktonic foraminifera to be enriched in heavy ^{13}C relative to ^{12}C because algal symbionts preferentially remove the lighter isotope from the DIC pool used in calcification (Spero and DeNiro, 1987). This effect increases with increasing test size because symbiont density increases through ontogeny (Berger *et al.*, 1978; Bouvier-Soumagnac and Duplessy ,1985; Spero and Williams, 1988; 1989; Spero *et al.*, 1991;

Spero, 1992; Spero and Lea, 1993; Ravelo and Fairbanks, 1995). The resulting strong positive correlation of $\delta^{13}C$ and test size has been used to provide evidence of symbiosis in extinct species (Pearson *et al.*, 1993; D'Hondt and Zachos, 1993; D'Hondt *et al.*, 1994; Norris, 1996; Quillévéré *et al.*, 2001). The absence of this $\delta^{13}C$ 'fingerprint' in *Subbotina* and *Parasubbotina* agrees well with previous findings and our $\delta^{18}O$ data, which imply these taxa were deep living and asymbiotic (Boersma and Premoli Silva, 1983; Pearson *et al.*, 1993; D'Hondt *et al.*, 1994; Norris, 1996; Kelly *et al.*, 1996; Quillévéré *et al.*, 2001).

In summary, the criteria for recognizing palaeosymbiosis in fossil species include having among the lightest $\delta^{18}O$ values, large intraspecific variability in $\delta^{13}C$ values and, often, clear $\delta^{13}C$ offset from other species (Figures 5.2 and 5.4; D'Hondt *et al.*, 1994; Pearson *et al.*, 1993; Norris, 1996; Houston *et al.*, 1999). These characteristics are illustrated in $\delta^{18}O$ vs. $\delta^{13}C$ cross plots (Figure 5.5 and Figure 5.6) that include size fraction data, which reveal two principal clusters corresponding to 1) asymbiotic and 2) shallow living symbiotic species. The asymbiotic clusters have low $\delta^{13}C$ and high $\delta^{18}O$ with weak to minimal correlation between $\delta^{18}O$ vs. $\delta^{13}C$ across size spectra. The inferred symbiotic clusters (Figures 5.5 C-F) have distinctly lower $\delta^{18}O$ and higher $\delta^{13}C$ and show a negative correlation between $\delta^{18}O$ vs. $\delta^{13}C$ across test-size spectra. The separation of the two clusters becomes more pronounced over time presumably as photosymbiosis becomes an increasingly important ecological strategy.

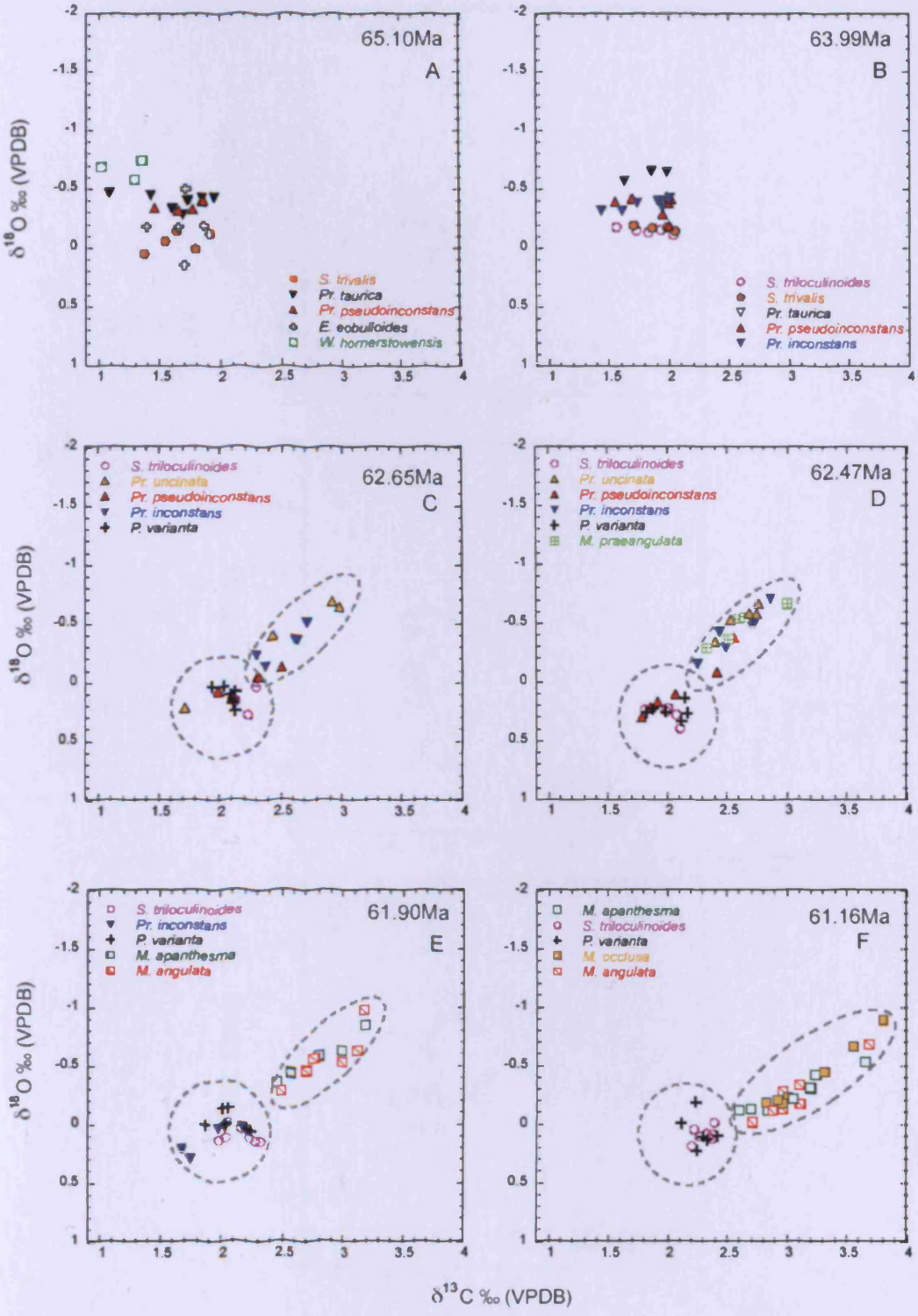

Figure 5.5 - Carbon isotope ($\delta^{13}C$) - oxygen isotope ($\delta^{18}O$) cross plots for 6 time slices during the Paleocene from ODP site 1262. Ages are based on the time scale from Westerhold *et al.*, (2008) with orbital chronology from site 1262. Genera abbreviations as Figure 5.2. Grey dashed ellipses indicate species with a photosymbiotic ecology, whereas grey dashed circles indicate asymbiotic ecology.

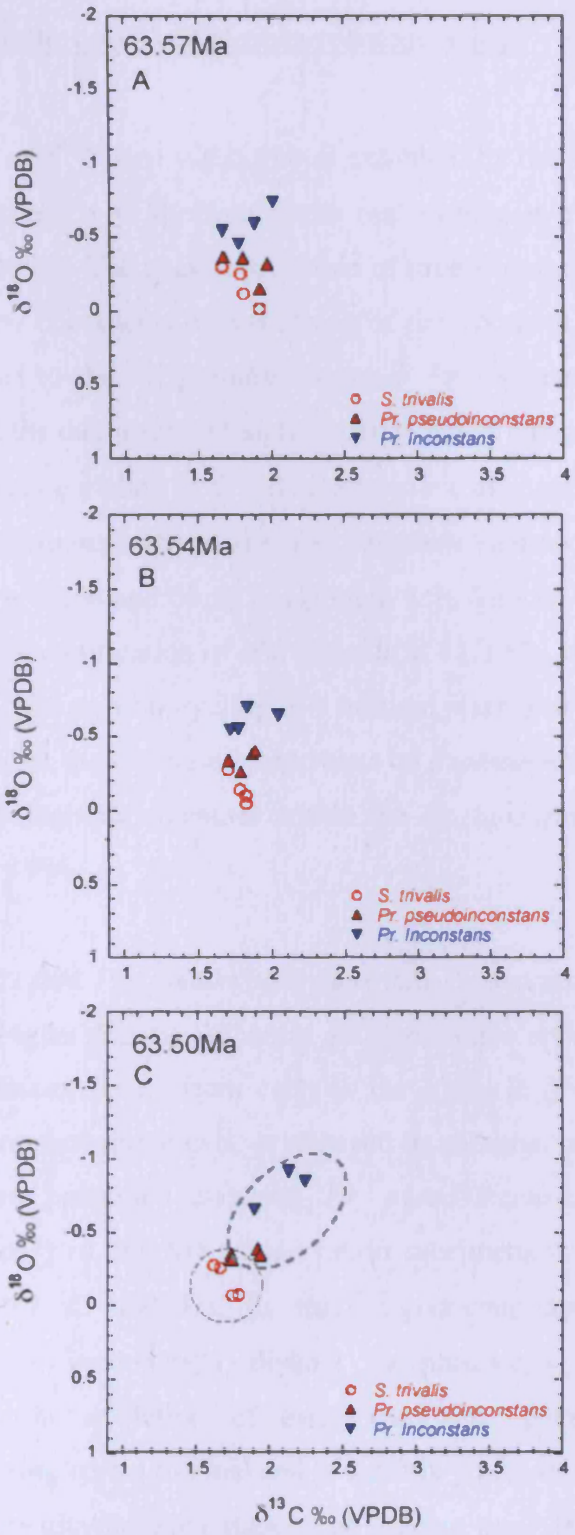

Figure 5.6 - Close up time slices showing carbon isotope ($\delta^{13}C$) - oxygen isotope ($\delta^{18}O$) cross plots (A-B) from between 63.99 and 62.65Ma (arrows in Figure 5.2 and 5.4). Ages are based on the time scale from Westerhold et al (2008) with orbital chronology from site 1262. Genera abbreviations as Figure 5.2. Grey dashed ellipse indicates species with a photosymbiotic ecology, whereas the grey dashed circle indicate asymbiotic ecology.

5.3.3. *Praemurica* and the origin of Paleocene photosymbiosis

The changing pattern of $\delta^{13}C$-size variability is exhibited by our multispecies isotopic analyses and is consistent with the hypothesis that symbiosis evolved in the genus *Praemurica* (Norris, 1996). The results, sequence of time slices and detailed Site 1262 age model provide new constraints on the timing of development of this ecology, pin-pointing its appearance to the *Pr. pseudoinconstans- Pr. inconstans* morphogroup by 63.5 Ma. Specifically, the data suggest that the acquisition of a photosymbiotic ecology, resulting in progressively enriched $\delta^{13}C$ (relative to co-existing species) with increasing test size, occurred simultaneously in the *Pr. pseudoinconstans* and *Pr. inconstans* morphogroups between 63.54 and 63.50 Ma (Figure 5.3). This is ~1Ma earlier than the origin and subsequent diversification of *Morozovella* at 62.2 Ma, which has been linked to the recovery of pelagic carbon cycling 3-4 million years post K/Pg (Coxall *et al.*, 2006) and ~0.9 Ma earlier than previous constraints on *Praemurica* evolution that report the first appear of the isotopic signature within the *Pr. inconstans* and *Pr. uncinata* morphogroup (Norris, 1996).

Our $\delta^{18}O$ data suggests that *Pr. pseudoinconstans* and *Pr. inconstans* initially lived at intermediate-depths (Figure 5.2 B). Whereas *Pr. inconstans* appears to have made a complete shift to shallower levels from early in the lifecycle (Figures 5.2 C and D), presumably to facilitate photosymbiosis, or changed its seasonal preference for growth. *Preamurica inconstans* presumed ancestor, *Pr. pseudoinconstans* appears to have adopted this ecology only in mid life stages, i.e. in specimens with mean test sizes of >180 μm (Figures 5.2 C and D). In this respect our data suggest that *Pr. pseudoinconstans* is an ecologically distinct morphospecies, that represented a transitional stage in the evolution of early Paleogene planktonic foraminiferal photosymbiosis, migrating across thermal and or salinity gradients to the well-lit surface mixed layer in post-juvenile/pre-adult stages and shifting away from ingesting alga as food to cultivating them. The smaller $\delta^{13}C$ offsets in *Pr. pseudoinconstans* compared to subsequent species of *Preamurica* and *Morozovella* may be a result of the type or density of the algal symbionts (D'Hondt & Zachos 1994; Houston and Huber 1998; D'Hondt & Zachos 1998), as is the case in the two types (Type I and II), of extant

species *Globigerinella siphonifera* (Bijma *et al.*, 1998). Culture experiments indicate that the weaker correlation between $\delta^{13}C$ and test size in the larger Type I *G. siphonifera* morphotype is due to lower symbiont density, hence lower photosynthetic rates, and a facultative rather than obligate symbiotic association. Type II *G. siphonifera*, in contrast, is more highly dependent on its symbionts and demonstrates a much stronger $\delta^{13}C$ -test size correlation (Bijma *et al.*, 1998). Another possibility is that *Pr. pseudoinconstans* possessed chrysophyte algal symbionts (Hemleben *et al.*, 1989), which in extant species produce smaller isotopic offsets, compared to the majority of symbiotic species that have developed associations with dinoflagellates (Hemleben *et al.*, 1989; Bijma *et al.* 1998). The slight decrease in $\delta^{13}C$ in the largest tests of both *Pr. pseudoinconstans* and *Pr. inconstans*, which coincides with a decrease in $\delta^{18}O$, is consistent with the hypothesis that these species, as well as other inferred symbiotic species, migrated to deeper water for reproduction and/or digested symbionts at terminal life stages (Houston and Huber, 1998).

Pr. inconstans displays the isotopic signal of symbiosis until 62.47 Ma (Figure 5.4 D), after which it appears to loose its symbionts (Figure 5.4 E) and returns to a thermocline habitat. This is demonstrated in Figure 5.5, which records shifts in *Praemurica* isotopic ecology from the asymbiotic to the symbiotic cluster and back again over the studied interval. A similar pattern of ecological shift was has been recorded in *Pr. inconstans* from the Atlantic (Boersma and Shackleton, 1979; Boersma *et al.* 1979; Boersma and Premoli Silva 1983). The timing of this return coincides with onset of diversification within the 'muricate' group (*Morozovella*, *Acarinina* and *Igorina*) at Site 1262 (Figure 5.1), a clade that dominates surface habitats over subsequent early Paleogene time. We suggest that *Pr. inconstans* was not as well adapted to the surface dwelling symbiotic niche as the increasingly specialized and highly successful *Morozovella*. The prevalence of the early species of *Praemurica* and subsequent *Morozovella* in surface waters from the Paleocene and younger deep sea sequences demonstrates that foraminiferal photosymbiosis was beneficial to early Paleocene planktonic foraminifera. Evolution of this ecological strategy might initially have been gradual but the subsequent rapid expansion of symbiotic species suggests that it allowed the 'muricate' group to diversify

into an expanding ecologic niche typified by food-poor oligotrophic pelagic environments at low latitudes (Coxall *et al.*, 2006; Fuqua *et al.* 2008).

5.3.4. Ontogenetic isotopic vital effects and thresholds on test size $\delta^{13}C$ values

Based on these results test size $\delta^{13}C$ thresholds can be identified, that help explain the observed isotopic trends and identify an optimal test-size window for studying early Paleocene carbon cycling. The results suggest that specimens with test diameters below 150 μm likely underestimate seawater $\delta^{13}C$ equilibrium values by ~ 0.3-0.5‰, corresponding to the range of variation in $\delta^{13}C$ exhibited by specimens in the 80-150 μm size range (Figs 5.4A and B), because of the metabolic vital effect described above. Tests larger than 200 μm, especially inferred photosymbiotic species, are likely to overestimate seawater $\delta^{13}C$ by 0.1-1.5‰ because of an increasing positive vital effect. Tests between 150 μm and 200 μm, that appear to fall between the strongest influence of these effects, may be expected to show the least departure from equilibrium values and, therefore, are most appropriate for isotopic studies. This concept is represented in a schematic model in Chapter 4, Figure 4.1. The ideal 150 μm and 200 μm corresponds broadly to the early onset of the 'adult' growth stage (Brummer *et al.*, 1987), although there is interspecies variation in this range. We note that even forms from this favourable test size window are likely to be slightly negatively offset from DIC $\delta^{13}C$ because their whole test $\delta^{13}C$ will include calcite formed during early ontogenetic stages under the influence of the negative metabolic disequilibrium (D'Hondt *et al.*, 1994). Therefore, although disequilibrium effects will manifest in all test sizes, specimens between 150-250 μm appear to be at least a useful standard to which other single species isotopic records can be compared.

5.4. Summary

- Positive correlations between $\delta^{13}C$ and test size for tests <150 μm, which includes small species and the small life stages of typically larger species, suggests an influence of isotopically depleted metabolic carbon on foraminiferal calcite $\delta^{13}C$ in very small tests <150 μm that depresses equilibrium calcite $\delta^{13}C$ values by ~0.3-0.5 ‰. This effect is especially pronounced in thin walled microperforate species that represent most of the post K/Pg survivor taxa as well as the early diversifying opportunists.

- From 62.65 Ma, pronounced correlations between test size and $\delta^{13}C$ appear in larger specimens (>150 μm) of the surface dwelling genus *Praemurica,* and later *Morozovella.* Together with interspecies depth-related $\delta^{18}O$ offsets, this is interpreted as the isotopic signature of photosymbiosis and suggests isotopic enrichment by 0.1-0.3 ‰ $\delta^{13}C$ in *Pr. pseudoinconstans* and *Pr. inconstans* >150 μm in size and 0.5-1.5 ‰ $\delta^{13}C$ in species of *Morozovella.* A similar negative correlation between test size and $\delta^{18}O$ for the same species likely represents movement into more surface waters to increase light levels for the symbiotic algae.

- The results lend support to the hypothesis that foraminiferal symbiosis evolved in the *Praemurica* lineage. The new data and detailed Site 1262 age model provide further constraints on the timing of development of this ecology, pin-pointing its appearance to the *Pr. pseudoinconstans- Pr. inconstans* morphogroup by 63.5 Ma, ~0.9 Ma earlier than previously suggested. All *Praemurica* species, excluding the first species *Pr. taurica,* and *Pr. inconstans* at the end of its evolutionary range, should therefore be expected to have slightly enriched $\delta^{13}C$ values.

- The results would suggest that 150-200 μm represents an optimal test size window for Paleocene isotopic analysis, that will minimize disequilibrium effects, and produce a standard to which other single species isotope records can be compared. This should optimize the potential for accurate reconstructions of the surface-to-deep ocean $\delta^{13}C$ gradient.

- These results underscore the importance of choice of species and use of narrow size fractions for producing accurate paleoceanographic reconstructions using foraminifera, particularly in the aftermath of the K/Pg when an entirely new set of species were evolving under extreme and unfamiliar oceanographic conditions.

6. Carbon System Recovery after the K/Pg

This chapter focuses on the carbon system recovery after the mass extinction event to further test the hypothesis that K/Pg pelagic extinctions were associated with a reduction in the strength of the carbon pump. This chapter also addresses the current conflict between benthic and planktonic foraminifera data over the timing and magnitude of carbon system recovery and organic carbon flux from the surface to the deep ocean.

6.1. Introduction

The marine biological pump (Figure 6.1) is the main process by which carbon is transferred from the atmosphere to the deep ocean, particularly on a local scale (Struck et al., 1993; Feely *et al.*, 2001), where it remains until deep water ventilation occurs. The amount of CO_2 in the surface oceans depends on the temperature and chemical properties of that area of water (Feely *et al.*, 2001). Temperate waters are sinks of CO_2 whereas tropical waters are sources and high latitudes tend to be characterised by only small fluxes (Takahashi *et al.*, 1997; Gruber et al., 2009). The biological pump not only transports and recycles materials in the sea but is thought to help remove excess CO_2 from the atmosphere over geological timescales, if part of the material transported is sequestered in the sediments (Turner, 2002). Understanding the role and behaviour of the biological pump is therefore critical for understanding climate and climate change on a range of timescales. Through reconstructions of the biological pump in the past we can improve our understanding of the factors that can affect it, the scale and duration of perturbations, as well as the consequences of perturbations for climate. The K/Pg boundary provides an excellent opportunity for assessing changes in the marine biological pump as global extinctions, especially of calcifying marine algae and zooplankton (Smit, 1982; Molina *et al.*, 1998; Olsson *et al.*, 1999; Huber *et al.*, 2002), are thought to have disrupted marine food webs and the role they played in pumping carbon between atmospheric and deep sea reservoirs (D'Hondt *et al.*, 1998; Coxall *et al.*, 2006; Fuqua *et al.*, 2008; Honjo *et al.*, 2008).

Evidence for large scale disruption in the carbon system after the K/Pg boundary is provided by a major decrease in the accumulation of calcium carbonate at the sea floor in all ocean basins (Hsü *et al.*, 1982; Zachos and Aurthur, 1986; Stott and Kennett, 1989; Zachos *et al.*, 1989; D'Hondt, 2005) and a flattening or, reversal in some locations, of the carbon isotope gradient ($\Delta\delta^{13}C$) between mixed layer dwelling planktonic foraminifera and benthic foraminifera (Zachos *et al.*, 1985; Arthur *et al.*, 1987; Zachos and Arthur, 1986; Zachos *et al.*, 1989; Zachos *et al.*, 1992; D'Hondt *et al.*, 1998). These observations have been interpreted as signalling a global collapse (Hsü and McKenzie, 1985; Kump, 1991) or at least a significant reduction (D'Hondt *et al.*, 1996; Adams *et al.*, 2004; Coxall *et al.*, 2006; Alegret and Thomas, 2007; Ridgwell, unpublished data) of marine biological carbon pumping that exports organic carbon from the photic zone to the deep ocean. The lack of significant extinction among deep-sea benthic foraminifera, however, challenges this hypothesis, as benthic foraminifera are proposed to rely on surface organic matter for food (Culver, 2003; Alegret and Thomas, 2007, 2009). Existing $\Delta\delta^{13}C$ data sets for the K/Pg boundary (Arthur *et al.*, 1987; Zachos and Arthur, 1986; Zachos *et al.*, 1989; D'Hondt *et al.*, 1998) include possible disequilibrium effects, which may distort $\Delta\delta^{13}C$ values and the duration of carbon pump perturbations. In addition to this the inferred carbon system changes have not been considered against the backdrop of ocean and planktonic foraminifera thermal stratification.

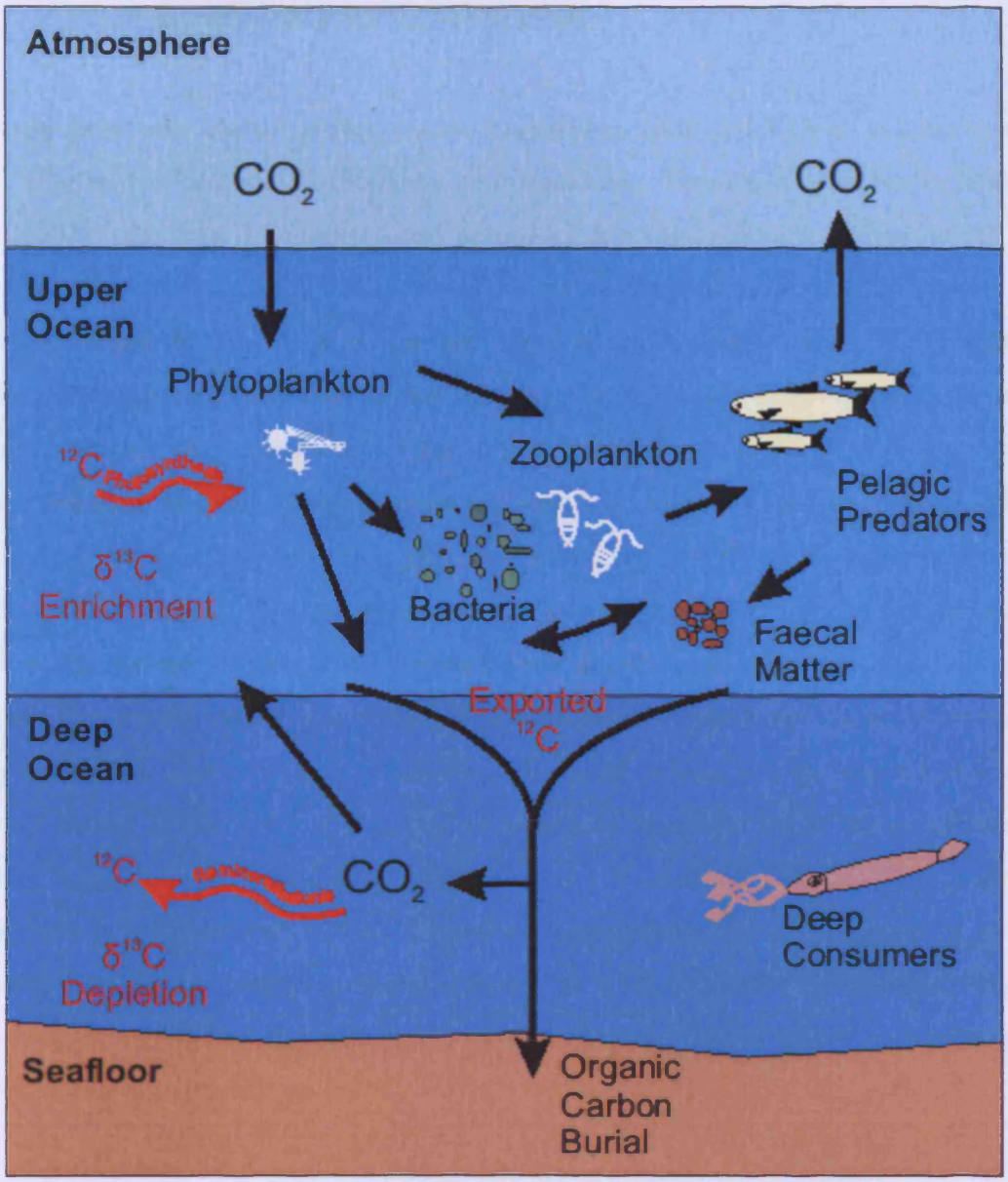

Figure 6.1 – Schematic of the marine biological pump adapted from Chisholm, (2000). The biological pump (black arrows) acts to transfer carbon from the atmosphere to the deep ocean, largely via food webs. Red arrows denote the movement of carbon isotopes and the gradient that exists between surface and deep waters due to the biological pump.

6.1.1. Carbon flux processes in the modern ocean

Primary producers in the surface ocean incorporate dissolved CO_2 to produce mostly POC (Particulate Organic Carbon) via photosynthesis. The majority (~ 80 %, Honjo *et al.*, 2008) of this POC is remineralised in the surface ocean through respiration (as POC has a density similar to that of seawater). A small proportion of organic carbon does however, reach the sea floor, as the sediments of the world's oceans testify (Leeder, 2001). The major constituents of the biogenic particles that settle through the water column are planktonic carbonate tests, opaline shells, and POM (particulate organic matter), which includes POC. The flux of organic matter to the sea floor is largely controlled by biological processes (Michaels and Silver, 1988) such as zooplankton and nekton faecal pellets, phytoplankton and marine snow (organic aggregates >500μm in size, Alldredge and Silver, 1988) formed from a variety of particles (including faecal pellets) that stick together due to microbially produced exopolymers or polysaccharides (Turner, 2002). The relative contributions of faecal pellets, marine snow and sinking phytoplankton to the vertical flux and recycling of materials in the water column are highly variable and dependent upon multiple interacting factors. These include variations in productivity, biomass, plankton size spectra, the composition of pelagic communities in the overlying water column, as well as trophic interactions between various components of the pelagic ecosystem (Turner, 2002), that vary across ocean basins, latitudes and seasonally.

Sediment trap experiments conducted by Honjo *et al.* (1982) in the Atlantic and Pacific have shown that 60 to 90% of the total particulate flux is of biogenic origin and carbonate hard parts accounted for 30 to 60% of this in temperate and tropical regions. Ballasting is also an important mechanism that aids POC in reaching the sea floor by providing extra density in the form of silicate, carbonate biominerals or dust (Armstrong *et al.*, 2002). Francois *et al.* (2002) found that ballasting by carbonate was extremely important as the fraction of the flux of organic carbon (C-org) exported from surface waters, was directly related to the accompanying flux of calcium carbonate. C-org flux was found to be inversely related to seasonality and unaffected by the flux of biogenic opal (Francois *et al.*, 2002).

Along with the transfer of particulate organic matter to the deep ocean, there is also the transfer of the light carbon isotope (^{12}C). This results from photosynthesis preferentially removing ^{12}C from the surface waters (to build organic tissue) leaving them, relatively speaking, enriched in the heavier ^{13}C isotope. The reverse occurs at depth as the ^{12}C enriched organic matter is remineralised, releasing the ^{12}C to the surrounding waters (Figure 6.1). The calcium carbonate tests of planktonic and benthic foraminifera that live throughout the water column and on the seafloor (in the case of benthic foraminifera), conveniently 'record' this vertical carbon isotope gradient ($\Delta\delta^{13}C$) and can be used to reconstruct the process of surface to deep carbon pumping today and also in the geological past (Broecker, 1982; Shackleton *et al.*, 1983). The $\delta^{13}C$ of seawater is affected by the amount of primary production occuring, through removal of ^{12}C, which is largely dependent on nutrient availability (Broecker, 1982; Shackleton *et al.*, 1983; Berger and Vincent, 1986). Variations in primary production, related to distribution of nutrients, can thus also affect $\Delta\delta^{13}C$. Additional factors also include; equilibration with the atmosphere in surface waters, mixing of different water masses and the preformed nutrient state of subsurface waters (Kroopnick, 1985; Mackersen *et al.*, 1993; Bickert and Wefer, 1999; Sigman and Boyle 2000).

6.1.2. Biological pump collapse at the K/Pg boundary

Interspecies planktonic and benthic $\delta^{13}C$ gradients suggest that the Cretaceous ocean showed a similar difference between surface and deep water carbon isotopes to the modern ocean, which is indicative of a 'normal' biological pump (D'Hondt, 2005). However, at the K/Pg boundary the carbon isotope gradient $\Delta\delta^{13}C$ collapsed (Figure 6.2) (Zachos *et al.*, 1989; D'Hondt *et al.*, 1998; D'Hondt, 2005 and Coxall *et al.*, 2006). Previous records suggest that these differences in $\delta^{13}C$ took over 3 million years to recover to the pre-extinction state (D'Hondt *et al.*, 1998; Adams *et al.*, 2004). The recovery can also be broken down into two stages (Figure 6.2); Initial recovery (bottom arrow) where $\Delta\delta^{13}C$ differences stabilised after initial K/Pg boundary $\Delta\delta^{13}C$ collapse

and final recovery (top arrow) where pre-extinction planktonic and benthic foraminifera $\delta^{13}C$ differences returned.

The explanation for this $\delta^{13}C$ pattern has been linked to K/Pg extinction, related disturbance to the pelagic ecosystem. A reduction in primary productivity was first proposed by Hsü *et al.* (1982) to be the cause of the breakdown of the carbon isotopic gradient in a so called 'strangelove' ocean (Broecker and Peng, 1982). This may have been true initially as the dust cloud from the impact would have led to global darkness and prevented photosynthesis. However, models of large impact events have dust clouds leaving the atmosphere after only approximately one year (Kring, 2000), which does not explain the 3 million year delay. D'Hondt *et al.*, (1998) proposed that primary production recovered quickly after the mass extinction event but that organic export production from the surface waters remained low over the 3 million year period following the boundary. This has been termed the 'Living Ocean Model' (D'Hondt *et al.*, 1998 and Adams *et al.*, 2004) invoking a modified, weaker carbon pump in the several million years after the widespread extinctions. The reduction in organic export has been attributed to an ecosystem re-organisation (D'Hondt *et al.*, 1998). The extinction of larger grazers, reduced $CaCO_3$ ballasting and a reduction in mean phytoplankton size would have resulted in smaller aggregates that could not survive dissolution before they reached the sea floor. Similar disruption to food webs has been found on land as well as in the ocean. Analysis of insect feeding damage on angiosperm leaves also found that food webs were severely unbalanced for 1 to 2 myr after the K/Pg event on land (Wilf *et al.*, 2006).

Two other lines of evidence also support the idea that there was a reduction of organic flux to the deep ocean after the K/Pg event (Zachos *et al.*, 1989). Firstly barium (Ba) behaves in a nutrient like manner in the modern ocean and its accumulation rates in sediment can be used as a proxy for carbon organic flux (however, there are some problems with using Ba as a proxy for organic matter and care should be taken when interpreting results; McManus *et al.*, 1998). Ba accumulation rates decreased at the K/Pg boundary indicating a reduction in organic matter flux (Shatsky Rise Site 577, Zachos *et al.*, 1989). Secondly, the boundary was marked by a decreased infaunal to

epifaunal $\delta^{13}C$ gradient in benthic foraminifera (Zachos *et al.*, 1989). The reduction in decay of organic matter in the upper few centimetres of sediment as inferred by a decreased organic flux would lead to a reduction of pore water $\delta^{13}C$ gradients.

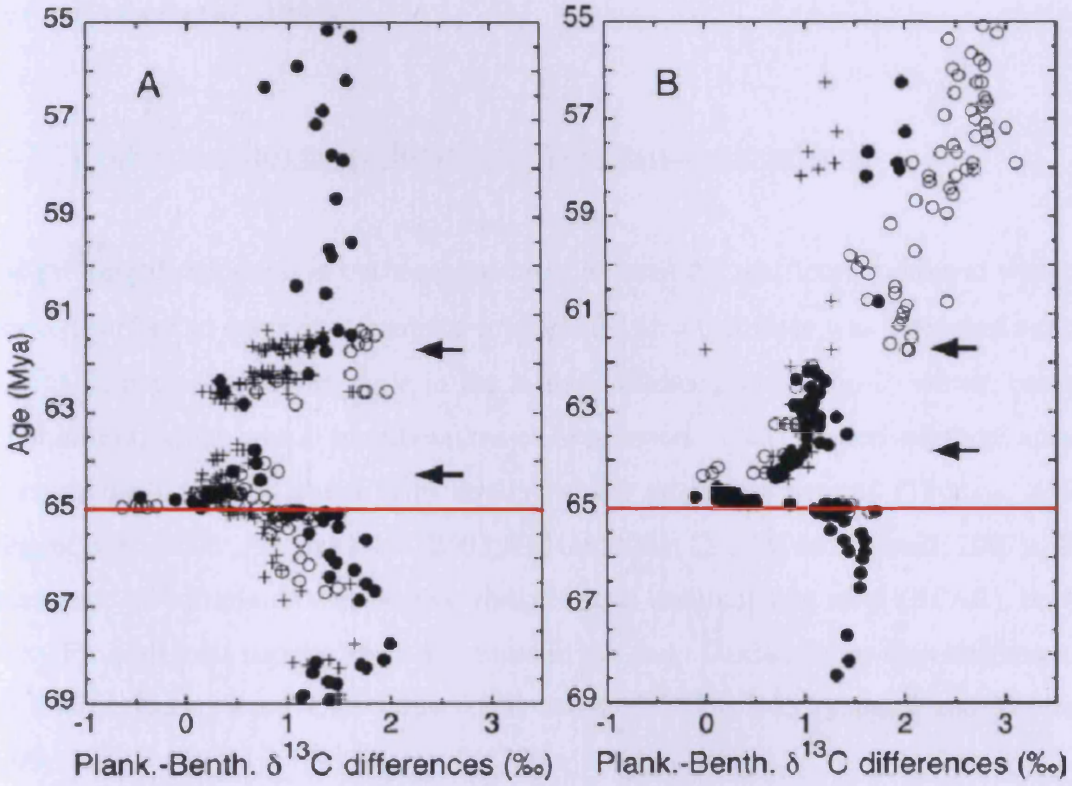

Figure 6.2 - Carbon isotopic $\delta^{13}C$ differences between planktic foraminifera and benthic foraminifera: (A) South Atlantic DSDP Site 528; (B) Central Pacific DSDP Site 577. The black circles represent $\delta^{13}C$ differences between fine carbonate (principally calcareous nannofossils) and benthic foraminifera, the white circles represent differences between mixed layer planktic foraminifera and benthic foraminifera, and the crosses represent differences between thermocline planktic foraminifera and benthic foraminifera. The K/Pg boundary (red line), the partial recovery of the $\delta^{13}C$ differences (bottom arrow in each panel), and the eventual recovery (top arrow in each panel). Isotopic data are from D'Hondt et al. (1998) and S. D'Hondt and J.C. Zachos (unpublished data). Adapted from D'Hondt, 2005. Ages are based on the Cande and Kent, (1995) time scale.

This inferred decrease in organic flux from the surface water could have led to increased nutrient recycling in the upper layers of the ocean and increased biomass production rather than a decrease in the photic zone (D'Hondt, 2005). This line of reasoning for increased biological productivity in surface waters is supported by the

research of Hollis *et al.* (1995) as they found an increase in siliceous sediments after the K/Pg, especially within the first few million years, when carbonate accumulation and planktonic-benthic $\Delta\delta^{13}C$ differences were still low. Silica is undersaturated in the worlds oceans and preservation in sediments only occurs in the modern ocean where the rain rate is extremely high (i.e. upwelling areas) or unusual bottom water conditions prevail (Leinen *et al.*, 1986).

6.1.3. Evidence against major disruptions of the marine carbon pump

The prolonged reduction in carbonate accumulation at the sea floor, combined with the reduced surface to deep $\delta^{13}C$ gradient supports the idea that there was a reduced supply of organic matter to the sea floor in the 3 myrs following the K/Pg. However, benthic foraminifera, which would have been major benefactors of surface derived food, appear to cross the boundary event with relatively few or no extinctions (Thomas, 1990; Alegret *et al.*, 2001; Alegret *et al.*, 2003; Culver, 2003; Coccini and Marsili, 2007). The abundance of buliminids and benthic foraminiferal accumulation rates (BFAR), both a proxy for high food supply, show increases in the early Danian rather than decreases in the Pacific Ocean from ODP Sites 1220 and DSDP Site 465 (Alegret and Thomas, 2009).

Only a short period of reduced organic flux, lasting no longer than planktonic foraminifera biozone P1a (~100 kyr) can be seen within some benthic foraminifera record (Alegret *et al.*, 2001; Alegret and Thomas, 2007). Additional studies (Kuhnt and Kaminski, 1993; Peryt *et al.*, 2002; Coccini and Marsili, 2007) show a change in community structure (e.g. an increase in epifaunal species and agglutinated forms) that was inferred to relate to a reduction of organic flux, as the pelagic food web collapsed. This however lasted for ~200 kyr and the specific pattern and timing of recovery is very dependent on paleogeography (Alegret *et al.*, 2003; Alegret, 2007). Many studies show low benthic diversity and an increase in opportunistic taxa, indicating environmental instability with food supply possibly increasing rather than decreasing in the early Danian. Food supply to the seafloor at this time is suggested to have been irregular and from opportunistic phytoplankton blooms (e.g. siliceous or bacterial) rather than from

calcifying nannoplankton (Alegret *et al.*, 2003; Alegret and Thomas, 2009), which suffered widespread extinction (Bernaola and Monechi, 2007).

Alegret and Thomas (2007) studied the benthic foraminifera assemblage changes at Site 1262. The benthic foraminifera at this site, as with elsewhere, show no net extinction but decreases in diversity and hetrogeneneity were noted. Three proxies; percentage buliminids, percentage infaunal taxa and benthic foraminiferal accumulation rates (BFAR) were interpreted to indicate high organic flux to the seafloor. None of these proxies however, were in agreement as percentage buliminid taxa decreased rapidly but the overall percentage of infaunal taxa remained constant, as agglutinated forms became more common. BFAR dropped at the boundary and fluctuated strongly in the early Paleocene. The changes in the three proxies therefore are likely (at best) to indicate changes in when organic carbon arrives at the seafloor rather than overall changes in flux (Alegret and Thomas, 2007).

This lack of significant extinction among deep-sea benthic foraminifera, has lead some authors (Culver, 2003; Alegret and Thomas, 2007, 2009) to challenge the idea of a prolonged (~3 myr) period of reduced carbon pumping and questions have been raised about the fidelity of the $\Delta\delta^{13}C$ proxy in recording surface to deep gradients. Using the superior stratigraphic sequence at ODP Site 1262, which benefits from a detailed astronomically tuned age model, new down hole planktonic and benthic foraminifera carbon and oxygen stable isotope records are produced here. This provides new constraints on early Paleocene nutrient and thermal stratification. The objective of this chapter is to further test the hypothesis that K/Pg pelagic extinctions were associated with a reduction in the strength of the carbon pump.

6.2. Results

6.2.1. Oxygen isotope record

The late Maastrichtian data measured here show separation between the benthic and planktonic $\delta^{18}O$ values of approximately 0.8 ‰ (Figure 6.3, Figure 6.4 and Figure 6.5). This separation is maintained until the K/Pg boundary, with a slight shift in all values to lighter $\delta^{18}O$ by 0.15 ‰ ~100 kyr before the K/Pg boundary. At the boundary, and immediately after, the difference between benthic and planktonic foraminifera decreases by 50 % (to ~0.4 ‰). By 65.6 Ma inter planktonic-benthic foraminifera $\delta^{18}O$ separation returns to almost pre-extinction levels (~0.6 ‰). During the first ~200 kyrs after the K/Pg boundary there is little or no separation between the thermocline dwelling planktonic and benthic foraminifera and the difference between benthic and planktonic foraminifera is maintained by the mixed layer species only. Between 64.6 and 64.2 Ma the differences in mixed layer dwelling planktonic and benthic foraminifera decrease to ~0.25 ‰ before returning to ~0.6 ‰. After this point benthic and surface dwelling planktonic foraminifera differences continue to increase to a maximum of 1.4 ‰ by 61.8 Ma. Although the differences between benthic and planktonic foraminifera stay relatively consistent above and below the K/Pg boundary, absolute $\delta^{18}O$ values increase by ~ 0.2 ‰ for both.

Figure 6.3 shows a pattern of succession in the $\delta^{18}O$ values of the mixed layer dwellers. When *Pr. taurica* first appears it has $\delta^{18}O$ values closer (separated by ~ 0.15 ‰) to that of *S. trivalis*. Soon after this, however *Pr. taurica* $\delta^{18}O$ values increase to 0.43 ‰ lighter than that of *S. trivalis*, until 64.6 Ma, when they decline to a value of only 0.1 ‰ lighter. This pattern of changing $\delta^{18}O$ values throughout a species range, is seen in the mixed layer dwellers *Pr. inconstans* and *M. angulata* but not in *M. praeangulata*. This pattern coincides with changing species composition (see Chapter 7 for details).

In summary overall planktonic and benthic offsets are maintained through the K/Pg, but at a reduced level. Benthic and thermocline planktonic foraminifera values converge for ~200 kys after the K/Pg boundary. A further convergence of benthic and planktonic

$\delta^{18}O$ values is seen between 64.2 and 64.6 Ma in conjunction with assemblage and habitat changes (see Chapter 5 and 7). Over the longer recovery phase (~4 Ma) strong planktonic-benthic $\delta^{18}O$ separation prevails. Subbotinids have the most constant $\delta^{18}O$ values, whilst benthic foraminifera values vary. The evolution of the morozovellid lineage is associated with major decreases in surface $\delta^{18}O$ values.

6.2.2. Carbon isotope record

In the Maastrichtian there is a clear separation of $\delta^{13}C$ values between benthic and planktonic mixed layer dwellers by ~1 ‰ for the non symbiotic species *Gl. falsostuarti* and *H. holmdelensis* and ~2.1 ‰ for the symbiotic species *R. fructicosa* (Figure 6.3, Figure 6.4 and Figure 6.5). From 65.75 Ma to the K/Pg boundary the differences between benthic and mixed layer dweller planktonic foraminifera are maintained but are all shifted to heavier $\delta^{13}C$ values by ~ 0.4 ‰ (Figure 6.4). At the K/Pg boundary the majority of the Cretaceous planktonic foraminifera become extinct and $\delta^{13}C$ values converge as benthic $\delta^{13}C$ values increase by a further ~ 0.1 ‰ and the survivor *H. holmdelensis* (as the other species did not survive the extinction) values decrease by ~0.9 ‰. The $\delta^{13}C$ of small microperforate species *G. cretacea* appears to change only slightly in $\delta^{13}C$ values across the boundary and has values that are ~ 0.5 ‰ lighter than the benthic values.

The convergence of benthic and planktonic $\delta^{13}C$ value persists until ~65.35 Ma when values begin to separate (~0.4 ‰). After initial separation benthic and planktonic foraminiferal $\delta^{13}C$ values continued to diverge over the interval studied, until ~64.1 Ma when a pre-extinction state of ~1.0 ‰ $\Delta\delta^{13}C$ offset returns (Figure 6.5) between benthic and the thermocline dwelling planktonic foraminifera (*S. trivalis*). There is very little or no difference between *S. trivalis* and mixed layer dwelling (interpreted from $\delta^{18}O$ values; see also Chapter 5) planktonic foraminifera (*Pr. taurica*) $\delta^{13}C$ values after the boundary until 63.5 Ma. After this point mixed layer dwelling planktonic foraminifera $\delta^{13}C$ values continue to increase to a maximum of ~3.6 ‰ at 61.4 Ma, after which $\delta^{13}C$ values stabilise. Similar to the corresponding $\delta^{18}O$ record, *Pr. inconstans* shows

increasing $\delta^{13}C$ values after its first appearance until ~62.5 Ma when its $\delta^{13}C$ values decrease to lower than the thermocline dweller *S. triloculinoides*.

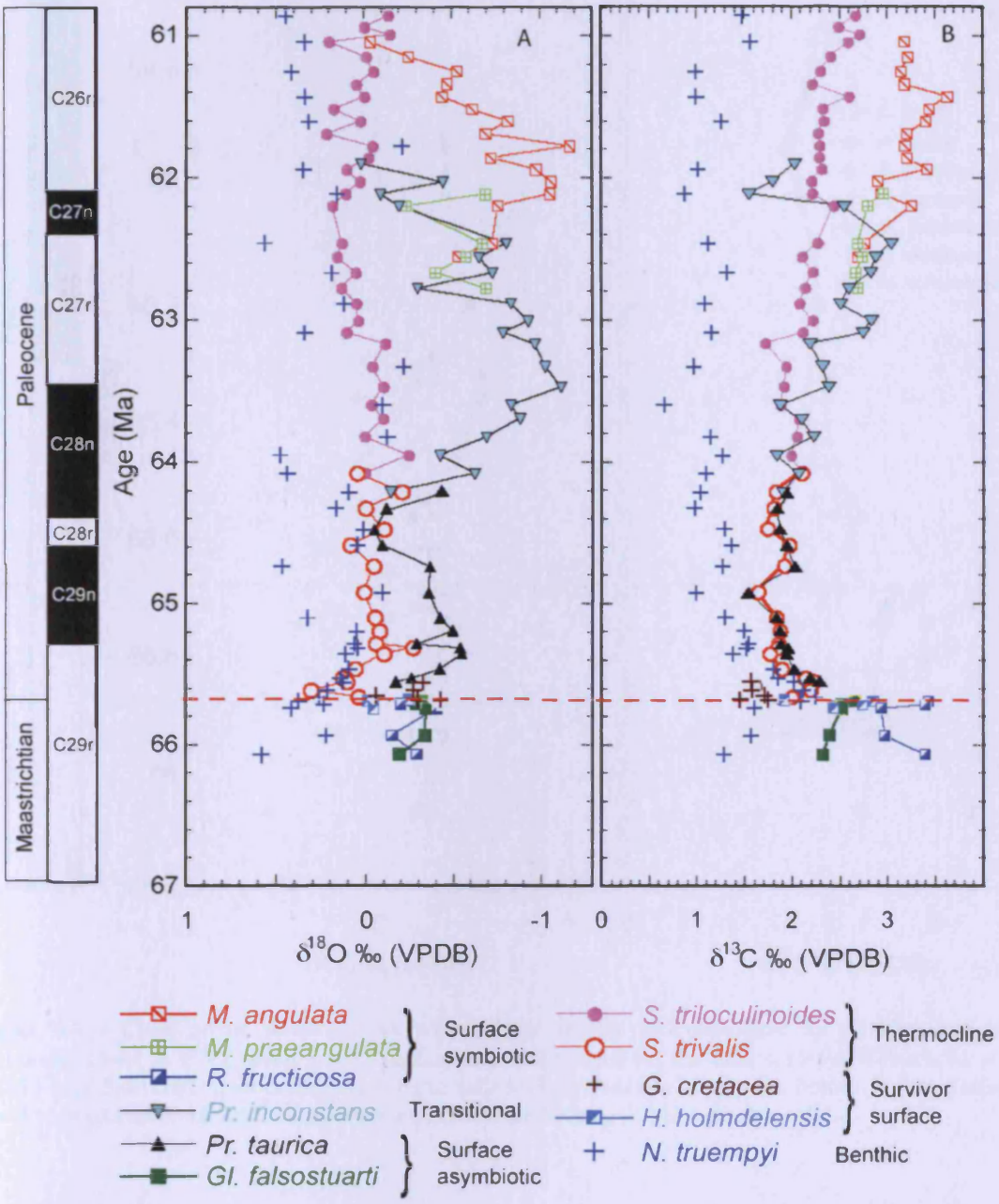

Figure 6.3 – Stable oxygen ($\delta^{18}O$), panel A and carbon ($\delta^{13}C$), panel B, isotope record from benthic and planktonic foraminifera against age (Ma) based on the time scale of Westerhold *et al,*. (2008), from Site 1262 (Appendix 11.1). Red line denotes the K/Pg boundary. Genera abbreviations as follows M= *Morozovella*, Pr = *Praemurica*, S = *Subbotina*, N = *Nuttallides*, R = *Racemiguembelina*, Gl = *Globotruncana*, G = *Guembelitria* and H = *Hedbergella*.

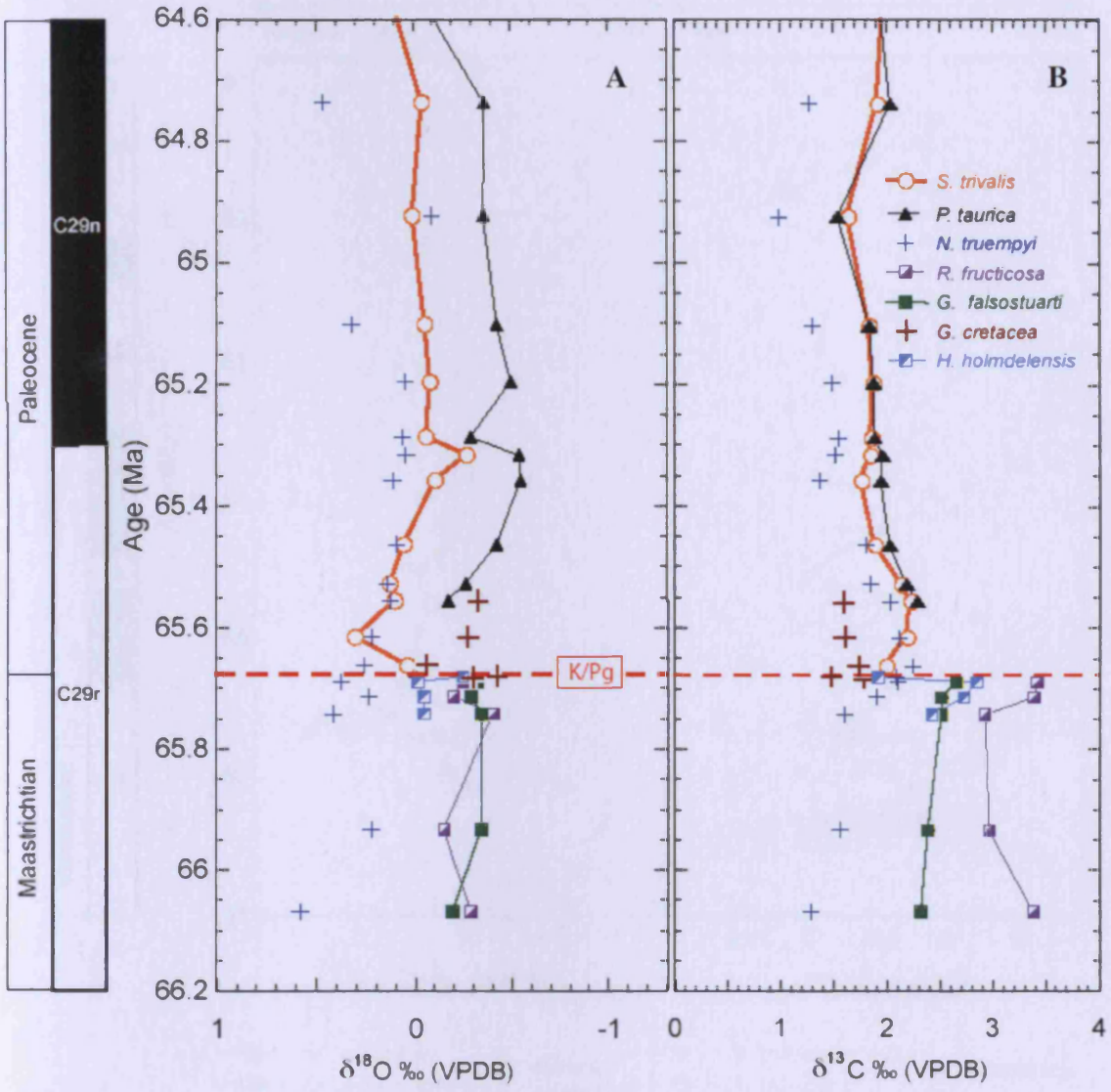

Figure 6.4 – Close up of stable isotope record from benthic and planktonic foraminifera and bulk carbonate. Panel A $\delta^{18}O$, panel B $\delta^{13}C$ against age (Ma) based on the time scale of Westerhold *et al.* (2008) from Site 1262. Genera abbreviations as follows Pr = *Praemurica*, S = *Subbotina*, N = *Nuttallides*, R = *Racemiguembelina*, Gl = *Globotruncana*, G = *Guembelitria* and H = *Hedbergella*.

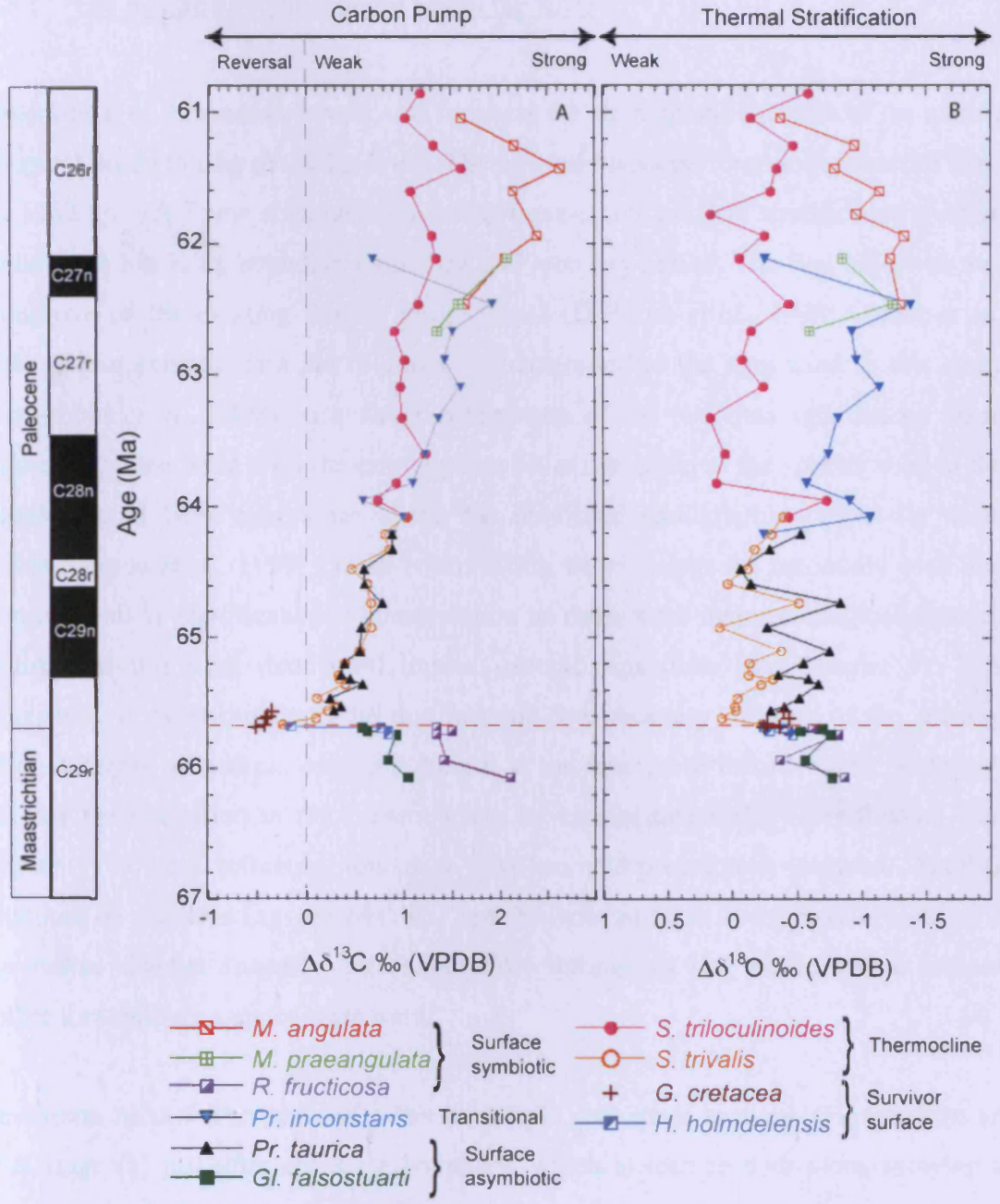

Figure 6.5 – Stable carbon ($\delta^{13}C$), panel A and oxygen ($\delta^{18}O$), panel B, isotope differences between the named planktonic foraminifera and benthic foraminifera against age (Ma) based on the time scale of Westerhold *et al.*, (2008) from Site 1262. Red line denotes the K/Pg boundary. Genera abbreviations as Figure 6.3.

6.3. Discussion

6.3.1. The marine biological pump across the K/Pg

A major goal of this research work was to assess the strength and function of the marine biological pump during the K/Pg event. The new multispecies foraminifera record from Site 1262 provided new constraints on ocean thermal and nutrient stratification over an extended ~4 Ma K/Pg boundary extinction and recovery period. The first objective was to improve on the existing Walvis Ridge record (D'Hondt *et al.*, 1998; Coxall *et al.*, 2006). These existing data are re-drawn and converted to the ages used in this study (Westerhold *et al.*, 2008) so a direct comparison of the two data sets can be made (Figure 6.6). One issue with the existing data set is that some of the species used in the isotopic record have ranges far above the published stratigraphic ranges for these species (Olsson *et al.*, 1999; Coxall *et al.*, 2006), which brings the taxonomy used into question. This is significant for interpretation as there were major ecological changes occurring at this time that could impact isotopic signatures (see Chapter 5). This discrepancy in taxonomy may be due to poor core recovery in parts of the section, and/or different taxonomic concepts present at the time these records were published. This has been rectified in the present study by careful taxonomic identification (see Chapter 3) so any influence this may have on interpretation is negated. Another limitation of the existing records was species selection, as there was a lack of a thermocline dweller (namely the subbotinids) throughout the record and a mix of benthic foraminifera species were used.

The carbon record after the K/Pg has been split into three sections (Figure 6.6): an initial stage (1) just after the K/Pg boundary, which is seen in both plots, showing a period when planktonic-benthic $\Delta\delta^{13}C$ were close to zero. In the second stage, seen again in both plots, planktonic-benthic $\Delta\delta^{13}C$ begin to return (between benthic and thermocline planktonic foraminifera) albeit at a reduced value compared to the Maastrichtian. Throughout this second stage of recovery the Site 1262 (Figure 6.6 – Plot A) $\Delta\delta^{13}C$ continues to increase and at ~64.1 Ma the pre-extinction difference of ~1.0 ‰ is reached, marking the return to a pre-extinction water column carbon gradient.

Following the idea of D'Hondt *et al.* (1998) interpretation of Site 1262 would indicate surface to deep ocean organic carbon export collapse at the K/Pg boundary, followed by a prolonged period of reduced carbon pump efficiency. The highly resolved Site 1262 age model indicates that marine biological pumping of carbon was suppressed for ~1.58 myr rather than the 3 myr that has previously been suggested (D'Hondt *et al.*, 1998; Adams *et al.*, 2004; D'Hondt, 2005; Coxall *et al.*, 2006) and provides new constraints for carbon system recovery. The final stage (3) of recovery sees the return of differences between mixed layer and thermocline planktonic foraminifera in the data presented here, however this is also coincident with the onset of photosymbiosis (see Chapter 5) and may just be an artefact of the exaggerated $\delta^{13}C$ values as a result of dependence of these foraminifera on their photosynthesising algae.

The mechanism to explain the inferred reduction in biological pumping is controversial. Reduced $\delta^{13}C$ gradients are unlikely to have been caused by prolonged cessation of biological production beyond a brief K/Pg event. Instead as suggested by D'Hondt *et al.* (1998) production would have quickly returned after any impact related effects, so that reduced $\delta^{13}C$ gradients must reflect interruptions to export. The data presented here are consistent with an initial recovery stage and the hypothesis of a return of biological production in surface waters, but a continued reduction in export over a longer recovery phase (D'Hondt *et al.*, 1998). However, the data here does not support the previous idea of stagnant $\Delta\delta^{13}C$ with no increase seen until a second stage of carbon recovery (D'Hondt *et al.*, 1998; Adams *et al.*, 2004; Coxall *et al.*, 2006). Site 1262 shows carbon export returned relatively quickly (~200 kyrs) after the K/Pg boundary, but at a reduced rate, which then steadily grew till pre-extinction values were restored at ~64.1 Ma. This gradual recovery is supported by other planktonic and benthic foraminifera stable isotope (ODP Site 690, Antarctic - Stott and Kennett, 1989) and bulk geochemical (Denmark - Sepúlveda *et al.*, 2009) studies that show a return of $\Delta\delta^{13}C$ soon after the K/Pg boundary and gradual increases thereafter for the extent (~1 Ma) of their studied interval. The second stage of recovery inferred by previous studies (D'Hondt *et al.*, 1998; Adams *et al.*, 2004; Coxall *et al.*, 2006) coincides with the evolution of photosymbiosis and likely represents an increased test $\delta^{13}C$ because of a vital effect rather than a real carbon flux signal (see Chapter 5).

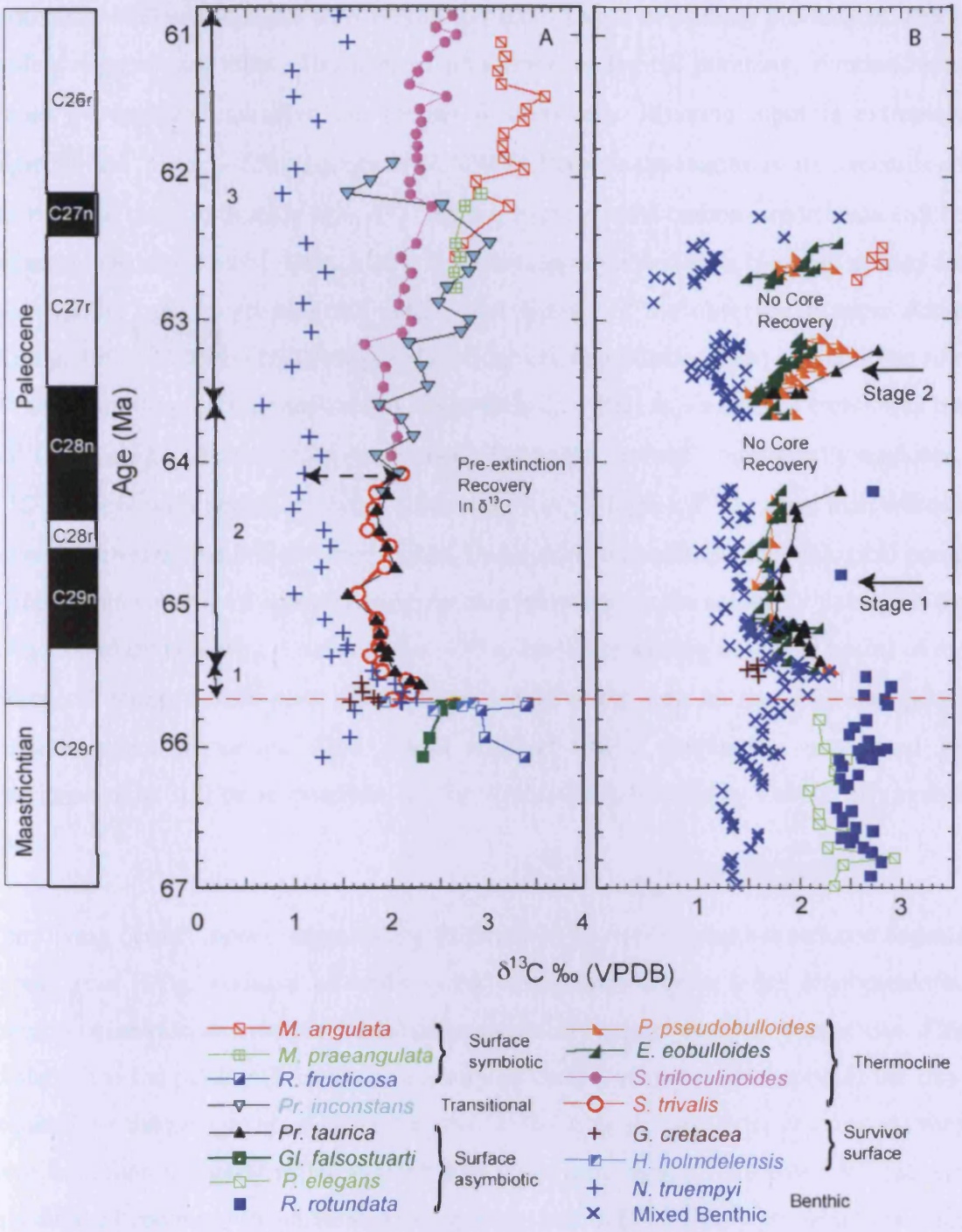

Figure 6.6 – Stable carbon ($\delta^{13}C$) isotope records from benthic and planktonic foraminifera from panel A - ODP Site 1262 and panel B - DSDP Site 528 (D'Hondt *et al.*, 1998; Coxall *et al.*, 2006) against age (Ma) based on the time scale of Westerhold *et al.*, (2008) note Site 528 ages were converted by linear interpolation from Cande and Kent (1995). Redline denotes the K/Pg boundary. Panel A 1= collapse of carbon pump, 2 = initial recovery of carbon pump and 3 = recovery of gradient between thermocline and surface layer dwelling planktonic foraminifera. Panel B - Stage 1 and 2 = recovery stages as interpreted by D'Hondt *et al*, (1998) Genera abbreviations as Figure 6.5 with additional genera as follows P = *Parasubbotina*, E = *Eoglobigerina*, Ps = *Pseudotextularia* and Rb = *Rugoglobigerina*.

Modelling studies also agree with a relatively quick return of primary production. These studies suggest that after ~100 kyrs of no marine biological pumping, riverine input would be expected to drive the marine $\delta^{13}C$ system. Riverine input is extremely depleted in $\delta^{13}C$ (e.g. -5 ‰, Lasaga *et al.*, 1985). Because the marine isotope records do not move to these extremely light $\delta^{13}C$ values, some vertical carbon export must still be occurring (Kump, 1991). Only a 10% reduction in organic carbon burial is needed for these model runs to produce the shape (and timing) of the observed isotopic curve (Kump, 1991). Another modelling study (Ridgwell, unpublished data) explored the role of the solubility pump (Broecker and Maier-Reimer, 1992) as a means of explaining the $\Delta\delta^{13}C$ reduction. The solubility pump acts to invert the 'normal' (biologically mediated) $\delta^{13}C$ gradient with depth, as colder polar waters (with higher $\delta^{13}C$ values than warmer waters) are ventilated into the deep ocean. Under normal conditions the biological pump is more than capable of compensating for this inversion by the solubility pump. At the K/Pg boundary however, a reduction of ~70 to 60 % (depending on ocean basin) of the biological pump would give the observed $\Delta\delta^{13}C$ trend seen as the solubility pump becomes more important. This would indicate that a mechanism unaffected by extinction must still be responsible for the ~30 to 40 % remaining transfer of organic matter.

The 'living ocean' model suggested by D'Hondt *et al.* (1998) assumes reduced organic export post K/Pg, because of wide spread extinctions among large phytoplankton, macrozooplankton and nekton faecal pellet producers higher up in the food chain. This explains the long delay (3 myr) in recovery of carbon pumping as it reflects the time required for the pelagic ecosystem to re-evolve these larger organisms and the role they have in carbon pumping to be re-established. The new record from Site 1262 reduces this delayed recovery to ~1.58 myr, suggesting that either, larger phytoplankton sizes and larger organisms evolved more quickly, or another mechanism was at work. As discussed in section 6.1.1 there are three main influences on how organic carbon is exported out of the photic zone. Firstly by packaging into larger sizes through ingestion e.g. faecal pellets, secondly by mineral ballasting ($CaCO_3$ is important in this process, Francois *et al.*, 2002) and lastly by aggregation into larger particles e.g. marine snow. The first mechanisms may have been impacted by extinctions among faecal pellet

producers, although the fossil record is incomplete. The effect of the $CaCO_3$ ballasting would have been greatly reduced due to 90 % extinction among calcareous planktonic foraminifera and nannoplankton (Smit, 1982). However, ballasting via silica would still remain and may even have increased as diatom and radiolarians are proposed to have bloomed in the aftermath of the extinction (Kitchell *et al.*, 1986; Hollis *et al.*, 1995; MacLeod *et al.*, 1997), although none were seen within the Site 1262 samples. The third mechanism of aggregate matter would have remained largely unaffected by the mass extinction, although differences in phytoplankton assemblage composition and the 'stickiness' of species specific secretions may have changed (Tallberg and Heiskanen, 1998; Thomas, 2007). These additional mechanisms would have provided some carbon export and may have slowly increased in importance after initial K/Pg event related disturbances, resulting in the steady increase of $\delta^{13}C$ gradients seen at Site 1262.

One result that was surprising was that despite obvious thermal stratification being present in the mixed layer (Figure 6.3) there was no evidence of stratification with regard to carbon isotopes between the proposed thermocline dweller (*S. trivalis*) and surface mixed layer dweller (*Pr. taurica*) (Figure 6.4) until the evolution of symbiosis and stage 3 of the recovery (Figure 6.6). *Praemurica taurica* over this time interval consistently gives the lightest $\delta^{18}O$ values and thus is the most likely candidate for a surface mixed layer dweller. D'Hondt *et al.* (1998) suggested that high rates of picoplankton rather than phytoplankton could lead to an increased fraction of production being moved through the microbial loop (Azam *et al.*, (1983). Increased patchiness of organic matter, due to the successive bloom of phytoplankton (Kitchell *et al.*, 1986; MacLeod *et al.*, 1997; Thomas, 2007) after the mass extinction, may have increased bacterial diversity and numbers (Azam, 1998) and may explain the increase in the microbial loop. An increase in recycling in the upper mixed layer would lead to an increase in light ^{12}C input at this depth and reduce the effect of photosynthesis stripping, which would effectively homogenise the upper part of the water column. Under these conditions the surface mixed layer would have a higher nutrient content and could be classed as mesotrophic. This could explain the lack of a $\delta^{13}C$ gradient between *Pr. taurica* and *S. trivalis*. Another explanation would be that *Pr. taurica* at the time was not living in the upper layers of the water column but at depths not much different from

S. trivalis. Temperature changes decrease greatly at the thermocline and could mean that a foraminifera could be experiencing very different temperatures over a small depth range, this could explain the lack of $\delta^{13}C$ gradient between them. The re-establishment of a $\delta^{13}C$ gradient between thermocline and surface mixed layer dwelling planktonic foraminifera occurs at the same time that the isotopic signature of photosymbiosis appears in the morozovellid lineage, when a surface habitat is essential. The $\delta^{18}O$ values document a shift in habitat in *Pr. inconstans* ($\delta^{18}O$ decreases) indicating a move to more surface waters (Figure 6.3), coincident with $\delta^{13}C$ signature of symbiosis (Chapter 5). A combination of increased microbial activity and decreased $\delta^{13}C$ gradient in the mixed layer, as well as a generally deeper habitat, probably combined to give the overall lack in surface-thermocline $\delta^{13}C$ gradients in stage 2 of the recovery. However, the influence of the microbial loop would have slowly been reduced as the export of organic carbon to deep waters increased and returned to normal at 64.15 Ma. This period coincides with a lack of $\delta^{18}O$ gradient as well as $\delta^{13}C$ gradient in the *Pr. taurica* and *S. trivalis* and thus may reflect a similar depth habitat, as another species takes over the niche of surface water dweller (see Chapter 7). Further analysis of a known non-symbiotic surface dweller (such as *Eoglobigerina spirals*, which were too rare to analyse in Site 1262 samples), may help to resolve this matter.

6.3.2. Reconciling benthic and planktonic foraminifera data.

The greatest challenge to the 'living ocean' suppressed carbon flux hypothesis came from the benthic community. Benthic foraminifera, which supposedly rely on export of surface derived organic carbon for nutrient and survival, showed no extinction at the K/Pg boundary, which provides evidence that the carbon pump (i.e. there food supply) was not significantly collapsed or perturbed (Thomas, 1990; Alegret *et al.*, 2001; Alegret *et al.*, 2003; Culver, 2003; Coccini and Marsili, 2007). Other arguments against the delayed carbon export hypothesis stem from the evidence that many other marine organisms survived the K/Pg event and bloomed in the early Danian. Surviving phytoplankton could be expected to bloom as soon as impact clouds receded and light returned. Catastrophic extinction (~90 %, Smit, 1982; Bown *et al.*, 2005) of calcareous

nannoplankton, the documented main primary producers in the Cretaceous, would have reduced competition for nutrients and potentially allowed siliceous phytoplankton species (that suffered less significant extinction) and bacterial primary producers to take over. Blooms in some coccolithophorids (e.g. *Braarudosphaera* and *Biscutum*), diatoms, cyanobacteria, and dinoflagellates (Kitchell *et al.*, 1986; Brinkhuis and Zachariasse, 1988; Gardin and Monechi, 1998; D'Hondt *et al.*, 1998; Bown *et al.*, 2005) have all been seen after the K/Pg boundary. These irregular bloom events may have been enough to sustain the benthic foraminifera while overall export production was reduced (Smith *et al.*, 1992). Despite these observations sediment accumulation records from a number of deep sea sites (Hsü *et al.*, 1982; Zachos and Arthur, 1986; Zachos *et al.*, 1989) indicate a major decrease in total sediment flux to the seafloor as a result of calcareous nannofossil extinction (Smit, 1982; Bown *et al.*, 2005).

The fact that $\delta^{18}O$ of Danian species in the Site 1262 data set records thermal stratification, is evidence that a typical range of depth habitats were exploited by Danian planktonic foraminifera, but that the surface to deep $\delta^{13}C$, and thus nutrient, gradient represents an altered carbon state compared to the late Maastrichtian. As discussed by D'Hondt *et al.* (1998) only a partial reduction in carbon organic flux is needed to reduce the surface to deep $\delta^{13}C$ gradient (supported by modelling studies, Ridgewell unpublished). The point being that the interpretation of extended carbon pump suppression is supported by the data presented here.

It has been argued in the past that the lack of $\delta^{13}C$ gradient may not be a result of a lack of export production but due to a number of other factors. These include; vital effects on planktonic foraminifera (through disequilibrium factors such as changing ecologies in the early Danian or reduced average test size), diagenesis, the use of different planktonic foraminifera above and below boundary or gas hydrate release (Day and Maslin, 2005), which would release ^{12}C into the oceans and effectively homogenise them (Thomas, 2007). Gas hydrate (characterised by a very light $\delta^{13}C$ signature [~ -60 ‰, Dickens *et al.*, 1995]) release at the K/Pg boundary has the potential to decrease water column $\delta^{13}C$ during its release. However, since there was no associated warming trend (Figure 6.4), that would be expected for a release of methane to the

system, this seems unlikely. Diagenesis also has the potential to alter $\delta^{18}O$ and to a lesser extent $\delta^{13}C$, but any such alteration would do so proportionally in all species such that any original signal between species and specimens is preserved (Sexton *et al.*, 2006). Moreover there is no evidence for significant preservation changes of Site 1262 material over the studied interval.

Site 1262 tackles the additional questions related to vital effects through evolutionary differences in planktonic foraminifera tracers with the use of detailed paleoecological investigations into early Paleocene species (Chapter 5). The down hole record uses planktonic foraminifera from carefully controlled size classes so vital effects should be kept to a minimum and the use of species that crossed the boundary, i.e. *G. cretacea* and *H. holmdelensis*, which are assumed to have constant ecology, ensures consistency. *Guembelitria cretacea* $\delta^{13}C$ changed little from the Maastrichtian to Danian. Its $\delta^{13}C$ signature is typically characterised by unusually depleted $\delta^{13}C$ values compared to other species, which is consistent with its inferred 'opportunistic' ecology. This species, as with other microperforate survivor species at the K/Pg boundary, has been suggested to have adopted both benthic and planktonic lifestyles termed 'tycho-pelagic' (Darling *et al.*, 2009). It is thought that this change in lifestyles allowed *G. cretacea* to survive the K/Pg event and dominate surface waters in the early Danian (Darling *et al.*, 2009). *Hedbergella holmdelensis*, a more oligotrophic 'typical' taxon, on the other hand, did show a significant shift to lighter $\delta^{13}C$ values at the boundary.

One suggestion for the survival of benthic foraminifera despite reduced organic flux is a reduced dependence of benthic foraminifera to surface derived food (bentho-pelagic coupling) in the warmer climates of the Paleogene (Alegret *et al.*, 2001; Thomas, 2003; Thomas, 2007). This is demonstrated in longer term records of benthic foraminiferal assemblages, where bentho-pelagic coupling is not suggested to have fully started until the Eocene/Oligocene boundary (Thomas and Gooday, 1996). 'Greenhouse' faunas contained rare photodetritus dependent species unlike the modern ocean (Alegret *et al.*, 2001; Gooday, 2003; Thomas, 2007) and instead early Paleogene assemblages mainly contained deposit feeders (feeds on decomposing organic matter), which may have helped them to survive periods of reduced food supply (Thomas, 2007). Extinction

selection studies (Sheehan *et al.*, 1996) also showed that deposit feeders in general survived the K/Pg boundary better than their primary or secondary consumer counterparts. Despite a suggested reduced benthic-pelagic coupling in the Paleocene, buliminids (a group that thrives on high food concentrations) see a decrease at the K/Pg boundary and remained low while changes in community structure to smaller, agglutinated and opportunistic forms of benthic foraminifera occurred (Kuhnt and Kaminski, 1993; Alegret *et al.*, 2001; Peryt *et al.*, 2002; Alegret and Thomas, 2007; Coccini and Marsili, 2007). These changes in benthic assemblages are reported to have lasted for ~200 kyr, which coincides with stage one (Figure 6.6) of the carbon recovery (Kuhnt and Kaminski, 1993; Peryt *et al.*, 2002; Coccini and Marsili, 2007). The constant fluctuations in benthic community structure stabilize at the very time when $\delta^{13}C$ gradients begin to return.

This study provides further evidence that the carbon pump was reduced past initial K/Pg event disruptions, for approximately 1.58 myr. After initial disruptions in stage 1 that lasted 200 kyr, $\delta^{13}C$ gradients first appeared and continued to steadily increase. Benthic assemblages fluctuate greatly within this first 200 kyr after the K/Pg, then when organic carbon flux (as indicated by $\delta^{13}C$ gradients) first starts to appear, albeit at a reduced rate, benthic assemblages become more stable. This data provides for the first time some links between benthic and planktonic foraminifera and may help to further reconciling the two data sets. This would be particularly true if in the reduced organic flux period (stage 2) bentho-pelagic coupling was reduced in the warmer Paleocene, negating the benthic foraminifera's need for surface derived food.

6.3.3. Re-calibrated marine biological pump

The new interpretation of early Paleocene planktonic foraminifera paleoecologies and their disequilibrium effects, as detailed in Chapter 5, will allow for a refined and more accurate assessment of water column $\delta^{13}C$ gradients and thus the strength of marine carbon pump recovery after the K/Pg boundary. The resulting metabolic fractionation on small (<150 μm) test sizes causes $\delta^{13}C$ values to be depressed by ~0.3 to 0.5 ‰. For this reason *G. cretacea* and *H. holmdelensis* were adjusted (Table 6.1) by adding 0.4 ‰

to each $\delta^{13}C$ value. The value of 0.4 ‰ was selected because the isotopic depletion is greatest in the smallest size fractions and the specimens available in the early Danian are particularly small (65-125 μm).

In some planktonic foraminifera species of larger test sizes (>150 μm) a relationship with symbiotic algae causes $\delta^{13}C$ values to be enriched by up to 1.5 ‰. The amount of $\delta^{13}C$ enrichment is dependent on the test size and the species in question. In early *Pr. inconstans* and *M. praeangulata*, when symbiosis as an ecological strategy was first appearing at 63.5 Ma, the enrichment was less pronounced than in later species. For this reason the adjustment factor for symbiosis has been split into two categories (Table 6.1); weak symbiosis and full symbiosis. Weak symbiosis sees enrichment between 0.1 and 0.3 ‰, as the specimens picked here were at the larger end of the spectrum (>212 μm) for these species, where enrichment would be greatest, an adjustment value of 0.3 ‰ will be taken from these species. Full symbiosis sees enrichment range from 0.5 to 1.5 ‰, as the specimens selected (*M. angulata*) were of medium to large size (212-250 μm) for this species, a adjustment value of 1.0 ‰ will be applied. *Praemurica taurica* and *Subbotina* sp. show no marked size related disequilibrium effects (Chapter 5) and therefore are not adjusted.

Test Size	Type of disequilibrium	$\delta^{13}C$ Offset Range	$\delta^{13}C$ Adjustment
<150 μm	Metabolic	- 0.3 - 0.5 ‰	+ 0.4 ‰
>150 μm	Weak symbiosis	+ 0.1 - 0.3 ‰	- 0.3 ‰
>150 μm	Full symbiosis	+ 0.5 - 1.5 ‰	- 1.0 ‰

Table 6.1 – Calculated $\delta^{13}C$ adjustment factors (option 1) applied to species with known isotopic disequilibrium effects, taken from Chapter 5. Weak symbiosis refers to an ecological state characterised by smaller $\delta^{13}C$ offsets displayed by the symbiotic planktonic foraminifera when this ecology first appears (see Chapter 5).

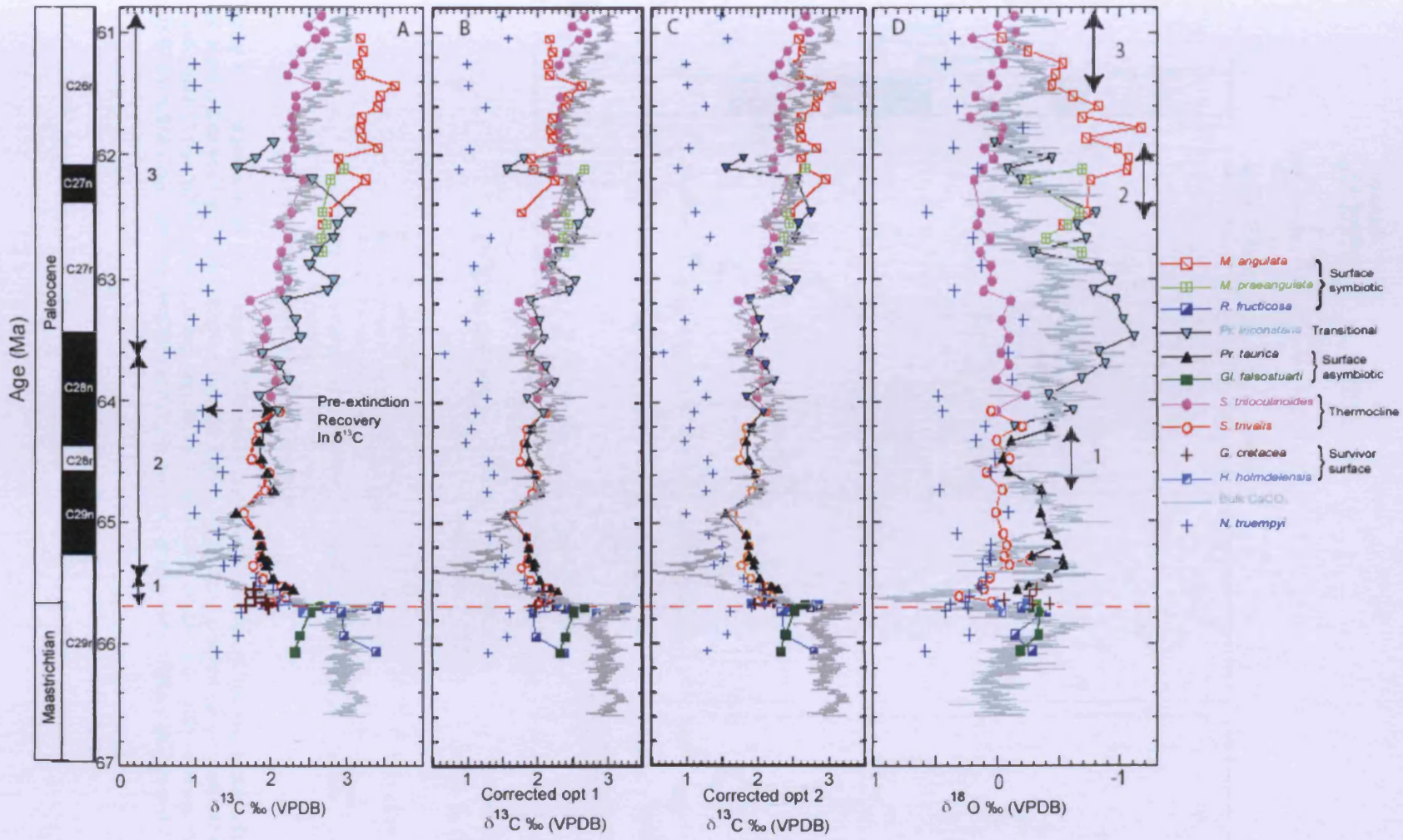

Figure 6.7 – ODP site 1262 benthic and planktonic foraminifera stable isotopes, A uncorrected $\delta^{13}C$, B corrected $\delta^{13}C$ option 1 and C corrected $\delta^{13}C$ option 2. D Stable oxygen ($\delta^{18}O$) isotope. Time scale of Westerhold *et al*,. (2008). Bulk isotope data taken from Kroon *et al*., (2007). Red line K/Pg boundary. Genera abbreviations as follows M= *Morozovella*, Pr = *Praemurica*, S = *Subbotina*, N = *Nuttallides*, R = *Racemiguembelina*, Gl = *Globotruncana*, G = *Guembelitria* and H = *Hedbergella*.

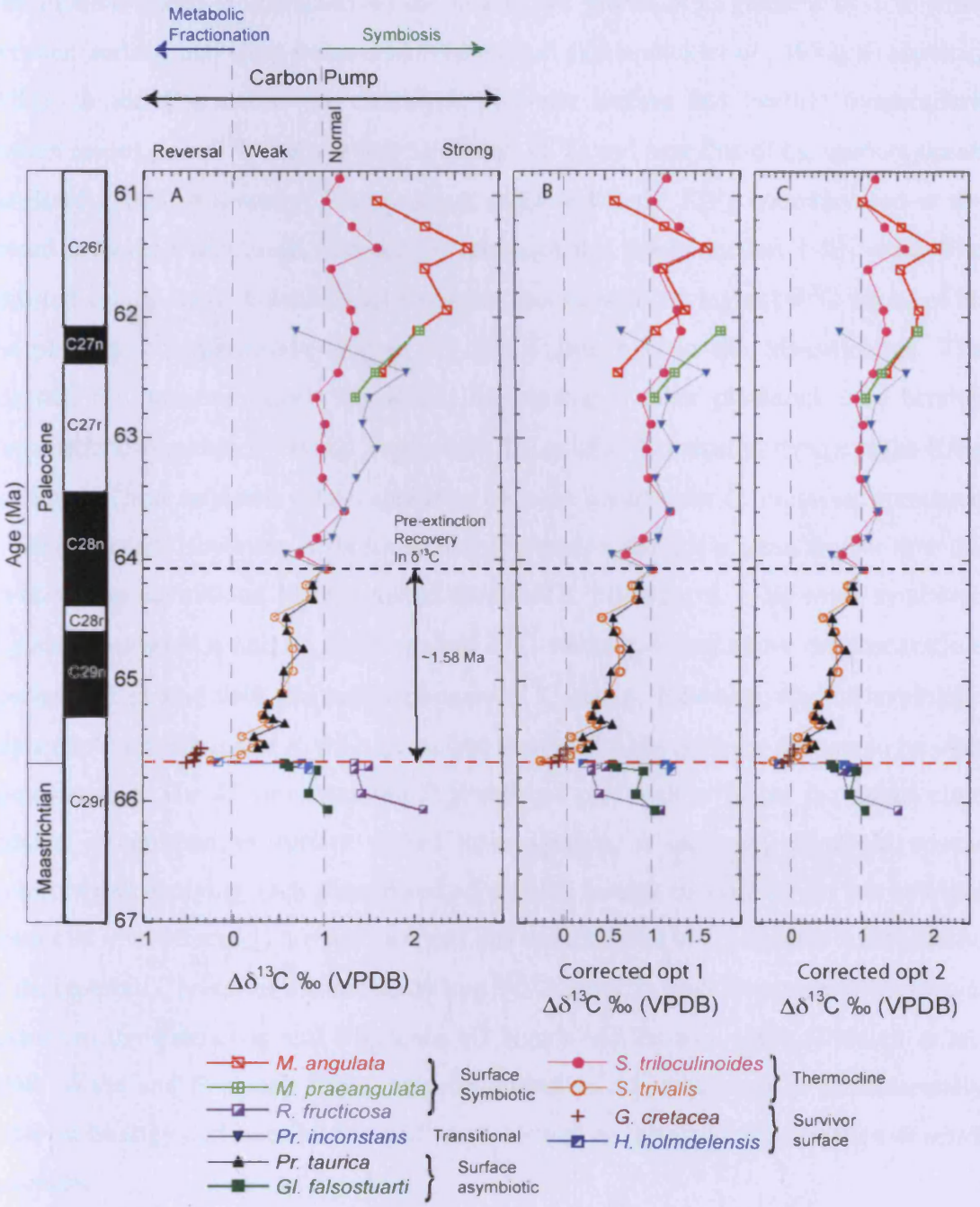

Figure 6.8 – Stable carbon ($\delta^{13}C$) isotope differences between individual planktonic foraminifera species and benthic foraminifera paired samples. Panel A before adjustment and panel B with adjustment option 1 and panel C with adjustment option 2, against age (Ma) based on the time scale of Westerhold *et al.*, (2008) from Site 1262. Red line denotes the K/Pg boundary. Genera abbreviations as Figure 6.7.

The modern ocean is characterised by an average global $\delta^{13}C$ gradient of 1 to 2 ‰ between surface and deep water dissolved carbon (Kroopnick *et al.*, 1972; Kroopnick, 1985). In the Cretaceous the difference between surface and benthic foraminifera (which record past $\delta^{13}C$ DIC) at Site 1262 was ~1 ‰ and near that of the modern ocean (D'Hondt, 2005; this study). This gradient collapsed at the K/Pg boundary and in the record presented here took 1.58 myr to return to this pre-extinction 1 ‰ value. The adjusted values for *H. holmdelensis* place this species with the highest $\delta^{13}C$ values of all the planktonic foraminifera (Figure 6.7 and Figure 6.8) in the Maastrichtian. The adjusted *G. cretacea* values fall within the cluster of other planktonic and benthic foraminifera (Figure 6.7 – B and Figure 6.8 - B), as all $\delta^{13}C$ values converge at the K/Pg boundary. These adjusted values appear to be more realistic for *G. cretacea*, compared to non-adjusted. However, *H. holmdelensis* in contrast, records a signal higher than the co-occurring asymbiotic surface mixed dweller *Gl. falsostuarti*. The weak symbiotic adjusted *Praemurica* and *M. praeangulata* $\delta^{13}C$ values plot just above the thermocline species and in line with the bulk carbonate $\delta^{13}C$ values. However, the full symbiotic adjusted *M. angulata* and *R. fructicosa*, like that of *H. holmdelensis*, appears to be over compensating. The *M. angulata* and *R. fructicosa* plot with or below the thermocline species, rather than as surface mixed layer species, as expected. It would appear therefore that applying such generalised adjustment factors, accounting for test size and symbiotic vital effects, is not justified and that species need to be assessed individually. In the case of *G. cretacea* the unusually low $\delta^{13}C$ values, as seen in other microperforate taxa from the Paleocene and Oligocene (D'Hondt and Zachos, 1993; D'Hondt *et al.*, 1998; Wade and Pearson, 2009), may be related to a combination of fundamentally different biology and calcification pathways, as well as metabolic fractionation at small test sizes.

With this is mind a second option (Option 2) for adjustment is presented (Figure 6.7 – C and Figure 6.8 – C), where small microperforate *G. cretacea*, but not the small macroperforate *H. holmdelensis*, are adjusted by addition of 0.4 ‰. *Praemurica inconstans* and *M. praeangulata* are left with their adjustment factor of 0.3 ‰. Symbiosis does not appear to be affecting the $\delta^{13}C$ gradient of *M. angulata* or *R. fructicosa* as strongly as anticipated, thus a new adjustment factor of 0.3 ‰ for early *M.*

angulata, similar to the *Praemurica* and *M. praeangulata* is applied. An adjustment factor of 0.6 ‰ is applied for later *M. angulata* and *R. fructicosa*, which brings these species in line with the bulk carbonate $\delta^{13}C$ values and the *Praemurica* and *M. praeangulata* values. This exercise re-affirms the need to take care when interpreting planktonic foraminifera test $\delta^{13}C$ values. Each species needs to be treated separately and test size $\delta^{13}C$ variability should be explored in all potential water mass tracer species, rather than generalising small and/or symbiotic ecologies. Option 2 appears to be a better interpretation of the adjusted $\delta^{13}C$ values of some species and will be used in further interpretations in this chapter. These adjustments now indicate that there was no obvious reversal in the $\delta^{13}C$ gradient only a reduction to zero and the large increase in $\delta^{13}C$ gradient seen after 63.6 Ma in the symbiotic species is now reduced.

The adjusted multispecies $\delta^{13}C$ records provide new constraints on the magnitude and timing of carbon system disturbance at Site 1262. A delayed recovery period is seen in the results presented here and agrees with the proposed model by D'Hondt *et al.* (1998). However, the recovery was found to not be as long (1.58 myr compared to 3 myr) in the new record presented here, which uses thermocline as well as surface mixed layer planktonic foraminifera. The $\delta^{13}C$ gradient between surface and deep waters is found to be present between the thermocline planktonic and benthic foraminifera. As the thermocline species (*Subbotina* and *Parasubbotina*) appear to be particularly stable (no recorded $\delta^{13}C$ size trends, Chapter 5) at this time period. Future studies should use these species rather than surface mixed layer planktonic foraminifera (with recorded $\delta^{13}C$ size trends, Chapter 5) for marine carbon pump interpretations within the Paleocene.

Within the recovery period of $\delta^{13}C$ gradient, there is no evidence here for a second stage in $\delta^{13}C$ gradient recovery. The second stage recognised by previous studies (D'Hondt *et al.*, 1998; Adams *et al.*, 2004; Coxall *et al.*, 2006) appeared to coincide with the onset of photosymbiosis (Chapter 5). The new adjusted record presented here will help decide whether this was a real carbon flux signal or a vital effect. A $\delta^{13}C$ gradient between thermocline and surface planktonic foraminifera still exists, now reduced to ~0.2 ‰, even with the applied 0.3 ‰ adjustment for photosymbiosis (Figure 6.7 and Figure 6.8). The average global modern gradient between the surface and thermocline $\delta^{13}C$ DIC is

approximately 0.4 – 0.6 ‰ (Kroopnick *et al.*, 1972; Kroopnick, 1985) if there are no unusual hydrographic conditions, such as upwelling occurring (Nathan and Leckie, 2009). The 0.2 ‰ $\delta^{13}C$ gradient can be interpreted as a real signal, though approximately half that of modern conditions. The reduced gradient compared to modern values could indicate different hydrographic conditions for the early Paleocene compared to today (MacLeod *et al.*, unpublished). Surface waters could have been more homogenised, due to increased mixing. Another possibility is diagenesis, which could have homogenised the sample slightly resulting in a decreased $\delta^{13}C$ gradient (Sexton *et al.*, 2006). Nathan and Leckie (2009) observed smaller $\delta^{13}C$ gradients in modern waters from the western equatorial Pacific when productivity was high (due to upwelling of nutrients) and the thermocline was shallow. Perhaps this was also the case in the early Paleocene, with a recently recovered carbon pump, productivity may still have been high in surface mixed layer waters. The parallel $\delta^{18}O$ record indicates thermal stratification (Figure 6.7) at this time, so any factors leading to homogenisation of the $\delta^{13}C$ gradient are not affecting the $\delta^{18}O$ record, which makes diagenesis (which generally effects $\delta^{18}O$ more than $\delta^{13}C$ values, Sexton *et al.*, 2006) unlikely.

The bulk $\delta^{13}C$ of carbonate largely represents the surface mixed layer nannoplankton fraction. However, major extinction and reduced flux of nannoplankton at the K/Pg boundary mean a reduced proportion of this bulk material is from nannoplankton and an increased proportion of bulk carbonate is represented by planktonic foraminifera (Zachos and Arthur, 1986; D'Hondt et al., 1996; D'Hondt 2005; see also Chapter 7). As the stable isotope test size fraction analysis (Chapter 5) and down hole stable isotope record indicate, these planktonic foraminifera were subject to a variety of disequilibrium affects, which may have affected the $\delta^{13}C$ of the bulk carbonates. The bulk record appears to track the *Subbotina* sp. record closely (Figure 6.7). At this time the smaller size fractions were dominated by assemblages of thermocline dwelling *Subbotina*, *Parasubbotina* and *Globanomalina* species (Chapter 7; Appendix 11.3), which may account for the bulk $\delta^{13}C$ record largely tracking the *Subbotina* sp. $\delta^{13}C$ record. It is not until the proportion of nannoplankton contribution to the sediment increases at ~61.2 Ma (Chapter 7) that a true surface bulk record is seen.

The $\delta^{18}O$ record indicates three intervals (Figure 6.7 – D, labelled 1 to 3) where surface mixed layer dwelling species (*Pr. taurica*, *Pr. inconstans* and *M. angulata*) appear to change their habitat and become thermocline dwellers (as noted earlier); Stage 1, *Pr. taurica* appears to be superseded by *Pr. pseudoinconstans*. Stage 2, *Pr. inconstans* is superseded by the newly evolving morozovellids. Stage 3, *M. angulata* is superseded by the evolution of the morozovellids primarily *M. apanthesma* and *M. occlusa* (Chapter 7, Figure 7.6 to 7.7). High species turnover is seen throughout the early Paleocene (Chapter 7). New species evolved within these lineages and appear to live in a common surface habitat, but the $\delta^{18}O$ values indicate that the ancestor is not as well adapted as it's descendent. The ancestor later migrates to a deeper thermocline habitat before disappearing. Competitive exclusion is seen in modern planktonic foraminifera, between different genetic types of *Globigerinoides ruber* (Aurahs *et al.*, 2009), but remains a largely unexplored phenomenon. The results here provide evidence that the recognised species maybe more than just arbitrary morphological separations and represent true biologically separate species. This constant species turnover (at greater rates than background species turnover, Gerstel *et al.*, 1987) and competitive exclusion probably results from changing environmental conditions (Gerstel *et al.*, 1987), as the pelagic ecosystem recovers from the K/Pg event. This influence appears to be greater in surface mixed layer dwellers than thermocline dwellers, which show a reduced species turnover and longer species ranges (Chapter 7, Figure 7.2 to 7.8). This suggests that the environmental change occurring is having a greater impact in surface mixed layer waters or that the thermocline species are more resistant.

6.4. Summary

- Stability of the carbon system starts ~200 kyrs after the K/Pg extinction, with the return of a small $\Delta\delta^{13}C$ gradient.
- Recovery of $\Delta\delta^{13}C$ values continues steadily and at ~1.58 myr after the K/Pg event the carbon system returns to pre-extinction conditions, far earlier than the previously quoted 3 myr.
- No second stage in $\Delta\delta^{13}C$ recovery is seen only a $\delta^{13}C$ gradient between mixed layer and thermocline planktonic foraminifera is evident. This may be the result of the evolution of photosymbiosis at this point and a return to surface mixed layer waters.
- Benthic foraminifera communities fluctuations stabilise at the same time as initial $\Delta\delta^{13}C$ gradients start to appear. These findings may finally resolve the benthic – planktonic foraminifera conflict that has surrounded the carbon recovery after the K/Pg boundary event.
  - When adjustments were made to account for these effects in the down hole $\delta^{13}C$ record there appears to be over compensation in some species. This re-affirms the need to take care when interpreting planktonic foraminifera test $\delta^{13}C$ values. Each species needs to be treated separately and test size $\delta^{13}C$ analysis is required for each potential tracer species rather than generalising small and/or symbiotic ecologies.
  - The occurrence of a $\delta^{13}C$ gradient between thermocline and surface mixed layer planktonic foraminifera appearing at ~63.5 Ma, which coincide with the onset of photosymbiosis. This $\delta^{13}C$ difference between thermocline and surface mixed layer planktonic foraminifera is still present after a photosymbiosis adjustment factor is applied and thus likely represents a real $\delta^{13}C$ signal.

7. Paleocene Planktonic Foraminifera Size and Diversity.

This chapter focuses on planktonic foraminifera assemblage turnover and test size distribution. This information is then used to asses the changing ecological function of planktonic foraminifera after the mass extinction and throughout the recovery period. In addition the weights of sieved planktonic foraminiferal size fractions are used to evaluate how the contribution of size differentiated planktonic foraminifera ecological groups affect carbonate accumulation at the sea floor have varied over time.

7.1. Introduction

Since Cretaceous times planktonic foraminifera have had three major intervals of morphological diversification (Cifelli, 1969). At the start of each interval planktonic foraminifera had small tests and were of globigerinid form (Luterbacher and Premoli Silva, 1964), before test size increased and ornamentation developed (Norris, 1991). The dominance, at the start of each new radiation, by small, simple, cosmopolitan foraminifera suggests that these species were better adapted to cross through periods of environmental change than larger more specialist forms. Large species also tend to have lower population densities than smaller ones and are, as a result, more prone to extinction, as the K/Pg boundary demonstrates (Norris, 1991). The increase in planktonic foraminiferal size in the Paleocene correlates with increases in species richness following the K/Pg extinction and is primarily caused by the diversification of the morozovellids (Schmidt *et al.*, 2004a).

Detailed sedimentological and assemblage studies have demonstrated a 90% loss in diversity of planktonic foraminifera at the K/Pg boundary (Smit, 1982; D'Hondt *et al.*, 1996; MacLeod *et al.*, 1997; Molina *et al.*, 1998). Only a few species of planktonic foraminifera occur consistently more than a few centimetres above the boundary horizon (D'Hondt, 2005) and could be classified as Cretaceous survivors. These few survivors are thought to have seeded the subsequent Paleogene evolutionary radiation of planktonic foraminifera (Olsson *et al.*, 1999). In particular, the extinction caused loss of

large (<500μm) ornate keeled species (e.g. *Globotruncana*, *Globotruncanita*) as well as multiserial species (e.g. *Planoglobulina*) that had dominated pelagic assemblages for tens of millions of years. These were replaced abruptly in the earliest Paleocene by tiny triserial and biserial species with very few chambers. Some of these were extinction survivors (Olsson *et al.*, 1999) and others evolved within the first ~100 kyrs after the extinction event. Other survivors were small trochospiral hedbergellids. Two waves of evolutionary expansion have been described (Coxall *et al.*, 2006), the first within the first 300 kyr establishing basic genera and the second increasing species diversity ~ 3 myr later. These two waves of diversification were found to correlate with the two stage recovery in carbon isotopes that are interpreted as evidence for major disruptions to the marine carbon pump (Coxall *et al.*, 2006: see also Chapter 6).

Although many studies have produced range charts displaying which species are present and /or absent above and below the boundary, few quantitative records of abundance exist and even fewer records span the extended multimillion year period of extinction and carbon system recovery (Boersma, 1984; Gerstel *et al.*, 1987; Brinkhuis and Zachariasse, 1988; D'Hondt and Keller, 1991; Molina *et al.*, 1998; Coxall *et al.*, 2006). The following chapter address this limitation and focuses on the ecological recovery of planktonic foraminifera after the K/Pg mass extinction, with a focus on faunal turnover (species assemblage changes) and changes in test size.

Organism size is an easily measured and obvious morphological characteristic that is present in the fossil record (Schmidt *et al.*, 2004b; Schmidt *et al.*, 2006). Test size in planktonic foraminifera reflects ecology and the environmental conditions within its habitat; hence changes in test size can indicate ecological or environmental change (Schmidt *et al.*, 2006). By looking at changes in the contribution of different test size fractions to sea floor sediment, together with examining changes in planktonic foraminiferal assemblage composition within the sieved size classes, an overall picture of the environment and ecological function of planktonic foraminifera can be made. In addition to ecological changes, test size changes will be assessed to evaluate the dramatic reduction in the average planktonic foraminifera size at the K/Pg boundary and the implications this has for $CaCO_3$ accumulation at the sea floor.

7.2. Results

7.2.1. Test size distributions

Before the K/Pg boundary, in the Maastrichtian, at Site 1262, the percent contribution of the different sieved planktonic foraminifera size fractions to the total sample weights is evenly distributed, with each size fraction contributing similar proportions. The K/Pg boundary extinction event can be seen clearly in Figure 7.1, as reflected by a dramatic decrease in the proportion of larger tests to the >38 μm sediment fraction. This dramatic decrease in average test size at the K/Pg boundary coincides with a major increase in the foram fraction (the sediment fraction >38 μm, which contains predominately only foraminifera, the <38 μm fraction was not available). The data show a corresponding two fold increase (40 % to ~ 80 %) in the proportion of smaller (<106 μm) planktonic foraminifera tests contributing to the sedimentary foram fraction. These smaller tests (<106 μm) remain the dominate sediment contributor for ~2 Ma. During the interval studied the values never seem to reach those of pre-boundary conditions although they do follow a general trend in that direction. After the boundary the 80-106 μm size fraction consistently appear to have the highest percent weight contribution to the overall sediments when compared to the other size fractions. The foram fraction weight shows a significant increase just above the K/Pg boundary, followed by a general trend of decreasing values, returning to near pre-extinction values at ~61 Ma (Stage A4 on Figure 7.1). Overprinted on this general decreasing trend are many fluctuations, particularly in the early stage A1 after the extinction, reducing through the subsequent stage A2 and A3. Peaks in total weight (ignoring the peaks around 63.2 Ma which correspond with samples where lithified black/brown lumps were found) appear to correlate with peaks in the contribution of the 80-106 μm test size fraction. Comparison of the foram fraction to the <38 μm size fraction can not be made at this time as the data is unavailable.

To assess how the planktonic foraminifera test size fractions and overall weight fluctuations may affect the accumulation of sediment on the seafloor, the weight percent of bulk carbonate and sedimentation rate taken from Kroon *et al.* (2007) are also shown (Figure 7.1, C and E). The percent carbonate plot shows a reduction at the boundary,

but the minimum of less than 10 % is just above the K/Pg boundary (~65.4 Ma). After this point percent carbonate fluctuates greatly (Stage C1) until ~64.6 Ma when values start to stabilise and gradually increase (Stage C2). Foram fraction weight appears to be positively correlated with % $CaCO_3$ in the early Danian (up to 64.6 Ma) but not in the Maastrichtian. Sedimentation rate decreases dramatically at the boundary and despite an early shift in recovery, values remain below those recorded in the Maastrichtian through the studied interval. Planktonic foraminifera average size has been studied from the same Site 1262 by Schmidt (unpublished) and is included to provide a comparison with the planktonic foraminifera test size fraction data presented here (Figure 7.1). The planktonic foraminifera average size in the Cretaceous is above 200 μm. At the K/Pg boundary these sizes drop to an average of <100 μm, after which values only increase slightly to a maximum of ~130 μm in the middle Paleocene.

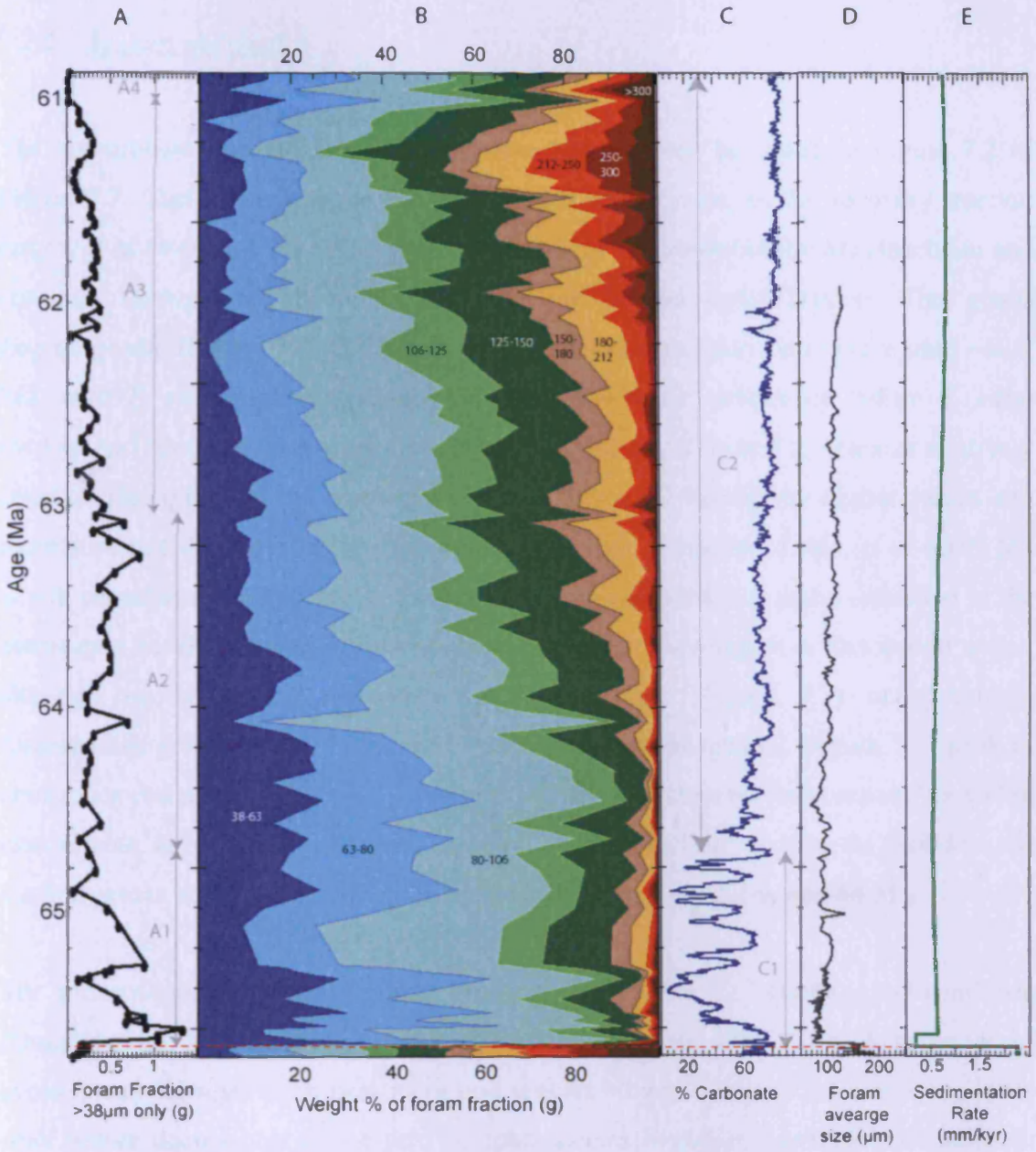

Figure 7.1 – Foraminiferal test size distributions and sediment carbonate content at Site 1262. Panel A = the coarse sediment fraction (>38µm) weights (g), consisting predominantly of planktonic foraminifera. Arrows denote the four main phases of recovery, A1 stage of greatest input and largest variability, A2 stage of reduced input and variability, A3 high stability and lower values and A4 return to pre-extinction values. Panel B = Coloured sections represent cumulative % weight (g) for the different test size fractions studied (Appendix 11.2). Panel C = the % carbonate data taken from Kroon *et al.*, (2007). Arrows denote two main phases, C1 high variability and C2 period of increased carbonate values and stability. Panel D = the average foraminifera size (µm) data from Schmidt (unpublished) based on the automotive method of Schmidt *et al.* (2006). Panel E = sedimentation rate (mm/kyr) data taken from Kroon *et al.*, (2007). All plots against sample age (Ma) based on the orbital time scale of Westerhold *et al.* (2008). Red dashed line denotes the K/Pg boundary.

7.2.2. Species abundance

The assemblage counts for all the Paleocene species can be found in Figure 7.2 to Figure 7.7. Cretaceous species counts have not been shown, as the recovery interval only was of interest here. ***Hedbergella*** (Figure 7.2) are present in the Maastrichtian and continue through the boundary, but die out in the early Danian. The genus ***Eoglobigerina*** (Figure 7.2) first appears soon after the boundary and ranges until ~62.9 Ma, with ***E. eobulloides*** appearing first and peaking in abundance before ***E. edita*** evolves and becomes more abundant. Benthic abundance (Figure 7.2) remains relatively constant throughout with abundance levels less than 10 %, slightly higher values and more variance do occur within the first 2 myr. The exception to this, is at 60.95 Ma where abundance reaches 75 %. This peak in benthic abundance and a reduction in the abundance in all planktonic foraminifera species would suggest a dissolution event, although no significant difference in % carbonate (Figure 7.1) or planktonic foraminifera preservation is observed. The microperforate genera (Figure 7.3) peak in abundance just after the boundary, but beyond this point their numbers remain low, with intermittent appearance for many species. The exception to this is ***Globoconusa daubjergensis***, which has a double peak in abundance at ~64.8 Ma and 64 Ma.

The genus ***Globanomalina*** (Figure 7.4) appears soon after the boundary and continues throughout the studied section, with a series of evolving species, which make up an evolutionary lineage. Each new incoming species slowly increases in abundance to its peak before decreasing, as the next morpho-species begins to increase in abundance. The exception to this pattern is ***G. archeocompressa*** and ***G. imitata***, which both have low abundances throughout their range. ***Subbotina*** and ***Parasubbotina*** (Figure 7.5) evolved soon after the boundary and continue throughout the studied interval, making up a significant and constant proportion of the assemblage. The subbotinids have relatively high abundances (40 to 50 % total abundance) throughout and follow a similar pattern to that of the globanomalinids, with new species evolving and apparently replacing existing ones. ***Parasubbotina pseudobulloides*** is rare throughout, unlike ***P. varianta*** which is common, and peaks in abundance (~50 % of total assemblage) around 62.2 Ma. Morozovellids (Figure 7.6) starts to appear at ~63 Ma with ***M. praeangulata***

but full diversity isn't reached until ~61.4 Ma where *M. apanthesma*, *M. angulata* and *M. occlusa* are the dominate species present. The genus *Igorina* (Figure 7.7) appears at 62.4 Ma, but never becomes abundant at Site 1262. *Praemurica* (Figure 7.7) evolves soon after the boundary and diversified to produce a succession of species before disappearing at ~62.2 Ma. The peak in abundance for this genus occurs at ~65 Ma, with the species *Pr. taurica* and *Pr. pseudoinconstans* dominating. Full tables of species counts can be found in Appendix 11.3.

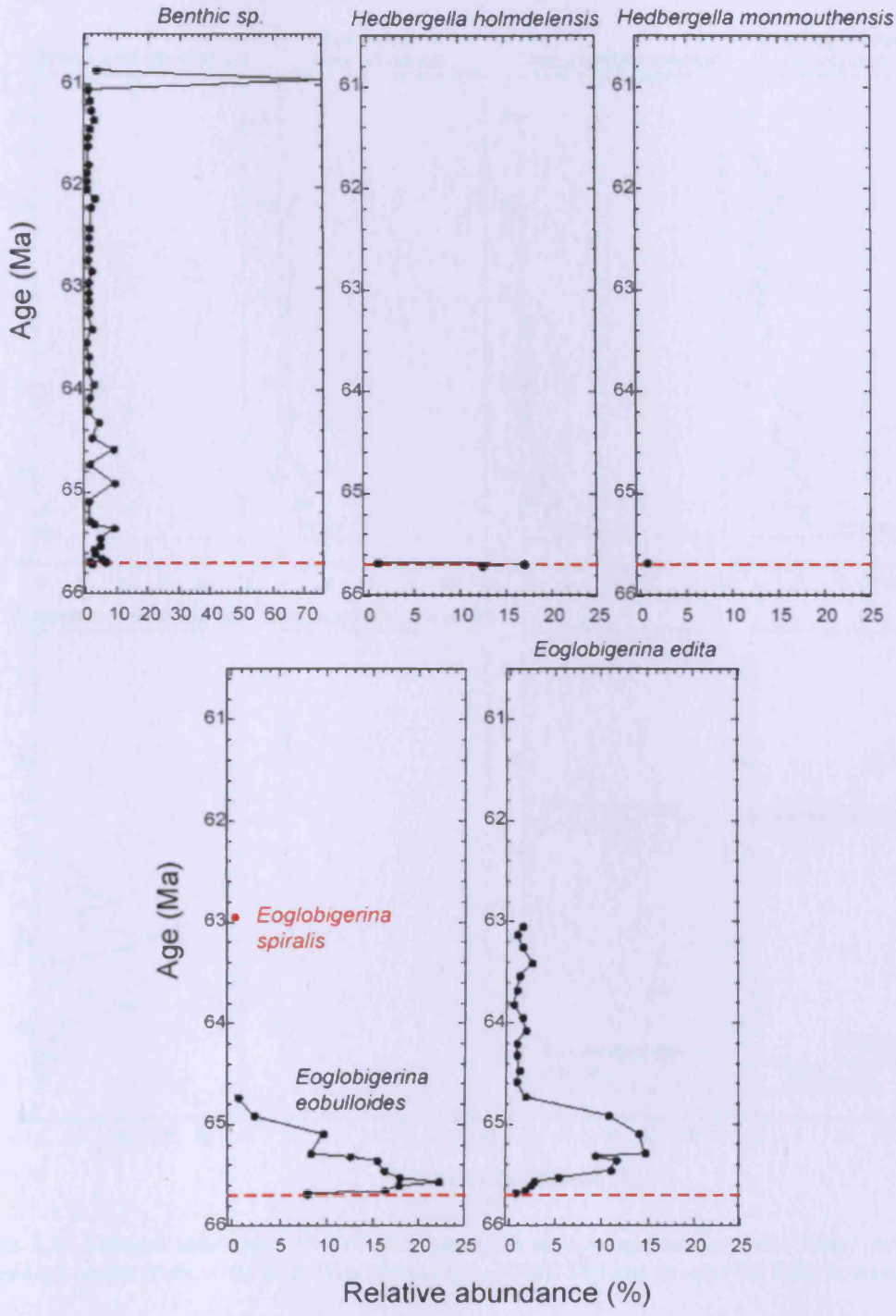

Figure 7.2 – Relative abundance (%) for species of *Hedbergella* and *Eoglobigerina* and benthic foraminifera (all species) against age (Ma) based on Site 1262 assemblage counts (time scale from Westerhold *et al.*, 2008). Red line denotes the K/Pg boundary.

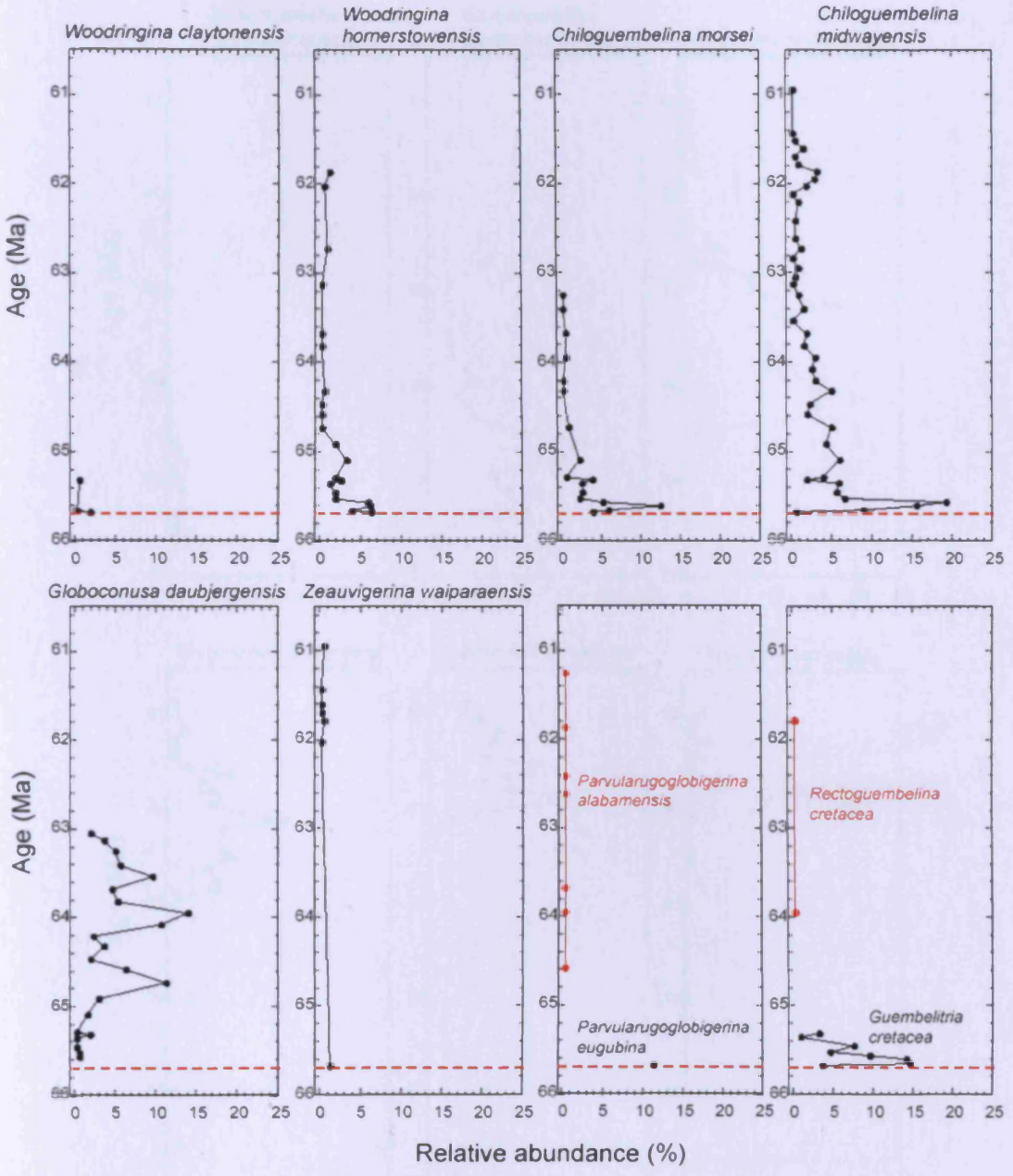

Figure 7.3 –Relative abundance (%) of microperforate species against age (Ma) based on Site 1262 assemblage counts (time scale from Westerhold *et al.*, 2008). Red line denotes the K/Pg boundary.

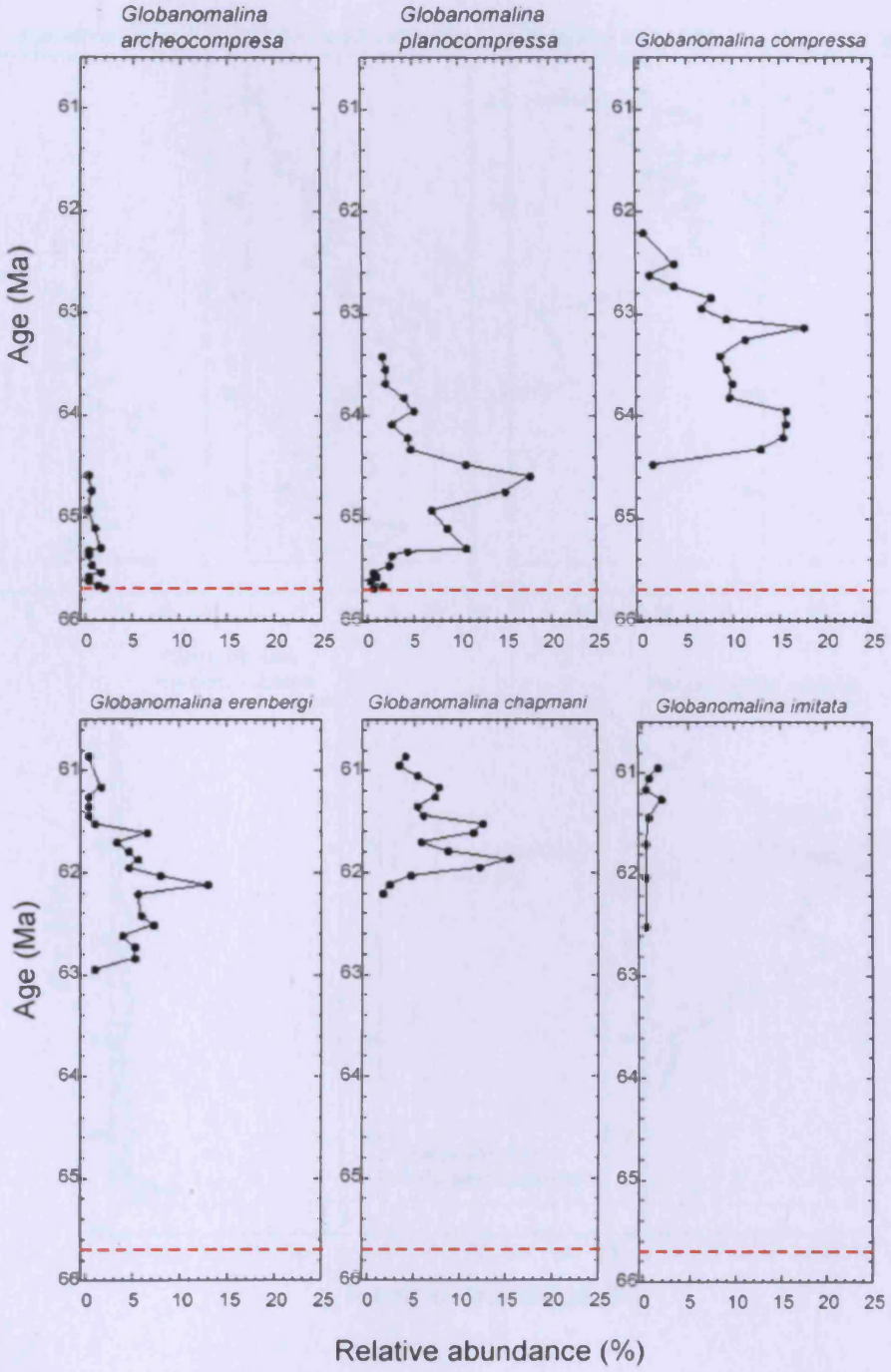

Figure 7.4 – Relative abundance (%) for species of *Globanomalina* against age (Ma) based on Site 1262 assemblage counts (time scale from Westerhold *et al.*, 2008). Red line denotes the K/Pg boundary.

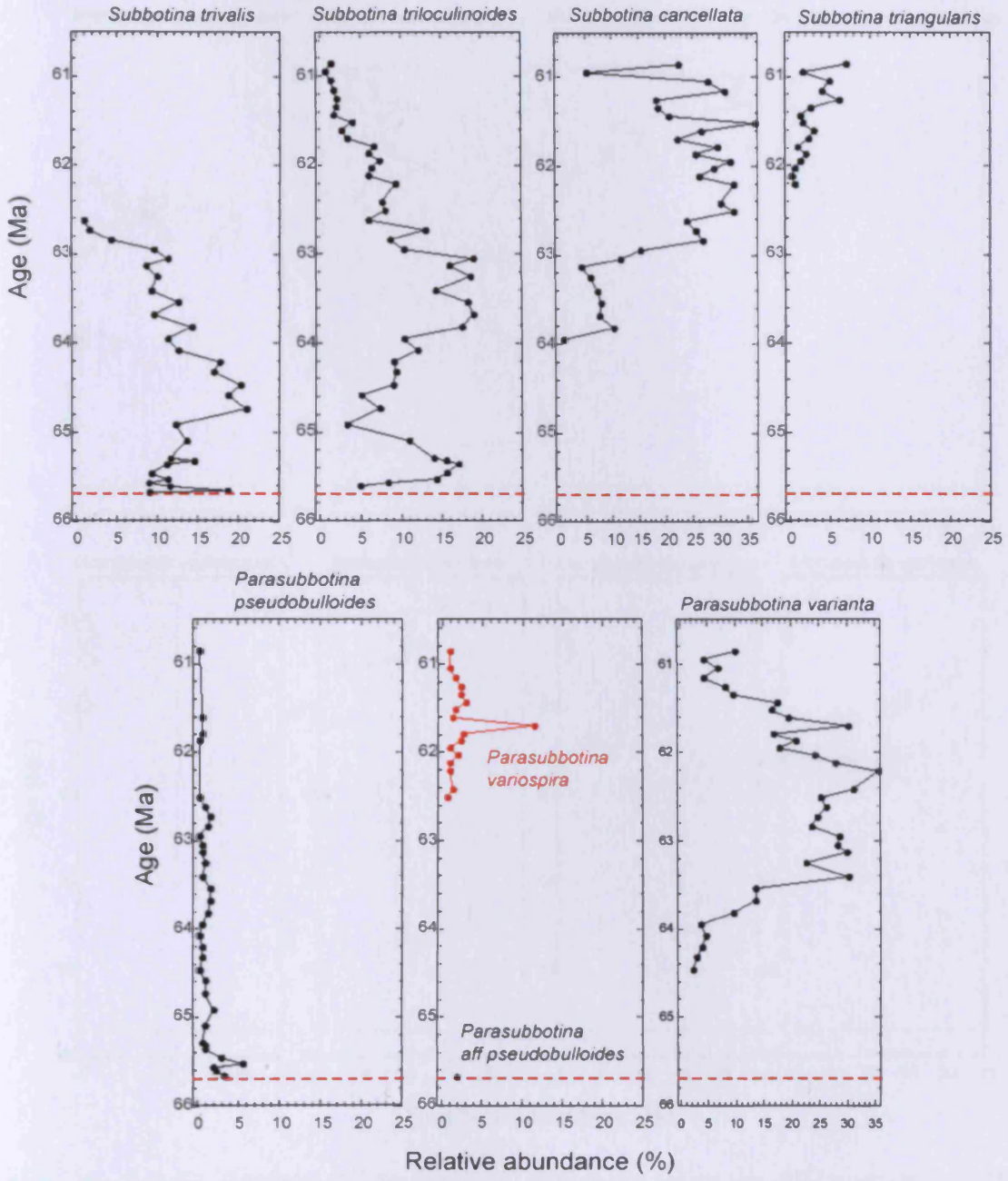

Figure 7.5 – Relative abundance (%) for species of *Subbotina* and *Parasubbotina* against age (Ma) based on Site 1262 assemblage counts (time scale from Westerhold *et al.*, 2008). Red line denotes the K/Pg boundary.

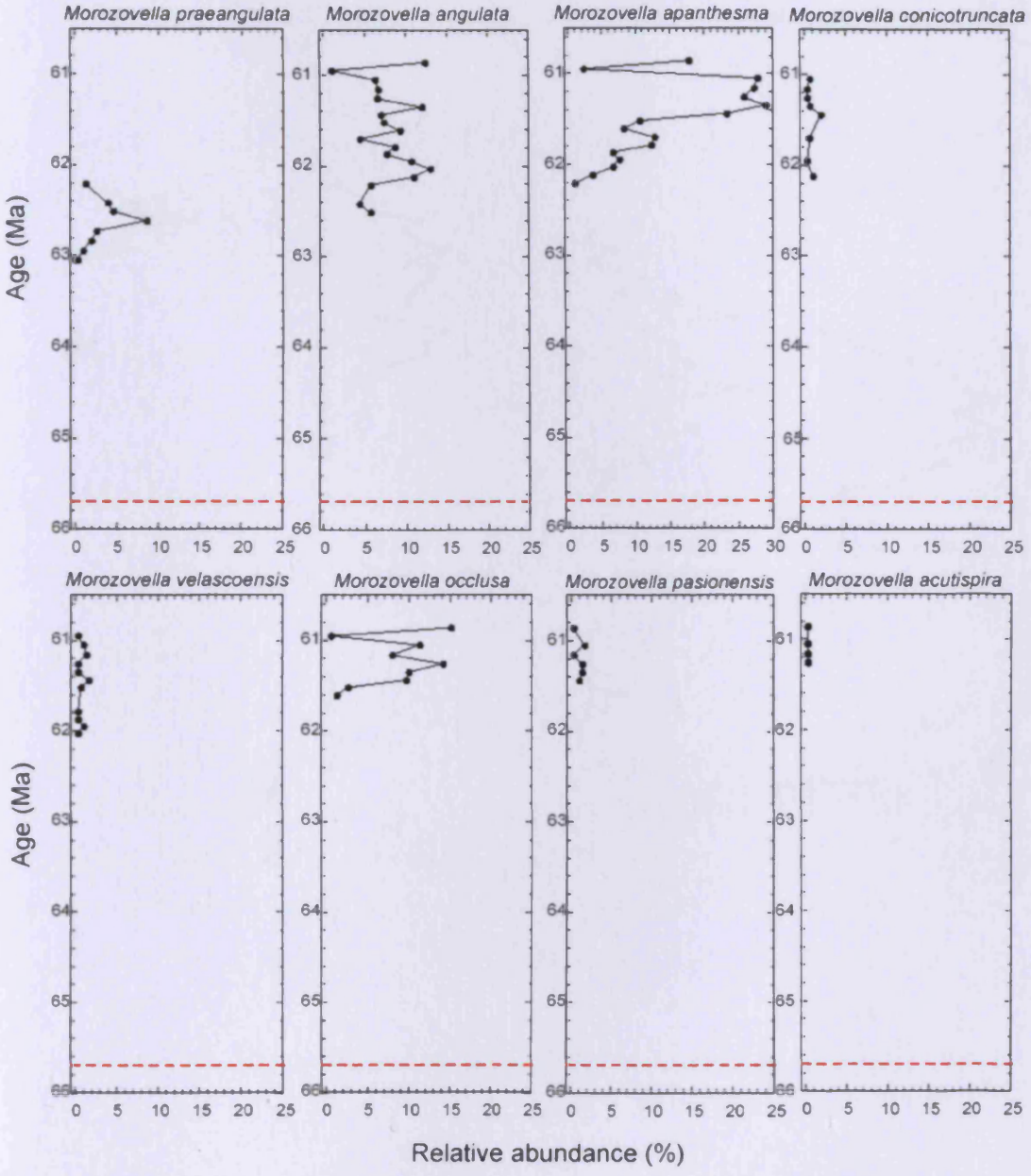

Figure 7.6 – Relative abundance (%) for species of *Morozovella* against age (Ma) based on Site 1262 assemblage counts (time scale from Westerhold *et al.*, 2008). Red line denotes the K/Pg boundary.

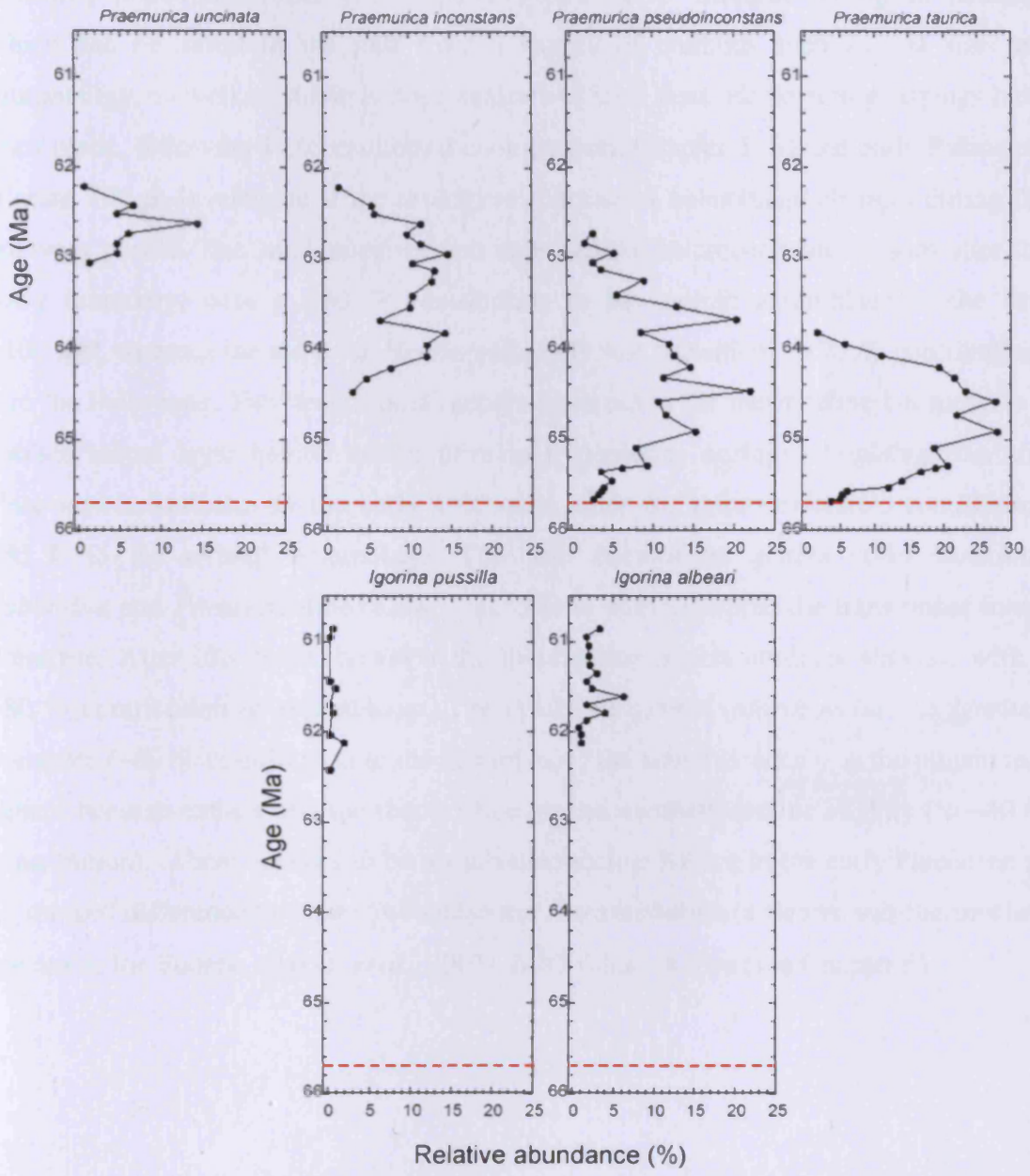

Figure 7.7 – Relative abundance (%) for species of *Praemurica* and *Igorina* against age (Ma) based on Site 1262 assemblage counts (time scale from Westerhold *et al.*, 2008). Red line denotes the K/Pg boundary.

7.2.3. Ecological grouping

Different planktonic foraminifera species/genera have different ecological habitats, which can be assed in the past from a variety of methods such as test size and morphology, as well as stable isotope analysis of their tests. Ecological groupings have been made, following isotope inferred ecology from Chapter 5, for the early Paleocene (Figure 7.8) to investigate if the ecological makeup of assemblage changes during the recovery period. The small survivor and opportunistic microperforates bloom after the K/Pg boundary, with a ~50 % contribution to the overall assemblage in the first ~100 kyr, whereas the survivor *Hedbergella* only just transitions (<20 % contribution) into the Paleocene. The 'transitional' genera (start out in the thermocline but move to a surface mixed layer habitat and/or develop a symbiotic ecology) *Eoglobigerina* and *Praemurica* dominate in the early Paleocene, after the microperforates, contributing ~85 % to the overall assemblage. The true thermocline genera (*Globinomalina*, *Subbotina* and *Parasubbotina*) slowly increase in number whilst the transitional forms dominate. After this point, however the thermocline genera numbers stabilise with a ~80 % contribution to assemblages. The symbiotic genera (*Morozovella* and *Igorina*) dominate (~60 % contribution to the assemblage) the later Paleocene, as the transitional genera become extinct and the thermocline genera numbers decline slightly (to ~40 % contribution). There appears to be no sub-thermocline habitat in the early Paleocene as no marked difference between *Subbotina* and *Parasubbotina* (a known sub-thermocline species in the Eocene, Coxall *et al.*, 2003), $\delta^{18}O$ values is seen (see Chapter 5).

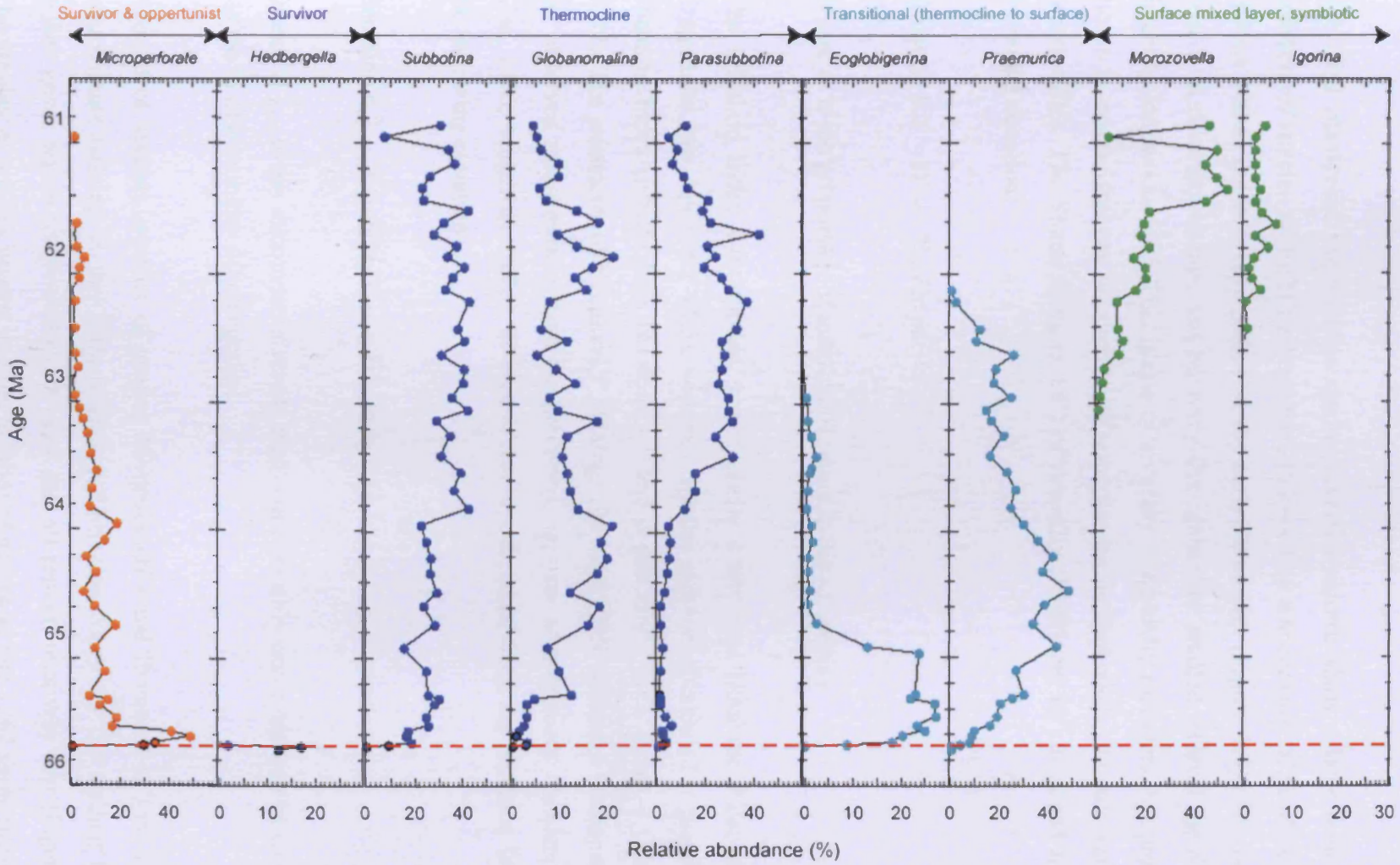

Figure 7.8 – Relative abundance (%) for Paleocene genera divided into ecological groupings based on the isotope analysis from this study (Chapter 5) and Olsson *et al.*, 1999. All against age (Ma) based on the time scale from Westerhold *et al.* (2008), for Site 1262. Red line denotes the K/Pg boundary.

7.2.4. Species diversity

Site 1262 planktonic foraminifera species diversity records show a large reduction in numbers of species at the K/Pg boundary, followed by a succession of newly evolving species within the recovery period of the early Paleocene (Figure 7.9). To assess the pattern in diversity change and recovery throughout the studied interval the Shannon diversity Index was used. This is one of a variety of diversity measures that provides a means to assess changes in community structure within biological and paleontological communities. The Shannon Index (H') of diversity (1949) can be calculated from the following equation:

Equation 6.1 $H' = - \Sigma pi \ln pi$

Where *pi* is the proportion of individuals found in the *i*th species.

The Shannon Index was applied to all species count data from the Paleocene and Cretaceous (see Appendix 11.3), with rare species only being counted if present. The Shannon Index usually falls between 1.5 and 3 and rarely goes above 4 (Margalef, 1972). The parameter of Evenness J' (Pielou, 1969 and 1975) measures the departure of the observed measurement from the predicted, i.e. how homogeneous the samples are (Zar, 1996; Magurran, 2005). Evenness can be calculated from the Shannon Index by the following equation:

Equation 6.2 $J' = H' / H_{max} = H' / \ln k$

Where H_{max} is the maximum diversity that could possibly occur and can be calculated via the ln of *k* (number of) categories.

Number of species, number of genera, Diversity (H') and Evenness (J') all show an approximate halving at the K/Pg boundary. Over the course of the studied interval values never return to pre-extinction ones and all remain relatively low (Figure 7.9). The number of species present and the number of genera at Site 1262 show fluctuations

throughout. However, species numbers fluctuate within a small range, whereas the number of genera shows a slight decrease over the studied interval. The number of genera in the 38-106 μm often fluctuates counter to the >106 μm size fraction, but is always greater in number. Diversity (H') and evenness (J') display two steps (or minimums) of decreasing then increasing within the recovery period centred around 64.6 and 62.2 Ma. The large decrease at 60.5 Ma is due to a sample containing mostly benthic foraminifera (Figure 7.2).

The number of microperforate verses macroperforate in the Cretaceous was small, with macroperforates dominating (Figure 7.10). At the boundary a significant increase in the microperforates is seen in both genera and species. Over the studied interval the number of microperforates decreases until pre-extinctions levels are reached at ~61 Ma. Over this general trend of decreasing microperforates, there are many fluctuations particularly in the species and genera >106 μm. The 38-106 μm size fraction shows overall greater numbers in microperforates compared to the >106 μm genera and species plots. The microperforates tend to be small opportunistic species, whereas the macroperforates tend to be larger specialists, which are more likely to be affected by the changing conditions at the K/Pg boundary.

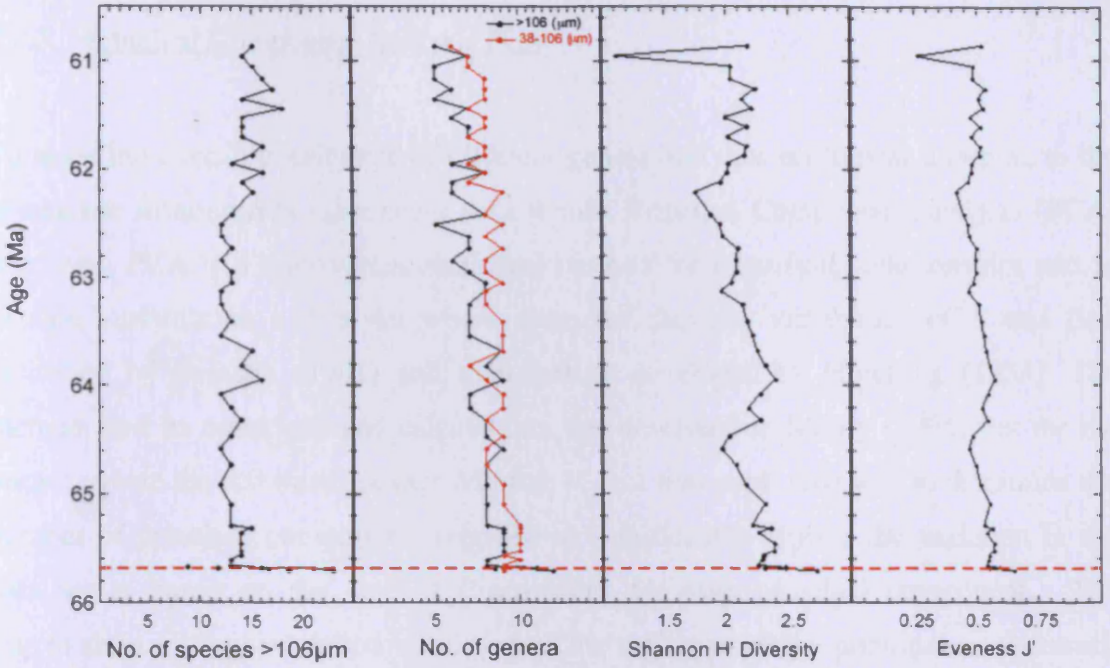

Figure 7.9 – From left to right: number of species >106 µm, number of genera >106 µm (black) and 38-106 µm (red), Shannon (H') diversity and Evenness (J'). All against age (Ma) based on the time scale from Westerhold *et al.* (2008), Site 1262. Red line denotes the K/Pg boundary.

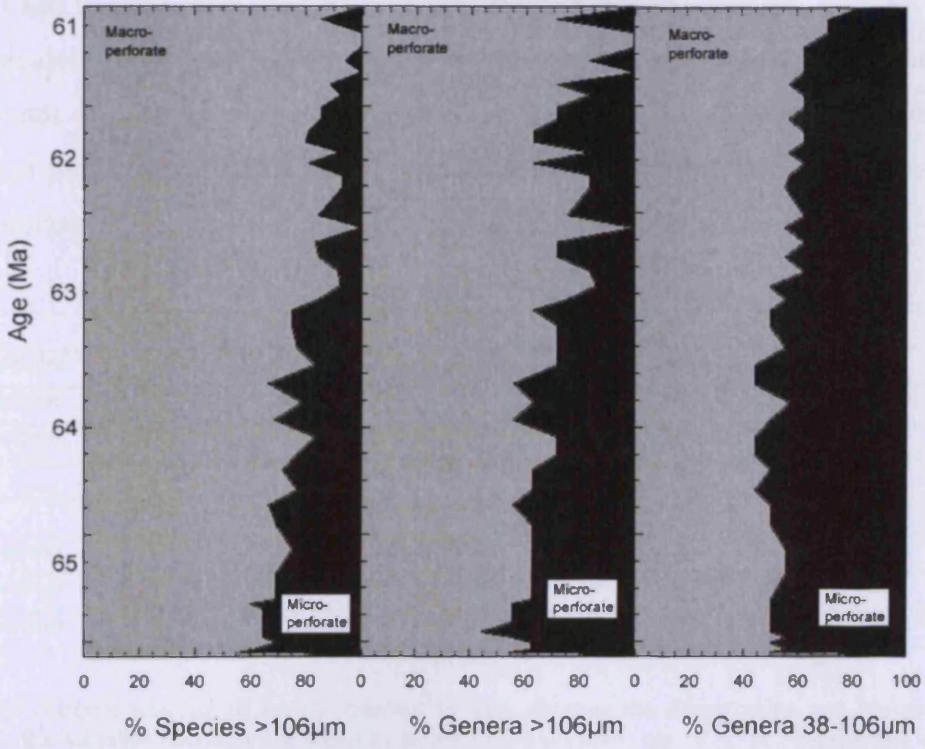

Figure 7.10 – Abundance (%) of Macroperfoarte (grey) vs Microperforate (black) genera for left – Species above 106µm, middle – Genera above 106µm and right – Genera between 38 - 106µm, all against age (Ma) based on the time scale from Westerhold *et al.* (2008), from Site 1262.

7.2.5. Principal Component Analysis PCA

To asses the overall importance of different genera and thus ecological grouping to the planktonic foraminifera assemblage as a whole, Principal Component Analysis (PCA) was used. PCA is a multivariate statistical method for identifying relationships and to explain variation in a data set where there are multiple variables. PCA was first described by Pearson (1901) and then further developed by Hotelling (1933). The method, and its equations and calculations, are described in Manly (1994) but for the purposes here the software package Minitab V 16.1 was used. One way to determine the number of principal components required to significantly explain the variation in the data set is based on the size of Eigenvalues for each principal component. The Eigenvalues of the correlation matrix equal the variances of the principal components. The number of principal components can be based on the amount of explained variance, retaining the components that cumulatively explain 90 % of the variance. Another technique is to analyze the bi-plot (Figure 7.11), which is an overlay of the score (not shown) and loading plots (Figure 7.12), for the first two components. For the latter, the interpretation of the spatial groupings of the data set has to be taken in conjunction with the amount of data set variation explained by the first two principal components alone (as the bi-plot is a two dimensional representation of the data spatially using these two components).

	PC1	PC2	PC3	PC4	PC5	PC6	PC7	PC8
Eigenvalue	**4.323**	**3.073**	**2.185**	**1.455**	**1.241**	0.866	0.801	0.654
Proportion	**0.270**	**0.192**	**0.137**	**0.091**	**0.078**	0.054	0.050	0.041
Cumulative	**0.270**	**0.462**	**0.599**	**0.690**	**0.767**	0.821	0.871	0.912
	PC9	PC10	PC11	PC12	PC13	PC14	PC15	PC16
Eigenvalue	0.541	0.311	0.228	0.121	0.101	0.065	0.035	0.002
Proportion	0.034	0.019	0.014	0.008	0.006	0.004	0.002	0.000
Cumulative	0.946	0.966	0.980	0.987	0.994	0.998	1.000	1.000

Table 7.1 – Eigen analysis of the Correlation Matrix, showing the Eigen value and the proportion of variance this variable accounts for when compared to the whole, out of 1. PC = Principle component. Numbers highlighted in bold represent Eigenvalue greater than 1 and are accepted to be the most representative.

The data matrix was constructed from the whole data set of percent counts. Individual species assemblage counts were combined to produce genera counts. Sixteen different Paleocene planktonic foraminifera genera and benthic foraminifera found at Site 1262 against the age of the sample were used in the PCA analysis. Table 7.1 shows that the first 5 principle components are above the generally excepted value of 1 for Eigen values and are thus the components that are most significant. These 5 components account for 76.7 % of the variability within the data matrix. The first component has a variance of 4.32, and accounts for 27 % of the data variability, and the second component has a variance of 3.07 and accounts for 19.2 % of the data variability.

These first two components account for 46.2 % of the data and are then plotted in the bi-plot of Figure 7.11. The bi-plot shows 5 outliers (highlighted with black circles) and by using the loading plot (Figure 7.12), the genera and therefore ecological group that are most influencing the distribution can be identified. Outlier 1 is influenced most by the survivor and microperforate genera (*Parvularugoglobigerina*, *Zeauvigerina* and *Hedbergella*). Outliers 2-4 are relatively close and are largely influenced by transitional and microperforate genera (*Guembelitria*, *Eoglobigerina*, *Chiloguembelina* and to a lesser extent by *Woodringina* and *Praemurica*). The distribution of the 3 main influential genera is slightly different (see species counts appendix 11.3), which is what separates these outliers. Outlier 5 is influenced by the symbiotic genera *Igorina* and *Morozovella* and by the microperforate genus *Zeauvigerina* and to a lesser extent by benthic sp. The rest of the data falls much closer to the centre plots and can be generally divided into 3 groups (indicated by green circles on Figure 7.11). Group A are influenced mostly by microperforate and transitional genera (*Guembelitria*, *Eoglobigerina*, *Chiloguembelina*, *Woodringina* and *Praemurica*), similar to outlier 2-4, but to a lesser extent. Group B are mostly influenced by the thermocline, microperforate and transitional genera (*Globanomalina*, *Subbotina*, *Globoconusa* and *Praemurica*). Group C is mostly influenced by the symbiotic and thermocline genera (*Morozovella*, *Igorina* and *Parasubbotina*). Note that less than 50% of the variation in the data set is explained by the first two principal components, indicating that care must be taken in interpreting these data patterns.

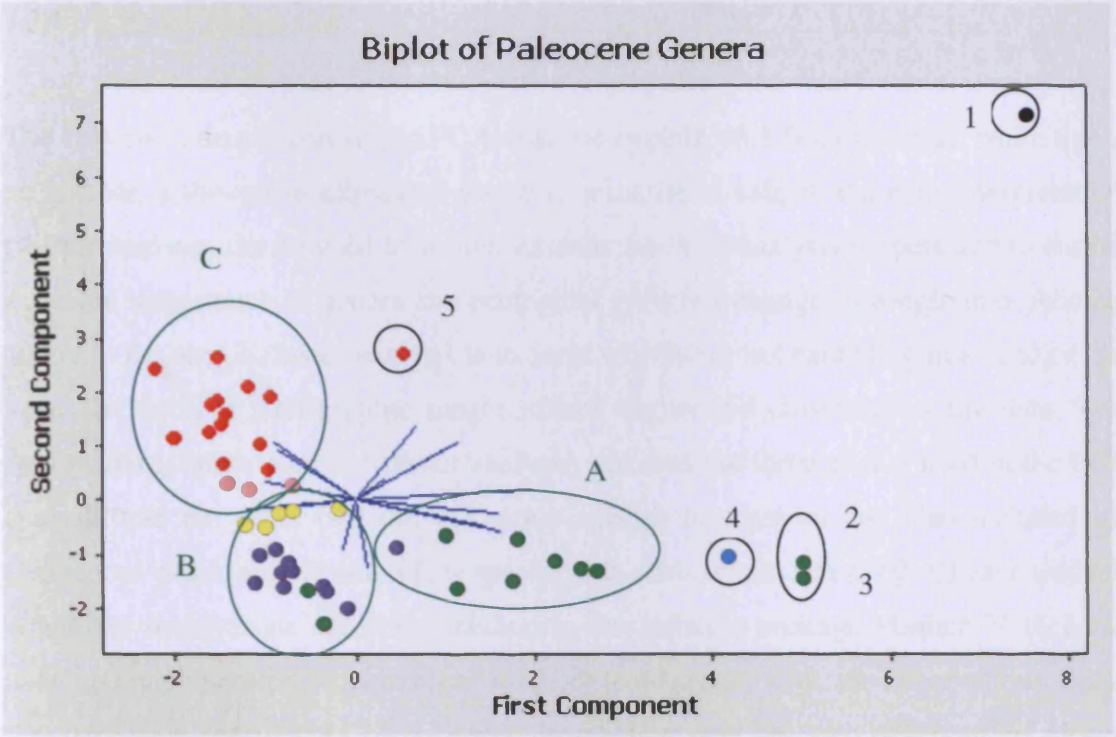

Figure 7.11– Biplot output from Minitab for the Paleocene Genera data from Appendix 11.3. Each dot represents an individual sample age, colours represent biozones black = Pα, blue = P1a, green = P1b, purple = P1c, yellow = P2, pink = P3a and red = P3b. Blue lines show the loading plot as shown in close up in Figure 7.12. Outlier's highlighted by black circle and main groups in green.

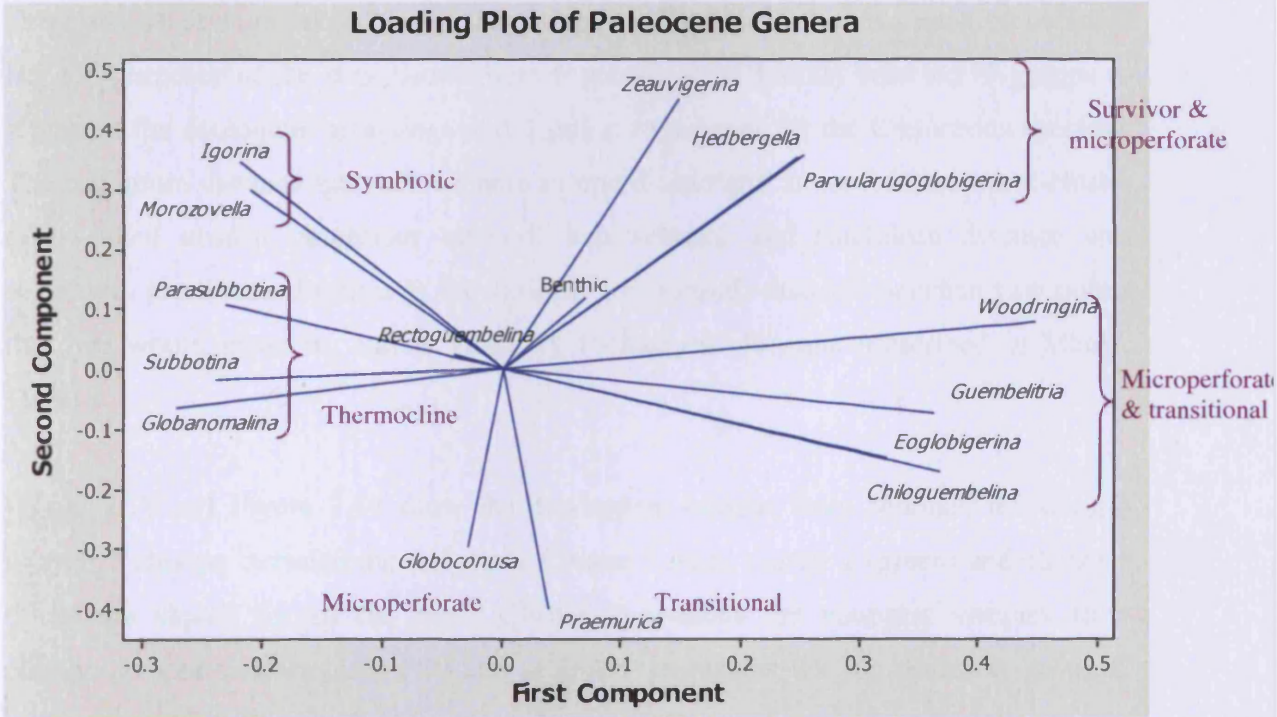

Figure 7.12– Loading Plot output from Minitab for the Paleocene Genera data from Appendix 11.3. Each line represents a vector created by the loading in 2D space. Purple brackets show ecological groupings.

7.2.6. Cluster analysis

The first two components of the PCA analysis explain 46.2 % of the data, while this is acceptable, although as explained above it necessitates care in the data interpretation. Cluster analysis can be used to further explain the PCA analysis outputs and to further asses the importance of genera and ecological grouping changes through time. Another aspect to the use of cluster analysis is to asses whether or not excluding rare species that have discontinues stratigraphic ranges affects the overall clustering of the data. Two data matrixes were used for cluster analysis; one was the same as that used in the PCA analysis and the other one did not group species into genera and also included the Cretaceous planktonic foraminifera species that occurred in Site 1262. Cluster analysis is another multivariate statistical method in the software package Minitab V 16.1 and uses an agglomerative hierarchical method that begins with all observations being separate, each forming its own cluster. In the first step, the two observations closest together are joined. In the next step, either a third observation joins the first two, or two other observations join together into a different cluster. This process is iterative until all clusters are joined into one (however, this single cluster is not useful for classification purposes). A decision as to how many groups are logical for the data must be decided. For the purposes of the data shown here 6 groups were initially selected (5 groups to represent the ecological groupings and 1 group to account for the Cretaceous species). The minimum distance between an item in one cluster and an item in the other cluster (also called nearest neighbour method) was selected and Euclidean distance was measured. Euclidean distance is the shortest (or normal) distance between two points that one would measure, and is given by Pythagoras' formula (described in Manly, 1994).

Figure 7.13 and Figure 7.14 show the dendogram outputs from Minitab, revealing a total of 7 clusters between the two plots. Cluster 1 (red), cluster 2 (green) and cluster 6 (blue) are shared by all the plots. Cluster 1 contains the youngest samples from planktonic foraminifera zone P3b and probably represents the top points in group C from the biplot (Figure 7.11), being largely influenced by the symbiotic genera (*Morozovella* and *Igorina*). Cluster 2 would be in cluster one from an age perspective,

but the large proportion of benthics and reduced numbers of other species (Figure 7.2 and appendix 11.3) isolates this sample. The biplot (Figure 7.11) also shows this isolation and cluster 2 corresponds to outlier 5. Cluster 6 contains the majority of samples ranging from biozone upper P1b to lower P3b samples, representing groups B and C on the biplot. Cluster 4 (orange) appears in the genera figure only (Figure 7.14) and makes up the samples from cluster 6 in the species dendogram that were not present in cluster 6 from the genera dendograms. They range from biozone P2 to lower P3b, these points fall at the upper edge of group B and lower edge of group C in the biplot and are largely influenced by the thermocline genera. Cluster 3 (purple) represents the two Cretaceous samples and as such is only present in Figure 7.13. Cluster 7 (pink in species dendogram and purple in genera dendogram) represents outlier 1 from the biplot, containing the microperforate and survivor genera. Of particular importance for cluster 7 are the species present in biozone Pα (*Parvularugoglobigerina eugubina* and *Hedbergella* species). The last Cluster 5 (orange in the species dendogram and pink in the genera dendogram) represents species from biozone P1b and group A on the biplot. The Paleocene genera dendogram (Figure 7.14) supports the PCA analysis well, as both show the outliers and main group divisions. The species clustering does not indicate any differences due to rare species. This would indicate that excluding these species when not present in a sample, despite knowing they could potentially be present from their stratigraphic range (Chapter 3), has little effect on the overall planktonic foraminifera assemblage.

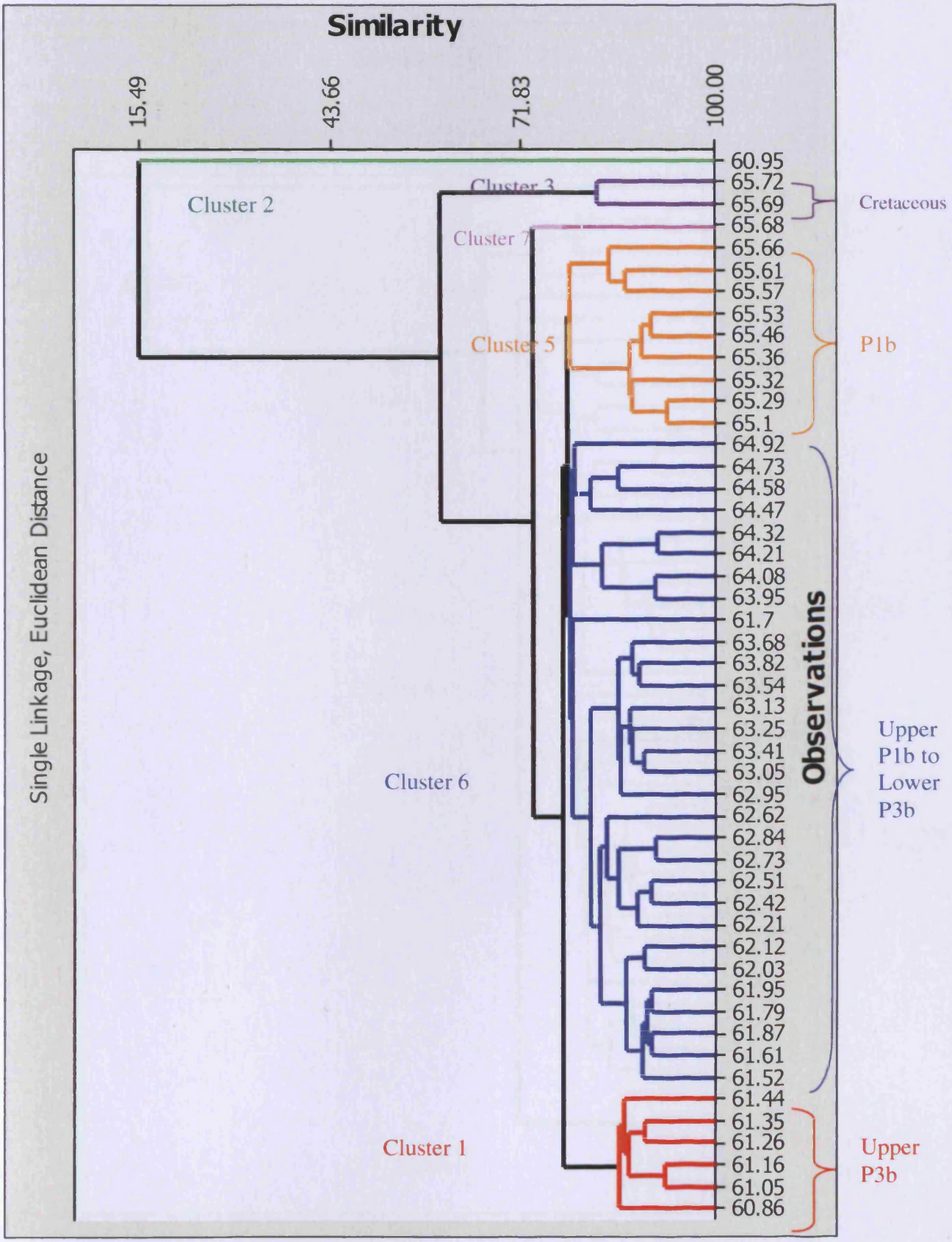

Figure 7.13– Dendrogram output from Minitab for all species found in samples, data from Appendix 11.3. The numbers on the right hand side of the plot reflect the age of each sample.

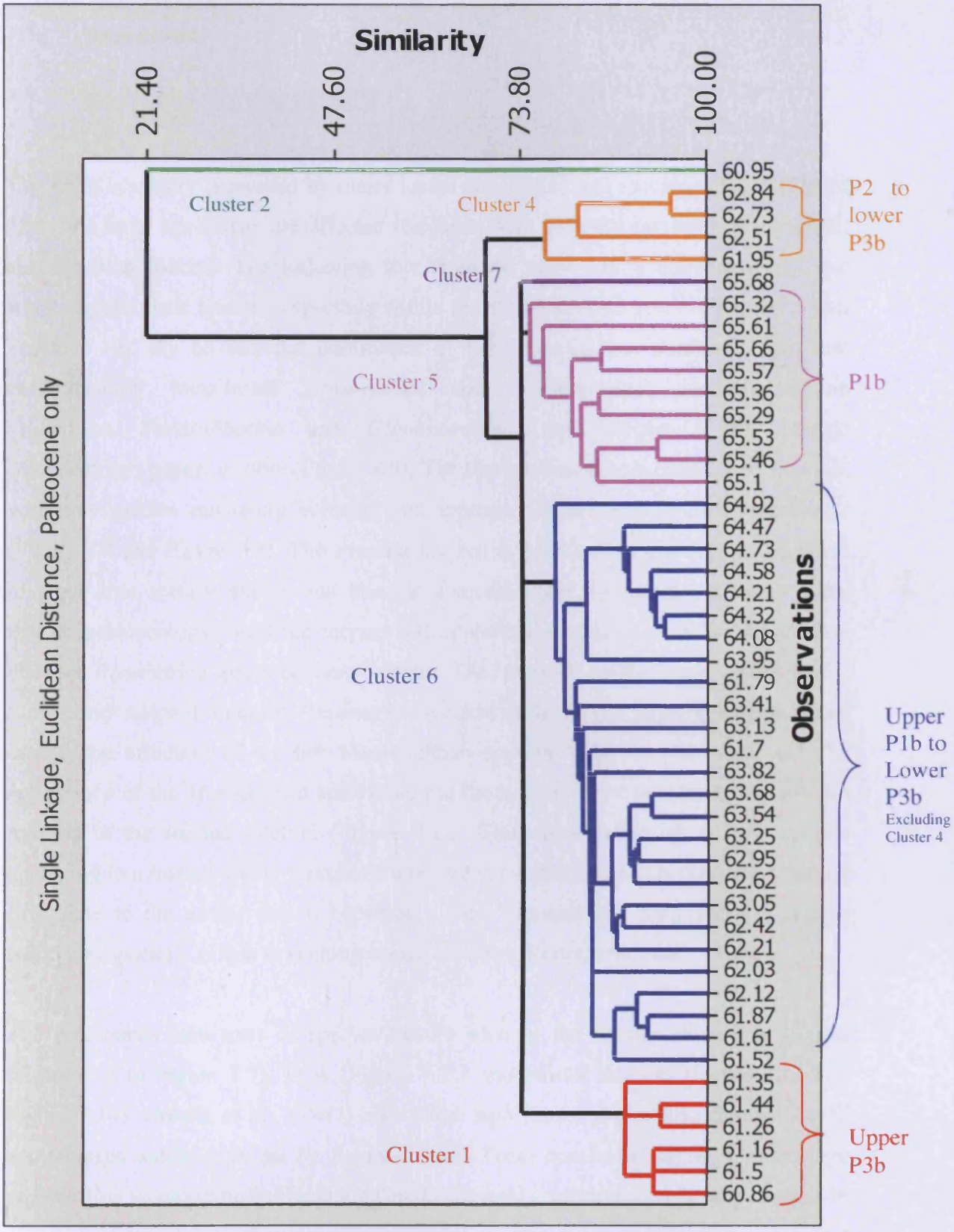

Figure 7.14– Dendrogram output from Minitab for all Paleocene Genera, data from Appendix 11.3. The numbers on the right hand side of the plot reflect the age of each sample.

7.3. Discussion

7.3.1. Species turnover after the K/Pg

The K/Pg boundary is marked by major losses in diversity and species richness (Figure 7.9). The large specialists are affected the most, with the only survivors being small, cosmopolitan species. The following few thousand years sees a dominance of these small opportunistic species, especially within the microperforate genera (Figure 7.3 and Figure 7.10). By 65 Ma the dominance of these species has diminished, as new predominantly transitional (*Praemurica* and *Eoglobigerina*) and thermocline (*Subbotina*, *Parasubbotina* and *Globanomalina*, see Chapter 5 for isotope paleoecology) genera evolve (Figure 7.8). The thermocline genera continue to flourish, with new species constantly evolving and appearing to outcompete their predecessor (Figure 7.4 and Figure 7.5). The *Praemurica* genus flourishes at this time and appears to move into surface waters and become a mixed layer dweller (see Chapter 5 for isotope paleoecology) until the morozovellids start to dominate ~61.8 Ma, when soon after the *Praemurica* genus becomes extinct. The larger *Morozovella* specialists appear to be better adapted, than the *Praemurica* species, to the mixed layer. The depth tiered assemblage structure of the late Maastrichtian appears to be re-established with the appearance of the *Morozovella* specialists but the large sizes of the Cretaceous are not reached in the studied interval (Figure 7.1). This constant change of new species appearing in a lineage likely represents anagenetic evolution (species gradually changes over time to the extent that it becomes a 'new' species but does not give rise to additional species), as few branching events are seen (Roopnarine *et al.*, 1999).

The continuous turn over of species can be seen in the species abundance figures (Figure 7.2 to Figure 7.7), PCA (Figure 7.11) and cluster analysis (Figure 7.13 and Figure 7.14). Gerstel *et al.*, (1987) also noted high faunal assemblage turnover, until assemblages stabilised in the *Pr. uncinata* zone. These constant changes in assemblage composition would indicate fluctuating environmental conditions comprising changes in physical and/or chemical water column structure that result in changing ecological

opportunities related to collapse of food webs at the K/Pg boundary (Gerstel *et al.*, 1987).

The results of the assemblage counts show that not all ecological groups were seen straight after the K/Pg boundary. The water column thermal and nutrient conditions favoured the small opportunists, as food availability probably remained highly variable, with opportunistic blooms (Alegret *et al.*, 2003; Alegret and Thomas, 2009). The lack of a sub-thermocline species, as indicated by $\delta^{18}O$ values (Chapter 5) is further evidence for a very weak or complete lack of marine biological pumping (see Chapter 6). Little or no food may have been transferred to the deeper layers of the water column, making this ecological strategy redundant. The specialists (e.g. symbiotic species) took time to re-appear and did not begin being the dominant ecological group (Figure 7.6 and Figure 7.8) till water column conditions were more stable and pre-extinction thermal and nutrient gradients appear to have been re-established (see Chapter 6). Planktonic foraminifera size can often be related to their ecology (Schmidt *et al.*, 2006), for example opportunistic species tend to be small and specialists tend to be larger (Armstrong and Brasier, 2005). This is clearly seen in the different sieved planktonic foraminifera size fractions (Figure 7.1), as the K/Pg boundary sees a dramatic increase in the smaller sizes fraction contribution and an increase in the small opportunistic species (Figure 7.8). The larger size fractions (>212 μm) do not contribute significantly to sediments till the time (~63 Ma) when the larger specialists return, in the case of the Paleocene it is the symbiotic morozovellids (Figure 7.6).

The progression from opportunistic to specialist species can be viewed in terms of ecological succession. Ecological succession refers to orderly changes in the composition and/or structure of an ecological community. Succession may be initiated either by formation of new, unoccupied habitat (e.g. a lava flow or severe landslide) or from disturbance (e.g. fire, storms and logging) of an existing community (Connell and Slatyer, 1977). In general, communities in early succession will be dominated by fast-growing, well-dispersed species (opportunist, fugitive, or r-selected strategies). As succession continues, these species will tend to be replaced by more competitive (k-selected) species, as resources become scarce (Clement, 1916; Connell and Slatyer, 1977). The K/Pg boundary event represents the re-setting of the environment, after

which the opportunistic microperforate forms thrive, with food resources high in surface waters due to lack of carbon pumping (see Chapter 6). As the environment stabilises and the carbon pump is restored, the export of nutrients to deeper waters reduces resources in surface waters. This allows the specialist symbiotic forams to become dominant as they are better adapted for the newly evolving conditions than the opportunistic species.

The initial wave of evolution appears to be somewhat dampened in the studied Site 1262 section. This may be because there is no planktonic foraminifera biozone P0 and only one Pα sample was studied due to the sampling resolution, these biozones represent a time when many new species (~ 17 from Olsson *et al.*, 1999) evolve. The lack of biozone P0 is common in deep sea site and may represent a hiatus at these deep marine locations (Norris *et al.*, 1999). An alternative suggestion proposed by Norris *et al.* (1999) is that biozone P0 is not a globally recognisable biozone and is only present in the shallower marine settings. Following the initial wave of evolution just above the boundary, when the majority of the Paleogene lineages appeared (Olsson *et al.*, 1999; Coxall *et al.*, 2006), there is little change, as the number of new species appears to balance the number of existing ones dying out at Site 1262 (Figure 7.10). This is counter to the findings of Coxall *et al.* (2006), where a second increase in species diversity is seen ~3 Ma after the boundary, with the addition of 3 genera and 16 new species. The differences in the two data sets may be a result of sampling resolution, as the data from Coxall *et al.* (2006) were placed into bins, whereas the data here were not. As a result of these bins the diversification of the *Acarinina* and continued diversification of the *Morozovella* in biochrone P4 (which was not investigated in this present study) would greatly increase the diversity of the bin present at ~3 Ma. However, two minimums in species diversity and evenness (Figure 7.9) are seen at Site 1262. These correspond to changing planktonic foraminifera assemblage structures. The first minimum occurs with the demise of the microperforates and *Eoglobigerina* sp. (~64.6 Ma) and the second with the demise in *Praemurica* sp. (~62.2 Ma), before the morozovellids had fully diversified. PCA (Figure 7.11) and cluster analysis (Figure 7.13 and Figure 7.14) also demonstrate this changing assemblage pattern, as groups and clusters follow the dominance from microperforates to transitional and thermocline through to thermocline and finally to the mixed layer dwelling and symbiotic species.

Comparison of the Site 1262 planktonic foraminifera with benthic foraminifera and nannoplankton diversity curves shows some similarities. The boundary marks a decrease in both benthic and planktonic diversity, but unlike the planktonic foraminifera, benthic diversity appears to return to pre-extinction levels by the end of biochrone Plc (~63.13 Ma in this study) (Alegret and Thomas, 2007; Coccioni and Marsili, 2007; Alegret and Thomas, 2009). Some parallels can be drawn between the benthic and planktonic foraminifera however, as smaller benthic species, just like the smaller planktonic species, saw the least amount of change at the K/Pg boundary (Culver, 2003). Nannoplankton diversity also shows a major decrease at the boundary, with up to 90 % of species becoming extinct (Bown, 2005) and like the planktonic foraminifera their diversity remains low for at least 1.5 myr (Bernaola and Monechi, 2007). Nannoplankton diversity does not appear to return to pre extinction levels within the Cenozoic (Bown et al., 2004). Jing *et al.* (2010) examined diversity (Shannon Index) in the nannoplankton. Their data showed a similar trend of reduced diversity from the Maastrichtian to the Danian followed by a gradual increase, until diversity levels out, yet remains lower than pre-extinction values, from ~50 kyrs after the K/Pg boundary. Non-metric multidimensional scaling (NMS) ordination was used and showed a range of ecologies in the species that appeared and a separation of taxa into survivor (high nutrient) and new taxa (low nutrient) within the first ~350 kyrs.

7.3.2. Carbonate sedimentation at the K/Pg boundary

The changes in sediment content (% $CaCO_3$) and $CaCO_3$ accumulation rate (Kroon *et al.*, 2005 - Figure 7.1) show a crash at the boundary and largely fluctuating values until stabilisation at approximately 64.2 Ma. This reduction at the boundary appears to have been a global phenomenon (Zachos and Arthur, 1986; Stott and Kennett, 1990; Rea *et al.*, 1990; D'Hondt, 2005, Figure 7.15). The decrease in $CaCO_3$ can be related to the extinction of calcareous nannoplankton and planktonic foraminifera rather than dissolution, due to the excellent preservation of early Danian fossils and lack of significant fragmentation (D'Hondt, 2005, Figure 7.15 - B). The sediment component that appears to have taken the place of the $CaCO_3$ at Site 1262 is clay (Ship Board Scientific Party, 2004).

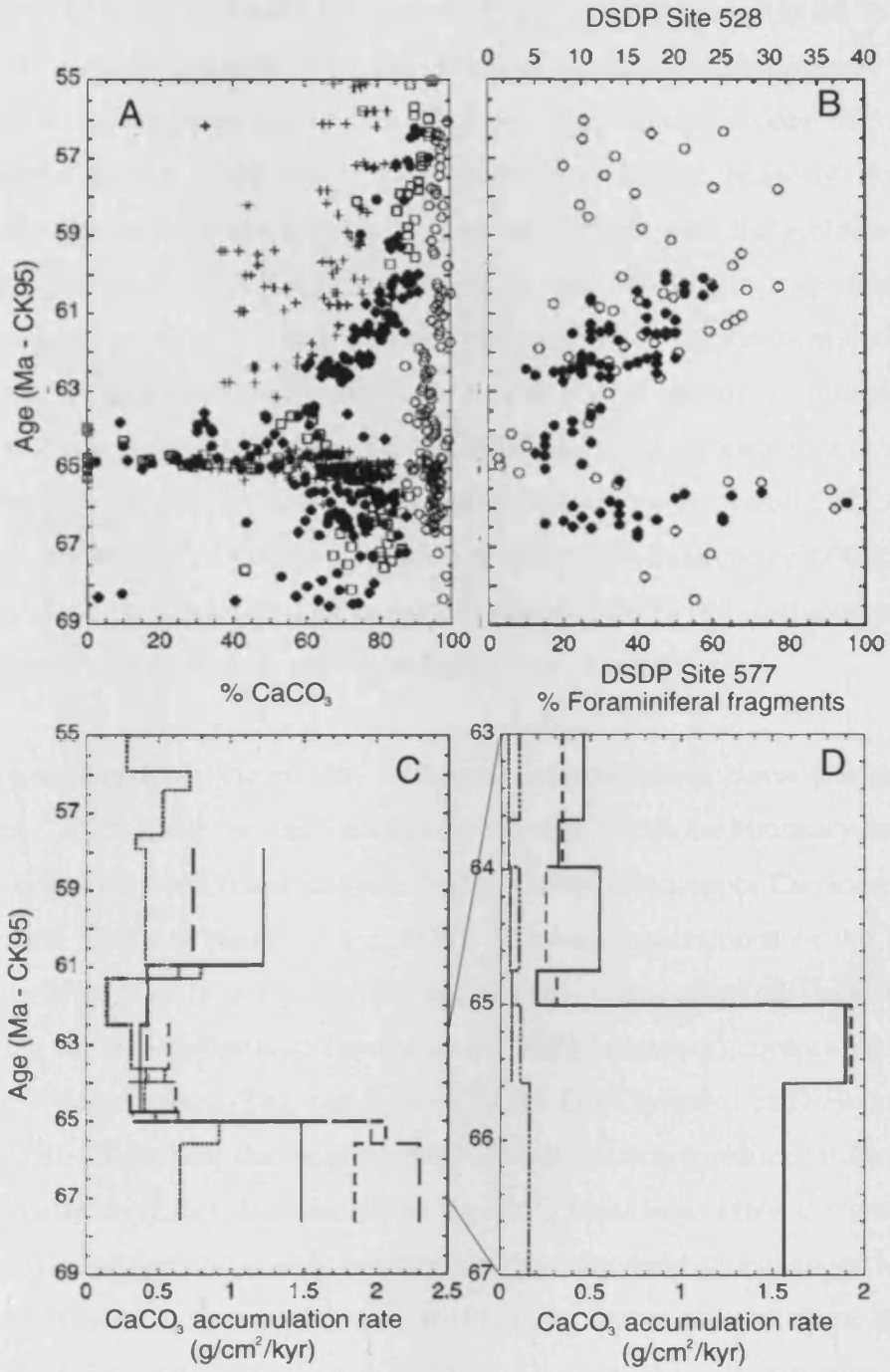

Figure 7.15 - Sediment patterns at the K/Pg boundary. Panel A = Carbonate concentrations (%) at Central Pacific DSDP Site 577 (white circles), South Atlantic DSDP Site 527 (white squares), South Atlantic DSDP Site 528 (black circles) and Caribbean ODP Site 1001A (crosses). Panel B = Percent foraminiferal fragments at Site 577 (white circles) and Site 528 (black circles). Panel C = Mean $CaCO_3$ accumulation rates at Site 577 (dotted line), Site 528 (line with short dashes), Site 527 (line with long dashes) and Site 1001A (solid line). Panel D = Accumulation of $CaCO_3$ in the >38 μm fraction at Site 527 (dotted line) and Site 528 (line of alternating dot and dashes) and the <38 μm fraction (predominately calcareous nannofossils) at Site 527 (dashed line) and Site 528 (solid line). Timescale is based on Cande and Kent (1995). Adapted from D'Hondt (2005).

The phase of high amplitude fluctuations in percent carbonate (65.68 to 64.6 Ma, stage C1) roughly correlates with the period of highest species turnover. This may represent a stage of opportunistic blooming taxa, with variable success of transporting the material to the sediments. During the early Paleocene phase of high $CaCO_3$ variability, the major peaks in percent carbonate coincide with the peaks in the foram fraction (>38 μm), which is when peaks in the 80-106 μm size fractions and minimums in the >106 μm size fractions contribution to the sediment occur (Figure 7.1). This is slightly counter-intuitive as a reduction in planktonic foraminifera test size would be expected to correspond to a reduction in the carbonate accumulation, as small tests are found to contribute only a small fraction to the overall $CaCO_3$ flux (e.g. Red Sea, Bijma *et al.* [1994]; NE Atlantic, Schiebel and Hemleben [2000]). However, it appears that a balance between size and abundance exists and is of most importance in the overall contribution to sediment during the early Paleocene.

Previous studies have shown that calcareous nannoplankton contribute the most to sediment $CaCO_3$ under 'normal' conditions and that before the boundary foraminifera contribute only a small fraction to the total carbonate in the upper Cretaceous (Zachos and Arthur, 1986; D'Hondt *et al.*, 1996). The major extinctions in the calcareous nannoplankton lead to early Danian sedimentary carbonates (not total sediments, which see an increase in clay content at the K/Pg boundary) comprising mostly of planktonic foraminifera. This can be seen in the $CaCO_3$ record of D'Hondt's (2005) (Figure 7.15 - D) where the proportion of <38 μm fraction (predominately calcareous nannofossils) decreases dramatically at the K/Pg boundary, while the proportion of >38 μm fraction (predominately foraminifera) remains largely unchanged at the K/Pg boundary. Since the accumulation of foraminifera carbonate sediments varies little over the K/Pg boundary (Figure 7.15 – D), but the average size decreases dramatically, the average flux of these small planktonic foraminifera must increase in the early Danian (D'Hondt, 2005). The low abundance of nannoplankton in post extinction sediments is unlikely caused by increased dissolution as nannofossils are more dissolution resistant then foraminifera (Ramsey *et al.*, 1973). If dissolution has not affected nannofossil content, then the question still remains, as to what has affected the proportion of nannofossil contribution, compared with planktonic foraminifera, when both suffered similar extinction rates.

Size is an obvious physical distinction between nannoplankton and planktonic foraminifera in the early Danian and could represent a threshold for the transfer of $CaCO_3$ to the deep sea that is centred around 38 μm. The nannoplankton in the immediate K/Pg boundary recovery interval are a mixture of Cretaceous survivors (3 and 10 μm), newly evolved Paleocene species (generally miniscule, 1–2 μm), and the 'disaster' taxa *Braarudosphaera* and *Thoracosphaera* (generally 20–40 μm), but *Thoracosphaera* often break into much smaller pieces (Bralower *et al.*, 2010). This size distinction may be the cause for a lack of nannofossils, but not planktonic foraminifera, in early Danian sediments. This is further illustrated in grain size analysis conducted at ODP Site 1212 (Shatsky Rise Pacific Ocean). This site shows an overall size increase and change from a unimodal distribution to a bimodal distribution, reflecting the extinction of Cretaceous nannoplankton and their replacement by small pieces of *Thoracosphaera*, combined with a larger grain size fraction composed of whole *Thoracosphaera* and small Danian planktonic foraminifera (Bralower *et al.*, 2010). Different transport mechanisms for the two size classes are another possibility for the difference between the contributions of nannofossils and planktonic foraminifera to early Danian sediments. The 'living ocean' model proposed by D'Hondt *et al.* (1998) (discussed in detail in Chapter 6) suggests that organic matter can be transported to the deep sea through ecological packing (into faecal pellets by organisms higher up in the food chain). However, this mechanism was severely affected by extinction at the K/Pg boundary. If this mechanism of ecological packing and transfer was important manly for nannofossils and not planktonic foraminifera, it would explain the discrepancies seen between the two constituents of the sediment, despite both suffering similar extinction patterns.

The continued gradual increase in percent carbonate after 64.2 Ma corresponds with the gradual decrease of the coarse foram sediment fraction (>38 μm) (Figure 7.1) and means something else is increasing its contribution to percent carbonate. This could represent an increase in the contribution of the finest fraction (<38 μm), predominately calcareous nannoplankton, to the sediment, but without the <38 μm weights no definitive conclusion can be made. Sediment records by D'Hondt (2005) and nannoplankton evolutionary records by Bown *et al.* (2004) do support this

conclusion. Nannofossil diversity starts to increase 2 myr after the K/Pg extinction event and by ~5 myr diversity had reached approximately half that of the late Maastrichtian (Bown *et al.*, 2004). The timing of this partial recovery of nannofossil diversity roughly coincides with the decrease in the foram fraction at Site 1262 (~61 Ma) and may represent full ecosystem recovery to a new altered state, as nannofossil diversity never reaches that of the late Cretaceous throughout the rest of the Cenozoic (Bown *et al.*, 2004).

7.4. Summary

- The K/Pg saw a reduction in species richness, diversity and size for planktonic foraminifera. Large specialists are the most severely hit, with only small cosmopolitan species surviving. Diversity and planktonic foraminifera size do not reach pre-extinction levels in the period studied.
- Dominance of small cosmopolitan species lasts for at least the first 600 kyrs. Evolutionary turnover was especially high during this period, with new species continually evolving and apparently replacing existing ones. After this period thermocline and transitional (thermocline to surface) species dominated before the appearance of the symbiotic surface dwellers at ~ 61.4 Ma, when these species dominate and a return to the hierarchical structure of the late Cretaceous is seen.
- A large reduction in percent carbonate is seen at the boundary. After the mass extinction percent carbonate fluctuates greatly and reaches minimum values. These fluctuations correlate with the highest planktonic foraminifera assemblage turnover and may indicate a need for stable ecosystem structure to facilitate carbonate accumulation in sediments.
- At the boundary the contribution of planktonic foraminifera to the carbonate portion of the sediment appears to increase, while percent carbonate values and thus the inferred proportion of nannoplankton reduces significantly; despite both suffering similar extinction patterns. Differences in size and export mechanisms may be responsible for this discrepancy.
- By ~61 Ma pre-extinction foram weight fractions are reached and the balance between nannoplankton and planktonic foraminiferal contribution to the sediment is re-established.

8. The search for the K/Pg boundary in Tanzania

This chapter focuses on the efforts of the Tanzania Drilling Project (TDP) to locate the K/Pg boundary in 2008 and 2009, when I participated in the expeditions. Lithology, biostratigraphy and palaeoenvironmental analysis of the two cores (Site TDP27 and TDP37) drilled are discussed. Despite the K/Pg boundary remaining elusive, early Paleocene clay containing well preserved 'glassy' planktonic foraminifera was recovered. This provided an accurate snap shot of early Paleocene low latitudes, Indian Ocean, paleotemperature estimates.

8.1. Introduction

The presence of Cretaceous and Paleogene marine sediments in coastal Tanzania was first mapped by Moore *et al.* (1963) and initial comments on stratigraphy were noted by Bornhardt (1990), before a synthesis of the geology of coastal Tanzania was made by Kent *et al.* (1971). This led to initial reconnaissance work where exceptionally well preserved examples of fossil foraminifera were collected from surface exposures (Pearson *et al.*, 2001; Nicholas *et al.*, 2006). The planktonic foraminifera were of particular importance since their test wall exhibited 'glassy' rather than 'frosty' (like the majority of partially recrystallized deep sea material) style of preservation, when examined under a light microscope (Sexton et al., 2006). The excellent preservation has been attributed to the relatively shallow burial depths and the impermeable, clay rich lithologies (Pearson *et al.*, 2004). The establishment of the Tanzanian Drilling Project (TDP) in 2002 followed the initial reconnaissance work. Many important Paleogene and Cretaceous sediment sequences have now been recovered through the TDP (Figure 8.1), yielding exceptionally well preserved microfossils (Pearson *et al.*, 2001; Stewart *et al.*, 2004; van Dougen *et al.*, 2006; Pearson *et al.*, 2007; Bown *et al.*, 2008; Handley *et al.*, 2008; Wade and Pearson, 2008; Lear *et al.*, 2008; Pearson *et al.*, 2008; Bown and Pearson, 2009). This has led to the area becoming important for Cretaceous and Cenozoic paleoclimate reconstructions, especially as a source of more reliable

temperature estimates for the tropics and sub-tropics (Pearson *et al.*, 2001; Stewart *et al.*, 2004; Pearson *et al.*, 2007; Lear *et al.*, 2008; Pearson *et al.*, 2008).

A primary objective of the TDP has been recovery of 'glassy' foraminifera, containing sequence spanning the K/Pg boundary mass extinction event. However, of the 26 sites drilled by the TDP before 2008 (Pearson *et al.*, 2004; Pearson *et al.*, 2006; Nicholas *et al.*, 2006; Jiménez Berrocoso *et al.*, 2010), the K/Pg boundary have not been recovered, despite a number of attempts (Figure 8.1). Although mid and upper Cretaceous sediments have been recovered at several sites, the oldest recovered zone in the Paleocene was planktonic foraminifera biochron P4a (late Paleocene). This was recovered at Site TDP19 in the Pande area of coastal Tanzania, where 42 m of late Paleocene sediment was recovered, before sitting above upper Cretaceous sediment (Nicholas *et al.*, 2006). The lack of lower Paleocene sediment has been attributed to faulting (Nicholas *et al.*, 2006). However, older early Paleocene planktonic foraminifera from biochron P1 have been noted by Blow and Banner (1962) and Blow (1979), using material from the 1950s BP-shell explorations.

In a further effort to locate the K/Pg in Tanzania, two additional drilling seasons (2008 and 2009) drilled cores at Kimamba Hill, in the Kilwa district. Kimamba Hill was selected as a candidate K/Pg site, because reconnaissance work had identified upper Maastrichtian clays in the Ukuli River bank on the south-western flank of the hill and the hill itself has been described as Paleocene from the limestones (Kent *et al.*, 1971 and Nicholas *et al.*, 2006). The aim to recover K/Pg sediments in Tanzania would allow for geochemical comparison of partially recrystallized ODP material with exceptionally well preserved 'glassy' planktonic foraminifera. This glassy material has the potential to produce the first 'realistic' paleotemperature estimates from the K/Pg boundary. The expedition logistics and drilling method are described in Chapter 2.

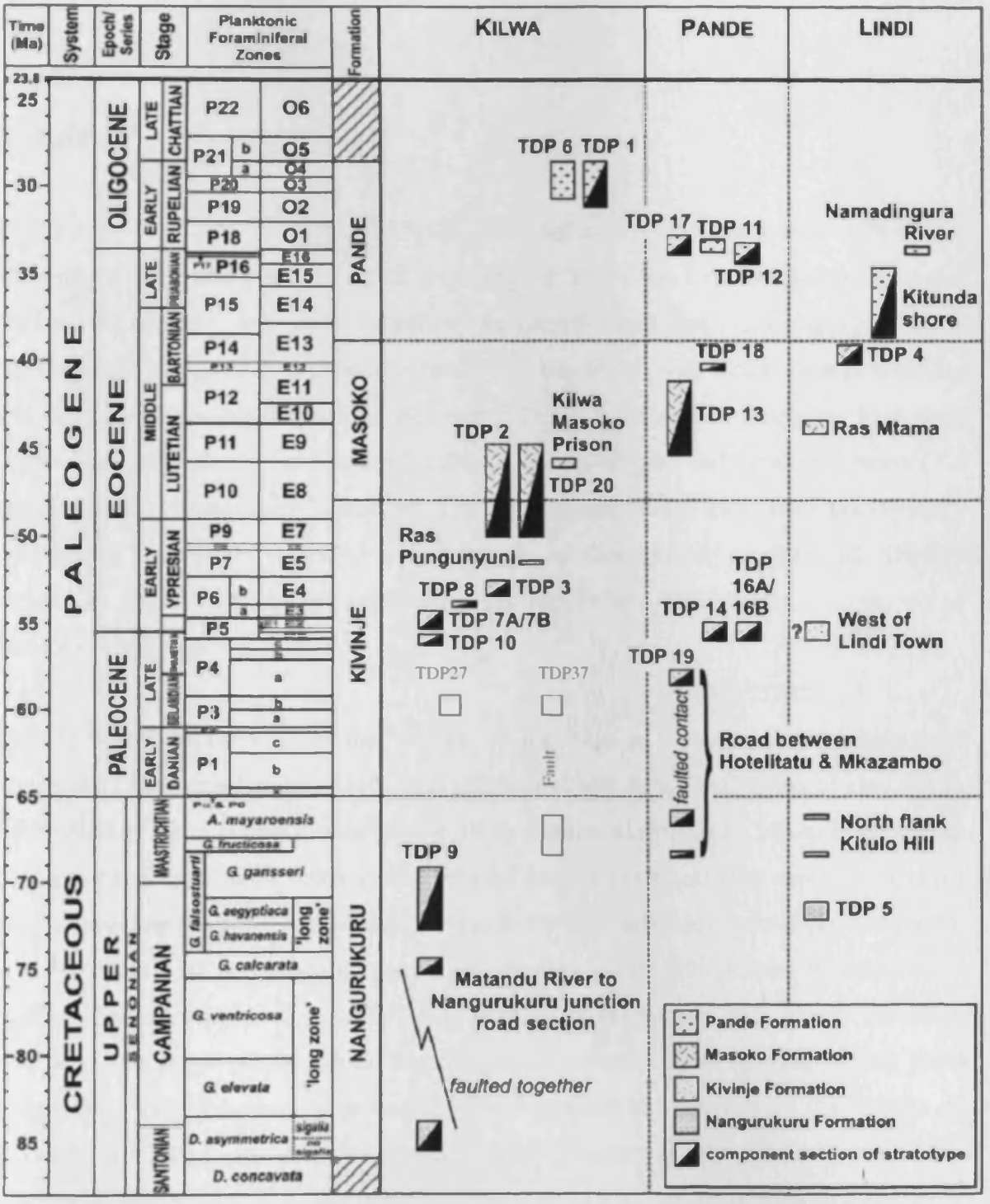

Figure 8.1- Chronostratigraphy of logged sections from TDP Sites within the Tanzanian Kilwa group, black = drilled prior to 2008, red = 2008 and 2009 K/Pg attempts. Cretaceous timescale is based on Gradstien *et al.*, (2004) and Paleogene timescale is based on Berggren and Pearson (2005). Taken from Nicholas *et al.* (2006).

8.2. Results

8.2.1. Lithologic description

TDP Site 27

Drilling at TDP site 27 recovered 18.2 m of sediment and limestones, with minor amounts of clay and poor core recovery (Figure 8.2). Unit I occurs below an initial ~0.2 m of lateritic soil and comprises weathered limestones. The upper 5 m is represented by greyish-orange weathered wacke limestone, with darker orange mottling and occasional bivalve fragments. Between 5.0-5.7 m the wacke limestone took on a light olive grey colour. Here macrofossils, including bivalve and coral fragments (1-4 cm diameter), became more abundant. The top and base of the limestones are typically broken and rubbly and in-filled with a matrix of dark yellow clayey-sand. Slightly sandier to chalky wackestone intervals occur locally and black specs, (micas) occur variably throughout.

Unit II occurs from 8 m to the bottom of the hole and comprises a sequence of brecciated limestones, interbedded, with sandstones and occasional layers of clay. From 8.0 to ~10 m a brecciated limestone involving angular clasts (up to 10 cm diameter) in dark orange to yellowish clayey-sand lithifed matrix, with variable amounts of olive grey sandy-clay mottling was found. Occasional black carbonaceous smears were seen. A short interval of soft, homogenous light olive grey clay was present between 10.0-10.8 m. This overlaid 2-3 m of (10.8-13.6 m) grey sandstones and gravel, with clay interbeds and large poorly sorted fossiliferous limestone clasts (gastropod and coral fragments), with the coarsest grained sediments occurring between 11.0 to 12.32 m. Between 13.3-13.6 m the sandstones became more weakly lithified and more calcareous. From 14.0 m to the bottom of the hole (18.35 m) the dominant lithology is light olive grey bioturbated limestone with dispersed shell fragments. This limestone is sandy between 14.0-15.7 m becoming finer grained and argillaceous down-core. This lower sequence is interrupted between 17.0-17.2 m by an interval of soft light olive grey clay, with broken claystone fragments and drilling slurry.

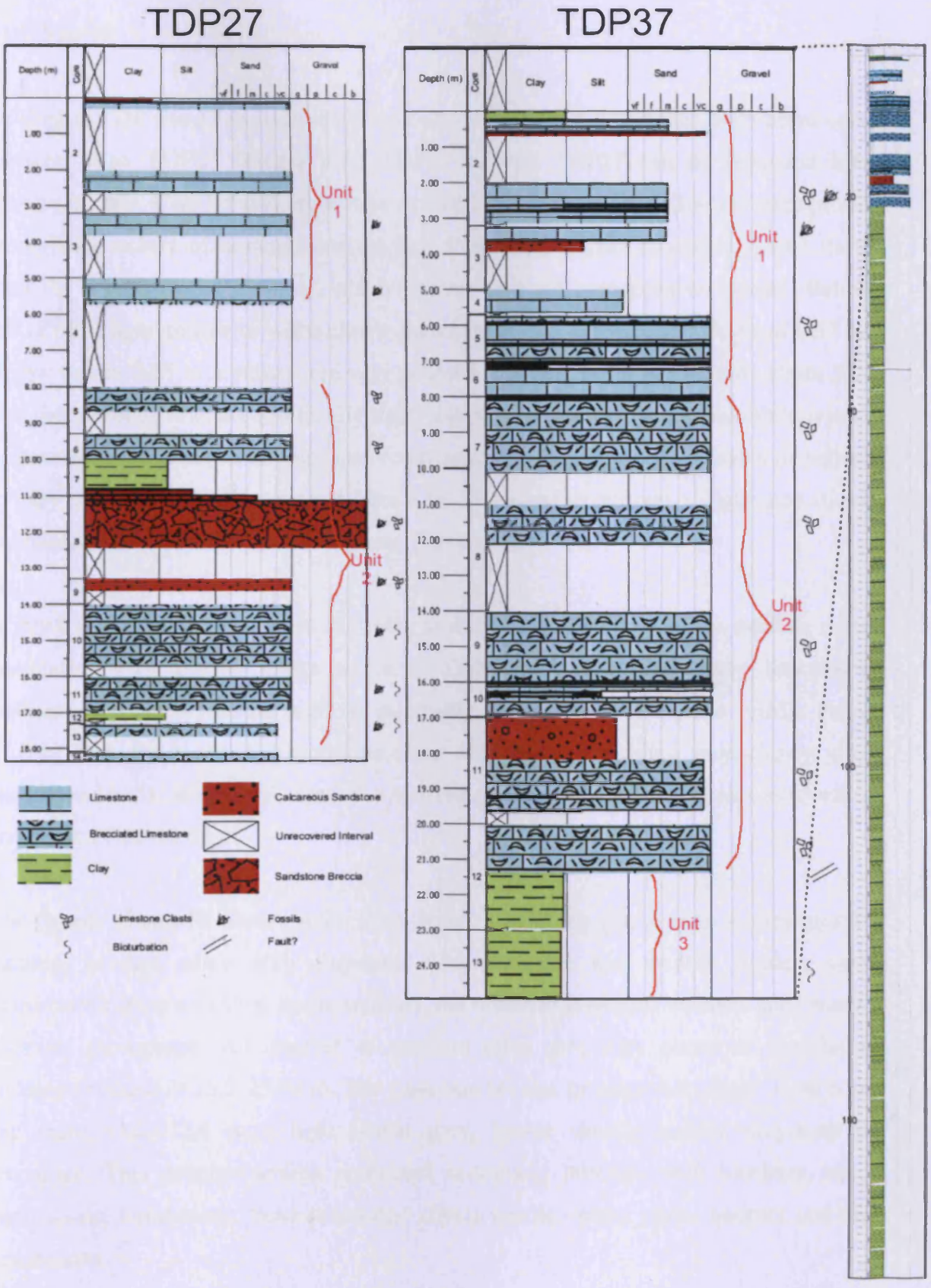

Figure 8.2 – Lithostratigraphy for Site TDP27 and TDP37 drilled at Kimamba Hill, Tanzania. Compilation of the lithostratigraphy was conducted by myself on site using the PSICAT software. The depth 0-25 m is shown in close up for TDP37 and full lithology 0-172.10 m is on the right.

TDP Site 37

Drilling at TDP site 37 recovered 172.1 m of sediments and limestones, with better core recovery than TDP27 (Figure 8.2). TDP37 as with TDP27 can be separated into lithologic units. Unit I and II are similar to TDP27, but a new Unit III is also recognised comprising mostly of homogenous medium to dark olive grey claystone. Unit I starts after the top 22 cm of the core, which yielded dark red homogeneous laterite. Below this depth a light yellow to white clastic limestone rubble occurred to a depth of 0.57 m. Below this to 0.65 m a yellow-red very coarse loose sand layer was present. From 2.0-8 m the lithology was predominately light yellow to moderately indurated white wacke limestones, with dissolution vugs and occasional shell fragments. Thin layers of yellow to grey clayey loose sand occurred from 3.63-3.9 m and an interval of light grey sticky unconsolidated clay was present between 7.09-7.21 m.

A move to Unit II occurs as ~8 m depth, as the white wacke limestones became more brecciated, with angular clasts within a silisiclastic matrix. Brecciated limestones continue from 11.0-16.9 m, with an increasing proportion of sandstone matrix. From 17.0-21.35 m the brecciated limestone clasts are contained within a grey, clayey, silty sandstone matrix. Within this section a medium to dark grey massive clayey siltstone is present at 19.62-19.65 m.

The change to unit III occurs at 21.35 m, where limestones give way to a homogenous medium to dark olive grey claystone. The claystone was weakly bedded, with bioturbation, faint mottling, pyrite nodules, tan coloured limestone nodules and 'waxy' intervals throughout. An interval of medium olive grey silty claystone that lacks bedding occurred at 25.2-25.94 m. The claystone became progressively bluer down core and from 53.0-172.1 m a light bluish grey, friable weakly bedded claystone is recognize. This deepest section contained occasional intervals with bioclasts, sand laminations, biturbation, 'beef structures' (fibres calcite veins), pyrite nodules and tan concretions.

8.2.2. Biostratigraphy – Washed residue and thin sections

TDP Site 27

Eight samples from the levels where soft sediment occur were analyzed for foraminiferal palaeontology and biostratigraphy (Table 8.1). Seven thin sections from rock samples were studied for stratigraphy and palaeoenvironmental analysis (Table 8.2 and Figure 8.3 to Figure 8.8). The washed residue samples (>63μm) contain rare planktonic foraminifera and common benthic foraminifera. Preservation is generally poor, with common calcite infilling, however, external wall preservation is occasionally good (glassy). Benthic assemblages include species of *Nuttallides*, *Lenticulina*, *Nodosarina*, *Cibicidoides*, *Anomalinoides*, *Dentalinoides*, *Noeflabellina*, and *Gyroidinoides*. Planktonic foraminifera assemblages variably contain *Morozovella angulata*, *M. velascoensis*, *M. pasionensis*, *M. apanthesma*, *Subbotina cancellata*, *S. triloculinoides*, *Parasubbotina varianta* and *Globanomalina chapmani* suggesting a mid-to upper Paleocene sediment age attributable to Biochron range P3-P4. The absence of *Igorina albeari*, which is the zonal marker for the base of P3b, but presence of other P3b species (e.g. *M. velascoensis* and *M. pasionensi*), prevents us from giving a more precise zonal assignment.

Planktonic foraminifera preservation and abundance improved markedly in Sample TDP27/7/1, 10-20cm. Here planktonic foraminifera out number benthic foraminifera and shell preservation is excellent despite infilling with sparry calcite (see Chapter 3 Figure 3.8). Species recorded include *M. angulata*, *M. praeangulata*, *S. cancellata*, *S. triangularis*, *S. triloculinoides*, *P. varianta*, *P. pseudobulloides*, *Praemurica uncinata*, *Pr. inconstans*, *Pr. pseudoinconstans*, *G. chapmani* and *G. ehrenbergi*. The lack of *M. velascoensis*-group morozovellids and the presence of *Pr. uncinata* and other species of *Praemurica* suggest an age for this sample of Biochron P3a. Sample TDP27/7/1, 10-20 cm sediments, therefore, appear to represent the stratigraphically lowest and oldest Paleocene sediment recovered thus far by TDP drilling.

Thin sections provide biostratigraphic and environmental indications for the limestones. In thin section all of the limestone samples can be described as bioclastic packstones. A few of the samples contain larger bioclasts and are described as rud-packstones. A third class have a higher percentage of mud supported matrix and are described as wacke-packstones. The bioclasts include coralline encrusting red algae, dasyclad green algae, corals, Paleocene peyssonnellid encrusting algae, as well as foraminifera in samples TDP27/1/1, 26-30 and TDP27/6/1, 0-5. In addition to bioclasts, quartz grains were often found. The remaining samples have a lower percentage of bioclasts and consist mainly of benthic and planktonic foraminifera, rather than a variety of algae and corals.

Only a handful of foraminifera are visible or identifiable in sectioned views. However, Paleocene planktonic species are very distinctive and *M. angulata,* and *M. velascoensis*-group morovollids (*M. pasionensis, M. occlusa*) where recognized, as well as somewhat compressed *Globanomalina* sp. by their keels and compressed form. These species occur in various combinations in samples from Cores TDP27/1, 6, 11 and 13 (Table 8.2). Interestingly all the limestone thin sections appear to contain morphologies diagnostic of slightly younger biochrons P3b-P4 (60 to 55.9 Ma), whereas the clay samples tend to suggest a biochron of P3a (61 to 60 Ma).

Washed residue (>63 μm)	Depth of sample	Lithology Description	Microfossils	Preservation	P/B ratio	Maximum Biochron Age
TDP27/6/1, 11-23	9.41-9.53m	Brecciated wackestone set in a lithified clayey-sand matrix	No planktonic forams only benthic.	-	-	-
TDP27/6/1, 53-61	9.83-9.91m	Brecciated wackestone set in a lithified clayey-sand matrix	Rare planktoinc forams (*S. triloculinoides, P. varianta, M. angulata, M. velascoensis, G. ehrenbergi*) lots benthics (Generally >212).	poor	-	P3b
TDP27/7/1, 10-20	10.20-10.30m	Soft homogenous light olive grey clay	Abundant planktics *S. triloculinoides, S. triangularis, S. cancellata, P. varianta, P. pseudobulloides, Pr. uncinata, Pr. inconstans, Pr. pseudoinconstans, G. compressa, G. ehrenbergi, M. angulata* and *M. praeangulata.*	V. G but infilled with sparry calcite shell material can be seperated	20:1 (benthic larger than planktics present)	P3a
TDP27/7/1, 32-48	10.42-10.58m	Soft homogenous light olive grey clay	Rare planktoinc forams (*S. triloculinoides, S. cancellata, P. varianta, Pr. uncinata* and *Pr. inconstans*) some benthics.	variable (poor to good)	1:1	P3a
TDP27/11/1, 26-28	16.26-16.28m	Light olive grey argillaceous limestone	No planktonics, rare benthics.	-	-	-
TDP27/12/1, 8-16	17.08-17.16m	Soft homogenous light olive grey clay	Two planktonics (*M. angulata* and *P. varianta*) rare benthics.	poor	-	P3a
TDP27/13/1, 43-44	17.73-17.74m	Light olive grey argillaceous limestone	One planktonic (*S. triloculinoides*) rare benthics.	poor	-	?
TDP27/14/1, 20-25	18.30-18.35m	Light olive grey argillaceous limestone	Rare planktonics (*M. angulata, P. varianta, Pr. uncinata* and *S. cancellata*) rare benthics some Miliolina.	poor	-	P3a

Table 8.1 – Biostratigraphy, preservation state and lithology of the washed residues from Site TDP27, Tanzania. P/B ratio indicates the number of planktonic to benthic foraminifera.

Thin section	Depth of sample	Lithology Description	Microfossils	Possible Biochron Range
TDP27/1/1, 26-30	0.26-0.30m	High % bioclastic pack-rudstone with some encrusting coralline algae and recrystalised coral. Quartz grains can also be seen.	*M. angulata*, biseriral planktic, *G.pseudomenardii*, *Subbotina* and benthics	At least P3 but maybe P4
TDP27/6/1, 0-5	9.3-9.35m	High % bioclatic pack-rudstone with red coralline algae, dasyclad green algae (<30m water depth), corals, Paleocene peyssonnellid encrusting algae and quarts grains.	*Parasubbotina* sp., benthics (generally >212), *M. occlusa*, *M. pasionensis*, possible *M. acuta* or *M. aequa* and *G.pseudomenardii* or *G. chapmani*.	At least P3b but maybe P4
TDP27/11/1, 56-58	16.56-16.58m	Low % bioclastic packstone with possble green algae	Possible *M. angulata*	P3a or P3b?
TDP27/13/1, 0-7	17.30-17.37m	Low % bioclastic wacke-packstone	*M. apanthesma*, *M. pasionensis*, *Parasubbotina* and benthics	P3b?
TDP27/13/1, 38-43	17.68-17.73m	Low % bioclastic wacke-packstone	*Morozovella* sp., *G. chapmani* and benthics	P3b?
TDP27/14/1, 0-6	18.10-18.16m	High % bioclastic packstone	*M. pasionensis*, *M. velascoensis*, *M. angulata* or *M. acuta* / *M. aequa*. Benthics (rotalids and miliolinas). Ostrcods	P3b or P4
TDP27/14/1, 20-25	18.30-18.35m	bioclastic packstone with some red algae.	Benthics, *Morozovella* sp., *M. velascoensis* / *M. pasionensis*, *G. chapmani*, *Acarinina* sp. and *Parasubbotina* sp.	P3b

Table 8.2 – Biostratigraphy and lithology of thin sections from Site TDP27, Tanzania. Corresponding thin section images can be found in Figure 8.4 to 8.9.

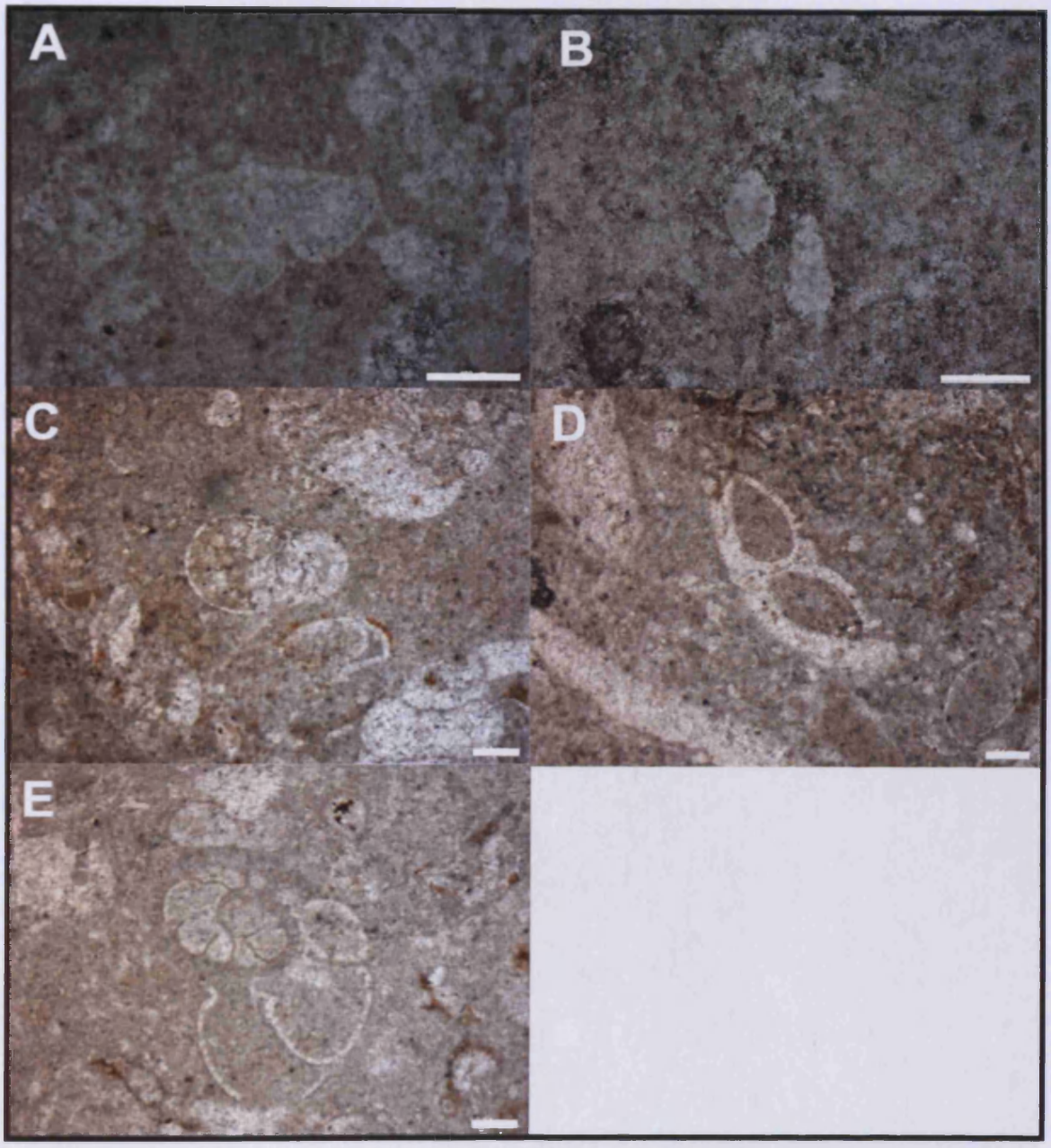

Figure 8.3 - TDP27/1/1, 26-30cm; A - *M. angulata* or *M. apanthesma*, B - Benthic or Biserial, C - *Subbotina* sp., D - *G. pseudomenardii*, E – Benthic spp. Scale bar = 100μm

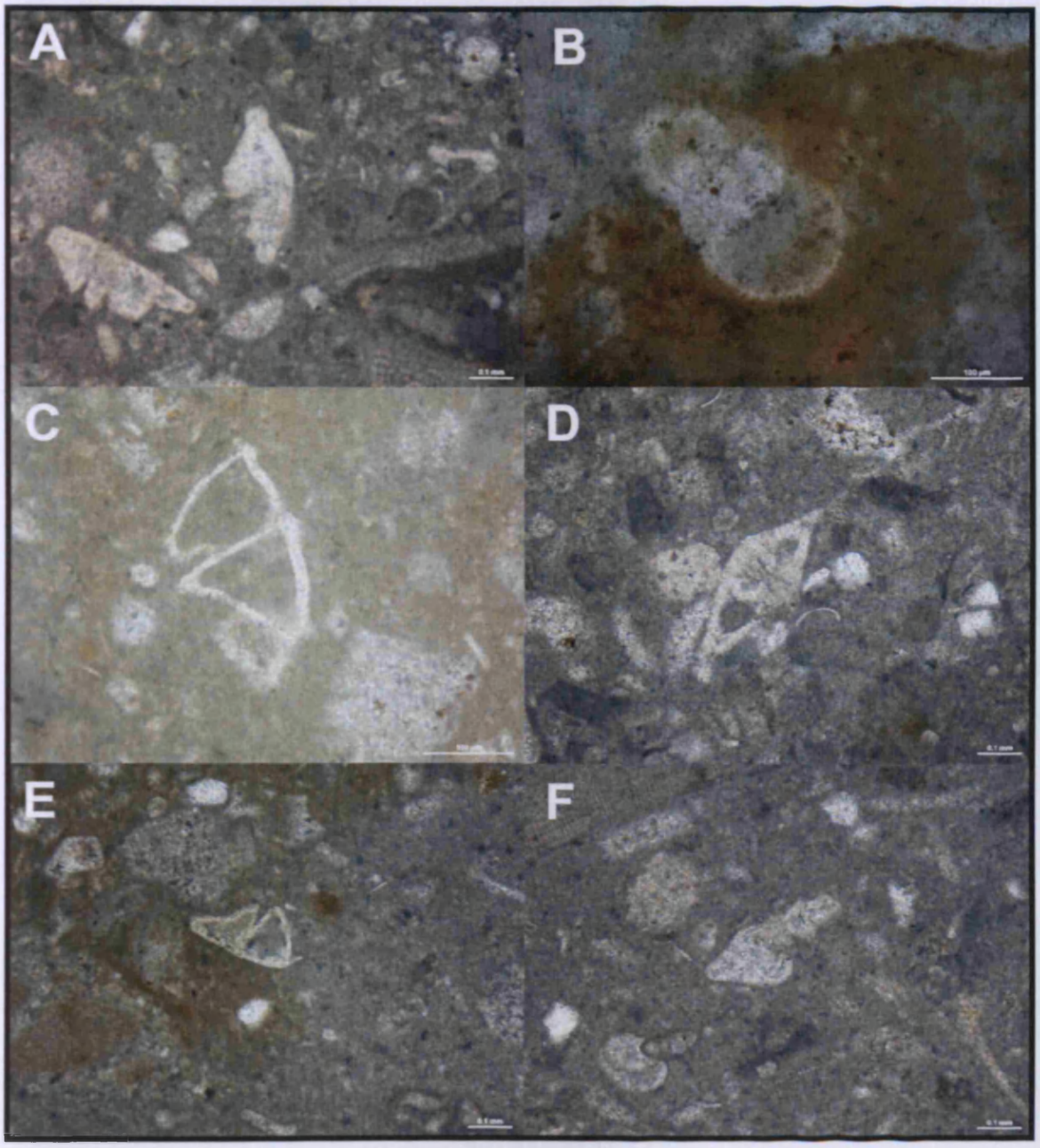

Figure 8.4 - TDP27/6/1, 0-5cm; A - *M. pasionensis* X2 , B - Parasubbotina sp., C - *M. angulata or M. acuta /M. aequa*, D - *M. occlusa* or *M. acutispira*, E - *M. angulata* or *M. acuta /M. aequa*, F - *G. chapmani*. Scale bar = 100µm.

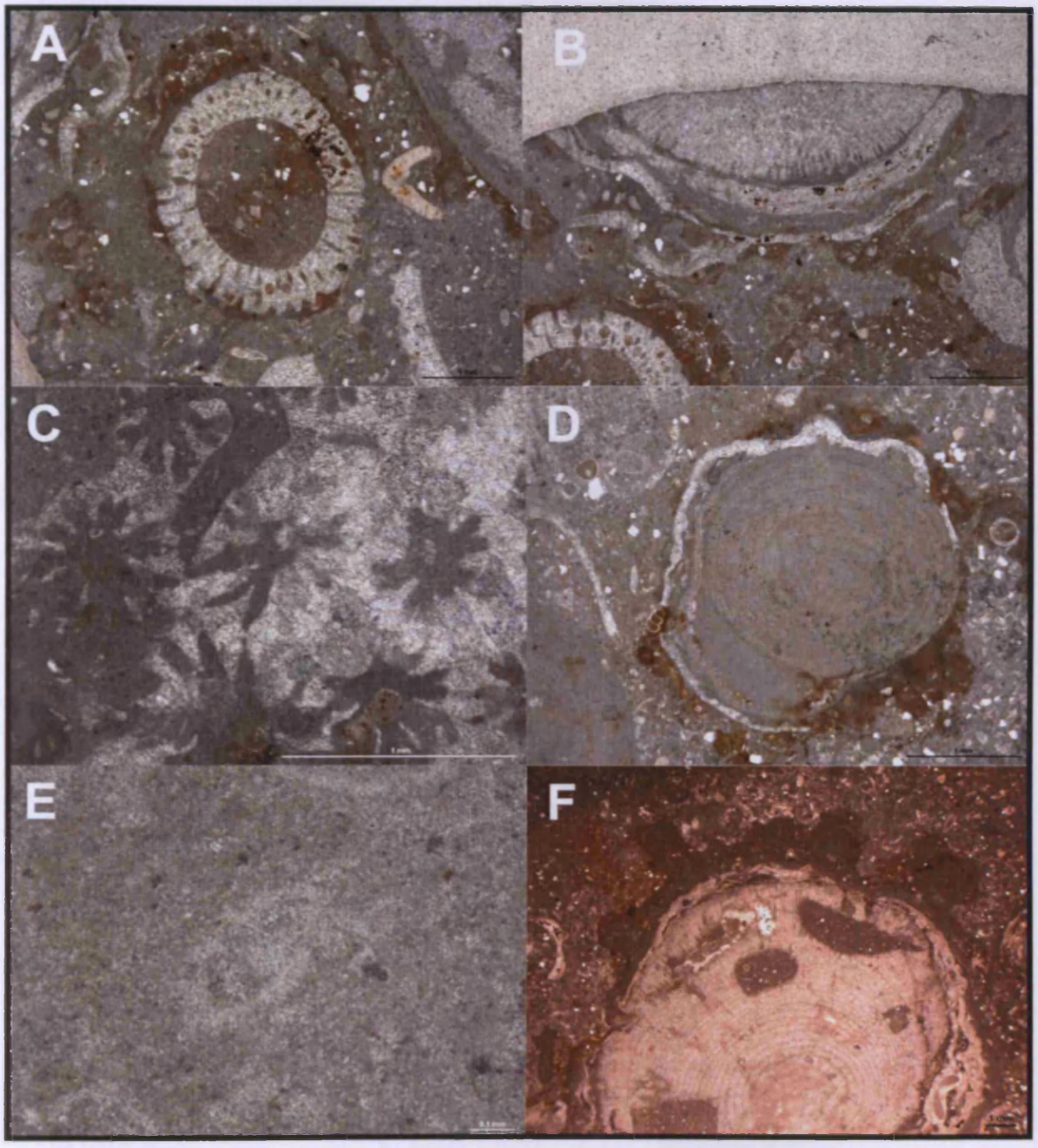

Figure 8.5 - TDP27/6/1, 0-5cm; A - Dasyclad green algae, B - Peyssonnellid algae, C - Coral, D - Red coralline algae, TDP27/11/1, 56-58cm; E - *M. angulata*?, F – Red coralline algae with bore holes and infill. Scale bar = 100µm.

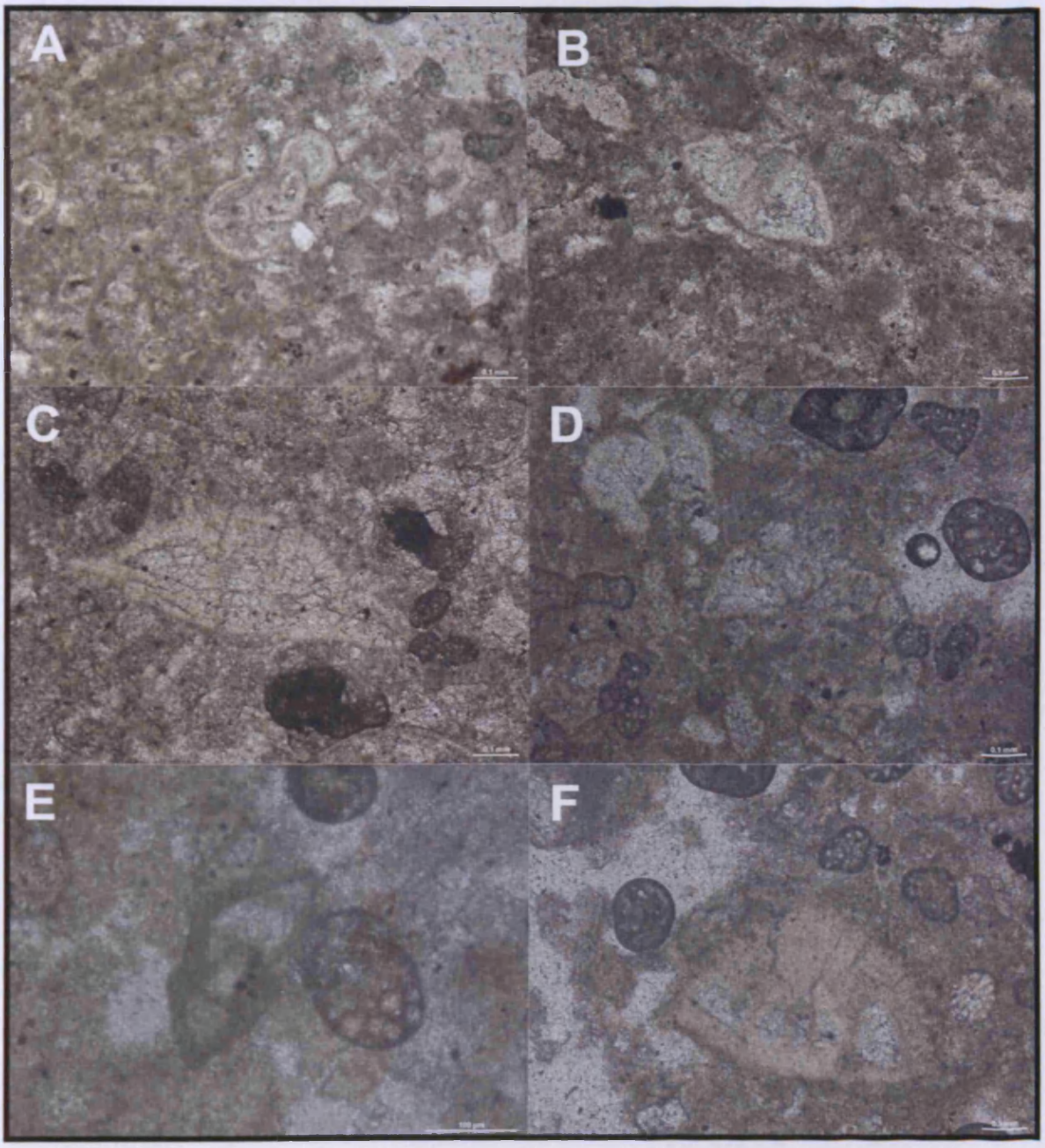

Figure 8.6 - TDP27/13/1, 0-7cm; A - *Parasubbotina* sp., B - *M. apanthesma*, C - *M. pasionensis*, TDP27/13/1, 38-43cm; D - *Morozovella* sp., E - *G. chapmani*, F – benthic sp. Scale bar = 100µm.

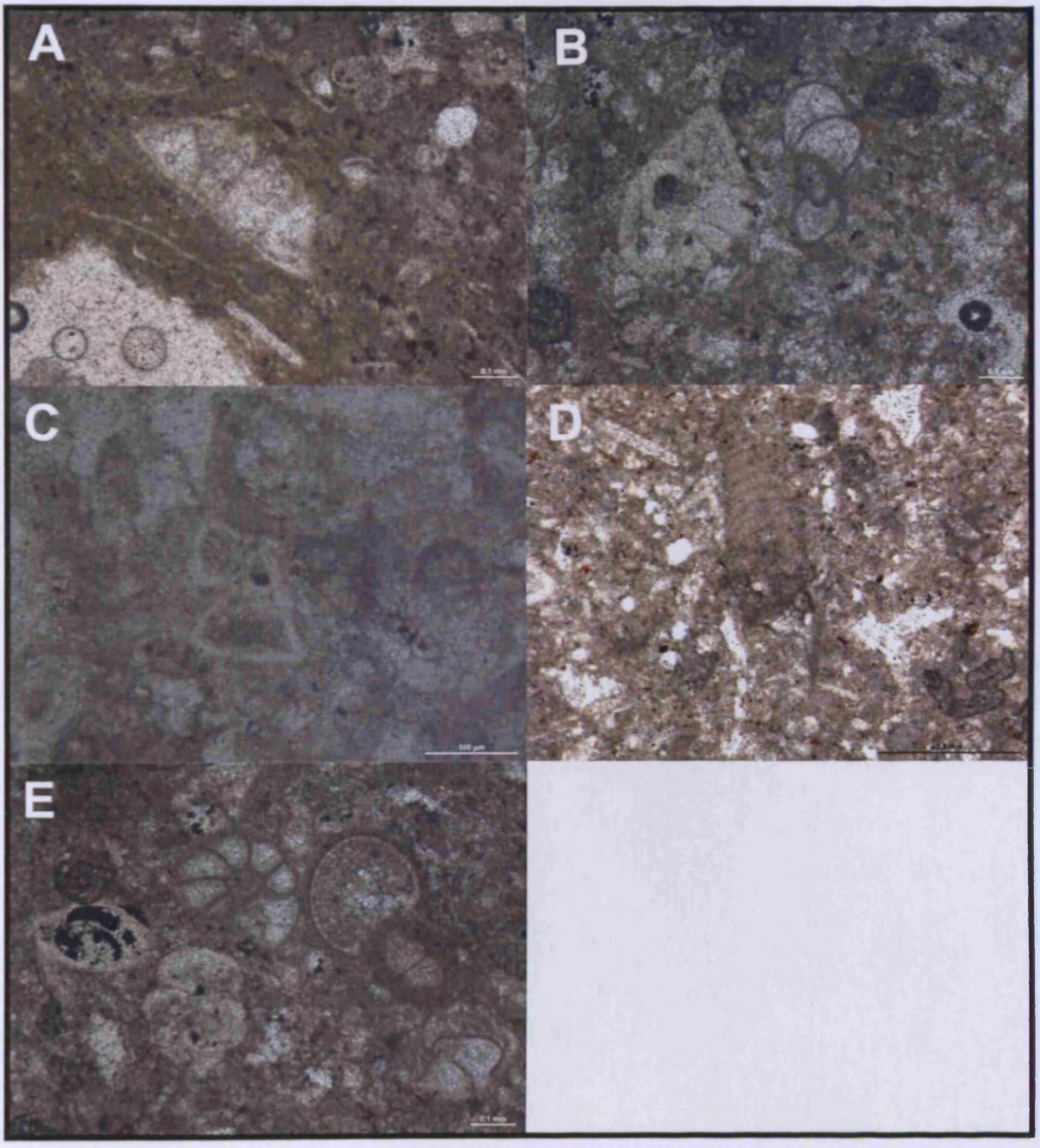

Figure 8.7 - TDP27/14/1, 0-6cm; A - *M. pasionensis* or *M. velascoensis*, B - *M. angulata*, C - *M. angulata* or possibly *M. acuta /M. aequa*, D - Red algae, E – benthic sp. Scale bar = 100µm.

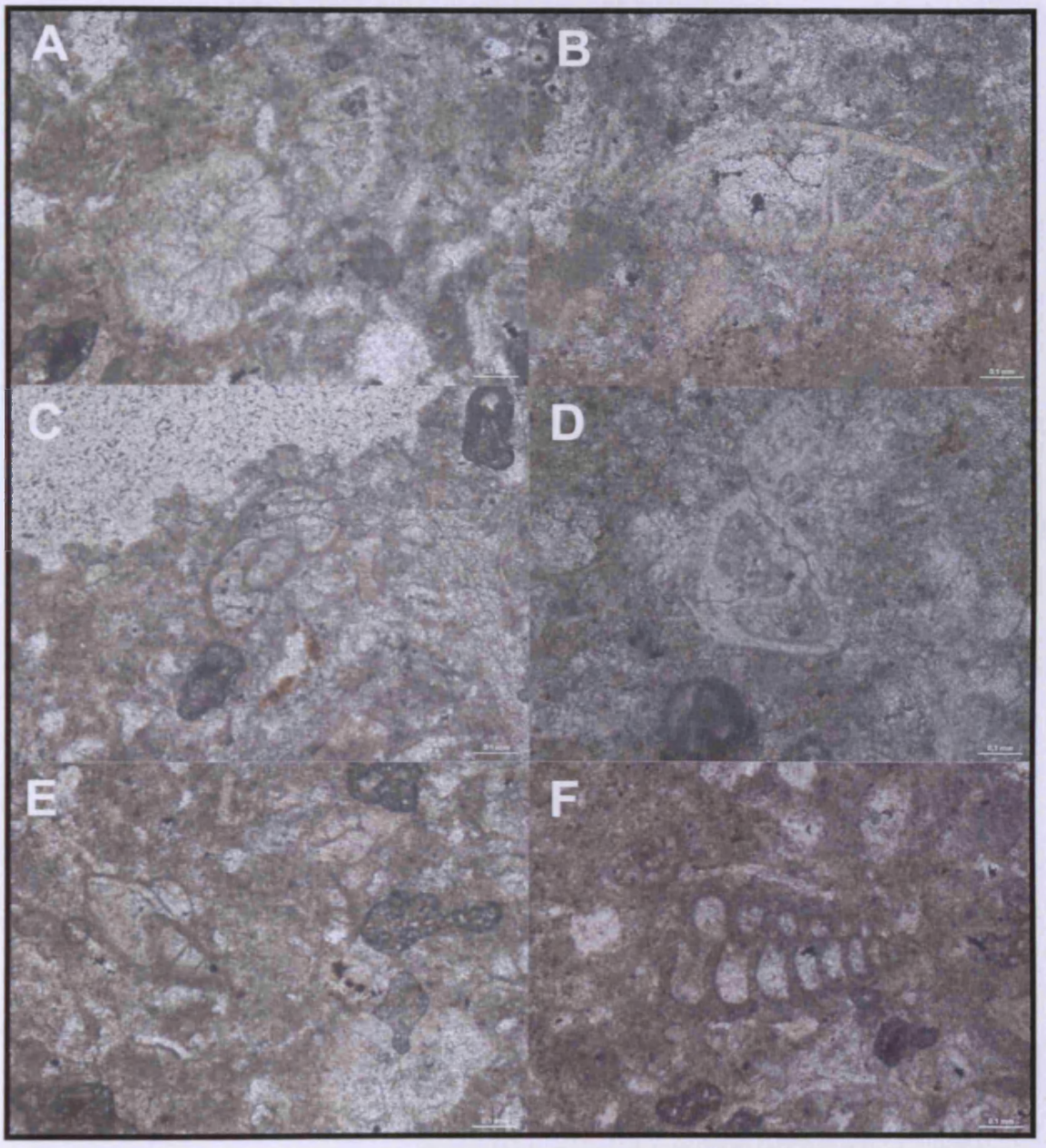

Figure 8.8 - TDP27/14/1, 20-25cm; A - *M. velascoensis* or *M. pasionensis* (right), benthic (left), B – benthic sp., C - *Parasubbotina* sp. or Benthic, D - *Morozovella* sp. or Benthic, E - *G. chapmani* and possible *Acarinina* sp. (Bottom right corner), F – benthic sp. Scale bar = 100µm.

TDP Site 37

Five washed samples of soft sediment and three thin sections were examined for foraminifera biostratigraphy (Table 8.3 and Table 8.4; Figure 8.9 and Figure 8.10). The washed residues are similar to those described from Site TDP27, with typically rare planktonic and more common benthic foraminifera and similar species composition. Benthic assemblages include species of *Nuttallides*, *Lenticulina*, *Nodosarina*, *Cibicidoides*, *Anomalinoides*, *Dentalinoides*, *Noeflabellina*, and *Gyroidinoides*. Preservation was mostly poor in the samples taken between 0-21.35 m, but the planktonic foraminifera *Morozovella angulata*, *M. velascoensis*, *M. pasionensis*, *M. apanthesma*, *M. occlusa*, *Subbotina cancellata*, *S. triangularis*, *S. triloculinoides*, *Parasubbotina varianta* and *Globanomalina chapmani* suggest a mid-to upper Paleocene sediment age (Bizone range P3-P4). The absence of *Igorina albeari*, which is the zonal marker for the base of P3b, prevents us from giving a precise zonal assignment, however the presence of the *M. velascoensis* and *M. pasionensis* group species, as well as *G. chapmani* suggests P3b-P4.

Foraminiferal assemblages recovered from the homogenous claystones that extended from 21.35 m to the bottom of the hole, contain abundant and diverse Cretaceous planktonic foraminifera. Calcitic benthic species are rare and the presence of agglutinated forms suggests low oxygen conditions at the seafloor, which is consistant with the dark colour and presence of pyrite. Foraminiferal preservation is good, but the majority of specimens are infilled with sparry calcite. Planktonic species in the upper part of this section (30.18-30.39m depth, sample TDP37/18/2, 18-39cm) include *Rosita contusa*, *Pseudotextularina elegans*, *Globotruncana aegyptica*, *Globotruncana falsostuarti*, *Globotruncana area*, *Globotruncanita stuarti*, *G. conica*, *G. stuartiformis*, *Racemiguembelina fructicosa*, *Pseudoguembelina costulata*, *P. palpebra*, *Rugoglobigerina rugosa*, *R. mareocephala*, *R. hexacamerata*, *Heterohelix navarroensis*, *Gansserina gansseri*, *Globigerinelloides subcarinata*, *Rosita fornicata*, *R. contusa*, *Globotruncanella havanensis* and *G. petaloidea*. The lack of *Abathomphalus mayaroensis* and presence of *Gansserina gansseri*, *Rosita contusa*, *Globotruncanella havanensis* and *Globotruncana aegyptica* would place this sample between three/four planktonic foraminiferal zones (depending on zonation scheme) near the end of the

Cretaceous period, within the Maastrichtian but before the *Abathomphalus mayaroensis* zone.

Thin sections provide biostratigraphic and environmental indications for the limestone age and formation, although currently we have information for Cores 2, 4 and 6 only. Similar to Site TDP27, Site TDP37 limestone samples are bioclastic packstones. One sample contains larger bioclasts and could be described as rud-packstones (Table 8.4). Planktonic foraminifera are rarer in TDP37 than in TDP27 and very few are visible or identifiable in sectioned view, but Paleocene planktonic species are very distinctive and *M. angulata*, and *M. pasionensis*, as well as somewhat compressed *Globanomalina* sp., *G. chapmani* can be recognized.

Washed residue (>63 μm)	Depth of sample	Lithology Description	Microfossils	Preservation	P/B ratio	Maximum Biochron Age
TDP37/2/1, 61-78	2.61-2.78m	Orange to gray mottled loose fine clay	Planktoinc forams (*S. triangularis, S. cancellata, M. apanthesma, M. angulata, M. velascoensis, M. occlusa* and *G. chapmani*) lots benthics.	poor	~1:20	P3b
TDP37/6/1, 9-21	7.09-7.21m	Light gray, sticky unconsolidated clay	Planktoinc forams (*S. triloculinoides, S. cancellata, P. varianta, M. apanthesma, M. angulata, M.conicotruncata*) lots benthics.	poor	~1:15	P3a/b
TDP37/11/1, 93-107	17.93-18.07m	Medium gray clayey, silty sandstone matrix supporting conglomerate	*M. angulata* and *M. conicotruncata* with Maastrichtian contamination.	-	-	P3a
TDP37/12/2, 70-100	21.70-22.0m	Homogeneous medium to dark olive gray claystone	Maastrichtian planktonic foraminifera including *A. mayaroensis*	-	-	*A. mayaroensis*
TDP37/18/2, 18-39	30.18-30.39m	Medium olive gray silty claystone	Planktonic foram speceis *R. contusa, P. elegans, G. aegyptica, G. falsostuarti, G. area, G. stuarti, G. conica, R. fructicosa, P. costulata, P. palpebra, R. rugosa, R. mareocephala, R. hexacamerata, H. navarroensis, G. gansseri, G. stuartiformis, G. subcarinata, R. fornicata, G. havanensis, G. petaloidea.*	Good but infilled	~3:1 (some agglutinated)	*G. gansseri, R. contuse, G. havanensis* and *G. aegyptica* zones

Table 8.3 – Biostratigraphy, preservation state and lithology of the washed residues from Site TDP37, Tanzania. P/B ratio indicates the number of planktonic to benthic foraminifera.

Thin section	Depth of sample	Lithology Description	Microfossils	Minimum Biochron
TDP37/2/1, 64-74	2.64-2.74m	bioclastic packstone with red algae	Subbotina sp., *G. chapmani*, *M. angulata*, *M. pasionensis*, Benthics and Bryozoans or Red algae	P3b
TDP37/4/1, 19-24	5.19-5.24m	High % bioclastic pack-rudstone with red algae, corals, Paleocene peyssonnellid encrusting algae and quarts grains.	*Morozovella* sp., Benthics	P3b
TDP37/6/1, 5-7	7.05-7.07m	Low % bioclastic packstone (baddly grounded)	*G. chapmani*, Morozovella sp. and Benthic (Miliolina)	P3b

Table 8.4 – Biostratigraphy and lithology of thin sections from Site TDP37, Tanzania. Corresponding thin section images can be found in Figure 8.10 to 8.11.

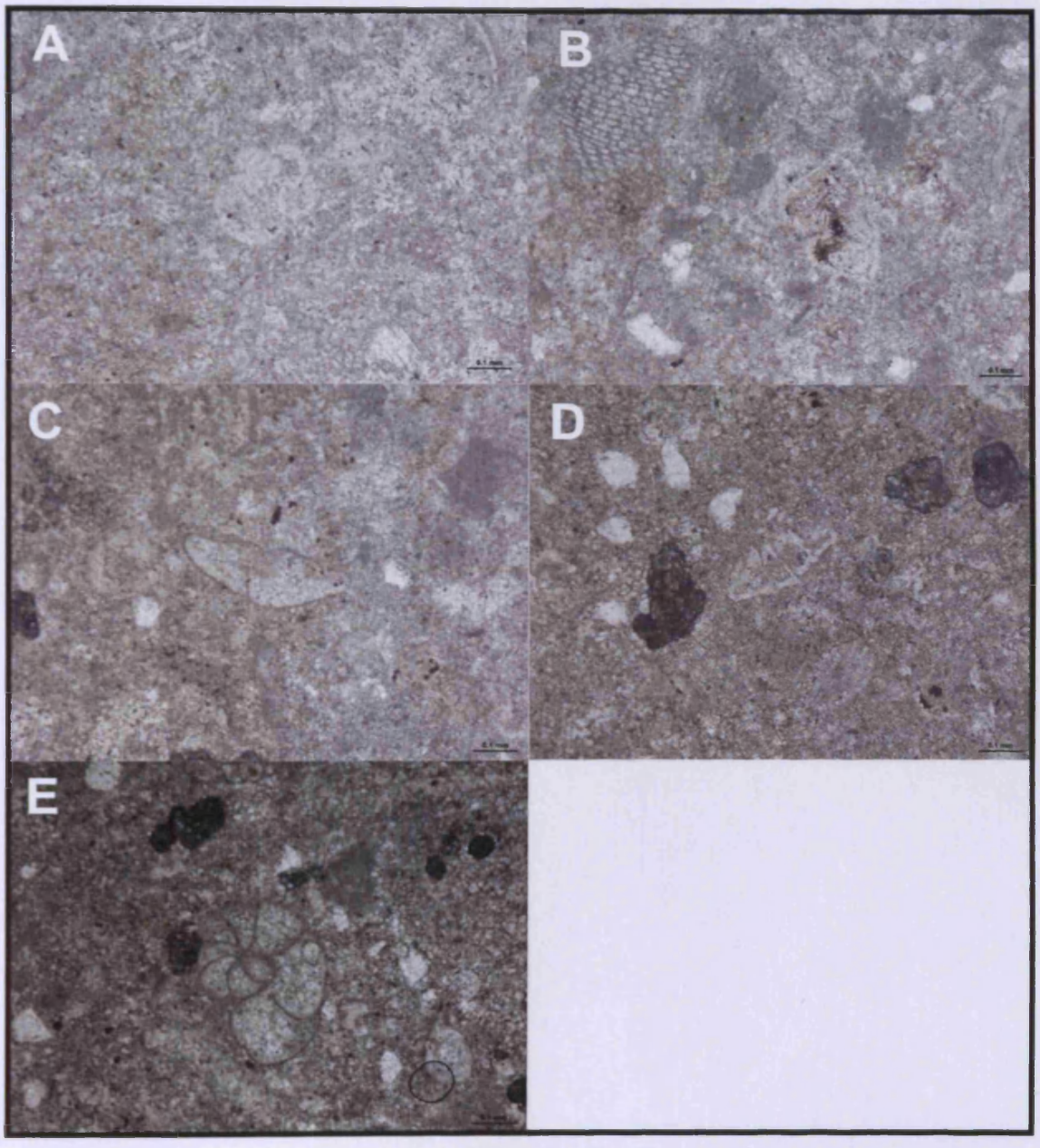

Figure 8.9 - TDP37/2/1, 64-74cm; A - *Subbotina* sp., B - *M. angulata* and bryozoan / red algae (top left corner), C - *G. chapmani*, D - *M. pasionensis*, E – benthic sp. Scale bar = 100µm.

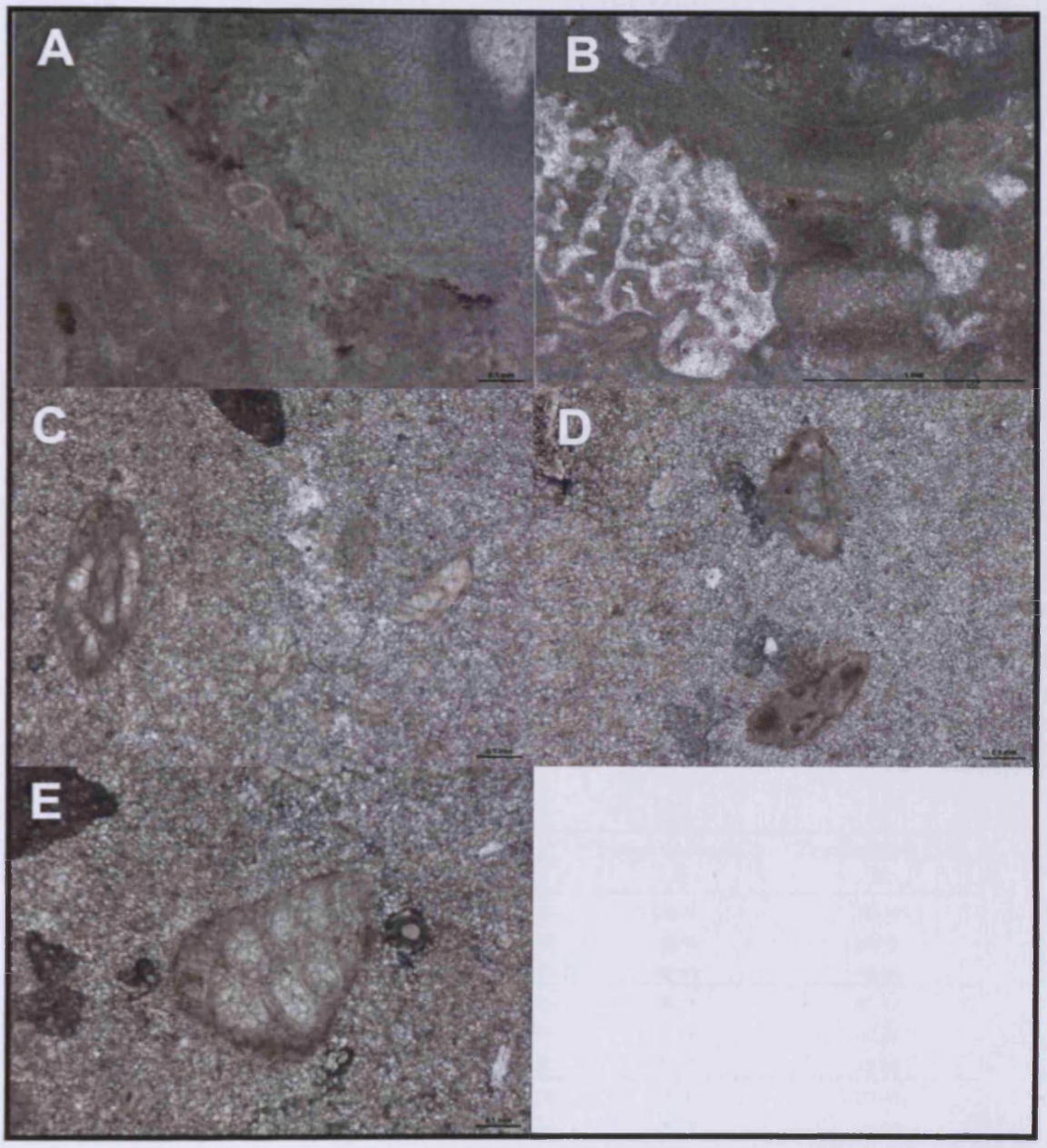

Figure 8.10 - TDP37/4/1, 19-24cm; A - *Morozovella* sp. or *Globanomalina* sp. and Red algae, B- Red algae (scale bar = 1mm). TDP37/6/1, 5-7cm C - *G. chapmani* (right) and benthic, miliolina (left), D - Benthic (bottom) *Morozovella* sp. (top), E – benthic sp. Scale bar = 100μm (all except B).

8.2.3. Stable isotopes analysis

Figure 8.11 displays the results of the isotopic analysis from the one sample containing well preserved planktonic foraminifera, TDP27/7/1, 10-20 cm. Only one sample for three species could be analysed, as large numbers of specimens were needed, due to the need to remove the test from the 'sparry' infill. Analysis of the test only, shows *M. angulata* with the lightest $\delta^{18}O$ values (by 0.8 ‰) compared to *Pr. uncinata* and *S. triangularis* (Table 8.5), with *Pr. uncinata* and *S. triangularis* having similar $\delta^{18}O$ values. The $\delta^{13}C$ values of *M. angulata* and *Pr. uncinata* are similar to each other and heavier (by ~2.0 ‰) than *S. triangularis*. The isolated 'sparry' infill from these species has similar $\delta^{18}O$ and $\delta^{13}C$ values, that are significantly lower ($\delta^{18}O$ by ~3.34 to 4.21 ‰ and $\delta^{13}C$ by ~0.32 to 2.05 ‰) compared to the test only samples. The samples containing a mix of test and infill have slightly heavier $\delta^{18}O$ values than the infill only samples. *Morozovella angulata* and *Pr. uncinata* cluster together in the mix plot, however *S. triangularis* plots slightly lighter in $\delta^{18}O$ (by ~0.2 ‰) and $\delta^{13}C$ (by ~0.8 ‰).

Species	Composition	$\delta^{13}C$	$\delta^{18}O$	Temperature (°C) A	Temperature (°C) B
M. angulata	Test	2.89	-3.49	29.59	30.76
	Infill	0.88	-6.83	45.50	46.71
	Mix	1.49	-5.89	40.96	42.16
Pr. uncinata	Test	2.83	-2.75	26.14	27.30
	Infill	0.78	-6.96	46.14	47.36
	Mix	1.45	-5.87	40.87	42.08
S. triangularis	Test	0.84	-2.78	26.30	27.46
	Infill	1.05	-6.86	45.65	46.87
	Mix	0.72	-6.08	41.88	43.09

Table 8.5 - Stable isotope data and paleotemperature estimates from TDP27/7/1, 10-20cm for three species of planktonic foraminifera. Three components were used for each species; crushed test only after removal from the sparry infill, the infill it's self and finally a mixture of the two. Temperature estimate use the equation from Erez and Luz (1983) with $\delta^{18}O$ of seawater for A = -0.75 ‰ from Pearson *et al.* (2007) and B = -0.5 ‰ from Tindall *et al.* (2010). Genera abbreviations as follows; M = *Morozovella*, Pr. = *Praemurica* and S = *Subbotina*.

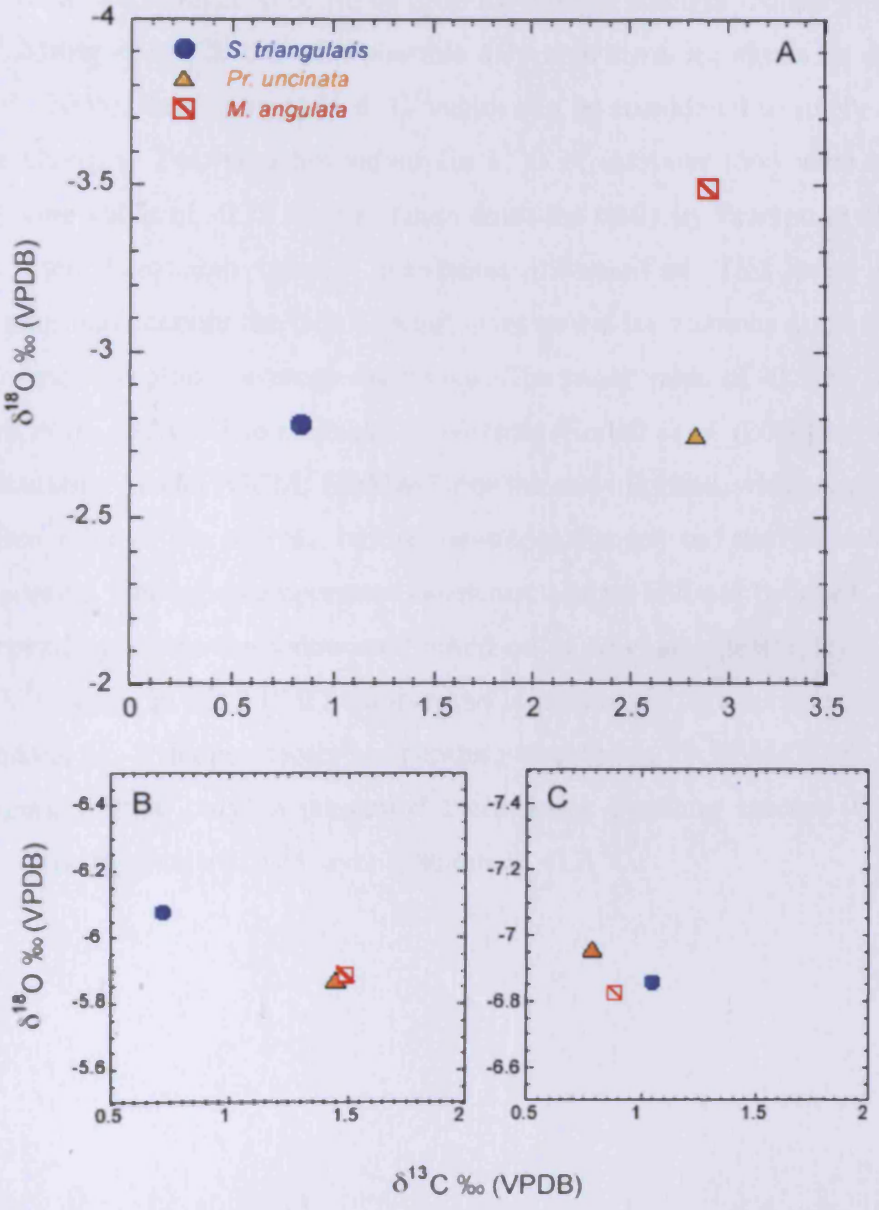

Figure 8.11 - Carbon isotope ($\delta^{13}C$) - oxygen isotope ($\delta^{18}O$) cross plots for A – planktonic foraminiferal test only, B- Mix of test and infill and C – Infill only from planktonic foraminifera biochron P3a, sample TDP27/7/1, 10-20cm. Genera abbreviations as follows M= *Morozovella*, Pr = *Praemurica* and S = *Subbotina*. Note varying scales.

The temperature equation of Erez and Luz (1983) was used to estimate early Paleocene sea surface temperatures (SSTs) (see Chapter 4, section 4.2.4 for details). Changes in $\delta^{18}O$ values can be due to either ice volume or temperature changes. However for this time period there are thought to be no or little ice volume changes (Miller *et al.*, 1987; Smit, 1990; Miller *et al.*, 2005), with possible only ephemeral ice sheets on Antarctica (Miller *et al.*, 2005), thus changes in $\delta^{18}O$ values can be considered to solely represent temperature changes. Two possible values for $\delta^{18}O$ of seawater (δw) were used here (Table 8.5). One value of -0.75 ‰ was taken from the study by Pearson *et al.* (2007), which also used Tanzanian 'glassy' planktonic foraminifera. This value has been adjusted to take into account the lack of significant global ice volumes in the Paleocene compared to modern global average δw values. The other value of -0.5 ‰ was taken from Tindall *et al.* (2010). The estimate of δw from Tindall *et al.* (2010) is based on a General Circulation Model (GCM; HadCM3) for the early Eocene, which uses an initial global ice free value of δw = -1 ‰, before the model was run and the full hydrological cycle incorporated. The paleotemperature estimates suggest SSTs of between 29.59 and 30.76 °C depending on the δw value used based on *M. angulata* (test only), which has the lowest $\delta^{18}O$ value in the TDP27 sample and is interpreted as a surface mixed layer dweller (Chapter 5). A deeper cooler temperature of between 26.30 and 27.46 °C based on *S. triangularis* (test only) a presumed thermocline dwelling species (Chapter 5) (Table 8.5). This suggests a mixed layer gradient of ~3.3 °C.

8.3. Discussion

8.3.1. TDP27 and TDP37 Paleoenvironment, late Cretaceous to Paleocene

The three lithological units recognised in TDP27 and TDP37 indicate changing depositional regimes in coastal southern Tanzania from the late Cretaceous to the Paleocene. Unit III, comprising of Maastrichtian hemipelagic clays containing diverse planktonic foraminifera assemblages at Site TDP37 (TDP37/12/2, 70-100 cm and TDP37/18/2, 18-39 cm), indicates deep outer slope conditions. The presence of fossilized red and green algae, corals and low planktonic to benthic foraminifera ratios (P/B) in many of the samples and thin sections (Table 8.1 to Table 8.4), in both site TDP27 and TDP37 (Units I and II), suggests shallow water deposition. Many samples also contain quartz grains, indicating the influence of fluvial sediments and proximity to land. Biomarkers, in other TDP drilling sites in the Kilwa area, found high levels of terrestrial organic matter suggesting shallow water environments and fluvial inputs (Pearson *et al.*, 2004). The presence of dasyclad green algae in TDP27/6/1, 0-5 cm, constrains the water depth to <30 m, which is the depth limit of this algal family and these delicate structures are rarely transported far (Flügel, 2004). Some of the red coralline algae have holes that appear to be the result of boring, which have subsequently been infilled with the surrounding sediment (TDP27/6/1, 0-5 cm, Figure 8.5 - F). This infilling generally only occurs if the coralline algae is already dead (Tribollet, 2008). The higher occurrence of these shallow water indicators and less brecciated limestones within Unit I, suggests a shallower environment than Unit II or III, and likely represents upper slope conditions. Unit II, comprises manly brecciated limestones, sands and clays, with fewer occurrences of red and green algae, suggesting a shallower water environment than unit III but deeper than unit 1, possibly low upper slope conditions.

The presence of a shallow carbonate body with open ocean influence would suggest a carbonate shelf (steep sided) was present in the Paleocene at the studied area (Flügel, 2004). This carbonate shelf is boarded by a reef, as indicated by the presence of corals

changes in litholog

during the late Cre

control of sedimen

impact, given the dy

8.3.2. Planktonic foraminifera stable isotope ecology and Paleocene climate of coastal southern Tanzania

The clay horizon derived from Site TDP27 provides important new paleotemperature constraint and paleoecology of early Paleogene, Tanzanian planktonic foraminifera. The depleted $\delta^{18}O$ values and enriched $\delta^{13}C$ values relative to *S. triangularis* of *M. angulata* are indicative of this species being a surface mixed layer dweller and symbiotic (D'Hondt and Zachos, 1993; Pearson *et al.*, 1993; D'Hondt *et al.*, 1994; Norris, 1996; Quillevere *et al.*, 2004; see Chapter 5). The enriched $\delta^{13}C$ values of *Pr. uncinata*, which are similar to the values of *M. angulata*, would indicate a symbiotic ecology for this species. However, the $\delta^{18}O$ values of *Pr. uncinata* are similar to *S. triangularis*, which is suggested to be a thermocline dweller (Boersma and Premoli Silva 1983; Corfield and Cartlidge, 1991; D'Hondt *et al.*, 1994; Norris, 1996; Kelly *et al.* 1996; Pearson *et al.* 1993; Quillévéré *et al.* 2001; Coxall *et al.*, 2000; 2007). If *Pr. uncinata* is a symbiotic species it would need to inhabit the well lit surface ocean rather than the thermocline, suggesting that the $\delta^{18}O$ values of either *Pr. uncinata* or *S. triangularis* may not be accurate.

Post burial diagenesis and recrystallisation under the influence of cooler deeper waters at the seafloor are often invoked to explain derivations in $\delta^{18}O$ values from the expected (Pearson *et al.*, 2001; Sexton *et al.*, 2006). However, the $\delta^{18}O$ values of the calcite infill are isotopically lower than predicted δw and thus is in the wrong direction for diagenesis and recrystallisation to be the cause. The $\delta^{18}O$ values may reflect diagenesis at higher temperatures during deeper burial (Stüben *et al.*, 2003). However, Tanzania material benefits from relatively shallow burial depths (Pearson *et al.*, 2004). Another possibility is the inclusion of isotopically light meteoric waters (Stüben *et al.*, 2003). Meteoric ground waters are characterized by lower $\delta^{18}O$ values, typically –10 ‰ in low latitudes (Faure, 1986). The close proximity to land of this area suggests that inclusion of some meteoric waters is the most likely cause of the depleted $\delta^{18}O$ values of the sparry infill.

$\delta^{18}O$ planktonic fora
1990; Huber and Sl
discrepancy between
Arthur, 1996; Pearso
the result of digenetic
2006). New records

yield much higher temperature estimates for the tropics that are in line with other proxies and modelling studies (Pearson *et al.*, 2001; Stewart *et al.*, 2004; Pearson *et al.*, 2007; Lear et al., 2008; Pearson *et al.*, 2008).

The clay horizon derived from Site TDP27 provides an important new paleotemperature constraint in the Tanzanian Paleogene temperature curve. The paleotemperature estimates presented here give a SST of between 29.59 and 30.76 °C for planktonic foraminifera biochron P3a. When $\delta^{18}O$ values from this and other Tanzanian studies (Pearson *et al.*, 2001; Pearson *et al.*, 2007) are plotted (Figure 8.12) with the overall Cenozoic deep sea record a correlation can clearly be seen between peaks in deep water temperatures and peaks in Tanzanian SST. The data from this study fall in line with the increasing $\delta^{18}O$ values and decreasing temperatures at the beginning of the Cenozoic, seen in both the deep sea and other Tanzanian SST records. Due to only one early Paleocene sample being collected no specific climatic features associated with the K/Pg boundary can be seen.

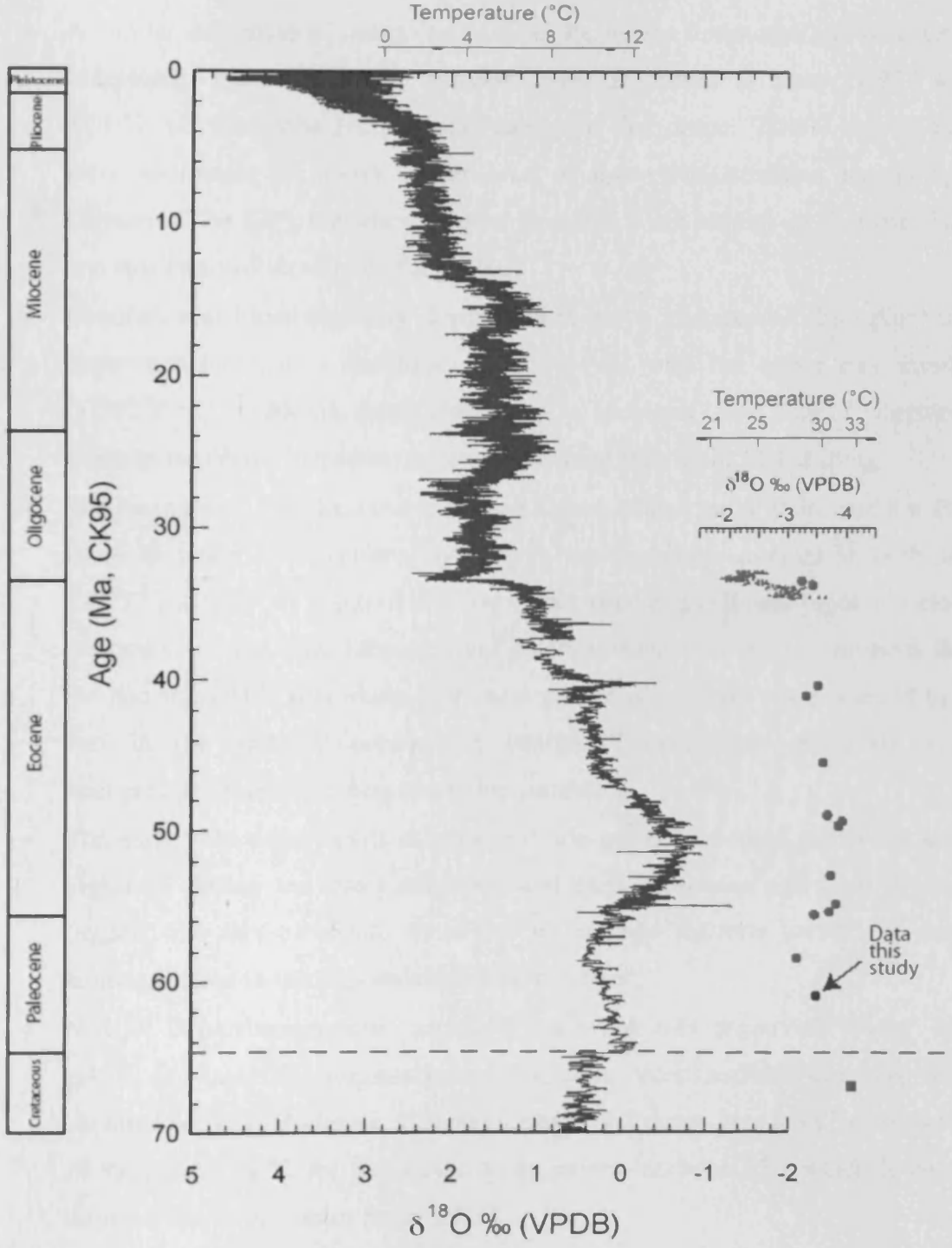

Figure 8.12 – Foraminifera $\delta^{18}O$ values for deep sea based on benthic foraminifera (Blue line) from Cramer *et al.* (2009) corrected to Oridorsalis via method of Katz *et al.* (2003), and sea surface based on planktonic foraminifera from Tanzania red circles from Pearson *et al.*, (2007), red square from Pearson *et al.* (2001), small red triangles from Pearson *et al.*, (2008) and green circle this study. All ages based on the Cande and Kent (1995) age model. For all planktonic foraminifera the lightest $\delta^{18}O$ values from an assemblage are plotted.

8.4. Summary

- A similar sequences of mid to early upper Paleocene limestones and brecciated limestones, with silisiclastic influence were recovered at Sites TDP27 and TDP37, on Kimamba Hill, coastal Tanzania. The deeper TDP37 reveals that these sediments sit above a sequence of upper Maastrichtian hemipelagic claystone. The K/Pg boundary interval therefore is not present on Kimamba Hill and still awaits discovery in Tanzania.
- Foraminiferal biostratigraphy derived from clays interspersed throughout the limestones indicates a biochron range P3-P4b, with the oldest clay sample (TDP27/7/1, 10-20cm) dated close to P3a biochron. Site TDP27, therefore contains the oldest Paleocene interval recovered thus far in TDP drilling.
- The presence of fossilized red and green algae, corals, quartz grains and low P/B ratios in many thin sections taken from the limestone samples in both site TDP27 and TDP37, suggests shallow water deposition, fluvial input and close proximity to land. The lithology and paleoenvironment evidence suggests that the Kimamba Hill area likely represents part of a carbonate shelf boarded by a reef in the early Paleocene. In contrast Maastrichtian sediments were hemipelagic clays indicating outer slop conditions.
- The early Paleocene reef is at odds with the general accepted global sea level highstand during the late Cretaceous and early Paleocene and local geology suggest that this carbonate shelf was an isolated platform created by local faulting related to the regional extension tectonics.
- New $\delta^{18}O$ paleotemperature estimates based on well preserved 'glassy' test calcite of planktonic foraminifera provide the oldest realistic Cenozoic SST obtained so far in Tanzania. Paleotemperature estimates give a SST of between 29.59 and 30.76 °C for planktonic foraminifera biochron P3a, which is just a little warmer than current modern SSTs.

9. Synthesis: Extinctions, Carbon Cycling and Climate

The main aim of this study was to further investigate the geochemical and biological recovery after the K/Pg mass extinction event. To build on the current knowledge and further explore the hypothesis that the long (3 myrs) delay in post K/Pg organic flux recovery, as indicated by reversed or reduced $\delta^{13}C$ gradients, was related to the ecological disruption of the pelagic ecosystem in the Paleocene. This hypothesis coined the 'living ocean model' was proposed by D'Hondt *et al.* (1989), but received opposition from the benthic foraminifera community. The lack of significant extinction among deep-sea benthic foraminifera, which are proposed to rely on surface organic matter for food (Culver, 2003; Alegret and Thomas, 2007, 2009) do not support the hypothesis for reduced organic flux. Further criticism has also been made on existing $\delta^{13}C$ gradient data sets for the K/Pg boundary (Arthur *et al.*, 1987; Zachos and Arthur, 1986; Zachos *et al.*, 1989; D'Hondt *et al.*, 1998), as they do not take into account the changing ecologies and depth habitats of the indicator species used. These possible disequilibrium effects may distort previous interpretations of $\delta^{13}C$ gradients and the duration of carbon pump reductions.

This research first addressed the problems of changing ecology in the early Danian by conducting multispecies size analysis on planktonic foraminifera (Chapter 5). As part of this research modern planktonic foraminifera were also analysed (Chapter 4), as their isotopic signal could be compared with known ecologies and provide analogues for the Paleocene species. This research then produced a new down hole isotope record from Maastrichtian to early Paleocene (~4 myr), from a recently drilled, continues, deep sea K/Pg sequence that benefited from an astronomically calibrated age model (Westerhold *et al.*, 2008). This record represents a development on previous work in that it includes a thermocline *Subbotina* sp., as well as the typical surface and benthic foraminifera used in other studies (Zachos *et al.*, 1989; D'Hondt *et al.*, 1998), which help provide new constraints on early Paleocene nutrient and thermal stratification (Chapter 6).

This synthesis takes a further look at the K/Pg recovery as a whole. First, an assessment of the evolutionary and geochemical recovery will be made to try and establish what drives the carbon system (Section 9.1). Secondly, a look into whether the K/Pg boundary event itself was directly associated with climate change (Section 9.2). Finally, a discussion of possible areas for future work is presented (Section 9.4).

9.1. Biogeochemical and ecological recovery

One question of interest at the start of this project relates to the driving mechanism behind disruptions and eventual recovery of the marine biological pump and the link between geochemical recovery and pelagic evolutionary recovery. The question at the K/Pg boundary is whether recovery of the marine carbon pump led to increased pelagic speciation due to the availability of new ecological niches. Or whether the eventual re-appearance of larger (specialist, e.g. symbiotic) species indicating return of the ecological system and its role in transferring organic matter to the deep sea and therefore playing a role in 'fixing' the marine carbon pump. Another important question is whether the evolution of photosymbiosis allowed the *Morozovella* to diversify.

In the modern ocean planktonic foraminifera with symbionts are at an advantage in clear waters and are able to inhabit low nutrient (oligotrophic) environments that their asymbiotic counterparts cannot. The symbionts provide their host with food, for example *Globigerinoides sacculifer* will only grow to about one third of its normal size if its symbionts are removed (Bé 1982; Bé et al. 1982). Carbon system recovery at Site 1262 appears to occur at ~64.1 Ma, as indicated by a return of a 1 ‰ $\delta^{13}C$ gradient (Chapter 6). This return of the carbon organic flux could indicate restoration of oligotrophic conditions in surface waters, where nutrients are stripped and released at depth. The return of this $\delta^{13}C$ gradient to pre-extinction, and modern, values precedes the origin of photosymbiosis occurring at 63.5 Ma. This suggests that geochemical recovery was needed before this ecological strategy re-evolved and became advantage to planktonic foraminifera. This is in broad agreement with the suggestion that

geochemical recovery was necessary for biological recovery of the photosymbiotic specialists (Coxall *et al.*, 2006).

Despite the return of the $\delta^{13}C$ gradient at ~64.1 Ma and the appearance of photosymbiosis at 63.50 Ma, the morozovellids did not start to diversify until after ~62.2 Ma (Chapter 6 and Chapter 7). The peak of diversification within the *Morozovella* genus occurs at ~61.4 Ma (Chapter 7, Figure 7.6). This coincides with *Morozovella* dominating ~60 % of the assemblage (surface mixed layer symbiotic dwellers are predominantly from the *Morozovella* genus - Chapter 7, Figure 7.8) and a decline in the dominance of thermocline species (Figure 9.1). The other photosymbiotic genera (*Acarinina* and *Igorina*) never diversified at Site 1262 in the period studied. Norris (1996) suggested that evolution of foraminiferal photosymbiosis was a trigger for diversification in this group. However, the data presented here suggests that photosymbiosis originated in *Praemurica*, 1.3 myr before the Morozovellides fully diversified and some other factor may have triggered the radiation. Photosymbiosis had a weaker effect on $\delta^{13}C$ values when it first appeared, reaching maximum values coincident with the diversification of the morozovellides. This would suggest that this ecological strategy hadn't fully developed until this time. Nannofossil assemblage data from the Atlantic (DSDP Site 384 and 528) Pacific (ODP Site 761) and Indian (ODP Site 1209) Oceans, show surface water conditions changed from mesotrophic to oligotrophic at ~62.2 Ma and in parallel with the *Morozovella* diversification at Site 1262 (Fuqua *et al.*, 2008). This suggests that development of oligotrophic conditions provided expanding ecological opportunities for species that harboured photosymbiotic algae, allowing them to exploit pelagic niches characterised by low food availability.

At a similar time to these assemblage changes, bulk $\delta^{13}C$ record appears to stop tracking the *Subbotina* $\delta^{13}C$ record (Figure 9.1). The percent contribution of foraminifera tests over 125 μm reaches ~50 % (dominated by large surface dwellers) and the contribution of the foram fraction to sediment has decreased significantly by this point (Figure 9.1). These sedimentological and bulk $\delta^{13}C$ changes likely represent an increased contribution of nannofossils to bulk $CaCO_3$ content, reflecting development of strong oligotrophic conditions in the S. Atlantic. Only when these oligotrophic conditions

developed did symbiosis become a distinct advantage, which in turn could have led to the diversification within the morozovellid lineage. The combination of these micropaleontological and sedimentological changes around the same time (within ~200 kyr) may indicate a full pelagic ecosystem recovery from the K/Pg boundary event. This would suggest that although the marine carbon pump recovered after 1.58 myr, the extended pelagic ecosystem especially calcareous plankton took far longer (4.28 myr) to recover fully to a pre-extinction state.

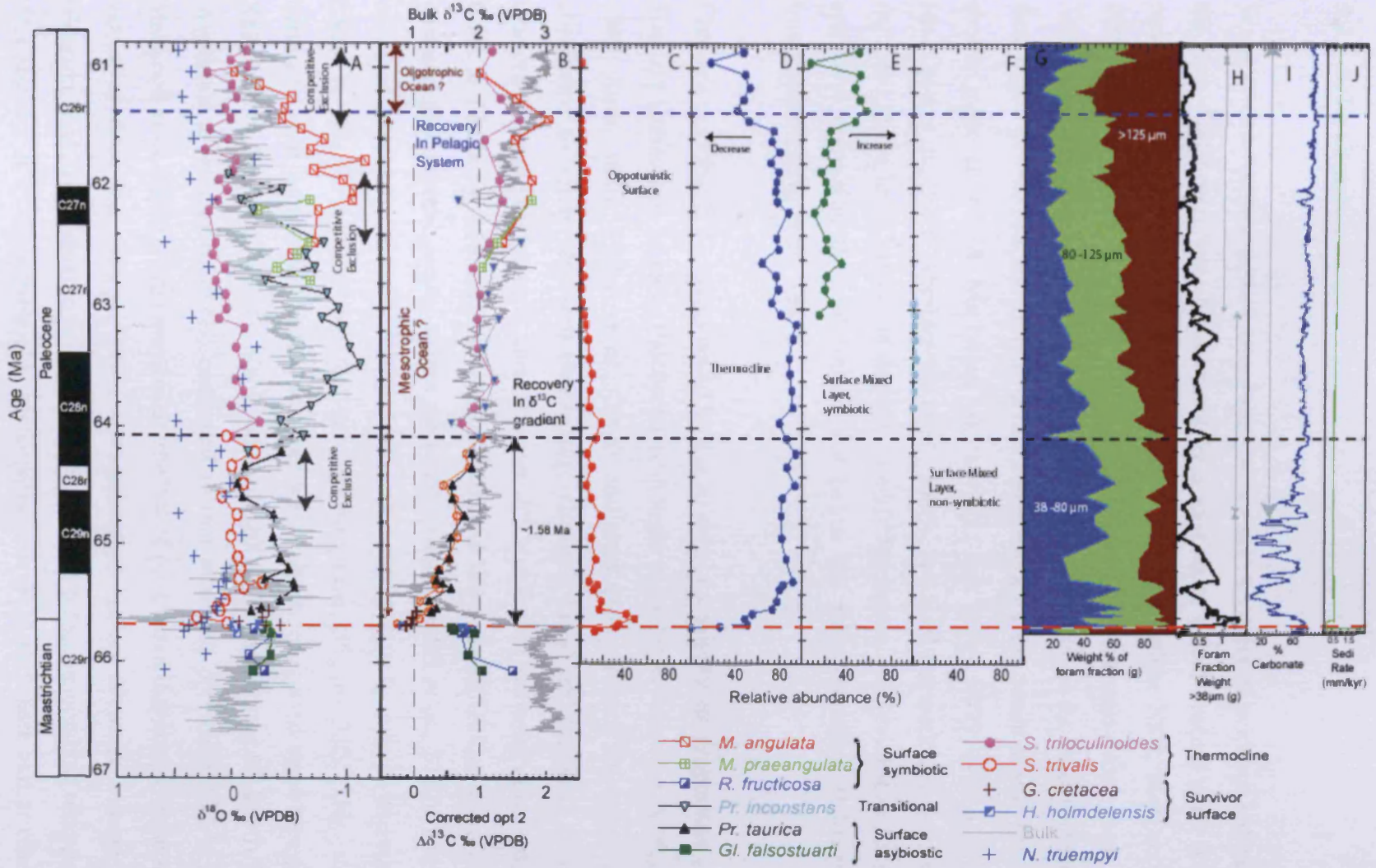

Figure 9.1 – Multiproxy K/Pg data sets from Site 1262. A and B - Stable isotope record from benthic and planktonic foraminifera. C to F - Relative abundance (%) for Paleocene ecological groupings modified from Aze *et al.*, (2011) and isotope analysis from this study (Chapter 5) and Olsson *et al.*, 1999. G to J - Foraminiferal test size distributions, sediment carbonate content and sedimentation rate (kroon *et al.*, 2007). Time scale from Westerhold *et al.* (2008). Red line denotes the K/Pg boundary.

9.2. K/Pg climate

Warm climates characterise most of the Cretaceous. A variety of evidence indicates that the Late Cretaceous was characterised by a long term global cooling trend (D'Hondt and Arthur, 1995; Bralower *et al.*, 2002; D'Hondt and Arthur, 2002; MacLeod *et al.*, 2005; Abramovich *et al.*, 2010). Paleosol pCO_2 levels also decrease (Nordt *et al.*, 2002). This trend was interrupted by two oceanic warming phases in the Maastrichtian. The first began at ~70 Ma and lasted ~2 myr, depending on the ocean basin. The second shorter pulse at ~65.78 Ma lasted ~0.2 Myr (Li and Keller, 1999; Wilf *et al.*, 2003; MacLeod *et al.*, 2005; Abramovich *et al.*, 2010). Sea level fluctuations have also been recorded in the late Cretaceous through to early Paleogene, with evidence of a marked sea level regression that culminated just before the K/Pg boundary, followed by a transgression (Haq *et al.*, 1987).

Changes in global $\delta^{18}O$ values could be due to either ice volume or temperature change. The late Cretaceous to early Paleocene is thought to be largely ice free (Miller *et al.*, 1987; Smit, 1990; Miller *et al.*, 2005) and thus changes in $\delta^{18}O$ values can be considered to solely represent temperature changes. Local and temporal changes in evaporation and precipitation can influence $\delta^{18}O$ values of seawater (Corfield, 1994; Cook and Rohling, 1999; Tindall *et al.*, 2010), but these are difficult to quantify in the past and global homogenous values are usually used (Tindall *et al.*, 2010). The results of mixed planktonic and bulk $\delta^{18}O$ values produced in this study indicate an increase in SSTs in the S. Atlantic for the late Maastrichtian (Figure 9.2). This warming corresponds in time with the second short warm phase recognised elsewhere (Li and Keller, 1999; Wilf *et al.*, 2003; MacLeod *et al.*, 2005; Abramovich *et al.*, 2010), but the magnitude is smaller (0.15 ‰) compared to that measured previously (0.5 – 1.5 ‰, MacLeod *et al.*, 2005). This may be an artefact of post burial diagenesis, because $\delta^{18}O$ values in deep sea sites are often an underrepresentation of water column values (Pearson *et al.*, 2001; Sexton *et al.*, 2006), or differing paleoceanographic settings of the sites studied. A $\delta^{13}C$ increase also accompanies the $\delta^{18}O$ shift here and at other sites (Stott and Kennett, 1989; MacLeod *et al.*, 2005). Nordt *et al.* (2002) related this SST

increase to pCO_2 increases just before the boundary and correlated them with volcanic activity associated with Deccan Trap volcanisum (Officer and Drake, 1985; Courtillot *et al.*, 1988). This would explain the increased $\delta^{18}O$ values, but not the corresponding $\delta^{13}C$ increases, as volcanic activity releases the lighter ^{12}C (Pineau *et al.*, 1976; Weinlich, 2005; Shangguan *et al.*, 2006) and would cause $\delta^{13}C$ values to be reduced and not increased. Instead higher $\delta^{13}C$ values might reflect a temporary increase in deep sea carbon organic burial caused by hypothesised changes in deep water circulation at this time (D'Hondt and Arthur, 2002; MacLeod *et al.*, 2005; MacLeod *et al.*, unpublished).

The climatic backdrop to the K/Pg extinction event was therefore dynamic and the question of whether the K/Pg boundary event itself had direct consequences for climate change is highly debated. Among the proxy records, some indicate cooling whilst others indicate warming (Toon *et al.*, 1982; Covey *et al.*, 1984; Rampino and Volk, 1988; Smit, 1990; Pope *et al.*, 1997; Beerling *et al.*, 2002; Galeotti *et al.*, 2004; Kring, 2007; Jiang *et al.*, 2010; Schulte *et al.*, 2010). The Site 1262 bulk, planktonic and benthic foraminifera data presented here suggests a warming of surface and deep water in the South Atlantic as indicated by $\delta^{18}O$ decreases. However, this appears to be a continuation of a trend started just before the boundary rather than a consequence of the K/Pg boundary event. The Site 1262 data suggest a decrease in thermal stratification in the earliest Paleocene since planktonic and benthic differences are reduced for ~0.6 myr. It is the apparent cooling shown by the surface mixed layer dwelling planktonic foraminifera that are mostly responsible for this reduction, resulting in convergence with thermocline dwellers. Alternatively the convergence could be related to a depth change in one or both species and a move to deeper waters. As mentioned in Chapter 1 the effects of an impact at the K/Pg boundary could have lead to fairly inhospitable conditions in surface waters with proposed increases in acidity (D'Hondt *et al.*, 1994; Schulte *et al.*, 2010) and heavy/trace metals (Jiang *et al.*, 2010), which could have prompted the change in depth habitat. These hostile conditions however, are unlikely to have persisted for as long as 0.6 myr, thus a surface cooling may have occurred after the K/Pg event. This shift to heavier $\delta^{18}O$ values at the K/Pg boundary is seen in other records from the Pacific (DSDP 577, Zachos *et al.*, 1989 and DSDP 465, Boersma and Shackleton, 1979) and Atlantic (DSDP 384, Boersma *et al.*, 1979).

The bulk $\delta^{13}C$ record shows a series of dramatic responses in the early Paleocene not captured in the foraminiferal record. Specifically following a ~1 ‰ decrease at the K/Pg boundary bulk $\delta^{13}C$ continue to decrease to a double minimum of ~0.5 ‰ at ~65.4 and 65.5 Ma (Figure 9.2). This corresponds with a decrease in bulk $\delta^{18}O$ values. One possible explanation for this is that the isotopic excursions represent a shift in nannofossil assemblage composition (reflecting different species with different ecologies and isotopic compositions). This is supported by increased abundances of the dinoflagellate *Thoracosphaera* sp. a dominant component of early Paleocene assemblages (Gardin and Monechi, 1998; Shipboard Scientific Party, 2004; Minoletti *et al.*, 2005; Fornaciari *et al.*, 2007). This genus is known to have extremely light $\delta^{13}C$ values (Minoletti *et al.*, 2005; Thomas, 2007). However, since the excursion is seen in bulk $\delta^{18}O$ values as well as $\delta^{13}C$ and has been reported elsewhere (Quillévéré *et al.*, 2008; Coccioni *et al.*, 2010) it may represent a global oceanographic event. On the Site 1262 timescale, this event is centred around 65.45 Ma with a duration of ~150 kyr, this corresponds closely to the timing of the 'Dan – C2 hyperthermal event' (Quillévéré *et al.*, 2008; Coccioni *et al.*, 2010). Quillévéré *et al.* (2008) suggested this event may be analogous to the Paleocene / Eocene Thermal Maximum (PETM) and other hyperthermal events of the early Paleogene. Day and Maslin (2005) have suggested that the K/Pg asteroid impact may have triggered the release of gas hydrates, which would provide a source of CO_2, as well as isotopically light carbon, to the system. However, the minimum in $\delta^{13}C$ values characteristic of the Dan-C2 event occurs ~0.2 myr after the boundary, whereas an impact induced release of gas hydrates would have occurred instantaneously (Day and Maslin, 2005). The planktonic and benthic $\delta^{13}C$ and $\delta^{18}O$ records presented here do not record the excursion. This may be an artefact of low sampling resolution in this study. A possible explanation for the extreme response in bulk $\delta^{13}C$ and $\delta^{18}O$ values is that bulk $CaCO_3$ contains an increased non-biogenic carbonate (any carbonate particle that does not exhibit biogenic structure, namely calcite microparticles and carbonate macrocrystals) component as the biogenic component is reduced through extinction. These non-biogenic carbonates have very depleted $\delta^{13}C$ and $\delta^{18}O$ values. Elevated concentrations of this non-biogenic component

in the early Danian sediments relative to biogenic carbonate might explain the shift in bulk isotopes (Minoletti *et al.*, 2005).

As the marine carbon pump plays an important role in transporting carbon from the atmosphere to the sediments and thus regulating global climates, understanding how disruptions affect this pump is important. Models have shown that complete cessation of oceanic productivity could lead to global warming of up to 3 °C due to increased pCO_2 levels by a factor of 2 or 3 on the time scale of a few 1,000 years (Caldeira *et al.*, 1988). The flux of organic matter, thus marine carbon pumps, was reduced for ~1.58 myr in this study. However, climate, as recorded by $\delta^{18}O$ values of planktonic foraminifera, increased (~2 °C decrease in surface waters) for a short period of time (~0.6 myr). A reduced organic flux, but a decrease of surface temperatures may indicate that enough export was still occurring (Kump 1991; Ridgwell, unpublished, see Chapter 6 for details). Alternatively, dust and sulphate aerosols, that are proposed to have been released on impact, caused colder conditions (Pope *et al.*, 1997) than the increase in pCO_2 could counter act. Return to pre-extinction temperatures followed quickly by ~0.6 myr after the K/Pg boundary. This quick return may be related to reduced carbon pumping, but as levels do not go much beyond pre-extinction values some other mechanism must be acting to stabilise the system. Though calcareous plankton were severely hit by extinction many other non-calcareous species bloomed (Kitchell *et al.*, 1986; Brinkhuis and Zachariasse, 1988; Gardin and Monechi, 1998; D'Hondt *et al.*, 1998; Bown *et al.*, 2005). These included siliceous diatom and radiolarians (Kitchell *et al.*, 1986; Hollis *et al.*, 1995; MacLeod *et al.*, 1997; Tozzi *et al.*, 2004). In the modern ocean diatoms rather than coccolithophores are suggested to dominate the sequestration of pCO_2 (Cermeño *et al.*, 2008) the increase in diatom abundance after the K/Pg event may have helped to decrease pCO_2 levels under a reduced marine carbon pump system.

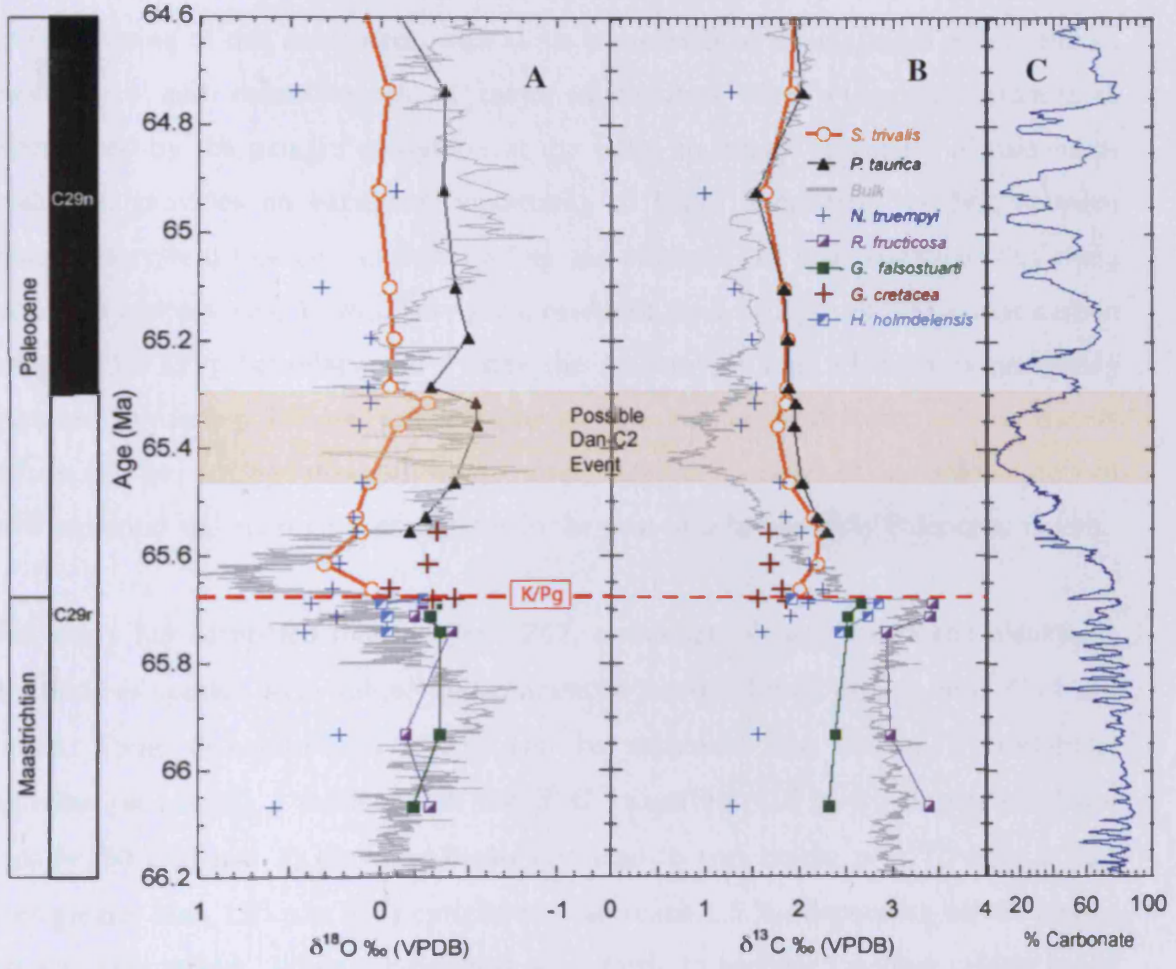

Figure 9.2 – Close up of ODP Site 1262 stable isotope record from benthic and planktonic foraminifera and bulk carbonate. A - $\delta^{18}O$, B - $\delta^{13}C$ both this study and C - % carbonate (Kroon *et al.*, 2007). Time scale of Westerhold *et al.* (2008). Bulk isotope data taken from Kroon *et al.*, (2007). Genera abbreviations as follows Pr = *Praemurica*, S = *Subbotina*, N = *Nuttallides*, R = *Racemiguembelina*, Gl = *Globotruncana*, G = *Guembelitria* and H = *Hedbergella*.

9.3. Conclusions

The pelagic ecosystem is thought to play an important role in regulating global climates by cycling carbon as biomineral skeletons and organic matter between ocean, sediments and atmospheric reservoirs. It's important therefore, to have a detailed understanding of the functioning of this ecosystem, with all its complexity as an integrated ecosystem, its response to and consequences of major disruptions. The widespread extinctions experienced by the pelagic ecosystem at the K/Pg boundary, especially of calcareous producers, provides an excellent opportunity to better understand the link between pelagic ecosystem function, carbon cycling and climate. The main questions this study wanted to address was; 1) was there good evidence for a collapse of the organic carbon pump at the K/Pg boundary and 2) was the recovery as long (3 myr) as previously proposed by carbon isotope gradients or are the geochemical water column tracers influenced by strong disequilibrium vital effects because of a unique set of environmental and ecological conditions in the post catastrophe early Paleocene Ocean.

This study has identified that, at Site 1262, a number of early Paleocene planktonic foraminifera species were subject to pronounced disequilibrium effects on $\delta^{13}C$ of test calcite. These disequilibrium effects can be separated into classes; 1) metabolic fractionation causing a reduction in test $\delta^{13}C$ values by ~0.3 to 0.5 ‰ for small test sizes (<150 μm) and 2) photosymbiosis can lead to enrichment in $\delta^{13}C$ value at test sizes greater than 150 μm. This enrichment can reach 1.5 ‰, depending on the largest test size and species. When adjustments were made to account for these effects in the down hole $\delta^{13}C$ record there appears to be over compensation in some species. This re-affirms the need to take care when interpreting planktonic foraminifera test $\delta^{13}C$ values. Each species needs to be treated separately and test size $\delta^{13}C$ analysis is required for each potential tracer species rather than generalising small and/or symbiotic ecologies.

The K/Pg boundary saw a crash in vertical ocean $\delta^{13}C$ gradients between planktonic and benthic foraminifera, which is interpreted as a break down in the marine carbon pump. Adjustments indicate there was no $\delta^{13}C$ gradient reversal and $\delta^{13}C$ values approximately

average at zero. Initial disruptions of the $\delta^{13}C$ record lasted ~200 kyr. There after the vertical $\delta^{13}C$ gradient gradually expanded until a pre-extinction gradient of 1 ‰ is reached signalling full carbon pump recovery returned at ~64.1 Ma, approximately 1.58 myr after the K/Pg event. This record helps to address the disagreement between the $\delta^{13}C$ record and the benthic foraminifera assemblage records. The lack of extinction in the latter, being interpreted as signalling no significant reduction in organic carbon flux. Despite the lack of no significant extinction benthic foraminifera assemblages fluctuate greatly within this first 200 kyr after the K/Pg, which corresponds to the $\delta^{13}C$ evidence for organic carbon pump suppression and initial $\delta^{13}C$ recovery. In the Site 1262 record this return to pre-extinction conditions occurs earlier than the previously suggested ~3 myr (D'Hondt *et al.*, 1998; Coxall *et al.*, 2006) and does so gradually, rather than in two steps. The proposed 'second stage' of previous studies (D'Hondt *et al.*, 1998; Adams *et al.*, 2004; Coxall *et al.*, 2006) is not supported by the new record. This is likely a consequence of the stratigraphic continuation and much better constrained age model at Site 1262, combined with detailed ecological control of the tracer species that pinpointed where isotopic adjustments were necessary. The occurrence of a $\delta^{13}C$ gradient between thermocline and surface mixed layer planktonic foraminifera appearing at ~63.5 Ma, which coincide with the onset of photosymbiosis. This $\delta^{13}C$ difference between thermocline and surface mixed layer planktonic foraminifera is still present after a photosymbiosis adjustment factor is applied and thus likely represents a real $\delta^{13}C$ signal.

The return of the planktonic – benthic foraminifera $\delta^{13}C$ gradient precedes the onset of photosymbiosis occurring at 63.5 Ma, which suggests that oceanic geochemical recovery was needed before this ecological strategy evolved in the Paleocene. Only once organic carbon pumping was returned and mixed layer nutrient recycling decreased was this ecological strategy advantage to planktonic foraminifera. The delay between the initial appearance of photosymbiosis (63.5 Ma) and substantial diversification of the morozovellids after ~62.2 Ma demonstrate that this ecology does not necessarily lead to diversification. In parallel to the morozovellid diversification, bulk $\delta^{13}C$ records appears to represent a true surface signal, the percent contribution of foraminifera tests over 125 μm reaches ~50 % and the contribution of the foram fraction

to sediment has decreased significantly by this point. These sedimentological, paleontological and bulk $\delta^{13}C$ changes likely reflect the disappearance of mesotrophic conditions and establishment of tropical ocean oligotrophic conditions, of which the calcareous nannoplankton are specialists. Only under these oligotrophic conditions is symbiosis a distinct advantage, which in turn led to the diversification within the *Morozovella* genus. The combination of these sedimentological and assemblage changes may indicate a full pelagic ecosystem recovery from the K/Pg boundary event. This would suggest that although the marine carbon system recovered after 1.58 myr the pelagic ecosystem may have taken far longer (4.28 myr) to fully recover.

9.4. Further work

This thesis provides new insight into the marine pelagic ecosystem and carbon system recovery after the K/Pg boundary. Possible important further work that has been highlighted by the results of this study fall in the following areas:-

- First and foremost repetition of this exercise at other K/Pg boundary sites with high quality records and age control at a variety of paleolatitudes, is needed to confirm the results here as global.

- One goal that this thesis could not meet was production of 'accurate' SST and organic carbon reconstructions across the K/Pg event using 'glassy' foraminifera. Drilling, as discussed in Chapter 8, in Tanzania failed to recover appropriate hemipelagic sediment across the K/Pg event. This is an area where further research from other potential 'glassy' foraminifera bearing sites is required (e.g. Mozambique or offshore Brazil). In addition to foraminiferal paleotemperature proxies other proxies, such as Mg/Ca analysis on planktonic foraminifera (Chave,1954; Barker *et al.*, 2005; Lear *et al.*, 2008) or organic proxies such as Tex 86 (based on the composition of tetraether membrane lipids produced by the aquatic microbe, Crenarchaeota, Schouten et al., 2002) and U_k^{37} (based on the saturation of alkenones from coccolithophores, Prahl and

Wakeham, 1987), could provide further insights into whether any climatic changes occurred as a result of the K/Pg event.

- The possible Dan-C2 event found by Quillévéré *et al.* (2008) was seen in the Site 1262 bulk record (Kroon *et al.*, 2007), but not in the planktonic foraminifera record presented here. Increased sampling of the target interval to increase the resolution of the foraminifera isotope record is a primary goal of future work.

- The $\delta^{18}O$ record shows two instances where the surface mixed layer record is not represented, due to species succession and changing depth habitats of the recorded species. Further isotopic paleoecological work (e.g. *Pr. pseudoinconstans*, *M. apanthesma* and *M. occlusa*) is required to fill these gaps and further improve the record of thermal and nutrient stratification. Such data would also provide a better assessment of the prevalence of ecological 'competitive exclusion' that appears to be occurring within evolutionary lineages throughout the interval studied.

- In addition to the surface (largely symbiotic) record, a surface asymbiotic record would be extremely useful, especially when assessing possible adjustment factors for the symbiotic species. This was not possible at Site 1262, due to the rarity of surface asymbiotic tracers, but maybe this would be possible at other locations.

- The $\delta^{18}O$ and $\delta^{13}C$ record presented reveal an absence of representatives of the sub-thermocline ecogroup in the Paleocene. *Parasubbotina*, a known sub-thermocline genus in the Eocene (Coxall *et al.*, 2003; 2007) do occur in the Site 1262 Paleocene assemblage but with stable isotopes revealing a thermocline habitat similar to *Subbotina* sp. A possible explaination for this is that a weakened organic carbon pump suggested less food below the thermocline, leaving this deep habitat unavailable. Geochemical data to constrain when this important depth ecology emerged would provide further insight into the evolution of Paleocene nutrient stratification.

- After the K/Pg extinction planktonic survivor taxa bloomed (Kitchell *et al.*, 1986; Brinkhuis and Zachariasse, 1988; Gardin and Monechi, 1998; D'Hondt *et al.*, 1998; Bown *et al.*, 2005). Test building planktonic foraminifera have an excellent fossil record. However, there were likely many other opportunistic species across different phytoplankton and zooplankton groups that may have been weakly calcified (Gardin and Monechi, 1998) or not calcified at all, and thus not left a fossil record. This makes assessment of the contribution of these other opportunistic species difficult (Alegret *et al.*, 2003; Alegret and Thomas, 2009). Analysis of biomarkers for these other non calcifying kinds of plankton (Werne *et al.*, 2000; Menzel *et al.*, 2003; Dahl *et al.*, 2004) would help quantify their contribution to primary production. Biomarker analysis requires organic rich sediments, which tend be scarcer further back in geological time. However, where organic rich sediments do occur analysis of the phytoplankton community through biomarkers can be made (e.g. Dumitrescu and Brassell, 2005).

- To help further constrain the mechanisms of carbon flux it may also be possible to use biomarkers as evidence of material being processed through an organisms gut or to analysis the sedimentary fabric and assess the contribution of faecal pellets verses aggregates. However, this type of analysis requires high organic content and undisturbed laminated sediments neither of which is likely in deep sea cores.

10. Bibliography

Abramovich, S., Yovel-Corem, S., Almogi-Labin, A. and Benjamini, C. (2010) Global climate change and planktic foraminiferal response in the Maastrichtian. *Paleoceanography* 25, doi 10.1029/2009pa001843.

Adams, G. C., Lee, D. E. and Rosen, B. R. (1990) Conflicting isotopic and biotic evidence for tropical sea-surface temperatures during the Tertiary. *Palaeogeography, Palaeoclimatology, Palaeoecology* 77 (3-4), 289-313.

Adams, J. B., Mann, W. E. and D'Hondt, S. (2004) The Cretaceous-Tertiary extinction: Modelling carbon flux and ecological response. *Paleoceanography* 19 (1), PA1002, doi: 1010,1029/2002PA000849.

Aguirre, J., Baceta, J. I. and Braga, J. C. (2007) Recovery of marine primary producers after the Cretaceous–Tertiary mass extinction: Paleocene calcareous red algae from the Iberian Peninsula. *Palaeogeography, Palaeoclimatology, Palaeoecology* 249 (3-4), 393-411.

Alegret, L. (2007) Recovery of the deep-sea floor after the Cretaceous-Paleogene boundary event: The benthic foraminiferal record in the Basque-Cantabrian basin and in South-eastern Spain. *Palaeogeography, Palaeoclimatology, Palaeoecology* 255, 181-194.

Alegret, L., Arenillas I, Arz J and E, M. (2004) Foraminiferal event-stratigraphy across the Cretaceous/Paleogene boundary. *N. Jb. Geol. Palaont. Abh* 234 (1-3), 25-50.

Alegret, L., Molina, E. and Thomas, E. (2001) Benthic foraminifera at the Cretaceous-Tertiary boundary around the Gulf of Mexico. *Geology* 29, 891-894.

Alegret, L., Molina, E. and Thomas, E. (2003) Benthic foraminiferal turnover across the Cretaceous/Paleogene boundary at Agost (southeathern Spain): paleoenvironmental inferences. *Marine Micropaleontology* 48, 251-279.

Alegret, L. and Thomas, E. (2004) Benthic foraminifera and environmental turnover across the Cretaceous/Paleogene boundary at Blake Nose (ODP Hole 1049C, Northwestern Atlantic). *Palaeogeography, Palaeoclimatology, Palaeoecology* 208 (1-2), 59-83.

Alegret, L. and Thomas, E. (2005) Cretaceous/Paleogene boundary bathyal paleo-environments in the central North Pacific (DSDP Site 465), the Northwestern Atlantic (ODP Site 1049), the Gulf of Mexico and the Tethys: The benthic foraminiferal record. *Palaeogeography, Palaeoclimatology, Palaeoecology* 224 (1-3), 53-82.

Alegret, L. and Thomas, E. (2007) Deep sea environments across the Cretaceous/Paleogene boundary in the eastern South Atlantic Ocean (ODP Leg 208, Walvis Ridge). *Marine Micropaleontology* 64, 1-17.

Alegret, L. and Thomas, E. (2009) Food supply to the seafloor in the Pacific Ocean after the Cretaceous/Paleogene boundary event. *Marine Micropaleontology* 73 (1-2), 105-116.

Ali, J. R. and Huber, M. (2010) Mammalian biodiversity on Madagascar controlled by ocean currents. *Nature* 463 (7281), 653-680.

Alldredge, A. L. and Silver, M. W. (1988) Characteristics, Dynamics and Significance of Marine Snow. *Progress In Oceanography* 20 (1), 41-82.

Al-Sabouni, N., Kucera, M. and Schmidt, D. N. (2007) Vertical niche separation control of diversity and size disparity in planktonic foraminifera. *Marine Micropaleontology* 63 (1-2), 75-90.

Alvarez, L. W., Alvarez, W., Asaro, F. and Michel, H. V. (1980) Extraterrestrial cause of the Cretaceous-Tertiary extinction. *Science* 208, 1095-1108.

Anand, P., Elderfield, H. and Conte, M. H. (2003) Calibration of Mg/Ca thermometry in planktonic foraminifera from a sediment trap time series. *Paleoceanography* 18 (2), doi:10.1029/2002kpa000846

Anderson, O. R., Spindler, M., Bé, A. W. H. and Hemleben, C. (1979) Trophic activity of planktonic foraminifera. *Journal of the Marine Biological Association of the United Kingdom* 59 (03), 791-799.

Antoine, D., André, J.-M. and Morel, A. (1996) Oceanic primary production: 2. Estimation at global scale from satellite (Coastal Zone Color Scanner) chlorophyll. *Global Biogeochem. Cycles* 10 (1), 57-69.

Armstrong, H. A. and Brasier, M. D. (2005) Microfossils second edition. Blackwell Publishing.

Armstrong, R. A., Lee, C., Hedges, J. I., Honjo, S. and Wakeham, S. G. (2002) A new, mechanistic model for organic carbon fluxes in the ocean based on the quantitative association of POC with ballast minerals. *Deep-Sea Research Part II -Topical Studies in Oceanography* 49 (1-3), 219-236.

Arthur, M. A., Zachos, J. C. and Jones, D. S. (1987) Primary productivity and the Cretaceous/Tertiary boundary event in the oceans. *Cretaceous Research* 8, 43-45.

Aurahs, R., Grimm, G. W., Hemleben, V., Hemleben, C. and Kucera, M. (2009) Geographical distribution of cryptic genetic types in the planktonic foraminifer Globigerinoides ruber. *Molecular Ecology* 18 (8), 1692-1706.

Azam, F. (1998) Microbial Control of Oceanic Carbon Flux: The Plot Thickens. *Science* 280 (5364), 694-696.

Azam, F., Fenchel, T., Field, J. G., Gray, J. S., Meyerreil, L. A. and Thingstad, F. (1983) The Ecological Role of Water-Column Microbes in the Sea. *Marine Ecology-Progress Series* 10 (3), 257-263.

Aze, T., Ezard, T. H. G., Purvis, A., Coxall, H. K., Stewart, D. R. M., Wade, B. S. and Pearson, P. N. (2011) A phylogeny of Cenozoic macroperforate planktonic foraminifera from fossil data. *Biological Reviews* doi: 10.1111/j.1469-1185X.2011.00178.x.

Barker, S., Cacho, I., Benway, H. and Tachikawa, K. (2005) Planktonic foraminiferal Mg/Ca as a proxy for past oceanic temperatures: a methodological overview and data compilation for the Last Glacial Maximum. *Quaternary Science Reviews* 24 (7-9), 821-834.

Baron-Szabo, R. C. (2006) Corals of the K/T-boundary: Scleractinian corals of the suborders Astrocoeniina, Faviina, Rhipidogyrina and Amphiastraeina. *Journal of Systematic Palaeontology* 4 (1), 1-108.

Barron, E. J. and Peterson, W. H. (1991) The Cenozoic Ocean Circulation Based on Ocean General-Circulation Model Results. *Palaeogeography Palaeoclimatology Palaeoecology* 83 (1-3), 1-28.

Be, A. W. H. (1960) Ecology of recent planktonic foraminifera: Part 2. Bathymetric and seasonal distributions in the Sargasso-Sea off Bermuda. *Micropaleontology* 6, 373-392.

Bé, A. W. H. (1982) Biology of planktonic foraminifera. In: Buzas, M. A., Sen Gupta, B. K. and Broadhead, T. W. (eds.) *Foraminifera, notes for a short course.* Knoxville: University of Tennesee.

Bé, A. W. H., Hemleben, C., Anderson, O. R., Spindler, M., Hacunda, J. and Tuntivate-Choy, S. (1977) Laboratory and field observations of living planktonic foraminifera. *Micropaleontology* 23 155-179.

Bé, A. W. H., Spero, H. J. and Anderson, O. R. (1982) Effects of symbiont elimination and reinfection on the life processes of planktonic foraminifer *Globigerineiodes sacculifer. Marine Biology* 70, 73-86.

Be, A. W. H. and Tolderlund, D. S. (1971) Distribution and ecology of living planktonic foraminifera in surface waters of the Atlantic and Indian Oceans. In: Funnel, B. M. and Riedel, W. R. (eds.) *The Micropaleontology of Oceans.*

Beerling, D. J., Lomax, B. H., Royer, D. L., Upchurch, G. R. and Kump, L. R. (2002) An atmospheric pCO2 reconstruction across the Cretaceous-Tertiary boundary from leaf megafossils. *Proceedings of the National Academy of Sciences of the United States of America* 99 (12), 7836-7840.

Bemis, B. E., Spero, H. J. and Thunell, R. C. (2002) Using species-specific paleotemperature equations with foraminifera: a case study in the Southern California Bight. *Marine Micropaleontology* 46 (3-4), 405-430.

Berger, W. (1969) Planktonic Foraminifera: Basic Morphology and Ecologic Implications. *Journal of Paleontology* 43 (6), 1369-1383.

Berger, W., Fischer, K., Lai, C. and Wu, G. (1988) Ocean carbon flux: global maps of primary production and export production. In: Agegian, C. R. (ed.) *Biogeochemical Cycling and Fluxes Between the Deep Euphotic Zone and Other Oceanic Realms.* Vol. 88-1. NOAA National Undersea Research Program, Research Report.

Berger, W. and Vincent, E. (1986) Deep-sea carbonates: Reading the carbon-isotope signal. *Geologische Rundschau* 75 (1), 249-269.

Berger, W. H., Killingley, J. S. and Vincent, E. (1978) Stable Isotopes in Deep-Sea Carbonates - Box Core Erdc-92, West Equatorial Pacific. *Oceanologica Acta* 1 (2), 203-216.

Berggren, W. A., Kent, D. V., Swisher, C. C. and Aubry, M.-P. (1995) A revised Cenozoic geochronology and chronostratigraphy. . In: W.A.Berggren, Kent, D. V., Aubry, M.-P. and Hardenbol, J. (eds.) *Geochronology, Time Scales and stratigraphic correlation. SEPM. Special publication.* Vol. 54.

Berggren, W. A. and Pearson, P. N. (2005) A revised tropical to subtropical Paleogene plnaktonic foraminifera zonation. *Journal of Foraminiferal Research* 35 (4), 279-298.

Bermudez, P. J. (1960) Foraminifcros planctonicos del Golfo de Venezuela: *Mem. Soc. Cicncias Nat. La Salle* 20, 58-76.

Bernaola, G. and Monechi, S. (2007) Calcareous nannofossil extinction and survivorship across the Cretaceous – Paleogene boundary at Walvis Ridge (ODP Hole 1262C, South Atlantic Ocean). *Palaeogeography, Palaeoclimatology, Palaeoecology* 255 (1-2), 132-156.

Bice, K. L. and Marotzke, J. (2001) Numerical evidence against reversed thermohaline circulation in the warm Paleocene/Eocene Ocean. *J. Geophys. Res.* 106 (C6), 11529-11542.

Bickert, T. and Wefer, G. (1999) South Atlantic and benthic foraminifer [delta]13C deviations: implications for reconstructing the Late Quaternary deep-water circulation. *Deep Sea Research Part II: Topical Studies in Oceanography* 46 (1-2), 437-452.

Bickert, T. and Wefer, G. (1999) South Atlantic and benthic foraminifer [delta]13C deviations: implications for reconstructing the Late Quaternary deep-water circulation. *Deep Sea Research Part II: Topical Studies in Oceanography* 46 (1-2), 437-452.

Bijma, J., Erez, J. and Hemleben, C. (1990) Lunar and semi-lunar reproductive cycles in some spinose planktonic foraminifers. *Journal of Foraminiferal Research* 20 (2), 117-127.

Bijma, J., Hemleben, C., Huber, B. T., Erlenkeuser, H. and Kroon, D. (1998) Experimental determination of the ontogenetic stable isotope variability in two morphotypes of *Globigerinella siphonifera* (d'Orbigny). *Marine Micropaleontology* 35 (3-4), 141-160.

Bijma, J., Hemleben, C. and Wellnitz, K. (1994) Lunar-influenced carbonate flux of the planktic foraminifer *Globigerinoides sacculifer* (Brady) from the central Red Sea. *Deep Sea Research Part I: Oceanographic Research Papers* 41 (3), 511-530.

Bijma, J., Spero, H. J. and Lea, D. W. (1999) Reassessing foraminiferal stable isotope geochemistry: Impact of the oceanic carbonate system. In: Fischer, G. and Wefer, G. (eds.) *Use of Proxies in Paleoceanography: Examples from the South Atlantic.* Springer-Verlag, Heidelberg.

Blow, W. H. (1979) *The Cainozoic Globigerinida: A Study of the Morphology, Taxonomy and Evolutionary Relationships and the Stratigraphical Distribution of Some Globigerinida (mainly Globigerinacea).* Leiden:

Blow, W. H. and Banner, F. T. (1962) The Mid-Tertiary (Upper Eocene to Aquitanian) Globigerinacea. In: Eames, F. T. (ed.) *Fundamentals of Mid-Tertiary Stratigraphic Correlation.* London Cambridge University Press.

Boersma, A. (1984) Cretaceous-Tertiary planktonic foraminifers from the southeastern Atlantic, Walvis Ridge Area, Deep Sea drilling Project Leg 74. In: Moore, T. C., Jr., Rabinowitz, P.D. et al. (ed.) *Initial Reports of the DSDP, 74.* Washington: U.S. Govt. Printing Office.

Boersma, A. and Premoli Silva, J. (1983) Paleocene planktonic foraminiferal biogeography and the paleoceanography of the Atlantic Ocean. . *Micropaleontology* 29, 355-381

Boersma, A., Shackleton, N., Hall, M. and Given, Q. (1979) Carbon and Oxygen isotope records at DSDP Site 384 (North Atlantic) and some Paleocene Paleotemperatures and carbon isotope variations in the Atlantic Ocean. In: Tucholke, B. E., Vogt, P. R., Murdmaa, I. O., Rothe, P., Houghton, R. L., Galehouse, J. S., Kaneps, A., McNulty, J. C. L., Okada, H., Kendrick, J. W., Demars, K. R. and McCave, I. N. (eds.) *Initial Reports of the Deep Sea Drilling Project,*. Vol. 43. Washington (U.S. Government Printing Office).

Boersma, A. and Shackleton, N. J. (1979) Oxygen and carbon isotope variations and planktonic foraminifer depth habitats, Late Cretaceous to Paleocene, Central Pacific, Deep Sea drilling project sites 463 and 465. *Initial Reports of the Deep Sea Drilling Project* 62, 513-526.

Bolli, H. M. (1957) The Genera *Globigerina* and *Globorotalia* in the Paleocene-Lower Eocene Lizard Springs Formation of Trinidad, B.W.I. In: Loeblich, A. R. J. and Collaborators (eds.) *Studies in Foraminifera.* Vol. 215. Bulletin of the United States National Museum.

Bolli, H. M., Saunders, J. B. and Perch-nielsen, K. (1985) *Plankton Stratigraphy* Cambridge Earth Science Series.

Bornhardt, W. (1900) *Zur Oberflächengestaltung und Geologie Deutsch-Ostafrikas. Deutsch-Ostafrika 7, Dietrich Reimer.* Berlin.

Bourget, J., Zaragosi, S., Garlan, T., Gabelotaud, I., Guyomard, P., Dennielou, B., Ellouz-Zimmermann, N. and Schneider, J. L. (2008) Discovery of a giant deep-sea valley in the Indian Ocean, off eastern Africa: The Tanzania channel. *Marine Geology* 255 (3-4), 179-185.

Bouvier-Soumagnac, Y. and Duplessy, J.-C. (1985) Carbon and oxygen isotopic composition of planktonic foraminifera from laboratory culture, plankton tows and recent sediment; implications for the reconstruction of paleoclimatic conditions and of the global carbon cycle. *Journal of Foraminiferal Research* 15 (4), 302-320.

Bowen, G. J., Beerling, D. J., Koch, P. L., Zachos, J. C. and Quattlebaum, T. (2004) A humid climate state during the Palaeocene/Eocene thermal maximum. *Nature* 432 (7016), 495-499.

Bown, P. (2005) Selective calcareous nannoplankton survivorship at the Cretaceous - Tertiary boundary. *Geology* 33 (8), 653-656.

Bown, P. and Pearson, P. (2009) Calcareous plankton evolution and the Paleocene/Eocene thermal maximum event: New evidence from Tanzania. *Marine Micropaleontology* 71 (1-2), 60-70.

Bown, P. R., Dunkley Jones, T., Lees, J. A., Randell, R. D., Mizzi, J. A., Pearson, P. N., Coxall, H. K., Young, J. R., Nicholas, C. J., Karega, A., Singano, J. and Wade, B. S. (2008) A Paleogene calcareous microfossil Konservat-Lagerstatte from the Kilwa Group of coastal Tanzania. *Geological Society of America Bulletin* 120 (1-2), 3-12.

Bown, P. R., Lees, J. A. and Young, J. R. (2004) Calcareous nannoplankton evolution and diversity through time. In: Thierstein, H. and Young, J. (eds.) *Coccolithophores: From Molecular Processes to Global Impact.* Berlin: Springer - Verlag.

Bradshaw, J. S. (1959) Ecology of living planktonic foraminifera in the North and Equatorial Pacific Ocean. *Cuchman Found. Foram. Res. Coutr.* 10, 25-64.

Brady, H. B. (1877) Supplementary note on the foraminifera of the chalk (?) of the New Britain Group. *Geol. Mag* 2 (4), 534-546.

Brady, H. B. (1882) Report on the foraminifera. In: Tizard and Murray, J. (eds.) *Exploration of lhe Faroe Channel, during the summer of 1880, in H.M.S. Knighl Errant, with subsidiary reports.*, Vol. 11. Roy. Soc. Edinburgh, Proc.

Bralower, T., Eccles, L., Kutz, J., Yancey, T., Schueth, J., Arthur, M. and Bice, D. (2010) Grain size of Cretaceous-Paleogene boundary sediments from Chicxulub to the open ocean: Implications for interpretation of the mass extinction event. *Geology* 38 (3), 199-202.

Bralower, T. J., Silva, I. P. and Malone, M. J. (2002) New evidence for abrupt climate change in the Cretaceous and Paleogene: An Ocean Drilling Program expedition to Shatsky Rise, northwest Pacific. *GSA Today* 12 (11), 4-10.

Bralower, T. J., Zachos, J. C., Thomas, E., Parrow, M., Paull, C. K., Kelly, D. C., Silva, I. P., Sliter, W. V. and Lohmann, K. C. (1995) Late Paleocene to Eocene Paleoceanography of the Equatorial Pacific Ocean: Stable Isotopes Recorded at Ocean Drilling Program Site 865, Allison Guyot. *Paleoceanography* 10 (4), 841-865.

Brass, G. W., Southam, J. R. and Peterson, W. H. (1982) Warm Saline Bottom Water in the Ancient Ocean. *Nature* 296 (5858), 620-623.

Brinkhuis, H. and Zachariasse, W. J. (1988) Dinoflagellate Cysts, Sea-Level Changes and Planktonic Foraminifers across the Cretaceous Tertiary Boundary at El Haria, Northwest Tunisia. *Marine Micropaleontology* 13 (2), 153-191.

Broecker, W. S. (1982) Glacial to interglacial changes in ocean chemistry. *Progress In Oceanography* 11 (2), 151-197.

Broecker, W. S. and Maier-Reimer, E. (1992) The influence of air and sea exchange on the carbon isotope distribution in the sea. *Global Biogeochemical Cycles* 6 (3), 315-320.

Broeker, W. S. and Peng, T.-H. (1982) *Tracers in the sea.* Palisades, New York: Lamont-Doherty Geological Oservatory, Colombia University.

Brösing, A. (2008) A reconstruction of an evolutionary scenario for the Brachyura (Decopoda) in the context of the Cretaceous- Tertiary boundary. *Crustaceana* 81 (3), 271-287.

Brummer, G. J. A., Hemleben, C. and Spindler, M. (1987) Ontogeny of Extant Spinose Planktonic-Foraminifera (Globigerinidae): A Concept Exemplified by *Globigerinoides sacculifer* (Brady) and *G. ruber* (D'orbigny). *Marine Micropaleontology* 12 (4), 357-381.

Buffetaut, E. (1990) Vertebrate extinctions and survival across the Cretaceous-Tertiary boundary. *Tectonophysics* 171 (1-4), 337-345.

Buzas, M. A. (1990) Another Look at Confidence-Limits for Species Proportions. *Journal of Paleontology* 64 (5), 842-843.

Buzas, M. A. and SenGupta, B. K. (1982) *Foraminifera: Notes for a short course.* University of Tennessee, Department of Geological Sciences

Caldeira, K. and Rampino, M. R. (1993) Aftermath of the End-Cretaceous Mass Extinction - Possible Biogeochemical Stabilization of the Carbon-Cycle and Climate. *Paleoceanography* 8 (4), 515-525.

Caldeira, K. G., Rampino, M. R. and Zachos, J. C. (1988) Atmospheric CO2 and the K/T Boundary. *Eos* 69, 377.

Cande, S. C. and Kent, D. V. (1995) Revised Calibration of the Geomagnetic Polarity Timescale for the Late Cretaceous and Cenozoic. *Journal of Geophysical Research-Solid Earth* 100 (B4), 6093-6095.

Canudo, J. I., Keller, G. and Molina, E. (1991) Cretaceous/Tertiary boundary extinction pattern and faunal turnover at Agost and Caravaca, S. E. Spain. *Marine Micropaleontology* 17, 319-341.

Cermeño, P., Dutkiewicz, S., Harris, R. P., Follows, M., Schofield, O. and Falkowski, P. G. (2008) The role of nutricline depth in regulating the ocean carbon cycle. *Proceedings of the National Academy of Sciences* 105 (51), 20344-20349.

Chave, K. E. (1954) Aspects of the Biogeochemistry of Magnesium .1. Calcareous Marine Organisms. *Journal of Geology* 62 (3), 266-283.

Chen, C. A. (1994) Vertical Distributions of pH and Fluorescence in the Western Tropical Indian Ocean-the INDIGO 2 Expedition. *Terrestrial, Atmospheric and Ocean Sciences* 5 (1), 77-89.

Chisholm, S. W. (2000) Oceanography - Stirring times in the Southern Ocean. *Nature* 407 (6805), 685-687.

Cifelli, R. (1969) Radiation of Cenozoic Foraminifera. *Systematic Zoology* 18, 154-168.

Clements, F. E. (1916) *Plant succession.* Carnegie Institute: Washington Pub.

Coccioni, R., Frontalini, F., Bancalà, G., Fornaciari, E., Jovane, L. and Sprovieri, M. (2010) The Dan-C2 hyperthermal event at Gubbio (Italy): Global implications, environmental effects, and cause(s). *Earth and Planetary Science Letters* 297 (1-2), 298-305.

Coccioni, R. and Marsili, A. (2007) The response of benthic foraminifer to the K-Pg boundary biotic crisis at Elles (northwestern Tunisia). *Palaeogeography, Palaeoclimatology, Palaeoecology* 255, 157-180.

Colling, A. (2001) *Ocean Circulation.* Open University.

Connell, J. H. and Slatyer, R. O. (1977) Mechanisms of Succession in Natural Communities and Their Role in Community Stability and Organization. *The American Naturalist* 111 (982), 1119-1144.

Cooke, S. and Rohling, E. (1999) Stable oxygen and carbon isotopes in foraminiferal carbonate shells. In: Barum, K. and Gupta, S. (eds.) *Modern foraminifera.* Kluwer Academic.

Corfield, R. M. (1994) Palaeocene oceans and climate: An isotopic perspective. *Earth-Science Reviews* 37 (3-4), 225-252.

Corfield, R. M. and Cartlidge, J. E. (1991) Isotopic evidence for the depth stratification of fossil and recent Globigerinina: A review. *Historical Biology* 5, 37-63.

Corfield, R. M. and Cartlidge, J. E. (1992) Oceanographic and Climatic Implications of the Paleocene Carbon Isotope Maximum. *Terra Nova* 4 (4), 443-455.

Corfield, R. M., Hall, M. A. and Brasier, M. D. (1990) Stable isotope evidence for foraminiferal habitats during the during of the Cenomanian/Turonian ocean anoxic event. *Geology* 18 (2), 175-178.

Corfield, R. M. and Norris, R. D. (1996) Deep water circulation in the Paleocene ocean. In: Knox, R. W. O. B., Corfield, R. M. and Dunay, R. E. (eds.) *Geological Society Special Publications.* Vol. 101.

Courtillot, V., Féraud, G., Maluski, H., Vandamme, D., Moreau, M. G. and Besse, J. (1988) Deccan flood basalts and the Cretaceous/Tertiary boundary. *Nature* 333, 843-846.

Covey, C., Schneider, S. H. and Thompson, S. L. (1984) Global Atmospheric Effects of Massive Smoke Injections from a Nuclear-War - Results from General-Circulation Model Simulations. *Nature* 308 (5954), 21-25.

Coxall, H. K., D'Hondt, S. and Zachos, J. C. (2006) Pelagic evolution and environmental recovery after the Cretaceous-Paleogene mass extinction. *Geology* 34 (4), 297-300.

Coxall, H. K., Huber, B. T. and Pearson, P. N. (2003) Origin and morphology of the Eocene planktonic foraminifera *Hantkenina. Journal of Foraminiferal Research* 33 (3), 237-261.

Coxall, H. K., Pearson, P. N., Shackleton, N. J. and Hall, M. A. (2000) Hantkeninid depth adaptation: An evolving life strategy in a changing ocean. *Geology* 28 (1), 87-90.

Coxall, H. K., Wilson, P. A., Pearson, P. N. and Sexton, P. F. (2007) Iterative evolution of digitate planktonic foraminifera. *Paleobiology* 33 (4), 495-516.

Cramer, B. S., Toggweiler, J. R., Wright, J. D., Katz, M. E. and Miller, K. G. (2009) Ocean overturning since the Late Cretaceous: Inferences from a new benthic

foraminiferal isotope compilation. *Paleoceanography* AGU. p. PA4216, doi: 4210.1029/2008pa001683

Crowley, T. J. and Zachos, J. C. (2000) Comparison of zonal temperature profiles for past warm time periods. In: Huber, B. T., MacLeod and Wing, S. L. (eds.) *Warm Climates in Earths History.*

Culver, S. J. (2003) Benthic foraminifera across the Cretaceous-Tertiary (K-T) boundary: a review. *Marine Micropaleontology* 47, 177-226.

Dahl, K. A., Repeta, D. J. and Goericke, R. (2004) Reconstructing the phytoplankton community of the Cariaco Basin during the Younger Dryas cold event using chlorin steryl esters. *Paleoceanography* 19 (1), PA1006, doi:1010.1029/2003pa000907

Darling, K. F., Thomas, E., Kasemann, S. A., Seears, H. A., Smart, C. W. and Wade, C. M. (2009) Surviving mass extinction by bridging the benthic/planktic divide. *Proceedings of the National Academy of Sciences* 106 (31), 12629-12633.

Day, S. and Maslin, M. (2005) Linking large impacts, gas hydrates, and carbon isotope excursions through widespread sediment liquefaction and continental slope failure: The example of the K-T boundary event. *Geological Society of America Special Papers* 384, 239-258.

Dekens, P. S., Lea, D. W., Pak, D. K. and Spero, H. J. (2002) Core top calibration of Mg/Ca in tropical foraminifera: Refining paleotemperature estimation. *Geochem. Geophys. Geosyst.* 3 (4), 1022.

Dennison, J. M. and Hay, W. W. (1967) Estimating the needed sampling area for subaquatic ecologic studies. *Journal of Paleontology* 41 (3), 706-708.

D'Hondt, S. (1991) Phylogenetic and stratigraphic analysis of earliest Paleocene biserial and triserial planktonic foraminifera. *Journal of Foraminiferal Research* 21 (2), 168-181.

D'Hondt, S. (1994a) The evidence for a meteorite impact at the Creataceous/Tertiary boundary. In: Molina, E. (ed.) *Extinction and the Fossil Record.* Seminario Interdisciplinar de la Universidad de Zaragoza (SIUZ).

D'Hondt, S. (2005) Consequences of the Cretaceous/Paleogene Mass Extinction for Marine Ecosystems. *Annual Reviews of Ecology, Evolution and Systematics* 36, 295-317.

D'Hondt, S. and Arthur, M. A. (1995) Interspecies Variation in Stable Isotopic Signals of Maastrichtian Planktonic Foraminifera. *Paleoceanography* 10 (1), 123-135.

D'Hondt, S. and Arthur, M. A. (1996) Late Cretaceous Oceans and the Cool Tropic Paradox. *Science* 271 (5257), 1838-1841.

D'Hondt, S. and Arthur, M. A. (2002) Deep water in the late Maastrichtian ocean. *Paleoceanography* 17 doi:10.1029/1999PA000486.

D'Hondt, S., Donaghay, P., Zachos, J. C., Luttenberg, D. and Lindinger, M. (1998) Organic carbon fluxes and ecological recovery from the Cretaceous-Tertiary mass extinctio. *Science* 282 (5387), 276-279.

D'Hondt, S. and Keller, G. (1991) Some patterns of planktic foraminiferal assemblage turnover at the Cretaceous-Tertiary boundary. *Marine Micropaleontology* 17 (1-2), 77-118.

D'Hondt, S., Pilson, M. E. Q., Sigurdsson, H., Hanson, A. K. and Carey, S. (1994c) Surface-Water Acidification and Extinction at the Cretaceous-Tertiary Boundary. *Geology* 22 (11), 983-986.

D'Hondt, S., Timothy, H. D., King, J. and Gibson, C. (1996) Planktic foraminifera, asteroids and marine production: Death and recovery at the Cretaceous-Teriary boundary. In: Ryder, G., Fastovsky, D. and Gartner, S. (eds.) *The Cretaceous-Tertiary Event and Other Catastrophes in Earth History*. Vol. 307. Boulder, Colorado: Geological Society of America Special Paper.

D'Hondt, S. and Zachos, J. C. (1993) On stable isotopic variation and earliest Paleocene planktonic foraminifera. *Paleoceanography* 8, 527-547.

D'Hondt, S. and Zachos, J. C. (1998) Cretaceous foraminifera and the evolutionary history of planktic photosymbiosis. *Palaeobiology* 24 (4), 512-523.

D'Hondt, S., Zachos, J. C. and Schultz, G. (1994b) Stable isotopic signals and photosymbiosis in late Paleocene planktic foraminifera. *Paleobiology* 20 (3), 391-406.

Dickens, G. R., O'Neil, J. R., Rea, D. K. and Owen, R. M. (1995) Dissociation of Oceanic Methane Hydrate as a Cause of the Carbon Isotope Excursion at the End of the Paleocene. *Paleoceanography* 10 (6), 965-971.

d'Orbigny, A. D. (1826) Tableau mdlhodiquc dc la classe des Cdphalopodes. *Ann. Sci. Nat.* 7, 245-314.

d'Orbigny, A. D. (1839) Foraminifdres des lies Canaries. In: Barker-Webb, P. and Berthelot, S. (eds.) *Histoire naturelle des lies Canaries 2, pt.2, Zool, Paris.*

Douglas, R. G. and Savin, S. M. (1978) Oxygen Isotopic Evidence for Depth Stratification of Tertiary and Cretaceous Planktic Foraminifera. *Marine Micropaleontology* 3 (2), 175-196.

Dumitrescu, M. and Brassell, S. C. (2005) Biogeochemical assessment of sources of organic matter and paleoproductivity during the early Aptian Oceanic Anoxic Event at Shatsky Rise, ODP Leg 198. *Organic Geochemistry* 36 (7), 1002-1022.

Duncan, R. A. and Pyle, D. G. (1988) Rapid eruption of the Deccan flood basalts at the Cretaceous/Tertiary boundary. *Nature* 333, 841-843.

Duplessy, J. C., Labeyrie, L., Juilletleclerc, A., Maitre, F., Duprat, J. and Sarnthein, M. (1991) Surface Salinity Reconstruction of the North-Atlantic Ocean during the Last Glacial Maximum. *Oceanologica Acta* 14 (4), 311-324.

Egger, J. G. (1893) Foraminifercn aus Meercsgrundproben, gelothet von 1874 bis 1876 von S.M.Seh. Gazelle. *K. Buyer, Akad. Wiss. Munchcn, M.-Ph. Cl, Abh* 2, 193-458.

Elderfield, H., Vautravers, M. and Cooper, M. (2002) The relationship between shell size and Mg/Ca, Sr/Ca, delta O-18, and delta C-13 of species of planktonic foraminifera. *Geochemistry Geophysics Geosystems* 3, doi: 10.1029/2001GC000194.

Emiliani, C. (1954) Depth habitats of some species of pelagic foraminifera as indicated by oxygen isotope ratios. *Am. J. Sci.* 252, 149-158.

Emiliani, C. (1971) Depth Habitats of Growth Stages of Pelagic Foraminifera. *Science* 173 (4002), 1122-1124.

Erez, J. (1978) Vital effect on stable-isotope composition seen in foraminifera and coral skeletons. *Nature* 273 (5659), 199-202.

Erez, J. and Honjo, S. (1981) Comparison of Isotopic Composition of Planktonic-Foraminifera in Plankton Tows, Sediment Traps and Sediments. *Palaeogeography Palaeoclimatology Palaeoecology* 33 (1-3), 129-156.

Erez, J. and Luz, B. (1983) Experimental Paleotemperature Equation for Planktonic-Foraminifera. *Geochimica Et Cosmochimica Acta* 47 (6), 1025-1031.

Erwin, D. H. (1998) The end and the beginning: Recoveries from mass extinctions. *Trends in Ecology and Evolution* 13, 344-349.

Fairbanks, R. G., Sverdlove, M., Free, R., Wiebe, P. H. and Be, A. W. H. (1982) Vertical-Distribution and Isotopic Fractionation of Living Planktonic-Foraminifera from the Panama Basin. *Nature* 298 (5877), 841-844.

Fairbanks, R. G. and Wiebe, P. H. (1980) Foraminifera and Chlorophyll Maximum - Vertical-Distribution, Seasonal Succession, and Paleoceanographic Significance. *Science* 209 (4464), 1524-1526.

Fairbanks, R. G., Wiebe, P. H. and Be, A. W. H. (1980) Vertical-Distribution and Isotopic Composition of Living Planktonic-Foraminifera in the Western North-Atlantic. *Science* 207 (4426), 61-63.

Faul, K. L., Ravelo, A. C. and Delaney, M. L. (2000) Reconstructions of upwelling, productivity, and photic zone depth in the eastern equatorial Pacific Ocean using planktonic foraminiferal stable isotopes and abundances. *Journal of Foraminiferal Research* 30 (2), 110-125.

Faure, G. (1986) *Principles of Isotope Geology, 2nd edn.* Wiley.

Feely, R. A., Sabine, C. L., Takahashi, T. and Wanninkhof, R. (2001) Uptake and Storage of Carbon Dioxide in the Ocean: The Global CO2 Survey. *Oceanography* 14, 18-32.

Flugel, E. (2004) *Microfacies of Carbonate Rocks: Analysis, Interpretation and Application.* Berlin; New York: Springer.

Fornaciari, E., Giusberti, L., Luciani, V., Tateo, F., Agnini, C., Backman, J., Oddone, M. and Rio, D. (2007) An expanded Cretaceous-Tertiary transition in a pelagic setting of the Southern Alps (central-western Tethys). *Palaeogeography, Palaeoclimatology, Palaeoecology* 255 (1-2), 98-131.

Francois, R., Honjo, S., Krishfield, R. and Aanganini, S. (2002) Factors controlling the flux of organic carbon to the bathypelagic zone of the ocean. *Global Biogeochemical Cycles* 16, 1087-1107.

Fuqua, L. M., Bralower, T. J., Arthur, M. A. and Patzkowsky, M. E. (2008) Evolution of calcareous nannoplankton and the recovery of marine food webs after the cretaceous-paleocene mass extinction. *Palaios* 23 (3-4), 185-194.

Futterer, D. K. (1990) Distribution of calcareous dinoflagellates at the Cretaceous-Tertiary boundary of Queen Maud Rise, eastern Weddell Sea, Antarctica (ODP Leg 113). In: Barker, P. F., Kennett, J.P., et al (ed.) *Proc. ODP, Sci. Results, 113: College Station, TX (Ocean Drilling Program).*

Galeotti, S., Brinkhuis, H. and Huber, M. (2004) Records of post-Cretaceous-Tertiary boundary millennial-scale cooling from the western Tethys: A smoking gun for the impact-winter hypothesis? *Geology* 32 (6), 529-532.

Gallagher, W. B. (2001) Oligotrophic Oceans and Minimalist Organisms: Restructuring the Marine Community After the K/T Mass Extinction. International Conference on Catastrophic Events and Mass Extinctions: Impacts and Beyond, 9-12 July 2000, Vienna, Austria, abstract no.3063.

Gardin, S. and Monechi, S. (1998) Palaeoecological change in middle to low latitude calcareous nannoplankton at the Cretaceous/Tertiary boundary. *Bulletin de la Societe Geologique de France* 169 (5), 709-723.

Gerstel, J., Thunell, R. and Erlich, R. (1987) Danian faunal succession; planktonic foraminiferal response to a changing marine environment. *Geology* 15, 665-668.

Gooday, A. J. (2003) Benthic foraminifera (protista) as tools in deep-water palaeoceanography: Environmental influences on faunal characteristics. *Advances in Marine Biology* 46, 1-90.

Gradstein, F. M. and Ogg, J. G. (2004) Geologic Time Scale 2004 - why, how, and where next! *Lethaia* 37 (2), 175-181.

Griffis, K. and Chapman, D. J. (1988) Survival of phytoplankton under prolonged darkness: implications for the Cretaceous-Tertiary boundary darkness hypothesis. *Palaeogeography, Palaeoclimatology, Palaeoecology* 67 (3-4), 305-314.

Gruber, N., Gloor, M., Mikaloff Fletcher, S. E., Doney, S. C., Dutkiewicz, S., Follows, M. J., Gerber, M., Jacobson, A. R., Joos, F., Lindsay, K., Menemenlis, D., Mouchet, A., Müller, S. A., Sarmiento, J. L. and Takahashi, T. (2009) Oceanic sources, sinks, and transport of atmospheric CO2. *Global Biogeochem. Cycles* 23 (1), doi: 10.1029/2008gb003349.

Guichard, S., Jorissen, F., Bertrand, P., Gervais, A., Martinez, P., Peypouquet, J.-P., Pujol, C. and Vergnaud-Grazzini, C. (1997) Foraminifères benthiques et paléoproductivité: réflexions sur une carotte de l'upwelling (NW africain). *Comptes Rendus de l'Académie des Sciences - Series IIA - Earth and Planetary Science* 325 (1), 65-70.

Handley, L., Pearson, P. N., McMillan, I. K. and Pancost, R. D. (2008) Large terrestrial and marine carbon and hydrogen isotope excursions in a new Paleocene/Eocene boundary section from Tanzania. *Earth and Planetary Science Letters* 275 (1-2), 17-25.

Hansen, T., Farrand, R. B., Montgomery, H. A., Billman, H. G. and Blechschmidt, G. (1987) Sedimentology and extinction patterns across the Cretaceous-Tertiary boundary interval in east Texas. *Cretaceous Research* 8 (3), 229-252.

Hansena, T. A., Kelleyb, P. H. and Haasl, D. M. (2004) Paleoecological patterns in molluscan extinctions and recoveries: comparison of the Cretaceous–Paleogene and Eocene–Oligocene extinctions in North America. *Palaeogeography, Palaeoclimatology, Palaeoecology* 214 (3), 233-242.

Haq, B. U., Hardenbol, J. and Vail., P. R. (1987) Chronology of fluctuating sea levels since the Triassic. (Vail sea level curves). *Science* 235, 1156-1166.

Hemleben, C. and Bijma, J. (1994) Foraminiferal population dynamics and stable carbon isotopes. In: Zahn, R. e. a. (ed.) *Carbon cycling in the glacial ocean: constraints on the ocean's role in global change.* Springer-Verlag Berlin Heidelberg.

Hemleben, C., Spindler, M. and Anderson, O. R. (1989) *Modern Planktonic Foraminifera.* New York: Springer-Verlag.

Henriksson, A. S. (1996) Calcareous nannoplankton productivity and succession across the Cretaceous–Tertiary boundary in the Pacific (DSDP Site 465) and Atlantic (DSDP Site 527) Oceans. *Cretaceous Research* 17 (4), 451-477.

Hildebrand, A. R., Penfield, G. T., Kring, D. A., Pilkington, M., Zanoguera, A. C., Jacobsen, S. B. and Boynton, W. V. (1991) Chicxulub Crater; a possible

Cretaceous/Tertiary boundary impact crater on the Yucatan Peninsula, Mexico. *Geology* 19, 867-871.

Hofker, J. (1956) Foraminifera Dentata, foraminifera of Satila tituz and Thaich Island, Virgin Archipelago, West Indies:. *Spolia Zool, Mus. Kobenhaven* 15, 1-237.

Hollis, C. J., Rodgers, K. A. and Parker, R. J. (1995) Siliceous plankton bloom in the earlist Tertiary of Marlborough, New Zealand. *Geology* 23 (9), 835-838.

Honjo, S., Manganini, J. S. and Cole, J. J. (1982) Sedimentation of biogenic matter in the deep ocean. *Deep Sea Research* 29, 609-625.

Honjo, S., Manganini, S. J., Krishfield, R. A. and Francois, R. (2008) Particulate organic carbon fluxes to the ocean interior and factors controlling the biological pump: A synthesis of global sediment trap programs since 1983. *Progress In Oceanography* 76 (3), 217-285.

Hotelling, H. (1933) Analysis of a complex of statistical variables into principal components. *Journal of Educational Psychology* 24, 417-441 and 498-520.

Houston, R. M. and Huber, B. T. (1998) Evidence of photosymbiosis in fossil taxa? Ontogenetic stable isotope trends in some Late Cretaceous planktonic foraminifera. *Marine Micropaleontology* 34, 29-46.

Houston, R. M., Huber, B. T. and Spero, H. J. (1999) Photosymbiosis and ontogenetic d18O and d13C trends in some Maastrichtian planktic foraminifera: A discussion of intraspecific variability and methodology. *Marine Micropaleontology* 36, 169-188.

Hsu, K. (1980) Terrestrial catastrophe caused by cometary impact at the end of Cretaceous. *Nature* 285, 201-203.

Hsü, K. J., He, Q., McKenzie, A., Weissert, H., Perch-Nielson, K., Oberhansli, H., Kelts, K., LaBrecque, J., Tauxe, L., Krahenbuhl, U., Percival, S. F., Wright, R., Karpoff, A. M., Petersen, N., Tucker, P., Poore, R. Z., Gombos, A. M., Posciotto, K., Carman, M. F. and Schreiber, E. (1982) Mass mortality and its environmental and evolutionary consequences. *Science* 216 (4543), 249-256.

Hsü, K. J. and McKenzie, A. (1985) "Strangelove" ocean in the earliest Tertiary. In: Broeker, W. S. and Sundquist, E. T. (eds.) *The carbon and atmospheric CO_2: Natural variations Archean to Present, Geophysics Monographs, Series.* Vol. 32. Washington D. C.: AGU.

Huber, B. T. (1996) Evidence for planktonic foraminifer reworking versus survivorship across the Cretaceous-Tertiary boundary at high latitudes. In: Ryder, G., Gartner, S. and Fastovsky, D. (eds.) *The Cretaceous-Tertiary Event and Other Catastrophes in Earth History.* Vol. 307. Boulder, Colorado: Geological Society of America Special Paper.

Huber, B. T., Bijma, J. and Darling, K. (1997) Cryptic speciation in the living planktonic foraminifer *Globigerinella siphonifera* (d'Orbigny). *Paleobiology* 23 (1), 33-62.

Huber, B. T., MacLeod, K. G. and Norris, R. D. (2002) Abrupt extinction and subsequent reworking of Cretaceous planktonic Foraminifera across the Cretaceous-Tertiary boundary: Evidence from the subtropical North Atlantic. *Geological Society of America Special Papers* 356, 277-289.

Huber, M. and Sloan, L. C. (2000) Climatic Responses to Tropical Sea Surface Temperature Changes on a 'Greenhouse' Earth. *Paleoceanography* 15 (4), 443-450.

Itou, M., Ono, T., Oba, T. and Noriki, S. (2001) Isotopic composition and morphology of living *Globorotalia scitula*: a new proxy of sub-intermediate ocean carbonate chemistry? *Marine Micropaleontology* 42 (3-4), 189-210.

Jiang, S. J., Bralower, T. J., Patzkowsky, M. E., Kump, L. R. and Schueth, J. D. (2010) Geographic controls on nannoplankton extinction across the Cretaceous/Palaeogene boundary. *Nature Geoscience* 3 (4), 280-285.

Jiménez Berrocoso, Á., MacLeod, K. G., Huber, B. T., Lees, J. A., Wendler, I., Bown, P. R., Mweneinda, A. K., Isaza Londoño, C. and Singano, J. M. (2010) Lithostratigraphy, biostratigraphy and chemostratigraphy of Upper Cretaceous sediments from southern Tanzania: Tanzania drilling project sites 21-26. *Journal of African Earth Sciences* 57 (1-2), 47-69.

Johnson, K. R., Nichols, D. J., Attrep Jr, M. and Orth, C. J. (1989) High-resolution leaf-fossil record spanning the Cretaceous/Tertiary boundary. *Nature* 340 708-711.

Kahn, M. I. (1979) Non-equilibrium Oxygen and Carbon Isotopic Fractionation in Tests of Living Planktonic-Foraminifera. *Oceanologica Acta* 2 (2), 195-208.

Katz, M. E., Katz, D. R., Wright, J. D., Miller, K. G., Pak, D. K., Shackleton, N. J. and Thomas, E. (2003) Early Cenozoic benthic foraminiferal isotopes: Species reliability and interspecies correction factors. *Paleoceanography* 18 (2), Artn 1024 doi: 1010.1029/2002pa000798.

Keller, G. (1988) Extinction, survivorship, and evolution across the Cretaceous/Tertiary boundary at El Kef. *Marine Micropaleontology* 13, 239-263.

Keller, G. R., Barrera, E., Schmitz, B. and Mattson, E. (1993) Gradual mass extinction, species survivorship, and long-term environmental changes across the Cretaceous-Tertiary boundary in high latitudes. *Geological Society of America Bulletin* 105 (8), 979-997.

Kelly, D. C., Arnold, A. J. and Parker, W. C. (1996) Paedomorphosis and the origin of the Paleogene planktonic foraminiferal genus Morozovella. *Paleobiology* 22 (2), 266-281.

Kennett, J. P. and Srinavasan, M. S. (1983) *Neogene planktonic foraminifera: A phylogenetic atlas* New York, NY: Hutchinson Ross Publishing Company.

Kent, P. E., Hunt, J. A. and Johnstone, D. W. (1971) The geology and geophysics of coastal Tanzania. *Geophysical paper* 6.

Kiessling, W. and Baron-Szabo, R. C. (2004) Extinction and recovery patterns of scleractinian corals at the Cretaceous-Tertiary boundary. *Palaeogeography, Palaeoclimatology, Palaeoecology* 214 (3), 195-223.

Kim, S. T. and O'Neil, J. R. (1997) Equilibrium and non-equilibrium oxygen isotope effects in synthetic calcites. *Geochimica Et Cosmochimica Acta* 61, 3461-3475.

Kirchner, J. W. and Weil, A. (2000) Delayed biological recovery from extinctions throughout the fossil record. *Nature* 404, 177-180.

Kitchell, J. A., Clark, D. L. and Gombos, A. M. (1986) Biological selectivity of extinction; a link between background and mass extinction. *Palaios* 1 (5), 504-511.

Kring, D. (ed.) (1993) *The Chicxulub impact event and possible causes of K/T boundary extinctions.* Mesa, Arizona: Mesa Southwest Museum and Southwest Paleontological Society.

Kring, D. (2000) Impact events and their effect on the origin, evolution and distribution of life. *GSA Today* 10 (8), 1-2.

Kring, D. A. (2007) The Chicxulub impact event and its environmental consequences at the Cretaceous–Tertiary boundary. *Palaeogeography, Palaeoclimatology, Palaeoecology* 255, 4-21.

Kriwet, J. and Benton, M. J. (2004) Neoselachian (Chondrichthyes, Elasmobranchii) diversity across the Cretaceous-Tertiary boundary. *Palaeogeography, Palaeoclimatology, Palaeoecology* 214 (3), 181-194.

Kroon, D. and Nederbragt, A. J. (1990) Ecology and Paleoecology of Triserial Planktic Foraminifera. *Marine Micropaleontology* 16 (1-2), 25-38.

Kroon, D., Zachos, J. C. and Leg 208 Scientific Party (2007) Leg 208 synthesis: Cenozoic climate cycles and excursions. In: Kroon, D., Zachos, J.C., and Richter, C. (Eds.) (ed.) *Proc. ODP, Sci. Results, 208: College Station, TX (Ocean Drilling Program).* Vol. 1–55. doi:10.2973/odp.proc.sr.208.201.2007.

Kroopnick, P. (1985) Distribution of ^{13}C of ΣCO_2 in the world oceans. *Deep Sea Research* 32, 57-84.

Kroopnick, P., Weiss, R. F. and Craig, H. (1972) Total CO2, 13C and Dissolved Oxygen - 18O at Geosecs-II in the North Atlantic. *Earth and Planetary Science Letters* 16 (1), 103-110.

Kuhnt, W. and Kaminski, M. (1993) Changes in the community structure of deep water agglutinated foraminifera across the K/T boundary in the Basque Basin (Northern Spain). *Revista Espanola Micropaleontolgia* 25, 57-92.

Kump, L. R. (1991) Interpreting Carbon-Isotope Excursions - Strangelove Oceans. *Geology* 19 (4), 299-302.

Lasaga, A. C., Berner, R. A. and Garrels, R. M. (1985) An improved geochemical model of atmospheric CO2 fluctuations over the past 100 million years. In: Sundquist, E. T. and Broecker, W. S. (eds.) *The carbon cycle and atmospheric CO2: natural variations Archean to present* Washington, D.C: American Geophysical Union; Geophysical Monograph 32.

Laskar, J., Robutel, P., Joutel, F., Gastineau, M., Correia, A. C. M. and Levrard, B. (2004) A long-term numerical solution for the insolation quantities of the Earth. *Astronomy & Astrophysics* 428 (1), 261-285.

Lear, C. H., Bailey, T. R., Pearson, P. N., Coxall, H. K. and Rosenthal, Y. (2008) Cooling and ice growth across the Eocene-Oligocene transition. *Geology* 36 (3), 251-254.

Leeder, M. (2001) *Sedimentology and sedimentary basins: From turbulence to tectonics*. Blackwell Science.

LeGrande, A. N. and Schmidt, G. A. (2006) Global gridded data set of the oxygen isotopic composition in seawater. *Geophysical Research Letters* 33 (12), doi: 10.1029/2006gl026011

Leinen, M., Cwienk, D., Heath, G. R., Biscaye, P. E., Kolla, V., Thiede, J. and Dauphin, J. P. (1986) Distribution of biogenic silica and quartz in recent deep-sea sediments. *Geology* 14 (3), 199-203.

Li, L. Q. and Keller, G. (1999) Variability in Late Cretaceous climate and deep waters: evidence from stable isotopes. *Marine Geology* 161 (2-4), 171-190.

Libes, S. M. (1992) *An introduction to marine biogeochemistry*. Wiley. New York. US.

Lipps, J. H. (1970) Plankton evolution. *Evolution* 24 (1), 1-22.

Liu, C. and Olsson, R. K. (1992) Evolutionary radiation of microperforate planktonic Foraminifera following the K/T mass extinction event. *Journal of Foraminiferal Research* 22 (4), 328-346.

Lockwood, R. (2004) The K/T event and infaunality: Morphological and ecological patterns of extinction and recovery in veneroid bivalves. *Paleobiology* 30 (4), 507-521.

Loeblich, A. R. J. and Tappan, H. (1957) *Planktonic foraminifera of Paleocene and Early Eocene age from the Gulf and Atlantic coastal plains*. Bulletin of the United States National Museum.

Lohmann, G. P. (1995) A Model for Variation in the Chemistry of Planktonic-Foraminifera Due to Secondary Calcification and Selective Dissolution. *Paleoceanography* 10 (3), 445-457.

Lohmann, G. P. and Schweitzer, P. N. (1990) *Globorotalia truncatulinoides'* Growth and chemistry as probes of the past thermocline: 1. Shell size. *Paleoceanography* 5, 55-75.

Luterbacher, H. P. and Premoli Silva, I. (1964) Biostratigrafia del limite Cretaceo-terziario nell' Appennino centrale. *Rivista Ital. Paleontol* 70, 67–117.

Mackensen, A., Hubberten, H. W., Bickert, T., Fischer, G. and Fütterer, D. K. (1993) The delta13C in Benthic Foraminiferal Tests of *Fontbotia Wuellerstorfi* (Schwager) Relative to the delta13C of Dissolved Inorganic Carbon in Southern Ocean Deep Water: Implications for Glacial Ocean Circulation Models. *Paleoceanography* 8 (5), 587-610.

MacLeod, K. G. and Huber, B. T. (1996) Strontium isotopic evidence for extensive reworking in sediments spanning the Cretaceous/Tertiary boundary at ODP Site 738. *Geology* 24, 463-466

MacLeod, K. G., Huber, B. T. and Isaza-Londono, C. (2005) North Atlantic warming during global cooling at the end of the Cretaceous. *Geology* 33 (6), 437-440.

MacLeod, K. G. and Keller, G. (1991) Hiatus distributions and mass extinctions at the Cretaceous/Tertiary boundary. *Geology* 19, 497-501.

MacLeod, K. G., Whitney, D. L., Huber, B. T. and Koeberl, C. (2007) Impact and extinction in remarkably complete Cretaceous-Tertiary boundary sections from Demerara Rise, tropical western North Atlantic. *Geological Society of America Bulletin* 119 (1-2), 101-115.

MacLeod, N., Rawson, P. F., Forey, P. L., Banner, F. T., BouDagher-Fadel, M. K., Bown, P. R., Burnett, J. A., Chambers, P., Culver, S., Evans, S. E., Jeffery, C., Kaminski, M. A., Lord, A. R., Milner, A. C., Milner, A. R., Morris, N., Owen, E., Rosen, B. R., Smith, A. B., Taylor, P. D., Urquhart, E. and Young, J. R. (1997) The Cretaceous-Tertiary biotic transition. *Journal of the Geological Society, London,* Vol, 154, pp. 265-292.

Magurran, A. E. (2005) *Measuring Biological diversity.* Blackwell Publishing.

Manly, B. F. J. (1994) *Multivariate Statistical methods: A Primer.* Chapman and Hall.

Margalef, R. (1972) Homage to Evelyn Hutchinson, or why is there an upper limit to diversity? *Trans. Connect. Acad. Arts Sci* 44, 211-235.

Markov, A. V. and Soloviev., A. N. (1997) Echninoids at the Cretaceous –Paleogene Boundary In: Rozanov, A. Y., Vickers-Rich, P. and Tassell, C. (eds.) *Evolution of the Biosphere.* Records of the Queen Victoria Museum No. 104, pp. 35-37.

Marshall, C. R. and Ward, P. D. (1996) Sudden and Gradual Molluscan Extinctions in the Latest Cretaceous of Western European Tethys. *Science* 274 (5291), 1360-1363.

McConnaughey, T. (1989a) C-13 and O-18 Isotopic Disequilibrium in Biological Carbonates .1. Patterns. *Geochimica Et Cosmochimica Acta* 53 (1), 151-162.

McConnaughey, T. (1989b) C-13 and O-18 Isotopic Disequilibrium in Biological Carbonates .2. Invitro Simulation of Kinetic Isotope Effects. *Geochimica Et Cosmochimica Acta* 53 (1), 163-171.

McManus, J., Berelson, W., Klinkhammer, G., Johnson, K., Coale, K., Anderson, R., Kumar, N., Burdige, D., Hammond, D., Brumsack, H., McCorkle, D. and Rushdi, A. (1998) Geochemistry of barium in marine sediments: implications for its use as a paleoproxy. *Geochimica Et Cosmochimica Acta* 62 (21-22), 3453-3473.

Menzel, D., van Bergen, P. F., Schouten, S. and Sinninghe Damsté, J. S. (2003) Reconstruction of changes in export productivity during Pliocene sapropel deposition: a biomarker approach. *Palaeogeography, Palaeoclimatology, Palaeoecology* 190, 273-287.

Michaels, A. F. and Silver, M. W. (1988) Primary Production, Sinking Fluxes and the Microbial Food Web. *Deep-Sea Research Part a-Oceanographic Research Papers* 35 (4), 473-490.

Miller, K. G., Fairbanks, R. G. and Mountain, G. S. (1987) Tertiary Oxygen Isotope Synthesis, Sea Level History, and Continental Margin Erosion. *Paleoceanography* 2 (1), 1-19.

Miller, K. G., Janecek, T. R., Katz, M. E. and Kei, D. J. (1987) Abyssal circulation and benthic foraminiferal changes near the Paleocene/Eocene boundary. *Paleoceanography* 2 (6), 741-761.

Miller, K. G., Kominz, M. A., Browning, J. V., Wright, J. D., Mountain, G. S., Katz, M. E., Sugarman, P. J., Cramer, B. S., Christie-Blick, N. and Pekar, S. F. (2005) The Phanerozoic Record of Global Sea-Level Change. *Science* 310 (5752), 1293-1298.

Milner, A. C. (1998) Timing and causes of vertebrate extinction across the Cretaceous-Tertiary boundary. *Geological Society Special Publication* 140, 247-257.

Minoletti, F., de Rafelis, M., Renard, M., Gardin, S. and Young, J. (2005) Changes in the pelagic fine fraction carbonate sedimentation during the Cretaceous-Paleocene transition: contribution of the separation technique to the study of Bidart section. *Palaeogeography Palaeoclimatology Palaeoecology* 216 (1-2), 119-137.

Molina, E., Arenillas, I. and Arz, J. A. (1998) Mass extinction in planktic foraminifera at the Cretaceous/Tertiary boundary in subtropical and temperate latitudes. *Bull. Soc. Géol. France* 169 (3), 351-363.

Moore, T. C., Rabinowitz, P. D., Boersma, A., Borella, P. E., Chave, A. D., Duée, G., Fütterer, D. K., Jiang, M., Kleinert, K., Lever, A., Manivit, H., O'Connell, S., Richardson, S. H. and Shackleton, N. J. (1984) *Initial Reports of the Deep Sea Drilling Project DSDP, 74, Introduction and explanatory notes.* Washington (U.S. Govt. Printing Office).

Moore, W. R., McBeath, D. M., Linton, R. E., Terris, A. P. and Stoneley, R. (1963) *Geological Survey of Tanganyika Quarter Degree Sheet 256 & 256E. 1:125 000. Kilwa.* Geological Survey Division, Dodoma.

Morozova, V. G. (1959) *Stratigrafiya Datsko-Montskikh otlozhenii Kryma po foraminiferam [Stratigraphy of the Danian-Montian Deposits of the Crimea According to the Foraminifera].* Doklady Akademiya Nauk SSSR.

Morozova, V. G. (1961) Datsko-Montskie planktonnye foraminifery yugu SSSR (Danian-Montian planktonic foraminifera of the Southern USSR). *Paleontologicheskiy Zhurnal* 2, 8-19.

Mulitza, S., Dürkoop, A., Hale, W., Wefer, G. and Stefan Niebler, H. (1997) Planktonic foraminifera as recorders of past surface-water stratification. *Geology* 25 (4), 335-338.

Murray, R. W. and Leinen, M. (1993) Chemical transport to the seafloor of the equatorial Pacific Ocean across a latitudinal transect at 135°W: Tracking sedimentary major, trace, and rare earth element fluxes at the Equator and the Intertropical Convergence Zone. *Geochimica Et Cosmochimica Acta* 57 (17), 4141-4163.

Naqvi, S. W. A. (2006) Oxygen deficiency in the north Indian Ocean. *Gayana (Concepción)* 70, 53-58.

Nathan, S. A. and Leckie, R. M. (2009) Early history of the Western Pacific Warm Pool during the middle to late Miocene (~ 13.2-5.8 Ma): Role of sea-level change and implications for equatorial circulation. *Palaeogeography, Palaeoclimatology, Palaeoecology* 274 (3-4), 140-159.

Natland, M. L. (1938) New species of foraminifera from off the west coast of North America and from the later Tertiary of the Los Angeles Basin. *Bull. Scripps. Inst. Oceanogr., Tech. Ser.* 4, 137-164.

Neveux, J. and de Billy, G. (1986) Spectrofluorometric determination of chlorophylls and pheophytins. Their distribution in the western part of the Indian Ocean (July to August 1979). *Deep Sea Research Part A. Oceanographic Research Papers* 33 (1), 1-14.

Nicholas, C. J., Pearson, P. N., Bown, P. R., Dunkley Jones, T., Huber, B. T., Karega, A., Lees, J. A., McMillan, I. K., O'Halloran, A., Singano, J. M. and Wade, B. S. (2006) Stratigraphy and sedimentology of the Upper Cretaceous to Paleogene Kilwa Group, southern coastal Tanzania. *Journal of African Earth Sciences* 45 (4-5), 431-466.

Nicholas, C. J., Pearson, P. N., McMillan, I. K. D., Ditchfield, P. W. and Singano, J. M. (2007) Structural evolution of southern coastal Tanzania since the Jurassic. *Journal of African Earth Sciences* 48 (4), 273-297.

Nichols, D. J. (2007) Selected plant microfossil records of the terminal Cretaceous event in terrestrial rocks, western North America. *Palaeogeography, Palaeoclimatology, Palaeoecology* 255 (1-2), 22-34.

Nordt, L., Atchley, S. and Dworkin, S. I. (2002) Paleosol barometer indicates extreme fluctuations in atmospheric CO2 across the Cretaceous-Tertiary boundary. *Geology* 30 (8), 703-706.

Norris, R. D. (1991) Biased extinction and evolutionary trends. *Paleobiology* 17 (4), 388-399.

Norris, R. D. (1996) Symbiosis as an evolutionary innovation in the radiation of Paleocene planktic foraminifera. *Paleobiology* 22, 461-480.

Norris, R. D., Huber, B. T. and Self-Trail, J. (1999) Synchroneity of the K-T oceanic mass extinction and meteorite impact. *Geology* 27 (5), 419-422.

Officer, C. B. and Drake, C. L. (1985) Terminal cretaceous environmental events. *Science* 227, 1161-1167.

Olsson, R. K. (1960) Foraminifera of Latest Cretaceous and Earliest Tertiary age in the New Jersey Coastal Plain. *Journal of Paleontology* 34, 1-58.

Olsson, R. K., Hemleben, C., Berggren, W. A. and Huber, B. T. (1999) *Atlas of Paleocene planktonic foraminifera.* Washington, DC: Smithsonian Inst.

Oms, O., Dinarès-Turell, J., Vicens, E., Estrada, R., Vila, B., Galobart, À. and Bravo, A. M. (2007) Integrated stratigraphy from the Vallcebre Basin (southeastern Pyrenees, Spain): New insights on the continental Cretaceous–Tertiary transition in southwest Europe. *Palaeogeography, Palaeoclimatology, Palaeoecology* 255 (1-2), 35-47.

Ortiz, J. D., Mix, A. C. and Collier, R. W. (1995) Environmental control of living symbiotic and asymbiotic foraminifera of the California Currnt. *Paleoceanography* 10 (6), 987-1009.

Ortiz, J. D., Mix, A. C., Rugh, W., Watkins, J. M. and Collier, R. W. (1996) Deep-dwelling planktonic foraminifera of the northeastern Pacific Ocean reveal environmental control of oxygen and carbon isotopic disequilibria. *Geochimica Et Cosmochimica Acta* 60 (22), 4509-4523.

Park, K. (1966) Deeo sea pH. *Science* 154, 1540-1542.

Pearson, K. (1901) On lines and planes of closest fit to a system of points in space. *Philosophical Magazine* 2, 557-572.

Pearson, P. N. (1995) Planktonic foraminifer biostratigraphy and the development of pelagic caps on guyots in the Marshall Islands group. *Proceedings of the Ocean Drilling Program, Scientific Results.* 144, 21-59.

Pearson, P. N., Ditchfield, P. W., Singano, J., Harcourt-Brown, K. G., Nicholas, C. J., Olsson, R. K., Shackleton, N. J. and Hall, M. A. (2001) Warm tropical sea surface temperatures in the Late Cretaceous and Eocene epochs. *Nature* 413 (6862), 481-487.

Pearson, P. N., McMillan, I. K., Wade, B. S., Jones, T. D., Coxall, H. K., Bown, P. R. and Lear, C. H. (2008) Extinction and environmental change across the Eocene-Oligocene boundary in Tanzania. *Geology* 36 (2), 179-182.

Pearson, P. N., Nicholas, C. J., Singano, J. M., Bown, P. R., Coxall, H. K., van Dongen, B. E., Huber, B. T., Karega, A., Lees, J. A., MacLeod, K., McMillan, I. K., Pancost, R. D., Pearson, M. and Msaky, E. (2006) Further Paleogene and Cretaceous sediment cores from the Kilwa area of coastal Tanzania: Tanzania Drilling Project Sites 6-10. *Journal of African Earth Sciences* 45 (3), 279-317.

Pearson, P. N., Nicholas, C. J., Singano, J. M., Bown, P. R., Coxall, H. K., van Dongen, B. E., Huber, B. T., Karega, A., Lees, J. A., Msaky, E., Pancost, R. D., Pearson, M. and Roberts, A. P. (2004) Paleogene and Cretaceous sediment cores from the Kilwa and Lindi areas of coastal Tanzania: Tanzania Drilling Project Sites 1-5. *Journal of African Earth Sciences* 39 (1-2), 25-62.

Pearson, P. N., Shackleton, N. J. and Hall, M. A. (1993) Stable Isotope Paleoecology of Middle Eocene Planktonic-Foraminifera and Multispecies Isotope Stratigraphy, Dsdp Site 523, South-Atlantic. *Journal of Foraminiferal Research* 23 (2), 123-140.

Pearson, P. N., van Dongen, B. E., Nicholas, C. J., Pancost, R. D., Schouten, S., Singano, J. M. and Wade, B. S. (2007) Stable warm tropical climate through the Eocene Epoch. *Geology* 35 (3), 211-214.

Pearson, P. N. and Wade, B. S. (2009) Taxonomy and Stable Isotope Paleoecology of Well-Preserved Planktonic Foraminifera from the Uppermost Oligocene of Trinidad. *Journal of Foraminiferal Research* 39 (3), 191-217.

Penfield, G. T. and Camargo, Z. (1981) Definition of a major igneous zone in the central Yucatan platform with aeromagnetics and gravity. *in Technical programs, abstracts and biographies (Society of exploration Geophysicists 51st annual international meeting): Los Angeles, Society of exploration Geophysicists.*

Peryt, D., Alegret, L. and Molina, E. (2002) The Cretaceous/Palaeogene (K/P) boundary at Aïn Settara, Tunisia: restructuring of benthic foraminiferal assemblages. *Terra Nova* 14 (2), 101-107.

Pielou, E. C. (1969) *An introduction to mathematical ecology.* New York: New York.

Pielou, E. C. (1975) *Ecological diversity.* New York: Wiley InterScience.

Pineau, F., Javoy, M. and Bottinga, Y. (1976) 13C/12C ratios of rocks and inclusions in popping rocks of the Mid-Atlantic Ridge and their bearing on the problem of isotopic composition of deep-seated carbon. *Earth and Planetary Science Letters* 29 (2), 413-421.

Plummer, H. J. (1926) *Foraminifera of the Midway Formation in Texas* University of Texas Bulletin.

Pollehne, F., Klein, B. and Zeitzschel, B. (1993) Low light adaptation and export production in the deep chlorophyll maximum layer in the northern Indian Ocean. *Deep Sea Research Part II: Topical Studies in Oceanography* 40 (3), 737-752.

Pope, K., Baines, K. H., Ocampo, A. C. and Ivanov, B. A. (1997) Energy, volatile production, and climate effects of the Chicxulub Cretaceous/Tertiary impact. *Journal of Geophysical Research* 102 (21), 645-664.

Pope, K., Fischer, A., Ocampo, A. C., Baines, K. H., King, D. and Grippo, A. (1997) Meteorite impact induced changes in the atmosphere and oceans at the Cretaceous/Tertiary boundary Anonymous. In *Geological Society of America, 1997 annual meeting* (Vol. Abstracts with Programs - Geological Society of America, 29 (6), pp. 212:). Salt Lake City, UT, United States.

Pope, K. O., D'Hondt, S. L. and Marshall, C. R. (1998) Meteorite impact and the mass extinction of species at the Cretaceous/Tertiary boundary. *Proceedings of the National Academy of Sciences, USA* 95 (19), 11028-11029.

Pospichal, J. (1994) Calcareous nannofossils at the K-T boundary, El Kef: no evidence for stepwise, gradual or sequential extinctions. *Geology* 22, 99-102.

Prahl, F. G. and Wakeham, S. G. (1987) Calibration of Unsaturation Patterns in Long-Chain Ketone Compositions for Paleotemperature Assessment. *Nature* 330 (6146), 367-369.

Quillevere, F., Norris, R. D., Kroon, D. and Wilson, P. A. (2008) Transient ocean warming and shifts in carbon reservoirs during the early Danian. *Earth and Planetary Science Letters* 265 (3-4), 600-615.

Quillévéré, F., Norris, R. D., Moussa, I. and Berggren, W. A. (2001) Role of photosymbiosis and biogeography in the diversification of early Paleogene acarninids (planktonic foraminifera). *Paleobiology* 27, 311-326.

Rampino, M. R. and Volk, T. (1988) Mass Extinctions, Atmospheric Sulfur and Climatic Warming at the K/T Boundary. *Nature* 332 (6159), 63-65.

Ramsey, A. T. S., Schneidermann, N. and Finch, J. W. (1973) Fluctuation in the Past Rates of Carbonate Solution in Site 149: A Comparison with Other Ocean Basins and an Interpretation of Their Significance. *Initial Reports of the Deep Sea Drilling Project* 15, doi:10.2973/dsdp.proc.2915.2122.1973.

Rao, R. R., Molinari, R. L. and Festa, J. F. (1989) Evolution of the Climatological Near-Surface Thermal Structure of the Tropical Indian Ocean 1. Description of Mean Monthly Mixed Layer Depth, and Sea Surface Temperature, Surface Current, and Surface Meteorological Fields. *J. Geophys. Res.* 94 (C8), 10801-10815.

Ravelo, A. C. and Fairbanks, R. G. (1995) Carbon Isotopic Fractionation in Multiple Species of Planktonic-Foraminifera from Core-Tops in the Tropical Atlantic. *Journal of Foraminiferal Research* 25 (1), 53-74.

Rea, D. K., Dehn, J., Driscoll, N. W., Farrell, J. W., Janecek, T. R., Owen, R. M., Pospichal, J. J. and Resiwati, P. (1990) Paleoceanography of the Eastern Indian-Ocean from Odp Leg-121 Drilling on Broken Ridge. *Geological Society of America Bulletin* 102 (5), 679-690.

Roopnarine, P. D., Byars, G. and Fitzgerald, P. (1999) Anagenetic Evolution, Stratophenetic Patterns, and Random Walk Models. *Paleobiology* 25, 41-57.

Salman, G. and Abdula, I. (1995) Development of the Mozambique and Ruvuma sedimentary basins, offshore Mozambique. *Sedimentary Geology* 96 (1-2), 7-41.

Sardessai, S., Shetye, S., Maya, M. V., Mangala, K. R. and Prasanna Kumar, S. (2010) Nutrient characteristics of the water masses and their seasonal variability in the eastern equatorial Indian Ocean. *Marine Environmental Research* 70 (3-4), 272-282.

Savin, S. M. (1977) History of Earths surface temperature during past 100 million years *Annual Review of Earth and Planetary Sciences* 5, 319-355.

Schiebel, R. (2002) Planktic foraminiferal sedimentation and the marine calcite budget. *Global Biogeochem. Cycles* 16 (4), 1065.

Schiebel, R., Bijma, J. and Hemleben, C. (1997) Population dynamics of the planktic foraminifer *Globigerina bulloides* from the eastern North Atlantic. *Deep Sea Research Part I: Oceanographic Research Papers* 44 (9-10), 1701-1713.

Schiebel, R. and Hemleben, C. (2000) Interannual variability of planktic foraminiferal populations and test flux in the eastern North Atlantic Ocean (JGOFS). *Deep-Sea Research Part II: Topical Studies in Oceanography* 47 (9-11), 1809-1852.

Schiebel, R. and Hemleben, C. (2005) Modern planktic foraminifera. *Paläontologische Zeitschrift* 79 (1), 135-148.

Schmidt, D. N., Elliott, T. and Kasemann, S. A. (2008) The influences of growth rates on planktic foraminifers as proxies for palaeostudies – a review. *Geological Society, London, Special Publications* 303 (1), 73-85.

Schmidt, D. N., Lazarus, D., Young, J. R. and Kucera, M. (2006) Biogeography and evolution of body size in marine plankton. *Earth-Science Reviews* 78 (3-4), 239-266.

Schmidt, D. N., Renaud, S., Bollmann, J., Schiebel, R. and Thierstein, H. R. (2004b) Size distribution of Holocene planktic foraminifer assemblages: biogeography, ecology and adaptation. *Marine Micropaleontology* 50 (3-4), 319– 338.

Schmidt, D. N., Thierstein, H. R. and Bollmann, J. (2004a) The evolutionary history of size variation of planktic foraminiferal assemblages in the Cenozoic. *Palaeogeography, Palaeoclimatology, Palaeoecology* 212, 159-180.

Schmidt, G. A., Bigg, G. R. and Rohling, E. J. (1999) Global Seawater Oxygen-18 Database http://data.giss.nasa.gov/o18data/.

Schott, F. A., Xie, S. P. and McCreary, J. P. (2009) Indian Ocean Circulation and Climate Variability. *Reviews of Geophysics* 47, doi:10.1029/2007RG000245.

Schouten, S., Hopmans, E. C., Schefuss, E. and Damste, J. S. S. (2002) Distributional variations in marine crenarchaeotal membrane lipids: a new tool for reconstructing ancient sea water temperatures? *Earth and Planetary Science Letters* 204 (1-2), 265-274.

Schulte, P., Alegret, L., Arenillas, I., Arz, J. A., Barton, P. J., Bown, P. R., Bralower, T. J., Christeson, G. L., Claeys, P., Cockell, C. S., Collins, G. S., Deutsch, A., Goldin, T. J., Goto, K., Grajales-Nishimura, J. M., Grieve, R. A. F., Gulick, S. P. S., Johnson, K. R., Kiessling, W., Koeberl, C., Kring, D. A., MacLeod, K. G., Matsui, T., Melosh, J., Montanari, A., Morgan, J. V., Neal, C. R., Nichols, D. J., Norris, R. D., Pierazzo, E., Ravizza, G., Rebolledo-Vieyra, M., Reimold, W. U., Robin, E., Salge, T., Speijer, R. P., Sweet, A. R., Urrutia-Fucugauchi, J., Vajda, V., Whalen, M. T. and Willumsen, P. S. (2010) The Chicxulub Asteroid Impact and Mass Extinction at the Cretaceous-Paleogene Boundary. *Science* 327 (5970), 1214-1218.

Sepkoski, J. J. (1996) Patterns of Phanerozoic extinction: a perspective from global databases. In: Walliser, O. H. (ed.) *Global Events and Event Stratigraphy*. Springer-Verlag, Berlin.

Sepkoski, J. J. J. (1998) Rates of speciation in the fossil record. *Philosophical Transactions of the Royal Society of London, Ser. B* 353, 315-316.

Sepulveda, J., Wendler, J. E., Summons, R. E. and Hinrichs, K. U. (2009) Rapid Resurgence of Marine Productivity After the Cretaceous-Paleogene Mass Extinction. *Science* 326 (5949), 129-132.

Sexton, P. F., Wilson, P. A. and Pearson, P. N. (2006) Microstructural and geochemical perspectives on planktic foraminiferal preservation: "Glassy" versus "Frosty". *Geochemistry Geophysics Geosystems* 7 Q12P19, doi:10.1029/2006GC001291.

Shackleton, N. and Boersma, A. (1981) The climate of the Eocene Ocean. *Geological Society of London* 138, 153-157.

Shackleton, N. J., Corfield, R. M. and Hall, M. A. (1985) Stable isotope data and the ontogeny of Paleocene planktonic foraminifera *Journal of Foraminiferal Research* 15 (4), 321-336.

Shackleton, N. J., Hall, M. A. and Boersma, A. (1984) Oxygen and Carbon Isotope Data from Leg-74 Foraminifers. *Initial Reports of the Deep Sea Drilling Project* 74 (Mar), 599-612.

Shackleton, N. J., Hall, M. A., Line, J. and Shuxi, C. (1983) Carbon isotope data in core V19-30 confirm reduced carbon dioxide concentration in the ice age atmosphere. *Nature* 306 (5941), 319-322.

Shackleton, N. J. and Opdyke, N. D. (1973) Oxygen isotope and palaeomagnetic stratigraphy of Equatorial Pacific core V28-238: Oxygen isotope temperatures and ice volumes on a 105 year and 106 year scale. *Quaternary Research* 3 (1), 39-55.

Shackleton, N. J. and Vincent, E. (1978) Oxygen and Carbon Isotope Studies in Recent Foraminifera from Southwest Indian-Ocean. *Marine Micropaleontology* 3 (1), 1-13.

Shangguan, Z. G., Zhao, C. P. and Gao, L. (2006) Carbon isotopic compositions of the methane derived from magma at the active volcanic regions in China. *Acta Petrologica Sinica* 22 (6), 1458-1464.

Shannon, C. E. and Weaver, W. (1949) *The mathematical theory of communication.* Urbana, IL: University of Illinois Press.

Sheehan, P. M., Coorough, P. J. and Fastovsky, D. E. (1996) Biotic selectivity during the K/T and Late Ordovician extinction events. In: Ryder, G., Fastovsky, D. and Gartner, S. (eds.) *The Cretaceous-Tertiary event and other catastrophes in Earth history*. Vol. 307. Special Paper - Geological Society of America.

Sheehan, P. M., Fastovsky, D. E., Hoffmann, R. G., Berghaus, C. B. and Gabriel, D. L. (1991) Sudden extinction of the dinosaurs: latest Cretaceous, upper Great Plains, USA. *Science* 254 (5033), 835-839.

Shipboard Scientific Party (2004): Explanatory notes. *In* Zachos, J.C., Kroon, D., Blum, P., et al., Proc. ODP, Init. Repts., 208: College Station, TX (Ocean Drilling Program). . 1-63.

Shipboard Scientific Party (2004) Leg 208 Summary. *In* Zachos, J.C., Kroon, D., Blum, P., et al., Proc. ODP, Init. Repts., 208: College Station, TX (Ocean Drilling Program). pp112.

Sigman, D. M. and Boyle, E. A. (2000) Glacial/interglacial variations in atmospheric carbon dioxide. *Nature* 407 (6806), 859-869.

Smit, J. (1982) Extinction and evolution of planktonic foraminifera at the Cretaceous/Tertiary boundary after a major impact. In: Silver, L. T. and Schultz, P. H.

(eds.) *Geological Implications of Impacts of Large Asteroids and Comets on the Earth, Geological Society of America Special Papers.* Vol. 190.

Smit, J. (1990) Meteorite impact, extinctions and the Cretaceous-Tertiary Boundary. *Geologie en Mijnbouw* (69), 187-204.

Spearman, C. (1904) The proof and measurement of association between two things. *American journal of Psychology* 15, 72-101.

Spero, H. J. (1992) Do Planktic Foraminifera Accurately Record Shifts in the Carbon Isotopic Composition of Seawater Sigma-Co2. *Marine Micropaleontology* 19 (4), 275-285.

Spero, H. J., Bijma, J., Lea, D. W. and Bemis, B. E. (1997) Effect of seawater carbonate concentration on foraminiferal carbon and oxygen isotopes. *Nature* 390 (6659), 497-500.

Spero, H. J. and DeNiro, M. J. (1987) The influence of symbiont photosynthesis on the δ18O and δ13Cvalues of planktonic foraminiferal shell calcite. *Symbiosis* 4, 213-228.

Spero, H. J. and Lea, D. W. (1993) Intraspecific Stable-Isotope Variability in the Planktic Foraminifera *Globigerinoides sacculifer* - Results from Laboratory Experiments. *Marine Micropaleontology* 22 (3), 221-234.

Spero, H. J. and Lea, D. W. (1996) Experimental determination of stable isotope variability in *Globigerina bulloides*: Implications for paleoceanographic reconstructions. *Marine Micropaleontology* 28 (3-4), 231-246.

Spero, H. J., Leche, I. and Williams, D. F. (1991) Opening the carbon isotope 'vital affects' box, 2, quantitative model for interpreting foraminiferal carbon isotope data. *Paleoceanography* 6, 639-655.

Spero, H. J. and Williams, D. F. (1988) Extracting Environmental Information from Planktonic Foraminiferal Delta-C-13 Data. *Nature* 335 (6192), 717-719.

Spero, H. J. and Williams, D. F. (1989) Opening the carbon isotope "vital effects" black box, 1. Seasonal temperatures in the euphotic zone. *Paleoceanography* 4, 593-601.

Srivastava, R., Ramesh, R., Jani, R. A., Anilkumar, N. and Sudhakar, M. (2010) Stable oxygen, hydrogen isotope ratios and salinity variations of the surface Southern Indian Ocean waters. *Current Science* 99, 1395-1399.

Stanley, S. M., Ries, J. B. and Hardie, L. A. (2005) Seawater chemistry, coccolithophore population growth, and the origin of Cretaceous chalk. *Geology* 33 (7), 593-596.

Stewart, D. R. M., Pearson, P. N., Ditchfield, P. W. and Singano, J. M. (2004) Miocene tropical Indian Ocean temperatures: Evidence from three exceptionally preserved

foraminiferal assemblages from Tanzania. *Journal of African Earth Sciences* 40 (3-4), 173-190.

Stott, L. D. and Kennett, J. P. (1989) New constraints on early Tertiary palaeoproductivity from carbon isotopes in foraminifera. *Nature* 342 (6249), 526-529.

Stott, L. D. and Kennett, J. P. (1990) The paleocenaographic and paleoclimatic signature of the Cretaceous/Tertiary boundary in the Antarctic: Stable isotopic results from ODP Leg 113.*Proceedings of the Ocean Drilling Program Scientific Results.* College Station: Ocean Drilling Program.

Struck, U., Sarnthein, M., Westerhausen, L., Barnola, J. M. and Raynaud, D. (1993) Ocean-atmosphere carbon exchange: impact of the "biological pump" in the Atlantic equatorial upwelling belt over the last 330,000 years. *Palaeogeography, Palaeoclimatology, Palaeoecology* 103 (1-2), 41-56.

Stüben, D., Kramar, U., Berner, Z. A., Meudt, M., Keller, G., Abramovich, S., Adatte, T., Hambach, U. and Stinnesbeck, W. (2003) Late Maastrichtian paleoclimatic and paleoceanographic changes inferred from Sr/Ca ratio and stable isotopes. *Palaeogeography, Palaeoclimatology, Palaeoecology* 199 (1-2), 107-127.

Subbotina, N. N. (1953) *Iskopaemye foraminifery SSSR (Globigerinidy, Khantkenininidy i Globorotaliidy) [Fossil Foraminifera of the USSR (Globigerinidae, Hantkeninidae and Globorotaliidae)].* Trudy Vsesoyznogo Neftyanogo Nauchno-Issledovatel 'skogo Geologo-Razvedochnogo Instituta (VNIGRI).

Tait, R. V. and Dipper, F. A. (1998) *Elements of marine ecology.* Butterworth-Heinemann.

Takahashi, T., Feely, R. A., Weiss, R. F., Wanninkhof, R. H., Chipman, D. W., Sutherland, S. C. and Takahashi, T. T. (1997) Global air-sea flux of CO2: An estimate based on measurements of sea–air pCO2 difference. *Proceedings of the National Academy of Sciences of the United States of America* 94 (16), 8292-8299.

Tallberg, P. and Heiskanen, A. S. (1998) Species-specific phytoplankton sedimentation in relation to primary production along an inshore-offshore gradient in the Baltic Sea. *Journal of Plankton Research* 20 (11), 2053-2070.

Thomas, E. (1990) Late Cretaceous-early Eocene mass extinction in the deep-sea. In: Shaprton, V. L. and Ward, P. D. (eds.) *Global catastrophies, Special Publication of the Geological Society of America.* Vol. 247.

Thomas, E. (2003) Extinction and food at the seafloor: A high-resolution benthic foraminiferal record across the initial Eocene thermal maximum, Southern Ocean site 690. *Geological Society of America Special Papers* 369, 319-332.

Thomas, E. (2007) Cenozoic mass extinctions in the deep sea: What perturbs the largest habitat on Earth? *Geological Society of America Special Papers* 424, 1-23.

Thomas, E. and Gooday, A. J. (1996) Cenozoic deep-sea benthic foraminifers: Tracers for changes in oceanic productivity? *Geology* 24 (4), 355-358.

Thomas, E., Zachos, J. C. and Timothy, J. B. (1999) Deep-sea environments on a warm earth: latest Paleocene-early Eocene In: Huber, B. T., Macleod, K. G. and Scott, L. W. (eds.) *Warm Climates in Earth History*. Cambridge University Press.

Toon, O. B., Pollack, J. B., Ackerman, T. P., Turco, R. P., McKay, C. P. and Liu, M. S. (1982) Evolution of an impact-generated dust cloud and the effect on the atmosphere. *GSA Special Paper* 190, 187–200.

Tozzi, S., Schofield, O. and Falkowski, P. (2004) Historical climate change and ocean turbulence as selective agents for two key phytoplankton functional groups. *Marine Ecology-Progress Series* 274, 123-132.

Tribollet, A. (2008) The boring microflora in modern coral reef ecosystems: a review of its roles. In: Wisshak, M. and Tapanila, L. (eds.) *Current Developments in Bioerosion.* Springer Berlin Heidelberg.

Tripati, A. and Zachos, J. (2002) Late Eocene tropical sea surface temperatures: A perspective from Panama. *Paleoceanography* 17 (3), 1032.

Tripati, A. K., Delaney, M. L., Zachos, J. C., Anderson, L. D., Kelly, D. C. and Elderfield, H. (2003) Tropical sea-surface temperature reconstruction for the early Paleogene using Mg/Ca ratios of planktonic foraminifera. *Paleoceanography* 18 (4), 1101.

Turner, J. T. (2002) Zooplankton faecal pellets, marine snow and sinking phytoplankton blooms. *Aquatic Microbial Ecology* 27 (1), 57-102.

Turner, J. V. (1982) Kinetic Fractionation of C-13 during Calcium-Carbonate Precipitation. *Geochimica Et Cosmochimica Acta* 46 (7), 1183-1191.

Uchikawa, J. and Zeebe, R. E. (2010) Examining possible effects of seawater pH decline on foraminiferal stable isotopes during the Paleocene-Eocene Thermal Maximum. *Paleoceanography* 25, doi: 10.1029/2009pa001864.

Urey, H. C. (1947) The thermodynamic properties of isotopic substances. *J. Chem. Soc.* 1, 562-581.

van Dongen, B. E., Talbot, H. M., Schouten, S., Pearson, P. N. and Pancost, R. D. (2006) Well preserved Palaeogene and Cretaceous biomarkers from the Kilwa area, Tanzania. *Organic Geochemistry* 37 (5), 539-557.

Varadi, F., Runnegar, B. and Ghil, M. (2003) Successive refinements in long-term integrations of planetary orbits. *Astrophysical Journal* 592 (1), 620-630.

Vecsei, A. and Moussavian, E. (1997) Paleocene reefs on the Maiella platform margin, Italy: An example of the effects of the Cretaceous/Tertiary boundary events on reefs and carbonate platforms. *Facies* 36, 123-139.

Wade, B., Al-Sabouni, N., Hemleben, C. and Kroon, D. (2008) Symbiont bleaching in fossil planktonic foraminifera. *Evolutionary Ecology* 22 (2), 253-265.

Wade, B. S. and Pearson, P. N. (2008) Planktonic foraminiferal turnover, diversity fluctuations and geochemical signals across the Eocene/Oligocene boundary in Tanzania. *Marine Micropaleontology* 68 (3-4), 244-255.

Wade, B. S., Pearson, P. N., Berggren, W. A. and Pälike, H. (2011) Review and revision of Cenozoic tropical planktonic foraminiferal biostratigraphy and calibration to the geomagnetic polarity and astronomical time scale. *Earth-Science Reviews* 104 (1-3), 111-142.

Walker, K. R. and Bambach, R. K. (1974) Feeding by benthic invertebrates: classification and terminology for paleo-ecological analysis. *Lethaia* 7 (1), 67-78.

Wefer, G. and Berger, W. H. (1991) Isotope paleontology: growth and composition of extant calcareous species. *Marine Geology* 100 (1-4), 207-248.

Wei, K.-Y. and Kennett, J. P. (1986) Taxonomic evolution of Neogene planktonic foraminifera and palaeoceanographic relations. *Paleoceanography* 1, 67-84.

Weinlich, F. H. (2005) Isotopically light carbon dioxide in nitrogen rich gases: the gas distribution pattern in the French Massif Central, the Eifel and the western Eger Rift. *Annals of Geophysics* 48 (1), 19-31.

Werne, J. P., Hollander, D. J., Lyons, T. W. and Peterson, L. C. (2000) Climate-Induced Variations in Productivity and Planktonic Ecosystem Structure from the Younger Dryas to Holocene in the Cariaco Basin, Venezuela. *Paleoceanography* 15 (1), 19-29.

Westerhold, T., Röh, U., Raffi, I., Fornaciari, E., Monechi, S., Reale, V., Bowles, J. and Evans, H. F. (2008) Astronomical calibration of the Paleocene time. *Palaeogeography, Palaeoclimatology, Palaeoecology* 257 (4), 377-403.

Westerhold, T., Rohl, U., Laskar, J., Raffi, I., Bowles, J., Lourens, L. J. and Zachos, J. C. (2007) On the duration of magnetochrons C24r and C25n and the timing of early Eocene global warming events: Implications from the Ocean Drilling Program Leg 208 Walvis Ridge depth transect. *Paleoceanography* 22 (1), ISI:000245584300001.

White, M. P. (1928) Some index foraminifera of the Tampico Embayment of Mexico, Part I and Part II. *Journal of Paleontology* 2, 177-215.

Wilf, P., Johnson, K. R. and Huber, B. T. (2003) Correlated terrestrial and marine evidence for global climate changes before mass extinction at the Cretaceous-Paleogene boundary. *Proceedings of the National Academy of Sciences of the United States of America* 100 (2), 599-604.

Wilf, P., Labandaira, C. C., Johnson, K. R. and Ellis, B. (2006) Decoupled plant and insect diversity after the end-cretaceous extinction. *Science* 313, 1112-1115.

Williams, M., Haywood, A. M., Taylor, S. P., Valdes, P. J., Sellwood, B. W. and Hillenbrand, C.-D. (2004) Evaluating the efficacy of planktonic foraminifer calcite [delta]18O data for sea surface temperature reconstruction for the Late Miocene. *Geobios* 38 (6), 843-863.

Wilson, C. and Qiu, X. (2008) Global distribution of summer chlorophyll blooms in the oligotrophic gyres. *Progress In Oceanography* 78 (2), 107-134.

Wit, J. C., Reichart, G. J., A Jung, S. J. and Kroon, D. (2010) *Approaches to unravel seasonality in sea surface temperatures using paired single-specimen foraminiferal $\delta^{18}O$ and Mg/Ca analyses.* http://dx.doi.org/10.1029/2009PA001857 Accessed: 4

Zachos, J. C. and Arthur, M. A. (1986) Paleoceanography of the Cretaceous-Tertiary boundary event: Inferences from stable isotopic and other data. *Paleoceanography* 1 (1), 5-26.

Zachos, J. C., Arthur, M. A. and Dean, W. E. (1989) Geochemical evidence for suppression of pelagic marine productivity at the Cretaceous/Tertiary boundary. *Nature* 337, 61-64.

Zachos, J. C., Arthur, M. A., Thunell, R., Williams, D. F. and Tappa, E. J. (1985) Stable isotope and trace element geochemistry of carbonate sediments across the Cretaceous/Tertiary boundary at Deep sea Drilling Project Hole 577, Leg 86. In: Heathe, J. R., Burckle, L. H. and al., e. (eds.) *Initial Reports of the Deep Sea Drilling Project.* Vol. 86. Washington: U.S. Government Printing Office.

Zachos, J. C., Aubry, M. P., Berggren, W. A., Ehrendorfer, T., Heider, F. and Lohmann, K. C. (1992) Chemobiostratigraphy of the Cretaceous/Paleocene boundary at Site 750, southern Kerguelen Plateau. *Proc., scientific results, ODP, Leg 120, central Kerguelen Plateau* 961-977.

Zachos, J. C., Pagani, M., Sloan, L., Thomas, E. and Billups, K. (2001) Trends, Rhythms, and Aberrations in Global Climate 65 Ma to Present. *Science* 292 (5517), 686 - 693.

Zachos, J. C., Stott, L. D. and Lohmann, K. C. (1994) Evolution of Early Cenozoic Marine Temperatures. *Paleoceanography* 9 (2), 353-387.

Zar, J. H. (1996) *Biostatistical Analysis.* Prentice-Hall International, INC.

11. Appendix

11.1 Down hole stable isotope data

11.2 Sample percent weights

11.3 Species counts down core and Paleocene only genera percent counts

11.4 Number of species, genera and diversity statistics

11.5 Number of macroperforate verses microperforate species and genera

			G. falsostuarti		*R. fructicosa*		*H. holmdelensis*		*G. cretacea*	
Sample	Depth (mcd)	Age (Ma)	$\delta^{13}C$	$\delta^{18}O$	$\delta^{13}C$	$\delta^{18}O$	$\delta^{13}C$	$\delta^{18}O$	$\delta^{13}C$	$\delta^{18}O$
1262B-19H-5	185.03	60.86								
1262C-10H-5	185.74	60.94								
1262C-10H-3	186.09	60.99								
1262C-10H-3	186.45	61.05								
1262C-10H-3	187.18	61.15								
1262C-10H-4	187.9	61.25								
1262C-10H-4	188.62	61.34								
1262C-10H-5	189.34	61.43								
1262C-10H-5	190.06	61.52								
1262C-10H-6	190.78	61.60								
1262B-20H-2	191.6	61.69								
1262B-20H-2	192.23	61.78								
1262B-20H-3	192.95	61.86								
1262B-20H-3	193.67	61.94								
1262B-20H-4	194.41	62.03								
1262B-20H-4	194.83	62.11								
1262C-11H-2	195.85	62.20								
1262C-11H-3	198.1	62.46								
1262C-11H-4	198.73	62.56								
1262C-11H-4	199.45	62.67								
1262C-11H-5	200.16	62.78								
1262C-11H-5	200.88	62.89								
1262C-11H-6	201.73	63.01								
1262B-21H-1	202.48	63.09								
1262B-21H-2	203.2	63.17								
1262C-12H-1	203.92	63.33								
1262C-12H-2	204.64	63.47								
1262C-12H-2	205.33	63.60								
1262C-12H-3	205.84	63.70								
1262C-12H-3	206.49	63.82								
1262C-12H-3	207.21	63.96								
1262C-12H-4	207.93	64.08								
1262C-12H-4	208.71	64.21								
1262C-12H-5	209.43	64.33								
1262C-12H-5	210.36	64.48								
1262C-12H-5	211.08	64.59								
1262C-22H-1	212.03	64.74								
1262C-22H-2	213.03	64.92								
1262C-22H-3	214	65.10								
1262C-22H-3	214.54	65.20								
1262C-13H-1	214.9	65.29								
1262C-22H-3	215.08	65.32								
1262C-22H-4	215.23	65.36								
1262C-12H-1	215.64	65.46								
1262C-13H-1	215.9	65.53								
1262C-13H-2	216.1	65.56							1.67	-0.32
1262C-13H-2	216.32	65.62							1.68	-0.27
1262C-13H-2	216.57	65.66							1.81	-0.06
1262C-13H-2	216.69	65.68					1.92	-0.24	1.56	-0.42
1262C-13H-2	216.77	65.68							1.85	-0.30
1262C-13H-2	216.87	65.69	2.66	-0.31	3.42	-0.24	2.84	-0.01	1.05	-1.60
1262C-13H-3	217.54	65.71	2.51	-0.28	3.39	-0.19	2.73	-0.04		
1262C-13H-3	218.32	65.74	2.51	-0.34	2.93	-0.40	2.43	-0.04		
1262C-13H-6	222.4	65.93	2.38	-0.33	2.97	-0.15				
1262B-23H-2	225.22	66.07	2.32	-0.19	3.38	-0.29				

Appendix 11.1 – Down hole stable oxygen and carbon isotopes analysis.

			S. trivalis		*S. triloculinoides*		*Pr. taurica*	
Sample	Depth (mcd)	Age (Ma)	$\delta^{13}C$	$\delta^{18}O$	$\delta^{13}C$	$\delta^{18}O$	$\delta^{13}C$	$\delta^{18}O$
1262B-19H-5	185.03	60.86			2.66	-0.14		
1262C-10H-5	185.74	60.94			2.49	0.00		
1262C-10H-3	186.09	60.99			2.71	-0.15		
1262C-10H-3	186.45	61.05			2.59	0.20		
1262C-10H-3	187.18	61.15			2.40	-0.01		
1262C-10H-4	187.9	61.25			2.30	-0.05		
1262C-10H-4	188.62	61.34			2.21	0.05		
1262C-10H-5	189.34	61.43			2.59	0.00		
1262C-10H-5	190.06	61.52			2.32	0.18		
1262C-10H-6	190.78	61.60			2.33	0.02		
1262B-20H-2	191.6	61.69			2.28	0.22		
1262B-20H-2	192.23	61.78			2.29	-0.04		
1262B-20H-3	192.95	61.86			2.28	-0.02		
1262B-20H-3	193.67	61.94			2.31	0.11		
1262B-20H-4	194.41	62.03			2.20	0.03		
1262B-20H-4	194.83	62.11			2.21	0.11		
1262C-11H-2	195.85	62.20			2.43	0.19		
1262C-11H-3	198.1	62.46			2.27	0.14		
1262C-11H-4	198.73	62.56			2.11	0.16		
1262C-11H-4	199.45	62.67			2.21	0.06		
1262C-11H-5	200.16	62.78			2.14	0.14		
1262C-11H-5	200.88	62.89			2.08	0.05		
1262C-11H-6	201.73	63.01			2.21	0.04		
1262B-21H-1	202.48	63.09			2.11	0.11		
1262B-21H-2	203.2	63.17			1.71	-0.11		
1262C-12H-1	203.92	63.33			1.93	-0.04		
1262C-12H-2	204.64	63.47			1.91	-0.10		
1262C-12H-2	205.33	63.60			1.87	-0.03		
1262C-12H-3	205.84	63.70			2.07	-0.10		
1262C-12H-3	206.49	63.82			2.05	0.01		
1262C-12H-3	207.21	63.96			1.99	-0.24		
1262C-12H-4	207.93	64.08	2.10	0.05	2.11	0.01		
1262C-12H-4	208.71	64.21	1.83	-0.20			1.90	-0.43
1262C-12H-5	209.43	64.33	1.80	0.00			1.84	-0.11
1262C-12H-5	210.36	64.48	1.74	-0.10			1.87	-0.05
1262C-12H-5	211.08	64.59	1.97	0.09			1.95	-0.09
1262C-22H-1	212.03	64.74	1.91	-0.04			2.03	-0.36
1262C-22H-2	213.03	64.92	1.64	0.01			1.54	-0.35
1262C-22H-3	214	65.10	1.83	-0.05			1.83	-0.42
1262C-22H-3	214.54	65.20	1.87	-0.08			1.87	-0.49
1262C-13H-1	214.9	65.29	1.85	-0.05			1.88	-0.28
1262C-22H-3	215.08	65.32	1.84	-0.26			1.95	-0.53
1262C-22H-4	215.23	65.36	1.76	-0.10			1.94	-0.54
1262C-12H-1	215.64	65.46	1.89	0.06			2.02	-0.42
1262C-13H-1	215.9	65.53	2.14	0.13			2.19	-0.25
1262C-13H-2	216.1	65.56	2.23	0.11			2.29	-0.17
1262C-13H-2	216.32	65.62	2.19	0.31				
1262C-13H-2	216.57	65.66	2.00	0.04				
1262C-13H-2	216.69	65.68						
1262C-13H-2	216.77	65.68						
1262C-13H-2	216.87	65.69						
1262C-13H-3	217.54	65.71						
1262C-13H-3	218.32	65.74						
1262C-13H-6	222.4	65.93						
1262B-23H-2	225.22	66.07						

Appendix 11.1 – continued.

			Pr. inconstans		*M. angulata*		*M. praeangulata*		*N. truempyi*	
Sample	Depth (mcd)	Age (Ma)	$\delta^{13}C$	$\delta^{18}O$	$\delta^{13}C$	$\delta^{18}O$	$\delta^{13}C$	$\delta^{18}O$	$\delta^{13}C$	$\delta^{18}O$
1262B-19H-5	185.03	60.86							1.48	0.45
1262C-10H-5	185.74	60.94								
1262C-10H-3	186.09	60.99								
1262C-10H-3	186.45	61.05			3.17	-0.03			1.57	0.34
1262C-10H-3	187.18	61.15			3.21	-0.25				
1262C-10H-4	187.9	61.25			3.14	-0.53			0.99	0.41
1262C-10H-4	188.62	61.34			3.18	-0.47				
1262C-10H-5	189.34	61.43			3.63	-0.45			0.99	0.34
1262C-10H-5	190.06	61.52			3.43	-0.61				
1262C-10H-6	190.78	61.60			3.40	-0.82			1.26	0.32
1262B-20H-2	191.6	61.69			3.20	-0.69				
1262B-20H-2	192.23	61.78			3.18	-1.17			-0.98	-0.21
1262B-20H-3	192.95	61.86			3.20	-0.72				
1262B-20H-3	193.67	61.94			3.41	-0.98			1.02	0.35
1262B-20H-4	194.41	62.03	1.80	-0.45	2.90	-1.06				
1262B-20H-4	194.83	62.11	1.55	-0.09	2.93	-1.06	2.96	-0.69	0.87	0.16
1262C-11H-2	195.85	62.20	2.55	-0.19	3.25	-0.76	2.79	-0.23		
1262C-11H-3	198.1	62.46	3.04	-0.81	2.76	-0.73	2.69	-0.67	1.12	0.57
1262C-11H-4	198.73	62.56	2.88	-0.65	2.68	-0.53	2.73	-0.57		
1262C-11H-4	199.45	62.67	2.82	-0.73			2.66	-0.40	1.32	0.19
1262C-11H-5	200.16	62.78	2.60	-0.30			2.69	-0.69		
1262C-11H-5	200.88	62.89	2.50	-0.83					1.08	0.12
1262C-11H-6	201.73	63.01	2.83	-0.93						
1262B-21H-1	202.48	63.09	2.74	-0.79					1.16	0.34
1262B-21H-2	203.2	63.17	2.19	-0.97						
1262C-12H-1	203.92	63.33	2.32	-1.03					0.97	-0.21
1262C-12H-2	204.64	63.47	2.38	-1.12						
1262C-12H-2	205.33	63.60	1.87	-0.83					0.66	-0.09
1262C-12H-3	205.84	63.70	2.10	-0.88						
1262C-12H-3	206.49	63.82	2.23	-0.69					1.14	-0.12
1262C-12H-3	207.21	63.96	1.84	-0.42					1.27	0.48
1262C-12H-4	207.93	64.08	2.07	-0.62					1.09	0.44
1262C-12H-4	208.71	64.21	1.91	-0.14					1.04	0.10
1262C-12H-5	209.43	64.33							0.97	0.17
1262C-12H-5	210.36	64.48							1.29	0.01
1262C-12H-5	211.08	64.59							1.36	0.05
1262C-22H-1	212.03	64.74							1.27	0.47
1262C-22H-2	213.03	64.92							0.99	-0.09
1262C-22H-3	214	65.10							1.30	0.32
1262C-22H-3	214.54	65.20							1.49	0.05
1262C-13H-1	214.9	65.29							1.54	0.07
1262C-22H-3	215.08	65.32							1.52	0.05
1262C-22H-4	215.23	65.36							1.38	0.12
1262C-12H-1	215.64	65.46							1.79	0.10
1262C-13H-1	215.9	65.53							1.85	0.14
1262C-13H-2	216.1	65.56							2.02	0.13
1262C-13H-2	216.32	65.62							2.11	0.22
1262C-13H-2	216.57	65.66							2.25	0.26
1262C-13H-2	216.69	65.68							2.08	0.00
1262C-13H-2	216.77	65.68								
1262C-13H-2	216.87	65.69							2.10	0.38
1262C-13H-3	217.54	65.71							1.90	0.24
1262C-13H-3	218.32	65.74							1.60	0.42
1262C-13H-6	222.4	65.93							1.56	0.22
1262B-23H-2	225.22	66.07							1.28	0.58

Appendix 11.1 – continued.

Sample	Depth (mcd)	Age (Ma)	% weight >300	% weight 250-300	% weight 212-250	% weight 180-212	% weight 150-180	% weight 125-150	% weight 106-125	% weight 80-106	% weight 63-80	% weight 38-63
1262B-19H-5	185.05	60.86	1.51	2.46	3.32	6.77	5.49	16.40	11.34	21.62	16.83	14.26
1262B-19H-5	185.41	60.90	3.30	2.85	4.46	5.61	4.72	12.75	10.16	21.84	19.96	14.35
1262C-10H-2	185.79	60.95	10.46	4.03	4.11	6.80	4.63	14.79	10.98	23.75	15.09	5.38
1262C-10H-3	186.15	61.00	2.53	1.82	2.92	5.39	4.09	12.13	9.34	22.32	21.03	18.43
1262C-10H-3	186.51	61.05	3.30	4.71	7.36	9.93	6.73	16.30	9.77	18.35	13.60	9.95
1262C-10H-3	186.87	61.11	2.76	4.14	4.32	10.82	8.66	20.06	12.05	20.57	16.62	0.00
1262C-10H-3	187.23	61.16	5.35	6.02	8.35	11.85	7.28	15.11	8.59	16.11	13.55	7.78
1262C-10H-4	187.59	61.21	4.07	5.81	9.34	13.43	8.24	15.64	11.57	19.09	7.90	4.91
1262C-10H-4	187.95	61.26	6.36	9.22	10.75	12.62	7.00	24.19	5.59	13.73	6.30	4.25
1262C-10H-4	188.31	61.31	5.73	9.72	11.90	11.75	6.24	11.49	6.52	15.56	11.78	9.31
1262C-10H-4	188.67	61.35	5.68	9.87	13.01	12.72	6.05	10.51	5.80	13.29	14.15	8.92
1262C-10H-5	189.03	61.40	5.50	6.19	9.48	12.85	7.27	13.53	7.80	16.13	11.66	9.57
1262C-10H-5	189.39	61.44	5.45	7.21	10.46	12.30	7.07	13.52	7.62	14.66	11.77	9.95
1262C-10H-5	189.75	61.48	0.94	2.51	5.63	9.26	6.66	16.58	11.91	24.43	13.98	8.09
1262C-10H-5	190.11	61.52	6.81	5.32	6.89	9.27	6.27	15.44	10.23	21.29	11.51	6.97
1262C-10H-5	190.47	61.57	3.10	3.70	5.60	9.90	6.74	16.33	13.56	23.41	10.02	7.65
1262C-10H-6	190.83	61.61	2.45	4.68	8.10	11.39	7.24	15.49	10.09	27.21	13.36	0.00
1262B-20H-2	191.2	61.66	3.91	5.65	8.27	10.92	7.05	16.45	9.66	21.59	11.12	5.38
1262B-20H-2	191.56	61.70	7.90	4.76	6.15	9.65	6.51	16.24	10.02	20.58	11.39	6.80
1262B-20H-2	191.92	61.74	3.63	2.73	4.51	8.11	6.39	17.36	13.54	28.39	10.79	4.55
1262B-20H-3	192.28	61.79	2.55	2.10	4.11	8.46	6.78	19.49	12.38	25.17	12.63	6.33
1262B-20H-3	192.64	61.83	1.38	1.75	4.29	9.20	7.00	19.71	11.48	27.44	12.34	5.41
1262B-20H-3	193	61.87	4.67	2.97	5.06	10.62	7.66	20.15	12.81	20.97	9.79	5.28
1262B-20H-3	193.36	61.91	2.49	2.65	5.61	9.99	6.71	18.17	11.57	22.89	13.17	6.75
1262B-20H-3	193.72	61.95	2.66	5.02	8.99	13.95	8.01	19.45	9.21	19.75	9.13	3.83
1262B-20H-4	194.08	61.99	3.64	2.69	6.14	11.71	8.25	18.59	11.60	20.66	10.08	6.65
1262B-20H-4	194.47	62.04	1.58	1.76	4.36	10.68	9.00	19.30	12.85	26.48	9.45	4.55
1262B-20H-4	194.83	62.08	2.18	2.72	6.66	10.09	6.51	15.28	10.12	20.08	15.92	10.44
1262B-20H-4	195.19	62.12	0.64	1.52	5.64	9.94	6.74	17.39	11.89	24.55	14.47	7.22
1262B-20H-5	195.55	62.17	10.25	3.33	3.72	10.74	3.51	7.26	4.36	6.18	4.31	2.47
1262C-11H-2	195.9	62.21	0.57	1.31	4.48	9.92	6.55	19.84	18.08	26.07	11.05	2.13
1262C-11H-2	196.26	62.25	0.69	1.11	4.48	10.67	8.26	18.15	17.78	25.07	11.81	1.97
1262C-11H-3	197.7	62.43	0.22	0.63	2.92	6.58	6.05	17.83	12.99	30.53	16.07	6.18
1262C-11H-3	198.06	62.47	1.18	1.31	4.57	9.30	6.26	16.12	12.62	29.64	15.31	3.70
1262C-11H-3	198.42	62.51	1.64	1.16	3.24	7.16	6.41	15.71	11.93	27.95	17.85	6.96
1262C-11H-4	198.78	62.57	1.59	0.85	2.64	6.45	5.83	18.19	13.20	30.20	13.17	7.87
1262C-11H-4	199.14	62.62	1.35	0.68	2.08	5.71	5.29	15.71	13.00	32.33	15.25	8.61
1262C-11H-4	199.5	62.68	0.74	0.90	2.86	6.31	7.10	16.39	12.29	28.49	15.87	9.04
1262C-11H-4	199.86	62.73	2.44	1.61	4.33	8.04	5.78	16.90	11.08	23.46	19.49	6.87
1262C-11H-5	200.22	62.79	0.32	1.22	4.32	7.03	6.78	17.54	11.60	23.53	16.89	10.77
1262C-11H-5	200.58	62.84	0.28	1.05	4.07	7.35	6.58	17.13	11.69	20.46	15.69	15.68
1262C-11H-5	200.94	62.90	0.55	0.80	3.30	7.90	6.15	16.99	11.97	25.92	15.23	11.18
1262C-11H-5	201.3	62.95	0.54	1.41	4.84	10.05	7.56	18.03	10.15	19.57	17.58	10.27
1262B-21H-1	201.75	63.01	3.85	1.93	3.81	7.92	6.18	15.91	10.18	21.01	15.07	14.14
1262B-21H-1	202.14	63.05	0.26	0.62	2.18	5.92	5.90	19.27	12.14	22.04	18.49	13.18
1262B-21H-1	202.5	63.09	1.41	2.13	5.47	11.26	8.15	19.13	10.30	18.72	15.68	7.74
1262B-21H-2	202.86	63.13	0.46	1.45	4.20	8.91	7.48	19.12	11.64	23.90	14.87	7.96

Appendix 11.2 – Weight percent of different size fractions above 38 μm.

Sample	Depth (mcd)	Age (Ma)	% weight >300	% weight 250-300	% weight 212-250	% weight 180-212	% weight 150-180	% weight 125-150	% weight 106-125	% weight 80-106	% weight 63-80	% weight 38-63
1262B-21H-2	203.22	63.17	0.27	0.72	3.36	8.84	6.72	18.61	11.58	24.51	14.54	10.84
1262C-12H-1	203.58	63.25	0.42	0.82	3.15	7.27	5.81	16.62	10.69	26.58	18.48	10.19
1262C-12H-1	203.94	63.34	0.17	0.34	1.75	5.81	5.51	17.40	11.93	26.72	19.46	10.92
1262C-12H-2	204.3	63.41	0.50	0.75	3.36	9.19	7.65	18.53	10.32	22.32	18.08	9.29
1262C-12H-2	204.66	63.48	0.57	1.48	4.47	8.83	6.54	17.95	9.54	28.75	13.86	8.01
1262C-12H-2	205.02	63.54	0.92	0.43	1.83	4.62	4.85	15.78	11.66	27.82	20.47	11.62
1262C-12H-2	205.38	63.61	0.38	0.86	2.78	7.10	6.22	18.66	12.39	24.61	17.43	9.57
1262C-12H-2	205.77	63.68	1.46	0.21	1.08	3.86	4.32	15.76	13.00	29.75	20.07	10.49
1262C-12H-3	206.13	63.75	0.06	0.31	1.41	4.53	4.41	14.83	10.40	24.80	21.44	17.83
1262C-12H-3	206.49	63.82	0.27	0.18	0.70	3.04	3.73	14.55	10.65	24.93	20.15	21.81
1262C-12H-3	206.85	63.89	0.65	0.15	0.62	2.69	3.40	14.75	12.22	29.60	19.30	16.61
1262C-12H-3	207.21	63.95	0.63	0.82	2.12	5.55	4.87	16.07	11.92	24.13	17.71	16.17
1262C-12H-4	207.57	64.02	0.09	0.32	0.77	3.03	3.31	13.59	12.50	30.03	22.69	13.68
1262C-12H-4	207.93	64.08	0.20	0.10	0.42	1.61	1.61	5.39	3.70	73.94	6.40	6.62
1262C-12H-4	208.29	64.14	0.23	0.13	0.87	4.07	4.67	15.60	10.93	24.40	20.47	18.63
1262C-12H-4	208.71	64.21	1.14	0.89	0.64	1.68	2.57	11.57	11.37	26.21	19.24	24.68
1262C-12H-5	209.07	64.27	0.30	0.30	0.38	1.36	2.16	9.91	10.33	27.50	24.17	23.60
1262C-12H-5	209.43	64.32	0.18	0.14	0.14	0.60	1.02	7.76	9.60	30.29	25.30	24.98
1262C-12H-5	209.79	64.38	0.56	0.41	0.41	0.92	1.22	6.46	9.10	33.67	31.84	15.41
1262C-12H-6	210.36	64.47	0.55	0.28	0.22	0.55	0.72	4.81	5.58	27.57	33.20	26.52
1262C-12H-6	211.08	64.58	0.50	0.42	0.66	2.67	3.31	14.41	11.37	27.51	23.27	15.87
1262C-12H-7	211.57	64.66	0.00	0.00	0.07	0.97	2.16	7.58	8.03	26.47	31.45	23.27
1262B-22H-1	212.03	64.73	0.00	0.04	0.62	3.59	3.92	14.32	9.74	21.34	27.03	19.40
1262B-22H-1	212.54	64.82	0.19	0.06	0.25	1.78	2.72	11.70	10.01	27.78	28.28	17.23
1262B-22H-2	213.03	64.92	1.45	0.90	1.27	1.63	4.88	7.59	6.15	20.61	29.66	25.86
1262B-22H-2	213.51	65.01	0.31	0.22	0.40	2.31	3.53	12.12	9.08	30.89	27.41	13.73
1262B-22H-3	214	65.10	0.22	0.36	1.14	4.39	4.39	13.97	9.97	40.37	15.78	9.40
1262C-13H-1	214.9	65.29	1.22	0.36	1.19	3.65	4.22	15.22	9.79	34.18	17.42	12.75
1262C-13H-1	214.99	65.31	1.11	0.28	0.63	2.26	3.05	11.30	9.34	29.56	23.62	18.85
1262B-22H-3	215.08	65.32	0.39	0.30	0.41	1.41	2.17	10.04	9.28	29.43	25.94	20.64
1262B-22H-4	215.17	65.34	0.56	0.52	0.52	0.92	1.28	6.54	7.37	25.07	31.45	25.79
1262B-22H-4	215.23	65.36	1.85	0.34	0.50	0.76	0.67	4.21	6.06	22.88	32.88	29.86
1262C-13H-1	215.04	65.46	0.62	0.56	0.83	2.31	6.90	10.83	9.53	28.15	22.52	17.75
1262C-13H-1	215.9	65.53	1.87	1.06	1.24	1.92	1.70	5.80	5.52	17.66	31.66	31.57
1262C-13H-1	215.98	65.55	0.58	0.34	0.61	1.24	1.27	6.75	6.11	32.85	30.60	19.64
1262C-13H-2	216.1	65.57	0.31	0.43	1.05	2.21	2.11	7.11	6.73	33.74	25.80	20.50
1262C-13H-2	216.22	65.59	0.42	0.47	0.52	1.01	1.52	4.47	4.96	21.89	37.44	27.29
1262C-13H-2	216.32	65.61	0.18	0.71	1.46	2.81	2.65	8.42	8.96	39.26	22.08	13.47
1262C-13H-2	216.46	65.64	0.47	0.39	0.75	1.61	1.70	7.42	9.94	37.04	26.30	14.37
1262C-13H-2	216.57	65.66	0.19	0.23	0.38	0.76	0.63	2.97	5.81	45.44	23.24	20.35
1262C-13H-2	216.69	65.68	2.62	1.67	2.39	2.92	1.73	4.65	4.23	12.88	29.93	36.97
1262C-13H-2	216.87	65.69	13.85	7.36	8.36	8.76	4.55	9.90	7.22	15.99	14.45	9.57
1262C-13H-2	217.17	65.70	21.16	8.87	8.65	8.87	4.54	8.27	6.08	14.52	11.65	7.41
1262C-13H-3	217.54	65.71	11.30	7.63	9.29	11.24	6.14	11.82	7.75	16.12	12.62	6.08
1262C-13H-3	217.9	65.72	11.63	8.94	10.08	10.98	5.45	10.33	6.26	16.02	13.41	6.91
1262C-13H-3	218.32	65.74	11.68	6.40	9.76	12.96	6.40	11.20	5.60	12.64	14.08	9.28
1262C-13H-3	218.71	65.76	19.75	10.60	10.40	10.24	4.90	8.46	5.30	11.61	10.12	8.62

Appendix 11.2 – Continued.

				Macroperforate Planktonic Foraminifera													
				Eoglobigerina			Globanomalina						Hedb-ergella		Igorina	
Sample	Depth (mcd)	PF Zone	Age (Ma)	edita	cobulloides	spiralis	archeocompressa	chapmani	compressa	ehrenbergi	imitata	planocompressa	holmdelensis	monmouthensis	albeari	pusilla
1262B-19H-5	185.05	P3b	60.86					12		1					10	2
1262C-10H-2	185.79	P3b	60.95					10			5				5	1
1262C-10H-3	186.51	P3b	61.05					16			2				6	
1262C-10H-3	187.23	P3b	61.16					23		5	1				6	
1262C-10H-4	187.95	P3b	61.26					21		1	6				6	
1262c-10h-4	188.67	P3b	61.35					16		1					9	
1262C-10H-5	189.39	P3b	61.44					18		1	2				5	1
1262C-10H-5	190.11	P3b	61.52					37		3					7	3
1262C-10H-6	190.83	P3b	61.61					34		20					19	
1262B-20H-2	191.56	P3b	61.70					17		10	1				5	1
1262B-20H-3	192.28	P3b	61.79					26		14					12	2
1262B-20H-3	193.00	P3b	61.87					46		17					5	
1262B-20H-3	193.72	P3b	61.95					36		14					2	
1262B-20H-4	194.47	P3b	62.03					14		24	1				3	1
1262B-20H-4	195.19	P3b	62.12					7		39					3	6
1262C-11H-2	195.90	P3a	62.21					5	1	17						
1262C-11H-3	197.70	P3a	62.42							18						1
1262C-11H-3	198.42	P3a	62.51						11	22	1					
1262C-11H-4	199.14	P2	62.62						3	12						
1262C-11H-4	199.86	P2	62.73						11	16						
1262C-11H-5	200.58	P2	62.84						23	16						
1262C-11H-5	201.30	P2	62.95			1			20	3						
1262B-21H-1	202.14	P2	63.05	4					28							
1262B-21H-2	202.86	P1c	63.13	2					53							
1262C-12H-1	203.58	P1c	63.25	4					34							
1262C-12H-2	204.30	P1c	63.41	7					26			5				
1262C-12H-2	205.02	P1c	63.54	3					28			6				
1262C-12H-2	205.77	P1c	63.68	2					30			6				
1262C-12H-3	206.49	P1c	63.82	1					29			12				
1262C-12H-3	207.21	P1c	63.95	4					47			15				
1262C-12H-4	207.93	P1c	64.08	5					47			8				
1262C-12H-4	208.71	P1c	64.21	2					46			13				
1262C-12H-5	209.43	P1c	64.32	2					39			14				
1262C-12H-6	210.36	P1c	64.47	3					4			32				
1262C-12H-6	211.08	P1b	64.58	2			1					53				
1262B-22H-1	212.03	P1b	64.73	5	2		2					45				
1262B-22H-2	213.03	P1b	64.92	32	7		1					21				
1262B-22H-3	214.00	P1b	65.10	42	29		3					26				
1262C-13H-1	214.90	P1b	65.29	44	25		5					32				
1262B-22H-3	215.08	P1b	65.32	28	38		1					13				
1262B-22H-4	215.23	P1b	65.36	35	47		1					8				
1262C-13H-1	215.64	P1b	65.46	33	49		2					7				
1262C-13H-1	215.90	P1b	65.53	16	54		5					2				
1262C-13H-2	216.10	P1b	65.57	8	67		1					3				
1262C-13H-2	216.32	P1b	65.61	7	54		1					1				
1262C-13H-2	216.57	P1a	65.66	5	49		4					5				
1262C-13H-2	216.69	Pα	65.68	2	24		6					2	3	2		
1262C-13H-2	216.87	Cretaceous	65.69										51			
1262C-13H-3	217.54	Cretaceous	65.71										37			

Appendix 11.3 - Species counts. PF Zone (Olsson et al. 1999; Berger & Pearson 2005)

				Macroperforate Planktonic Foraminifera												
				Morozovella								Praemurica				
Sample	Depth (mcd)	PF Zone	Age (Ma)	acutispira	angulata	apanthesma	conicotruncata	occlusa	pasionensis	praeangulata	velascoensis	inconstans	pseudoinconstans	taurica	uncinata
1262B-19H-5	185.05	P3b	60.86	1	37	53		45	1						
1262C-10H-2	185.79	P3b	60.95		3	7		2			1				
1262C-10H-3	186.51	P3b	61.05	1	19	84	2	34	5		3				
1262C-10H-3	187.23	P3b	61.16	1	20	82	1	24	1		4				
1262C-10H-4	187.95	P3b	61.26	1	19	75	1	41	4		1				
1262c-10h-4	188.67	P3b	61.35		36	87	2	30	4		1				
1262C-10H-5	189.39	P3b	61.44		21	70	6	29	3		5				
1262C-10H-5	190.11	P3b	61.52		22	32		8			2				
1262C-10H-6	190.83	P3b	61.61		28	25		4							
1262B-20H-2	191.56	P3b	61.70		13	38	2								
1262B-20H-3	192.28	P3b	61.79		26	37					1				
1262B-20H-3	193.00	P3b	61.87		23	20					1				
1262B-20H-3	193.72	P3b	61.95		32	23	1				3				
1262B-20H-4	194.47	P3b	62.03		39	20					1				
1262B-20H-4	195.19	P3b	62.12		33	11	3								
1262C-11H-2	195.90	P3a	62.21		17	3				4		4			2
1262C-11H-3	197.70	P3a	62.42		13					12		16			20
1262C-11H-3	198.42	P3a	62.51		17					14		17			14
1262C-11H-4	199.14	P2	62.62							26		34			43
1262C-11H-4	199.86	P2	62.73							8		29	8		18
1262C-11H-5	200.58	P2	62.84							6		34	5		14
1262C-11H-5	201.30	P2	62.95							3		44	16		14
1262B-21H-1	202.14	P2	63.05							1		31	8		4
1262B-21H-2	202.86	P1c	63.13									39	11		
1262C-12H-1	203.58	P1c	63.25									38	27		
1262C-12H-2	204.30	P1c	63.41									31	17		
1262C-12H-2	205.02	P1c	63.54									30	39		
1262C-12H-2	205.77	P1c	63.68									19	61		
1262C-12H-3	206.49	P1c	63.82									43	26	5	
1262C-12H-3	207.21	P1c	63.95									36	36	17	
1262C-12H-4	207.93	P1c	64.08									36	38	33	
1262C-12H-4	208.71	P1c	64.21									23	44	58	
1262C-12H-5	209.43	P1c	64.32									14	34	65	
1262C-12H-6	210.36	P1c	64.47									9	66	70	
1262C-12H-6	211.08	P1b	64.58										32	83	
1262B-22H-1	212.03	P1b	64.73										35	66	
1262B-22H-2	213.03	P1b	64.92										46	84	
1262B-22H-3	214.00	P1b	65.10										24	56	
1262C-13H-1	214.90	P1b	65.29										28	62	
1262B-22H-3	215.08	P1b	65.32										19	57	
1262B-22H-4	215.23	P1b	65.36										11	51	
1262C-13H-1	215.64	P1b	65.46										15	42	
1262C-13H-1	215.90	P1b	65.53										12	36	
1262C-13H-2	216.10	P1b	65.57										11	18	
1262C-13H-2	216.32	P1b	65.61										10	16	
1262C-13H-2	216.57	P1a	65.66										8	15	
1262C-13H-2	216.69	Pα	65.68											11	
1262C-13H-2	216.87	Cretaceous	65.69												
1262C-13H-3	217.54	Cretaceous	65.71												

Appendix 11.3 – Continued.

				Macroperforate Planktonic Foraminifera							
				Parasubbotina				Subbotina			
Sample	Depth (mcd)	PF Zone	Age (Ma)	aff pseudobulloides	pseudobulloides	varianta	variospira	cancellata	triangularis	trilocullinoides	trivalis
1262B-19H-5	185.05	P3b	60.86		1	30	3	67	21	4	
1262C-10H-2	185.79	P3b	60.95			13		16	5	2	
1262C-10H-3	186.51	P3b	61.05			21	3	84	15	4	
1262C-10H-3	187.23	P3b	61.16			13	5	93	12	5	
1262C-10H-4	187.95	P3b	61.26			24	7	53	18	6	
1262c-10h-4	188.67	P3b	61.35			29	7	56	8	6	
1262C-10H-5	189.39	P3b	61.44			53	9	62	4	5	
1262C-10H-5	190.11	P3b	61.52			50	5	110	5	12	
1262C-10H-6	190.83	P3b	61.61		2	59	4	80	9	8	
1262B-20H-2	191.56	P3b	61.70			90	34	66	7	10	
1262B-20H-3	192.28	P3b	61.79		2	51	8	89	3	20	
1262B-20H-3	193.00	P3b	61.87		1	63	7	77	6	18	
1262B-20H-3	193.72	P3b	61.95			54	3	96	4	22	
1262B-20H-4	194.47	P3b	62.03			73	6	87	2	19	
1262B-20H-4	195.19	P3b	62.12			84	3	79	1	18	
1262C-11H-2	195.90	P3a	62.21			107	3	98	2	28	
1262C-11H-3	197.70	P3a	62.42			94	4	91		23	
1262C-11H-3	198.42	P3a	62.51		1	76	2	98		24	
1262C-11H-4	199.14	P2	62.62		3	79		72		18	3
1262C-11H-4	199.86	P2	62.73		5	74		77		39	5
1262C-11H-5	200.58	P2	62.84		4	71		81		26	13
1262C-11H-5	201.30	P2	62.95		1	86		46		31	29
1262B-21H-1	202.14	P2	63.05		2	85		35		57	34
1262B-21H-2	202.86	P1c	63.13		2	90		13		48	26
1262C-12H-1	203.58	P1c	63.25		3	68		18		56	30
1262C-12H-2	204.30	P1c	63.41		2	91		22		43	28
1262C-12H-2	205.02	P1c	63.54		5	41		24		55	38
1262C-12H-2	205.77	P1c	63.68		5	41		23		57	29
1262C-12H-3	206.49	P1c	63.82		4	29		31		53	43
1262C-12H-3	207.21	P1c	63.95		2	11		3		31	34
1262C-12H-4	207.93	P1c	64.08		1	14				36	38
1262C-12H-4	208.71	P1c	64.21		2	12				27	53
1262C-12H-5	209.43	P1c	64.32		2	9				28	51
1262C-12H-6	210.36	P1c	64.47		1	7				27	61
1262C-12H-6	211.08	P1b	64.58		3					15	56
1262B-22H-1	212.03	P1b	64.73		3					22	63
1262B-22H-2	213.03	P1b	64.92		6					10	37
1262B-22H-3	214.00	P1b	65.10		3					33	41
1262C-13H-1	214.90	P1b	65.29		2					42	35
1262B-22H-3	215.08	P1b	65.32		3					47	44
1262B-22H-4	215.23	P1b	65.36		3					52	34
1262C-13H-1	215.64	P1b	65.46		9					47	28
1262C-13H-1	215.90	P1b	65.53		17					43	34
1262C-13H-2	216.10	P1b	65.57		6					25	27
1262C-13H-2	216.32	P1b	65.61		7					15	35
1262C-13H-2	216.57	P1a	65.66		10						56
1262C-13H-2	216.69	Pα	65.68	6							27
1262C-13H-2	216.87	Cretaceous	65.69								
1262C-13H-3	217.54	Cretaceous	65.71								

Appendix 11.3 - Continued.

Sample	Depth (mcd)	PF Zone	Age (Ma)	Benthic	Microperforate Planktonic Foraminifera									
					Globoconusa daubergensis	Guembelitria cretacea	Chiloguembelina midwayensis	Chiloguembelina morsei	Parvularugoglobigerina alabamensis	Parvularugoglobigerina eugubina	Rectoguembelina cretacea	Woodringina claytonensis	Woodringina hornestownensis	Zeauvigerina waiparaensis
1262B-19H-5	185.05	P3b	60.86	10										
1262C-10H-2	185.79	P3b	60.95	225			1							2
1262C-10H-3	186.51	P3b	61.05	2										
1262C-10H-3	187.23	P3b	61.16	4										
1262C-10H-4	187.95	P3b	61.26	5					1					
1262c-10h-4	188.67	P3b	61.35	8										
1262C-10H-5	189.39	P3b	61.44	4			1							1
1262C-10H-5	190.11	P3b	61.52	2			2							
1262C-10H-6	190.83	P3b	61.61	2			5							1
1262B-20H-2	191.56	P3b	61.70				2							1
1262B-20H-3	192.28	P3b	61.79	3			3				1			2
1262B-20H-3	193.00	P3b	61.87	1			10		1				4	
1262B-20H-3	193.72	P3b	61.95	1			9							
1262B-20H-4	194.47	P3b	62.03	1			6						2	1
1262B-20H-4	195.19	P3b	62.12	9			1							
1262C-11H-2	195.90	P3a	62.21	5			3							
1262C-11H-3	197.70	P3a	62.42	4			2		1					
1262C-11H-3	198.42	P3a	62.51	3										
1262C-11H-4	199.14	P2	62.62	4			2		1					
1262C-11H-4	199.86	P2	62.73	2			4						3	
1262C-11H-5	200.58	P2	62.84	6			1							
1262C-11H-5	201.30	P2	62.95	3			3							
1262B-21H-1	202.14	P2	63.05	3	6		2							
1262B-21H-2	202.86	P1c	63.13	3	11		1						1	
1262C-12H-1	203.58	P1c	63.25	3	15		3	1						
1262C-12H-2	204.30	P1c	63.41	6	17		5	1						
1262C-12H-2	205.02	P1c	63.54	1	29		1							
1262C-12H-2	205.77	P1c	63.68	3	14		6	2	1				1	
1262C-12H-3	206.49	P1c	63.82	3	16		5						1	
1262C-12H-3	207.21	P1c	63.95	8	42		9	2	1		1			
1262C-12H-4	207.93	P1c	64.08	4	32		8							
1262C-12H-4	208.71	P1c	64.21	2	7		9	1						
1262C-12H-5	209.43	P1c	64.32	13	11		15	1					2	
1262C-12H-6	210.36	P1c	64.47	6	6		7						1	
1262C-12H-6	211.08	P1b	64.58	27	19		6		1				1	
1262B-22H-1	212.03	P1b	64.73	4	34		15	3					1	
1262B-22H-2	213.03	P1b	64.92	28	9		13						6	
1262B-22H-3	214.00	P1b	65.10	3	5		18	7					10	
1262C-13H-1	214.90	P1b	65.29	4	1		12	2					6	
1262B-22H-3	215.08	P1b	65.32	8	6	10	6	12				2	8	
1262B-22H-4	215.23	P1b	65.36	28	1	3	18	8					4	
1262C-13H-1	215.64	P1b	65.46	14	1	23	17	8					6	
1262C-13H-1	215.90	P1b	65.53	14	2	14	20	7					6	
1262C-13H-2	216.10	P1b	65.57	8	2	29	58	16					18	
1262C-13H-2	216.32	P1b	65.61	9		43	47	38					19	
1262C-13H-2	216.57	P1a	65.66	15		44	27	18				1	12	
1262C-13H-2	216.69	Pα	65.68	19		11	2	12		34		6	19	4
1262C-13H-2	216.87	Cretaceous	65.69	4										
1262C-13H-3	217.54	Cretaceous	65.71	6										

Appendix 11.3 – Continued.

Sample	Depth (mcd)	PF Zone	Age (Ma)	Cretaceous Planktonic Foraminifera												
				Cretaceous reworking	Abathomphalus mayaroensis	Globotruncanella citae	Globigerinelloides subcarinata	Globotruncana aegyptica	Globotruncana arca	Globotruncana falsostuarti	Globotruncanella havanensis	Globotruncanella petaloidea	Globotruncanita conica	Globotruncanita stuarti	Heterohelix navarroensis
1262B-19H-5	185.05	P3b	60.86												
1262C-10H-2	185.79	P3b	60.95												
1262C-10H-3	186.51	P3b	61.05												
1262C-10H-3	187.23	P3b	61.16												
1262C-10H-4	187.95	P3b	61.26												
1262c-10h-4	188.67	P3b	61.35												
1262C-10H-5	189.39	P3b	61.44												
1262C-10H-5	190.11	P3b	61.52												
1262C-10H-6	190.83	P3b	61.61												
1262B-20H-2	191.56	P3b	61.70												
1262B-20H-3	192.28	P3b	61.79												
1262B-20H-3	193.00	P3b	61.87												
1262B-20H-3	193.72	P3b	61.95												
1262B-20H-4	194.47	P3b	62.03												
1262B-20H-4	195.19	P3b	62.12												
1262C-11H-2	195.90	P3a	62.21												
1262C-11H-3	197.70	P3a	62.42												
1262C-11H-3	198.42	P3a	62.51												
1262C-11H-4	199.14	P2	62.62												
1262C-11H-4	199.86	P2	62.73												
1262C-11H-5	200.58	P2	62.84												
1262C-11H-5	201.30	P2	62.95												
1262B-21H-1	202.14	P2	63.05												
1262B-21H-2	202.86	P1c	63.13												
1262C-12H-1	203.58	P1c	63.25												
1262C-12H-2	204.30	P1c	63.41												
1262C-12H-2	205.02	P1c	63.54												
1262C-12H-2	205.77	P1c	63.68												
1262C-12H-3	206.49	P1c	63.82												
1262C-12H-3	207.21	P1c	63.95												
1262C-12H-4	207.93	P1c	64.08												
1262C-12H-4	208.71	P1c	64.21												
1262C-12H-5	209.43	P1c	64.32												
1262C-12H-6	210.36	P1c	64.47												
1262C-12H-6	211.08	P1b	64.58												
1262B-22H-1	212.03	P1b	64.73												
1262B-22H-2	213.03	P1b	64.92												
1262B-22H-3	214.00	P1b	65.10												
1262C-13H-1	214.90	P1b	65.29												
1262B-22H-3	215.08	P1b	65.32												
1262B-22H-4	215.23	P1b	65.36												
1262C-13H-1	215.64	P1b	65.46												
1262C-13H-1	215.90	P1b	65.53	18											
1262C-13H-2	216.10	P1b	65.57	4											
1262C-13H-2	216.32	P1b	65.61												
1262C-13H-2	216.57	P1a	65.66	31											
1262C-13H-2	216.69	Pα	65.68	109											
1262C-13H-2	216.87	Cretaceous	65.69					3	12	6	2	5	3	1	87
1262C-13H-3	217.54	Cretaceous	65.71		2	1	1	5	15	11	2	12	6	3	51

Appendix 11.3 – Continued.

				Cretaceous Planktonic Foraminifera											
Sample	Depth (mcd)	PF Zone	Age (Ma)	Pseudoguembelina costulata	Pseudoguembelina palpebra	Pseudotextularia elegans	Racemiguembelina fructicosa	Racemiguembelina glabrata	Rosita contusa	Rugoglobigerina hexacamerata	Rugoglobigerina macrocephala	Rugoglobigerina reicheli	Rugoglobigerina rugosa	Rugoglobigerina scotti
1262B-19H-5	185.05	P3b	60.86											
1262C-10H-2	185.79	P3b	60.95											
1262C-10H-3	186.51	P3b	61.05											
1262C-10H-3	187.23	P3b	61.16											
1262C-10H-4	187.95	P3b	61.26											
1262c-10h-4	188.67	P3b	61.35											
1262C-10H-5	189.39	P3b	61.44											
1262C-10H-5	190.11	P3b	61.52											
1262C-10H-6	190.83	P3b	61.61											
1262B-20H-2	191.56	P3b	61.70											
1262B-20H-3	192.28	P3b	61.79											
1262B-20H-3	193.00	P3b	61.87											
1262B-20H-3	193.72	P3b	61.95											
1262B-20H-4	194.47	P3b	62.03											
1262B-20H-4	195.19	P3b	62.12											
1262C-11H-2	195.90	P3a	62.21											
1262C-11H-3	197.70	P3a	62.42											
1262C-11H-3	198.42	P3a	62.51											
1262C-11H-4	199.14	P2	62.62											
1262C-11H-4	199.86	P2	62.73											
1262C-11H-5	200.58	P2	62.84											
1262C-11H-5	201.30	P2	62.95											
1262B-21H-1	202.14	P2	63.05											
1262B-21H-2	202.86	P1c	63.13											
1262C-12H-1	203.58	P1c	63.25											
1262C-12H-2	204.30	P1c	63.41											
1262C-12H-2	205.02	P1c	63.54											
1262C-12H-2	205.77	P1c	63.68											
1262C-12H-3	206.49	P1c	63.82											
1262C-12H-3	207.21	P1c	63.95											
1262C-12H-4	207.93	P1c	64.08											
1262C-12H-4	208.71	P1c	64.21											
1262C-12H-5	209.43	P1c	64.32											
1262C-12H-6	210.36	P1c	64.47											
1262C-12H-6	211.08	P1b	64.58											
1262B-22H-1	212.03	P1b	64.73											
1262B-22H-2	213.03	P1b	64.92											
1262B-22H-3	214.00	P1b	65.10											
1262C-13H-1	214.90	P1b	65.29											
1262B-22H-3	215.08	P1b	65.32											
1262B-22H-4	215.23	P1b	65.36											
1262C-13H-1	215.64	P1b	65.46											
1262C-13H-1	215.90	P1b	65.53											
1262C-13H-2	216.10	P1b	65.57											
1262C-13H-2	216.32	P1b	65.61											
1262C-13H-2	216.57	P1a	65.66											
1262C-13H-2	216.69	Pα	65.68											
1262C-13H-2	216.87	Cretaceous	65.69	12	36	23	21	18	3	2	2	6	2	1
1262C-13H-3	217.54	Cretaceous	65.71	21	26	27	22	20	3	10	7	1	8	3

Appendix 11.3 – Continued.

Sample	Depth (MCD)	PF Zone	Age Opt. 2 Ma	*Eoglobigerina*	*Globanomalina*	*Hedbergella*	*Igorina*	*Morozovella*	*Parasubbotina*	*Praemurica*	*Subbotina*	microperforates
1262B-19H-5	185.50	P3b	60.86	0.0	4.4	0.0	4.3	46.0	11.5	0.0	3.9	0.0
1262C-1H-2	185.79	P3b	60.95	0.0	5.3	0.0	2.1	4.4	4.4	0.0	7.7	1.0
1262C-1H-3	186.51	P3b	61.50	0.0	6.0	0.0	2.0	49.2	8.0	0.0	34.2	0.0
1262C-1H-3	187.23	P3b	61.16	0.0	9.7	0.0	2.0	44.3	6.0	0.0	36.7	0.0
1262C-1H-4	187.95	P3b	61.26	0.0	9.7	0.0	2.7	49.0	1.7	0.0	26.6	0.3
1262c-1h-4	188.67	P3b	61.35	0.0	5.7	0.0	3.0	53.3	12.0	0.0	23.3	0.0
1262C-1H-5	189.39	P3b	61.44	0.0	7.0	0.0	2.0	44.7	2.7	0.0	23.7	0.7
1262C-1H-5	19.11	P3b	61.52	0.0	13.3	0.0	3.3	21.3	18.3	0.0	42.3	0.7
1262C-1H-6	19.83	P3b	61.61	0.0	18.0	0.0	6.3	19.0	21.7	0.0	32.3	2.0
1262B-2H-2	191.56	P3b	61.70	0.0	9.4	0.0	2.2	17.8	41.8	0.0	27.9	1.0
1262B-2H-3	192.28	P3b	61.79	0.0	13.3	0.0	4.7	21.3	2.3	0.0	37.3	2.0
1262B-2H-3	193.00	P3b	61.87	0.0	21.0	0.0	1.7	14.7	23.7	0.0	33.7	5.0
1262B-2H-3	193.72	P3b	61.95	0.0	16.7	0.0	0.7	19.7	19.0	0.0	4.7	3.0
1262B-2H-4	194.47	P3b	62.30	0.0	13.0	0.0	1.3	2.0	26.3	0.0	36.0	3.0
1262B-2H-4	195.19	P3b	62.12	0.0	15.3	0.0	3.0	15.7	29.0	0.0	32.7	0.3
1262C-11H-2	195.90	P3a	62.21	0.0	7.7	0.0	0.0	8.0	36.7	2.0	42.7	1.0
1262C-11H-3	197.70	P3a	62.42	0.0	6.0	0.0	0.3	8.4	32.6	12.0	37.9	1.0
1262C-11H-3	198.42	P3a	62.51	0.0	11.3	0.0	0.0	1.3	26.3	1.3	4.7	0.0
1262C-11H-4	199.14	P2	62.62	0.0	5.0	0.0	0.0	8.7	27.3	25.7	31.0	1.0
1262C-11H-4	199.86	P2	62.73	0.0	9.3	0.0	0.0	2.7	26.4	18.4	4.5	2.7
1262C-11H-5	2.58	P2	62.84	0.0	13.0	0.0	0.0	2.0	25.0	17.7	4.0	0.3
1262C-11H-5	21.30	P2	62.95	0.3	7.7	0.0	0.0	1.0	29.0	24.7	35.3	1.0
1262B-21H-1	22.14	P2	63.50	1.3	9.3	0.0	0.0	0.3	29.0	14.3	42.0	2.7
1262B-21H-2	22.86	P1c	63.13	0.7	17.7	0.0	0.0	0.0	3.7	16.7	29.0	4.3
1262C-12H-1	23.58	P1c	63.25	1.3	11.3	0.0	0.0	0.0	23.7	21.7	34.7	6.3
1262C-12H-2	24.30	P1c	63.41	2.3	1.3	0.0	0.0	0.0	3.9	15.9	3.9	7.6
1262C-12H-2	25.20	P1c	63.54	1.0	11.3	0.0	0.0	0.0	15.3	23.0	39.0	10.0
1262C-12H-2	25.77	P1c	63.68	0.7	12.0	0.0	0.0	0.0	15.3	26.7	36.3	8.0
1262C-12H-3	26.49	P1c	63.82	0.3	13.6	0.0	0.0	0.0	2.0	24.6	42.2	7.3
1262C-12H-3	27.21	P1c	63.95	1.3	2.7	0.0	0.0	0.0	4.3	29.8	22.7	18.8
1262C-12H-4	27.93	P1c	64.08	1.7	18.3	0.0	0.0	0.0	5.0	35.7	24.7	4.3
1262C-12H-4	28.71	P1c	64.21	0.7	19.7	0.0	0.0	0.0	4.7	41.9	26.8	5.7
1262C-12H-5	29.43	P1c	64.32	0.7	17.7	0.0	0.0	0.0	3.7	37.7	26.3	9.7
1262C-12H-6	21.36	P1c	64.47	1.0	12.0	0.0	0.0	0.0	2.7	48.3	29.3	4.7
1262C-12H-6	211.80	P1b	64.58	0.7	18.6	0.0	0.0	0.0	1.3	38.5	23.7	9.7
1262B-22H-1	212.30	P1b	64.73	2.3	15.7	0.0	0.0	0.0	1.0	33.7	28.3	17.7
1262B-22H-2	213.30	P1b	64.92	13.0	7.3	0.0	0.0	0.0	2.0	43.3	15.7	9.3
1262B-22H-3	214.00	P1b	65.97	23.7	9.7	0.0	0.0	0.0	1.0	26.7	24.7	13.3
1262C-13H-1	214.90	P1b	65.29	23.0	12.3	0.0	0.0	0.0	0.7	3.0	25.7	7.0
1262B-22H-3	215.80	P1b	65.32	21.9	4.6	0.0	0.0	0.0	1.0	25.2	3.1	14.6
1262B-22H-4	215.23	P1b	65.36	27.0	3.0	0.0	0.0	0.0	1.0	2.4	28.3	11.2
1262C-13H-1	215.64	P1b	65.46	27.2	3.0	0.0	0.0	0.0	3.0	18.9	24.9	18.3
1262C-13H-1	215.90	P1b	65.53	23.3	2.3	0.0	0.0	0.0	5.7	16.0	25.7	16.3
1262C-13H-2	216.10	P1b	65.57	24.9	1.3	0.0	0.0	0.0	2.0	9.6	17.3	40.9
1262C-13H-2	216.32	P1b	65.61	2.2	0.7	0.0	0.0	0.0	2.3	8.7	16.6	48.7
1262C-13H-2	216.57	P1a	65.66	18.0	3.0	0.0	0.0	0.0	3.3	7.7	18.7	34.0
1262C-13H-2	216.69	Pα	65.68	8.7	2.7	1.7	0.0	0.0	2.7	3.7	9.3	29.4

Appendix 11.3 – Paleocene only genera percent counts.

Sample	Depth (mcd)	Age (Ma)	No. of species >106 (ex. Benthic)	No. of genera >106 (ex. Benthic)	No. of genera 38 - 106 (ex. Benthic)	Shannon - H'	Evenness - J'
1262B-19H-5	185.05	60.86	15	5	6	2.18	0.520
1262C-10H-2	185.79	60.95	14	7	7	1.12	0.267
1262C-10H-3	186.51	61.05	15	5	7	2.04	0.487
1262C-10H-3	187.23	61.16	16	5	8	2.04	0.486
1262C-10H-4	187.95	61.26	17	6	8	2.24	0.535
1262c-10h-4	188.67	61.35	14	5	8	2.13	0.509
1262C-10H-5	189.39	61.44	18	7	7	2.21	0.528
1262C-10H-5	190.11	61.52	14	6	8	2.00	0.477
1262C-10H-6	190.83	61.61	14	7	8	2.17	0.519
1262B-20H-2	191.56	61.70	14	7	7	2.02	0.482
1262B-20H-3	192.28	61.79	16	8	8	2.17	0.518
1262B-20H-3	193.00	61.87	15	8	8	2.15	0.514
1262B-20H-3	193.72	61.95	13	6	7	2.02	0.483
1262B-20H-4	194.47	62.03	16	8	8	2.01	0.481
1262B-20H-4	195.19	62.12	14	6	7	1.96	0.468
1262C-11H-2	195.90	62.21	15	6	9	1.76	0.420
1262C-11H-3	197.70	62.42	13	8	8	1.88	0.449
1262C-11H-3	198.42	62.51	12	5	9	1.96	0.467
1262C-11H-4	199.14	62.62	12	7	8	1.98	0.472
1262C-11H-4	199.86	62.73	13	7	9	2.10	0.502
1262C-11H-5	200.58	62.84	12	6	8	2.09	0.498
1262C-11H-5	201.30	62.95	13	7	8	2.09	0.499
1262B-21H-1	202.14	63.05	13	8	9	2.05	0.489
1262B-21H-2	202.86	63.13	12	8	8	1.97	0.470
1262C-12H-1	203.58	63.25	12	7	8	2.14	0.510
1262C-12H-2	204.30	63.41	13	7	9	2.18	0.519
1262C-12H-2	205.02	63.54	12	7	9	2.22	0.530
1262C-12H-2	205.77	63.68	15	9	9	2.26	0.539
1262C-12H-3	206.49	63.82	14	8	7	2.32	0.554
1262C-12H-3	207.21	63.95	16	9	8	2.40	0.574
1262C-12H-4	207.93	64.08	12	7	9	2.29	0.545
1262C-12H-4	208.71	64.21	13	7	9	2.19	0.522
1262C-12H-5	209.43	64.32	14	8	8	2.28	0.545
1262C-12H-6	210.36	64.47	13	8	9	2.03	0.485
1262C-12H-6	211.08	64.58	12	9	8	1.97	0.471
1262B-22H-1	212.03	64.73	13	8	8	2.09	0.498
1262B-22H-2	213.03	64.92	12	8	9	2.17	0.517
1262B-22H-3	214.00	65.10	13	8	9	2.32	0.554
1262C-13H-1	214.90	65.29	13	8	10	2.22	0.530
1262B-22H-3	215.08	65.32	15	9	10	2.36	0.564
1262B-22H-4	215.23	65.36	14	9	10	2.27	0.541
1262C-13H-1	215.64	65.46	14	9	10	2.39	0.571
1262C-13H-1	215.90	65.53	14	9	10	2.39	0.570
1262C-13H-2	216.10	65.57	14	9	9	2.30	0.549
1262C-13H-2	216.32	65.61	13	8	10	2.29	0.548
1262C-13H-2	216.57	65.66	13	8	9	2.26	0.540
1262C-13H-2	216.69	65.68	16	11	10	2.48	0.591
1262C-13H-2	216.87	65.69	21	10	9	2.32	0.553
1262C-13H-3	217.54	65.71	23	12	9	2.73	0.652

Appendix 11.4 – Number of species and genera in each sample as well as diversity indices Shannon Index and Evenness.

Sample	Depth (mcd)	Age (Ma)	No. of Macro-perforate species > 106	No. of Micro-perforate species > 106	No. of Macro-perforate genera >106	No. of Micro-perforate genera >106	No. of Macro-perforate genera 38 - 106	No. of Micro-perforate genera 38 - 106
1262B-19H-5	185.05	60.86	15	0	5	0	5	1
1262C-10H-2	185.79	60.95	12	2	5	2	5	2
1262C-10H-3	186.51	61.05	15	0	5	0	5	2
1262C-10H-3	187.23	61.16	16	0	5	0	5	3
1262C-10H-4	187.95	61.26	16	1	5	1	5	3
1262c-10h-4	188.67	61.35	14	0	5	0	5	3
1262C-10H-5	189.39	61.44	16	2	5	2	4	3
1262C-10H-5	190.11	61.52	13	1	5	1	5	3
1262C-10H-6	190.83	61.61	12	2	5	2	5	3
1262B-20H-2	191.56	61.70	12	2	5	2	4	3
1262B-20H-3	192.28	61.79	13	3	5	3	5	3
1262B-20H-3	193.00	61.87	12	3	5	3	5	3
1262B-20H-3	193.72	61.95	12	1	5	1	4	3
1262B-20H-4	194.47	62.03	13	3	5	3	5	3
1262B-20H-4	195.19	62.12	13	1	5	1	4	3
1262C-11H-2	195.90	62.21	14	1	5	1	5	4
1262C-11H-3	197.70	62.42	11	2	6	2	5	3
1262C-11H-3	198.42	62.51	12	0	5	0	5	4
1262C-11H-4	199.14	62.62	10	2	5	2	5	3
1262C-11H-4	199.86	62.73	11	2	5	2	5	4
1262C-11H-5	200.58	62.84	11	1	5	1	5	3
1262C-11H-5	201.30	62.95	12	1	6	1	4	4
1262B-21H-1	202.14	63.05	11	2	6	2	5	4
1262B-21H-2	202.86	63.13	9	3	5	3	4	4
1262C-12H-1	203.58	63.25	9	3	5	2	4	4
1262C-12H-2	204.30	63.41	10	3	5	2	5	4
1262C-12H-2	205.02	63.54	10	2	5	2	4	5
1262C-12H-2	205.77	63.68	10	5	5	4	4	5
1262C-12H-3	206.49	63.82	11	3	5	3	4	3
1262C-12H-3	207.21	63.95	11	5	5	4	4	4
1262C-12H-4	207.93	64.08	10	2	5	2	4	5
1262C-12H-4	208.71	64.21	10	3	5	2	4	5
1262C-12H-5	209.43	64.32	10	4	5	3	4	4
1262C-12H-6	210.36	64.47	10	3	5	3	4	5
1262C-12H-6	211.08	64.58	8	4	5	4	4	4
1262B-22H-1	212.03	64.73	9	4	5	3	4	4
1262B-22H-2	213.03	64.92	9	3	5	3	5	4
1262B-22H-3	214.00	65.10	9	4	5	3	5	4
1262C-13H-1	214.90	65.29	9	4	5	3	5	5
1262B-22H-3	215.08	65.32	9	6	5	4	5	5
1262B-22H-4	215.23	65.36	9	5	5	4	5	5
1262C-13H-1	215.64	65.46	9	5	5	4	5	5
1262C-13H-1	215.90	65.53	9	5	4	4	5	5
1262C-13H-2	216.10	65.57	9	5	5	4	5	4
1262C-13H-2	216.32	65.61	9	4	5	3	5	5
1262C-13H-2	216.57	65.66	8	5	5	3	5	4
1262C-13H-2	216.69	65.68	9	7	6	5	5	5
1262C-13H-2	216.87	65.69	19	2	9	1	8	1
1262C-13H-3	217.54	65.71	21	2	11	1	8	1

Appendix 11.5 - Number of macroperforate verses microperforate species and genera